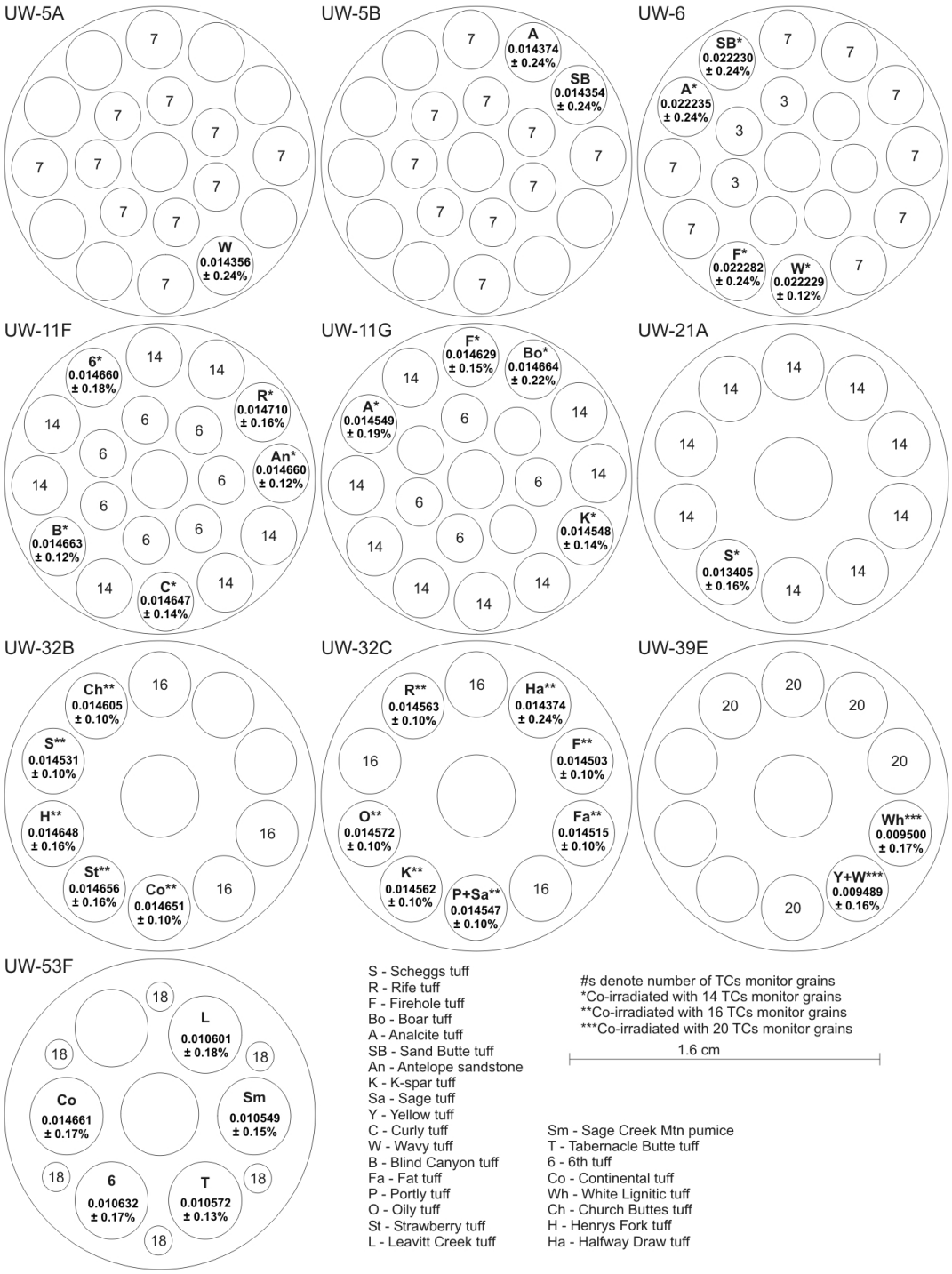

Figure DR1. Sanidine flux moniter and sample positions within stacked aluminum irradiation discs and resulting *J* values, calculated for sample positions using a distance-weighted interpolation algorithm.

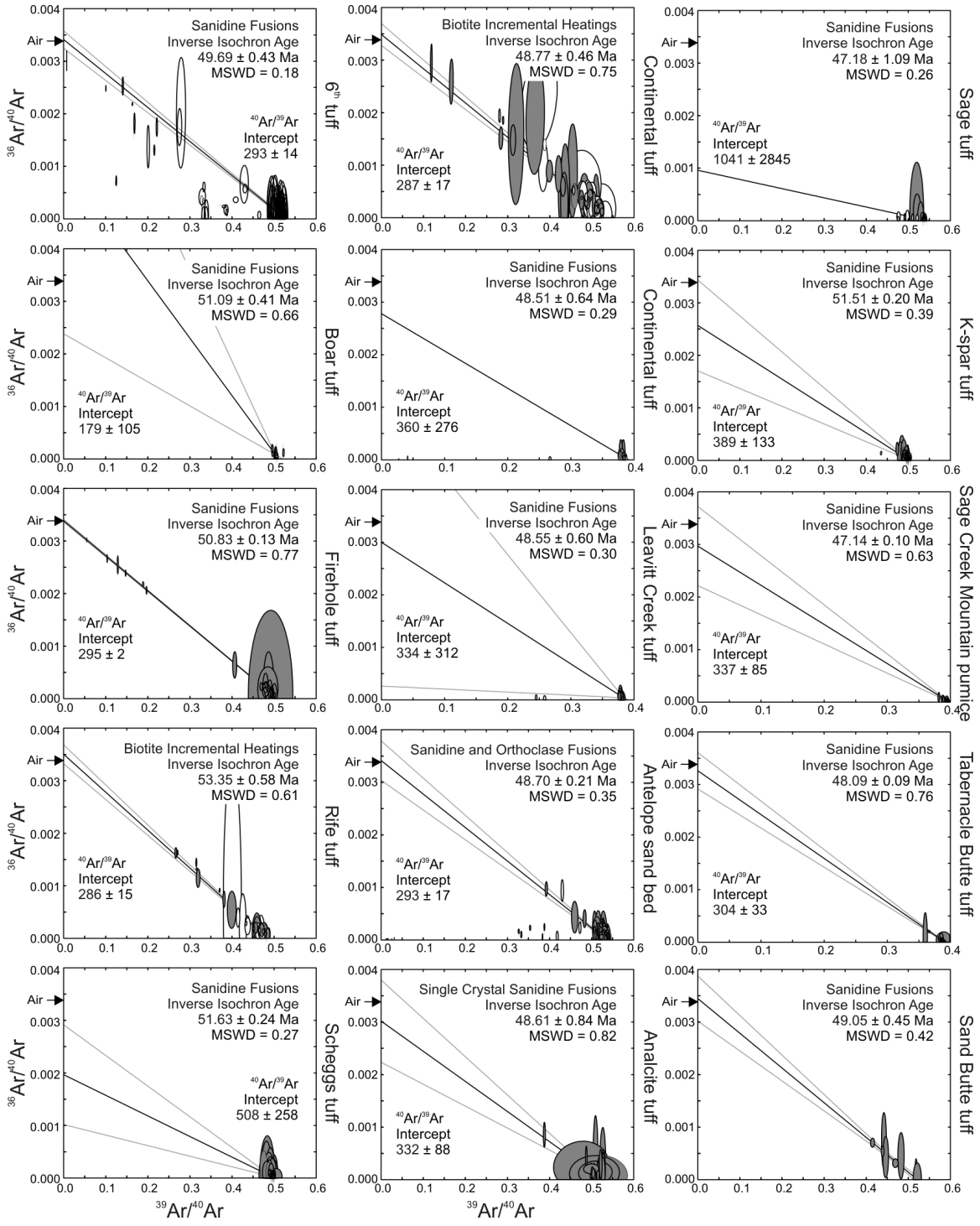

Figure DR2. Inverse isochron diagrams for dated ash beds. Ellipses represent 2σ uncertainties for individual analyses.

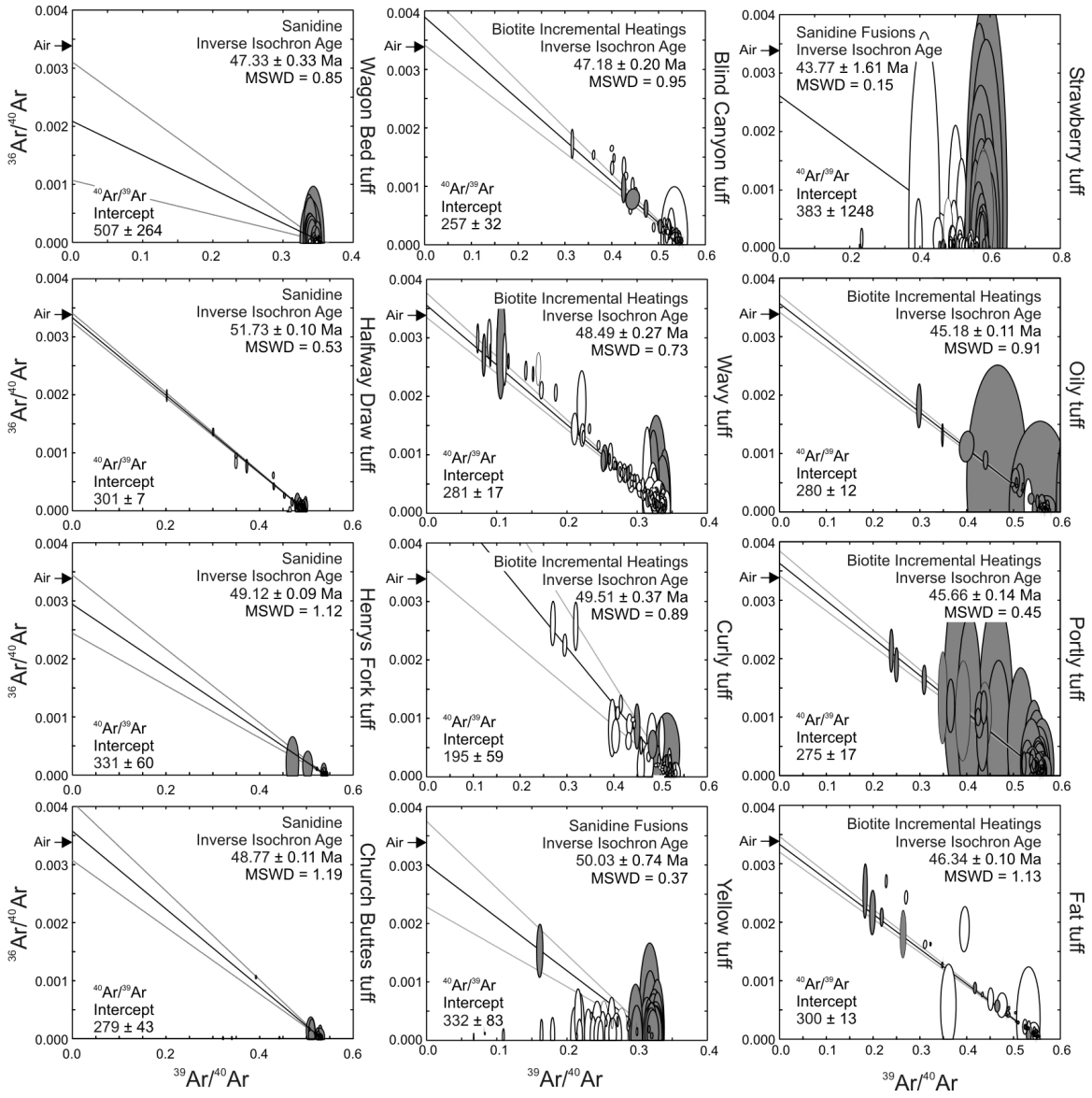

Figure DR2. Inverse isochron diagrams for dated ash beds. Ellipses represent 2σ uncertainties for individual analyses.

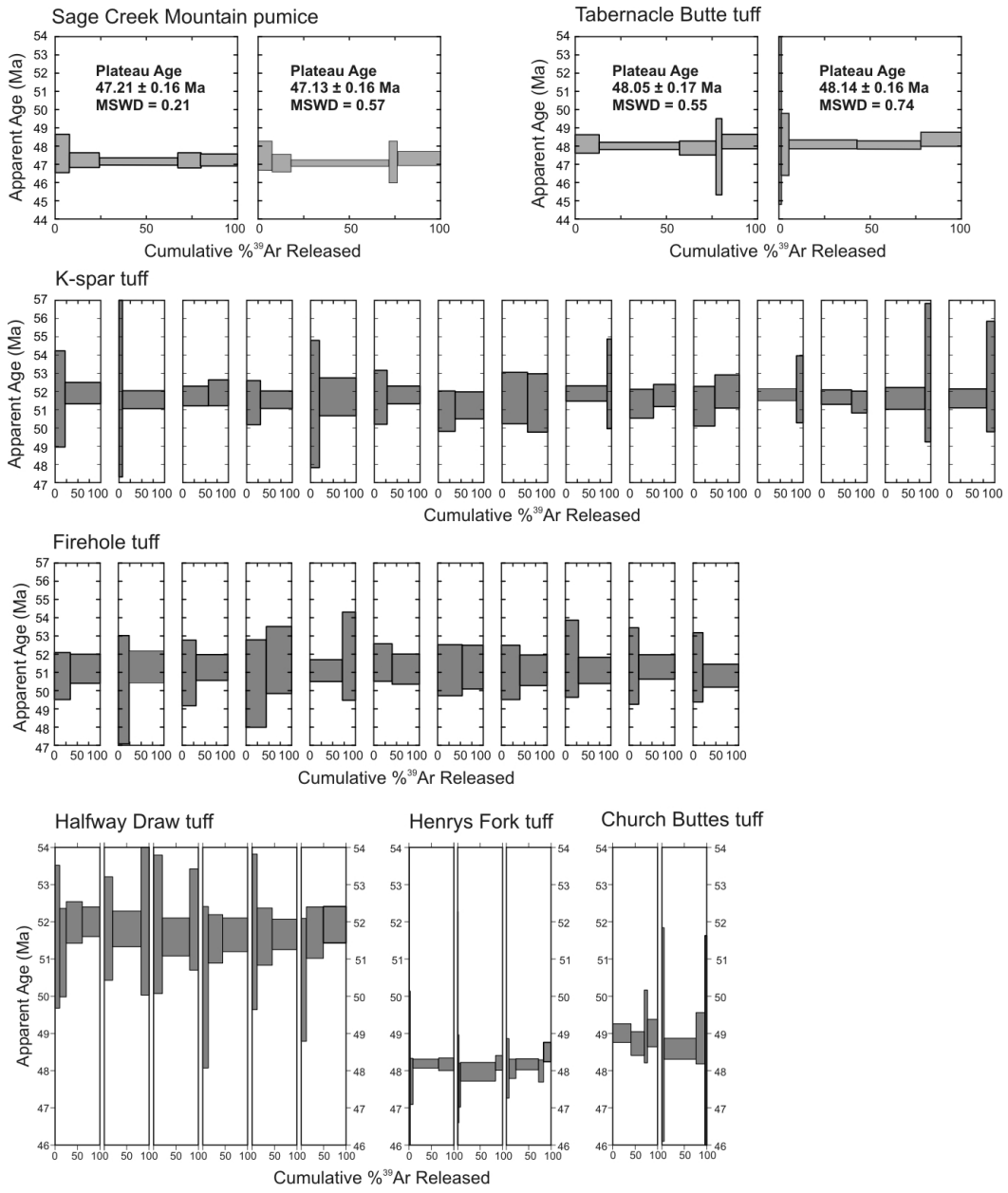

Figure DR3. Age specta diagrams for incrementally heated sanidine. Shown with 2σ uncertainties for each heating step.

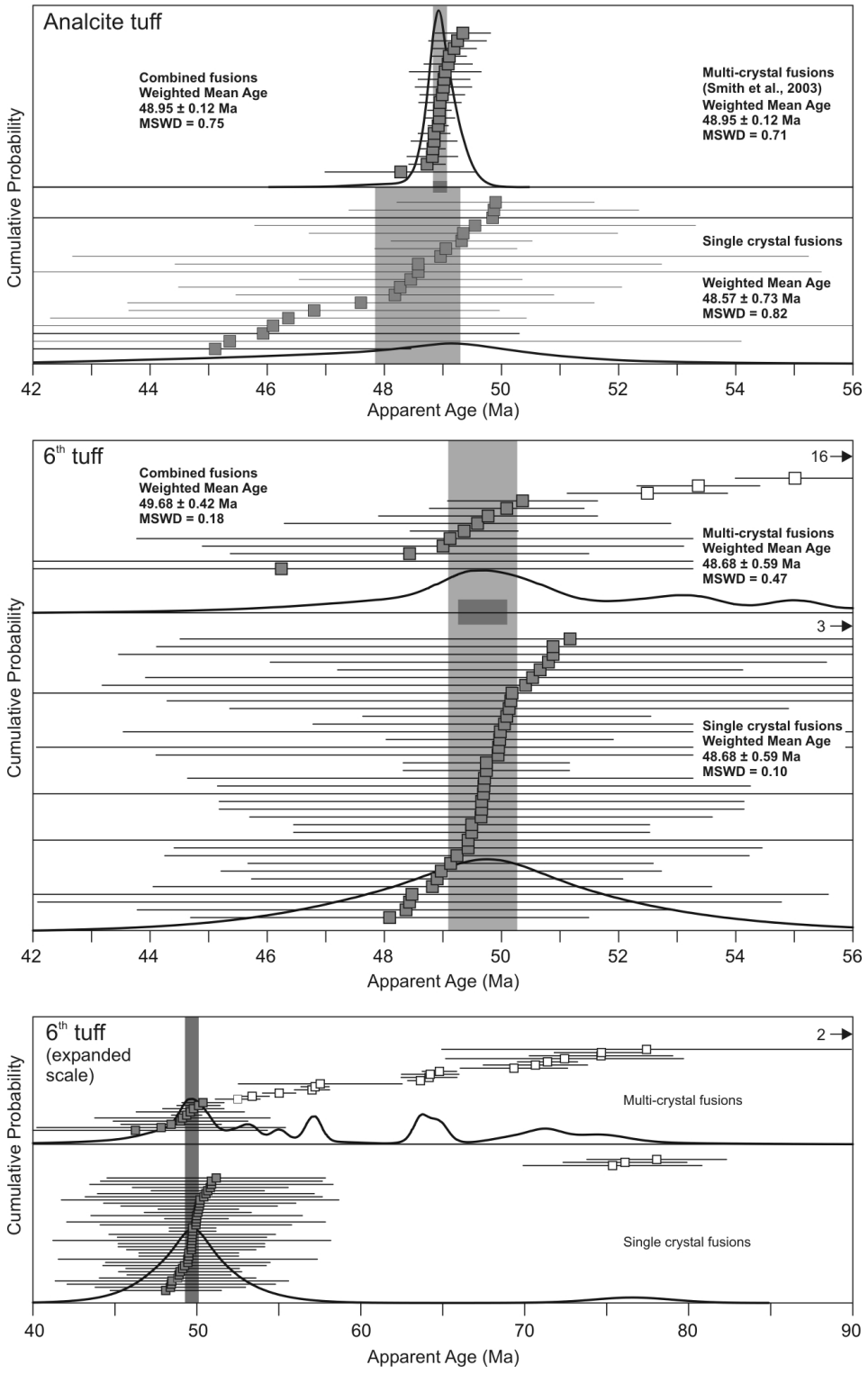

Figure DR4. Cumulative probability plots of single and multi-crystal laser fusion analyses of sanidine from the Analcite and 6th tuffs. Bars represent 2σ uncertainties for individual analyses.

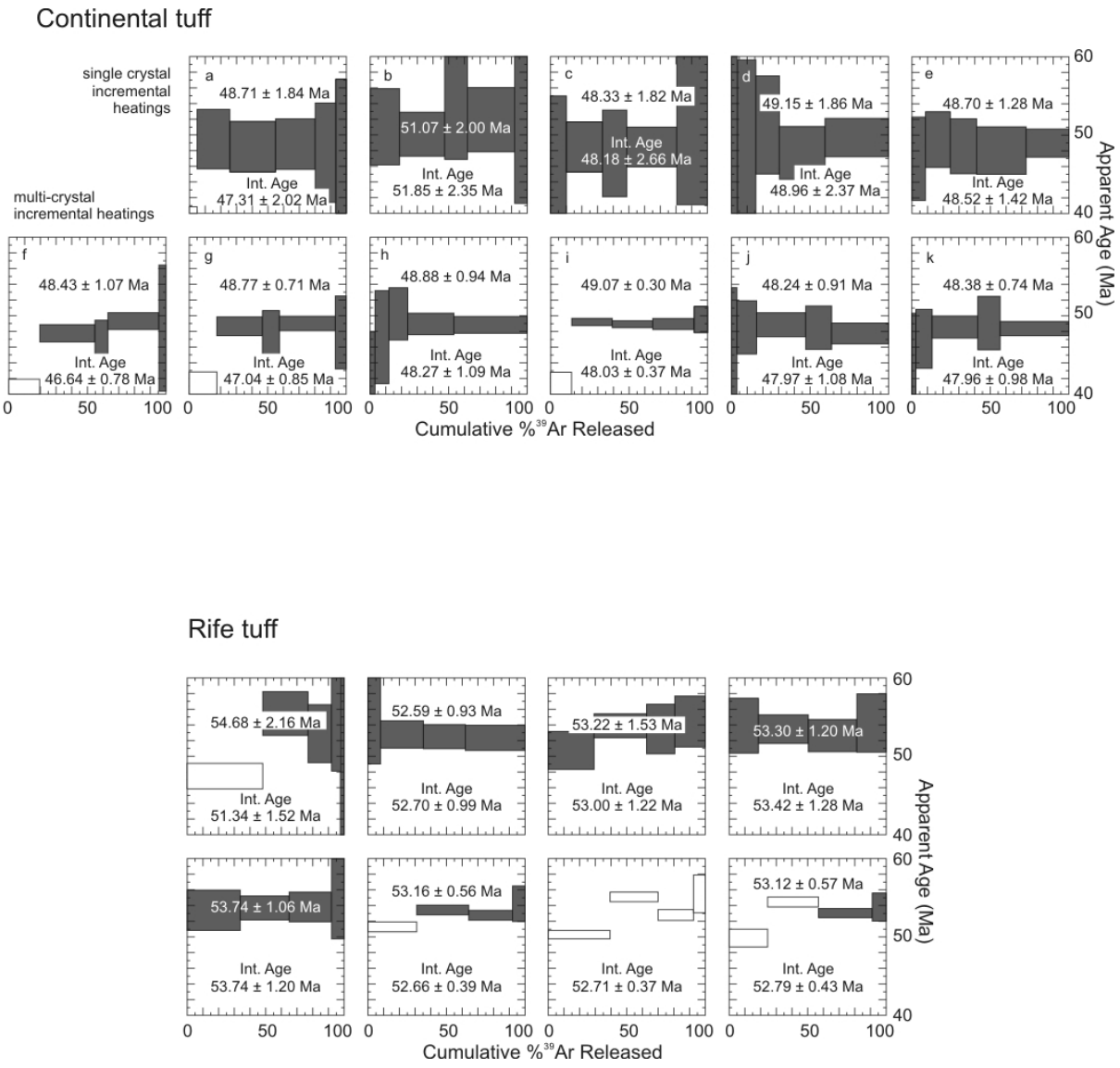

Figure DR5. Age specta diagrams for laser incrementally heated biotite. Shown with 2σ uncertainties for each heating step.

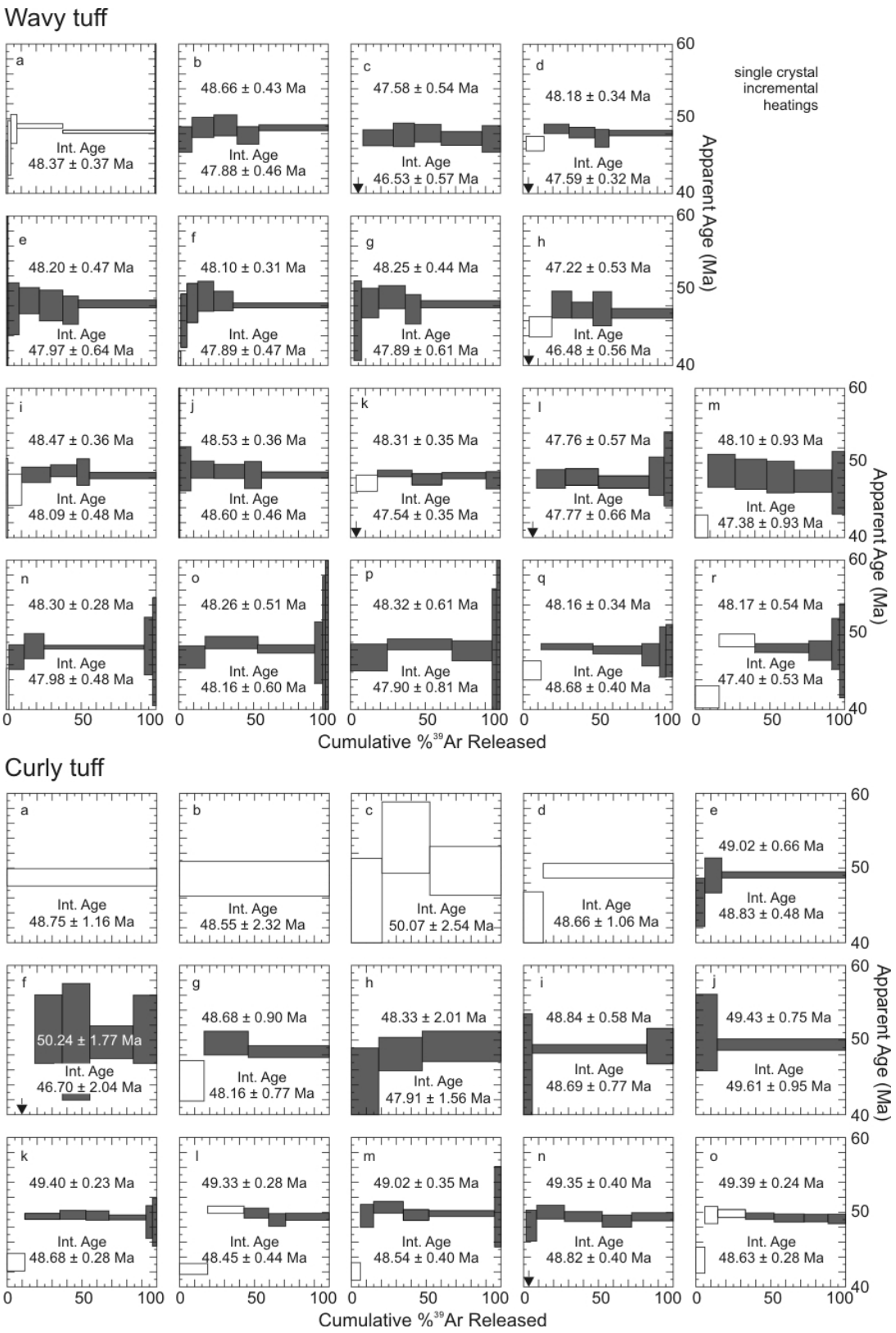

Figure DR5. Age specta diagrams for laser incrementally heated biotite. Shown with 2σ uncertainties for each heating step.

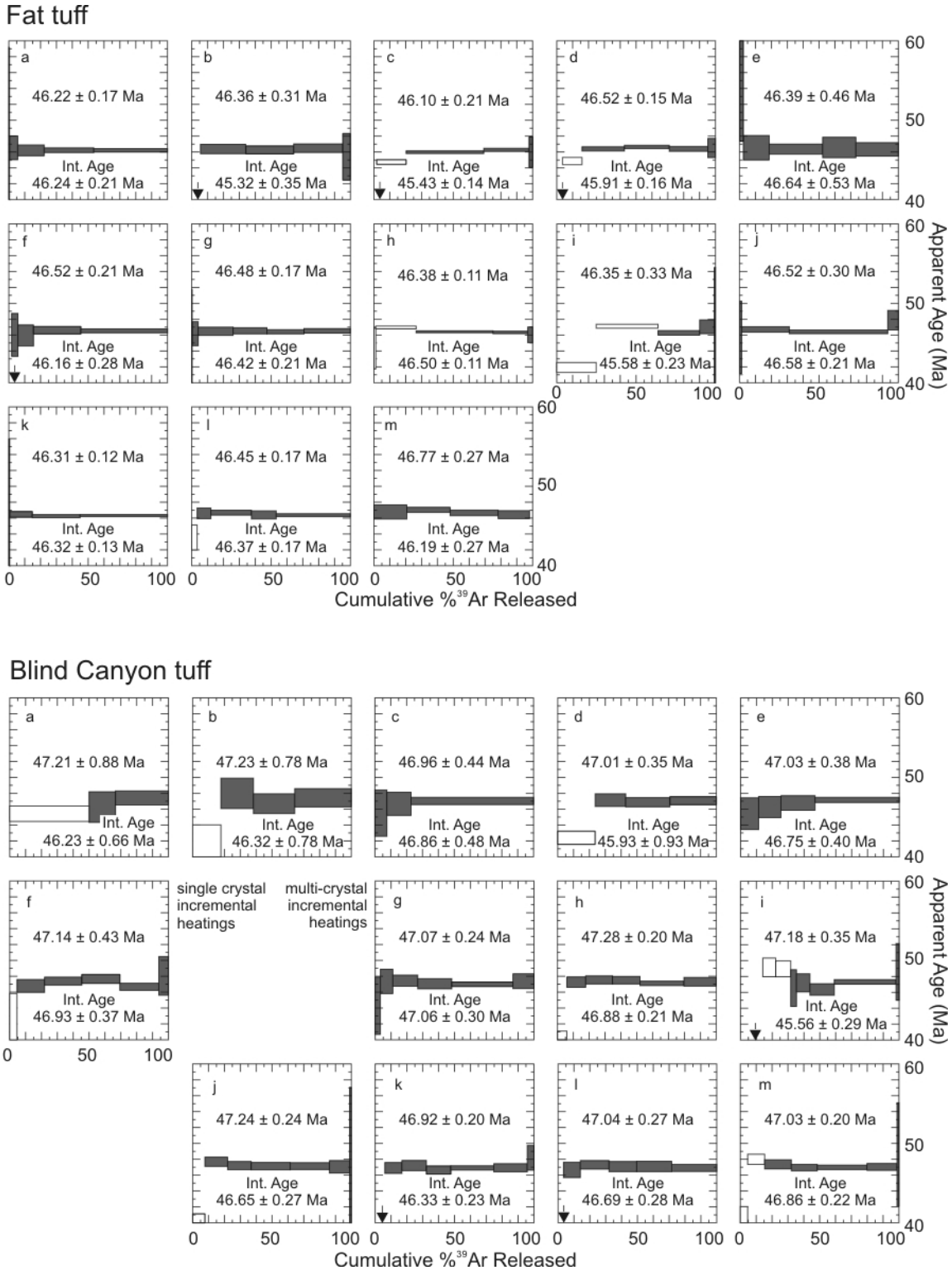

Figure DR5. Age specta diagrams for laser incrementally heated biotite. Shown with 2σ uncertainties for each heating step.

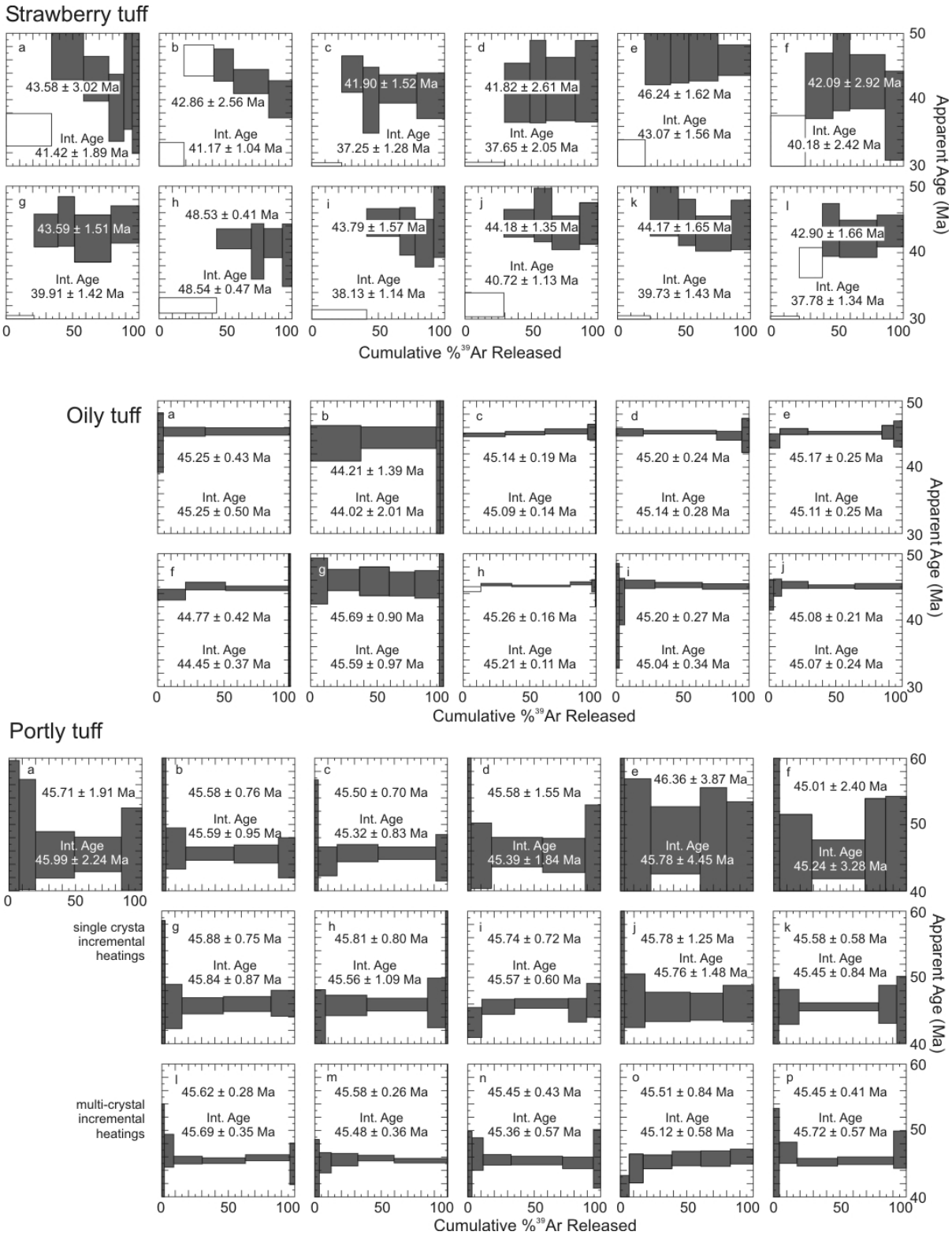

Figure DR5. Age specta diagrams for laser incrementally heated biotite. Shown with 2σ uncertainties for each heating step.

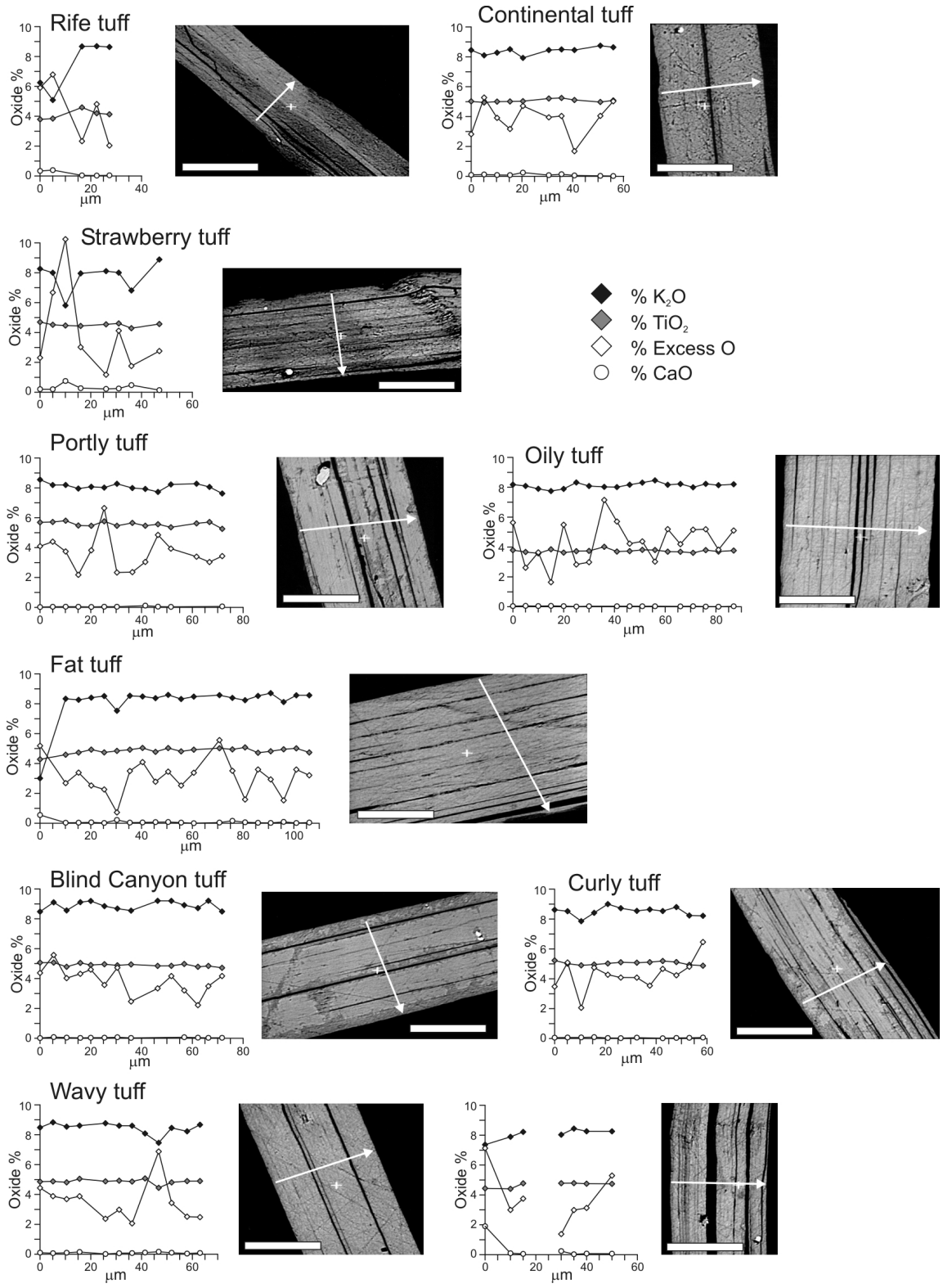

Figure DR6. Electron microprobe transects across biotite from dated ash beds. Analyses yielding less than 8 oxide % K are characteristic of partial alteration (c.f. Smith et al., 2007). See Table DR9 for explanation of analysis and “excess O”.

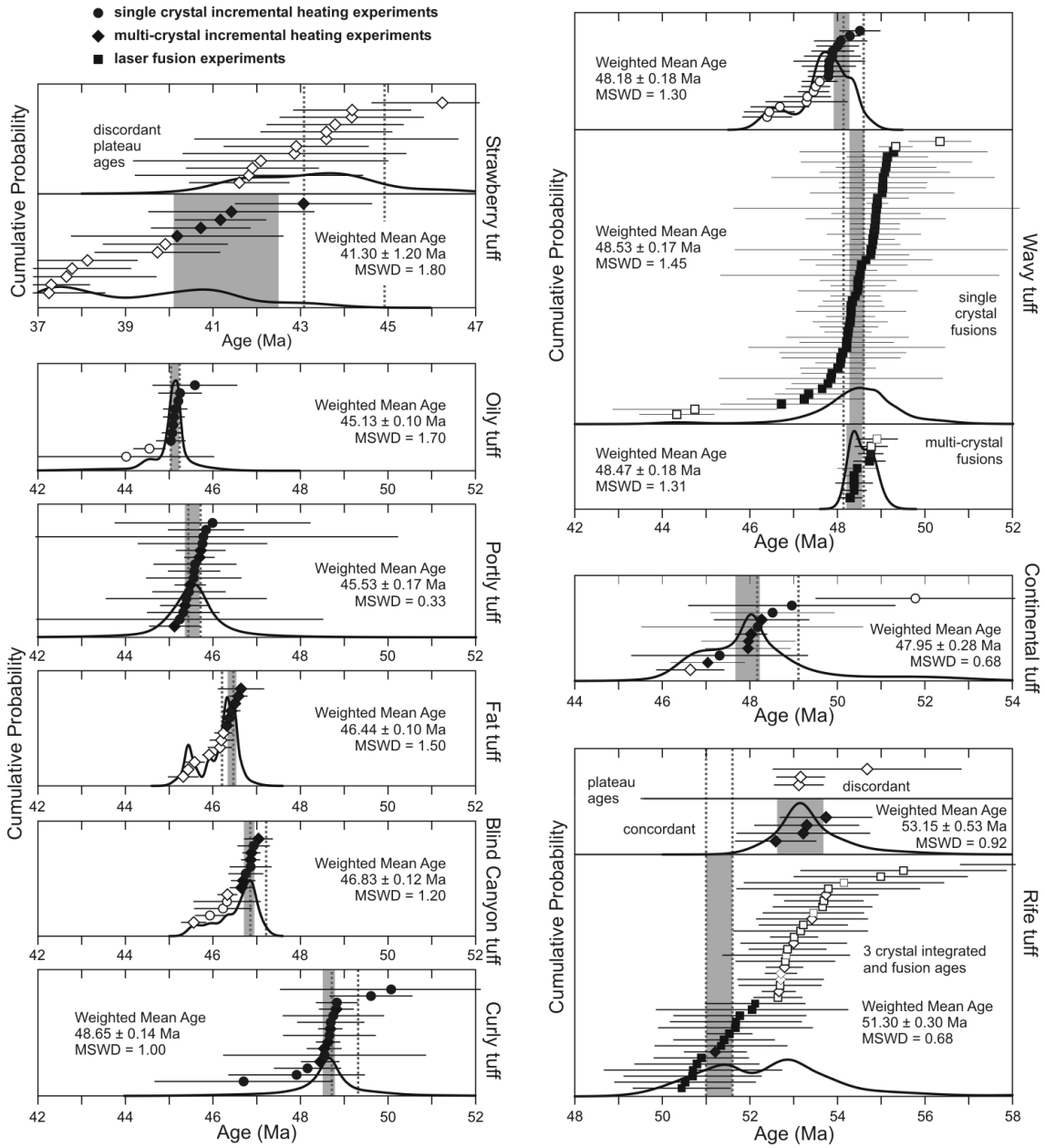

Figure DR7. Cumulative probability plots of biotite integrated and total fusion ages. Gray bars indicate envelope of uncertainty for shown analyses. Dashed lines indicate preferred age for tuff bed (see Table 1 and Figure 4). Analyses shown are integrated ages from biotite incremental heating experiments unless otherwise indicated. Bars represent 2σ uncertainties.

Table DR1. References for Laramide Basins and Volcanic Fields

Basin or Field	Floral References	Stratigraphic References	Biostratigraphic References
Greater Green River	(Knowlton, 1923; Brown, 1929; Berry, 1930; Brown, 1934; Leopold and MacGinitie, 1972; Grande, 1984; Roehler, 1993; Wolfe et al., 1998; Wilf, 2000)	(Hayden, 1869; Powell, 1876; Emmons, 1877; Veatch, 1907; Matthew, 1909; Schultz, 1920; Sears and Bradley, 1924; Bradley, 1926, 1929; Nightingale, 1930; Nace, 1939; Brown, 1950; Donovan, 1950; Anderman, 1955; Pipiringos, 1955; Bradley, 1959; Koenig, 1960; Culbertson, 1961; Oriel, 1961; Pipiringos, 1961; Sheridan et al., 1961; Culbertson, 1962; Dickey, 1962; Oriel, 1962; Deardorff, 1963; Lawrence, 1963; Stuart, 1963; Bradley, 1964; Love, 1964; Stephens and Healey, 1964; Wiegman, 1964; Culbertson, 1965; Hansen, 1965; Lawrence, 1965; Roehler, 1965; Stuart, 1965; Culbertson, 1966; Wood, 1966; Roehler, 1968; Bradley and Eugster, 1969; Culbertson, 1969; Pledge, 1969; Roehler, 1969; Steidtmann, 1969; Love, 1970; McGrew and Sullivan, 1970; Pipringos and Denson, 1970; Simnacher, 1970; Culbertson, 1971; Turnbull, 1972; Kistner, 1973; Roehler, 1973a, b; Trudell et al., 1973; West, 1973; Denson and Pipiringos, 1974; Gustav, 1974; Eugster and Hardie, 1975; West, 1976; Dorr et al., 1977; Buchheim, 1978; Stanley and Surdam, 1978; Burnside and Culbertson, 1979; Schmidtt, 1979; Surdam and Stanley, 1979; Sullivan, 1980; Surdam and Stanley, 1980b; Roehler and Trudell, 1981; West and Huchison, 1981; McGee, 1983; Smoot, 1983; Roehler, 1985; Rowley et al., 1985; Sullivan, 1985; Loen, 1986; Steidtmann et al., 1986; Groll and Steidtmann, 1987; Mason, 1987; Roehler, 1988, 1991b, c; Steidtmann and Middleton, 1991; M'Gonigle and Dover, 1992; Roehler, 1992a; Crews and Ethridge, 1993; Dover and M'Gonigle, 1993; Roehler, 1993; Horsfield et al., 1994; Love, 1995; Clyde et al., 1997; Buchheim and Eugster, 1998; Culbertson, 1998; Evanoff et al., 1998; Buchheim et al., 2000; Clyde et al., 2001; Leggitt and Cushman, 2001; Pietras et al., 2003a; Pietras et al., 2003b; Zonneveld et al., 2003)	(Matthew, 1909; Osborn, 1929; Wood, 1934; Morris, 1954; Knight, 1955; McGrew and Berman, 1955; McKenna, 1955; McGrew, 1959; McGrew and Roehler, 1960; Gazin, 1962, 1965; Dorr, 1969; McGrew and Sullivan, 1970; West, 1970; West and Atkins, 1970; Savage et al., 1972; Turnbull, 1972; Roehler, 1973b; West, 1973; West and Dawson, 1973, 1975; Gazin, 1976; Dorr, 1978; Turnbull, 1978; Gingerich, 1979; West and Huchison, 1981; Honey, 1988; West, 1990; Evanoff et al., 1994; Gunnell and Bartels, 1994; McCarroll et al., 1996b, a; Stucky et al., 1996; Clyde et al., 1997; Covert et al., 1998; Evanoff et al., 1998; Gunnell, 1998; Gunnell and Bartels, 1999; Gunnell and Yarborough, 2000; Holroyd and Smith, 2000; Anemone, 2001; Clyde et al., 2001; Smith and Holroyd, 2003)
Fossil-Fowkes	(Brown, 1929; Grande, 1984)	(Tracey et al., 1961; Oriel and Tracey, 1970; Nelson, 1972; Rubey et al., 1975, 1980; Hurst, 1984; Hurst and Steidtmann, 1986; M'Gonigle and Dover, 1992; Dover and M'Gonigle, 1993; Buchheim, 1994; Grande and Buchheim, 1994; Dover, 1995; Oaks et al., 1999)	(Gazin, 1962; Nelson, 1972, 1973; Ambrose et al., 1997; Froehlich and Breithaupt, 1998)
Piceance Creek	(MacGinitie, 1969; Manchester, 1989)	(Peale, 1876; Bradley, 1931; Duncan and Belser, 1950; Donnell, 1961b, a; Ritzma, 1965; Donnell, 1969; Dyni, 1969; Dyni et al., 1970; Snow, 1970; Trudell et al., 1970; Brobst and Tucker, 1973; Cashion and Donnell, 1974; Duncan et al., 1974; Dyni, 1974; O'Sullivan, 1974; Robb and Smith, 1974; Roehler, 1974; Trudell et al., 1974; Lundell and Surdam, 1975; O'Sullivan, 1975; Pipiringos and Johnson, 1975; Hail, 1987; O'Sullivan, 1987; Hail and Smith, 1994)	(Kihm, 1984; Izett et al., 1985; Krishtalka and Stucky, 1986; Honey, 1990; Lucas, 1998)
Uinta	(MacGinitie, 1969; Grande, 1984; Manchester, 1989)	(Comstock, 1875; Osborn, 1895; Douglass, 1914; Kay, 1934; Stagner, 1941; Spieker, 1946, 1949; Muessig, 1951; Schoff, 1951; Dane, 1954, 1955; Picard, 1955; Ray et al., 1956; Abbott, 1957; Picard, 1957a, b, 1959; McGookey, 1960; Chatfield, 1965; Sanborn and Goodwin, 1965; Cashion, 1967; Picard, 1967; Marcantel and Weiss, 1968; Picard and High, 1968; Moussa, 1969; Anderson and Picard, 1972; Doelling, 1972; Anderson and Picard, 1974; Cashion, 1974; Cashion and Donnell, 1974; Dyni, 1976; Fouch, 1976; Fouch et al., 1976; Peterson, 1976; Ryder et al., 1976; Sheliga, 1980; Fouch, 1981; Fouch et al., 1982; Trudell et al., 1982; Weiss, 1982; Zawiskie et al., 1982; Fouch et al., 1983; Smith, 1984; Dyni et al., 1985; Johnson, 1985; Rowley et al., 1985; Bruhn et al., 1986; Cashion, 1986; Dickinson et al., 1986; Franczyk et al., 1989; Weiss et al., 1990; Morris et al., 1991; Bryant, 1992; Remy, 1992; Garner and Morris, 1996; Weiss and Warner, 2001; Pusca, 2003)	(Osborn, 1895; Douglass, 1914; Kay, 1934; Parker, 1970; Nelson et al., 1980a; Doi, 1990; Miller and Hall, 1990; Prothero, 1996; Gunnell and Bartels, 1999; Rasmussen, 1999; Rasmussen et al., 1999)
Bighorn	(Wing et al., 1991; Bown et al., 1994; Wing et al., 1995; Wing et al., 2000)	(Rohrer, 1964a, b; Rohrer and Gazin, 1965; Rohrer, 1966b; Neasham and Vondra, 1972; Bown, 1982; Krause, 1985; Dutcher et al., 1986; DeCelles et al., 1991; Wing et al., 1991; Seeland, 1998)	(Rohrer and Gazin, 1965; Gingerich, 1983; Bown et al., 1994; Wing et al., 1995; Gingerich and Clyde, 2001)

Table DR1. References for Laramide Basins and Volcanic Fields

Basin or Field	Floral References	Stratigraphic References	Biostratigraphic References
Powder River	(Brown, 1948; Mapel, 1959)	(Brown, 1948; Mapel, 1959; Flores and Ethridge, 1985; Seeland, 1992)	(Brown, 1948; Mapel, 1959)
Wind River	(Berry, 1930; Bay, 1969; MacGinitie, 1974)	(Murphy and Roberts, 1954; Love, 1964; Keefer, 1965; Rohrer, 1966a; Soister, 1968; Bay, 1969; Love, 1970; Seeland, 1978a, b; Thaden, 1980a, b; Korth, 1982; Ver Ploeg, 1992)	(Sinclair and Granger, 1911; Korth, 1982; Stucky, 1982; Winterfield and Conard, 1983; Stucky, 1984a; Stucky et al., 1989; Winterfield, 1990)
Gros Ventre	(MacGinitie, 1974)	(Love, 1947; Love et al., 1951; Rohrer, 1968, 1969; Love et al., 1972; MacGinitie, 1974; Antweiler et al., 1989; Love et al., 1992)	(Love, 1947; McKenna, 1972; MacGinitie, 1974; McKenna, 1980)
Shirley	(Harshman, 1972)	(Harshman, 1968; Denson and Harshman, 1969; Harshman, 1972; Blackstone, 1975)	(McGrew, 1953; Harshman, 1972; Blackstone, 1975)
Laramie		(Blackstone, 1975)	(McGrew, 1953; Prichinello, 1971; Blackstone, 1975; Davidson, 1987)
Hanna		(Blackstone, 1975)	(Prichinello, 1971; Blackstone, 1975)
North-Middle Park	(Hail and Leopold, 1960; Stands, 1992)	(Hail, 1965, 1968)	(Hail and Leopold, 1960; Hail, 1965; Stands, 1992)
South Park		(De Voto, 1964; Ettinger, 1964)	(Siems, 1964)
Denver		(Bryant et al., 1981; Hicks et al., 2003)	
Raton		(Berner and Briggs, 1958; Johnson, 1959)	(Robinson, 1966)
San Juan		(Tweto, 1980; Fassett, 1985; Smith et al., 1985)	(Krishtalka and Stucky, 1986)
Claron		(Anderson and Rowley, 1975; Bowers, 1990; Goldstrand, 1994)	(Eaton, 1995; Eaton et al., 1999)
Sheep Pass		(Winfrey, 1958, 1960; Fouch, 1979; Fouch et al., 1979)	(Emry, 1990)
Cherty Limestone		(Decker, 1962; Brokaw, 1967; Fouch, 1979; Fouch et al., 1979; Solomon et al., 1979; Solomon, 1981; Moore and Solomon, 1982)	
Challis Volcanics	(Axelrod, 1968)	(McIntyre et al., 1982; Ekren, 1985; Moye et al., 1988; Snider and Moye, 1989; Fisher et al., 1992; Janecke and Snee, 1993; Snider, 1995; Janecke et al., 1997; Palmer and Shawkey, 1997)	
Basins of SW Montana		(Wood, 1934; Fields et al., 1985; Hanneman, 1989; Ripley, 1995; Thomas et al., 1995; M'Gonigle and Dalrymple, 1996; Tabrum et al., 1996; Vandenburg et al., 1998; Janecke et al., 1999; Janecke et al., 2000; Rasmussen, 2003; Sears and Ryan, 2003)	(Douglass, 1903; Wood, 1934; Tabrum et al., 1996; Rasmussen, 2003)
Lowland Creek Volcanics		(Smedes, 1962; Smedes and Hanna, 1977; Ispolatov et al., 1996)	
Absaroka Volcanic Province	(Dorf, 1960; MacGinitie, 1974; Fritz, 1980; Yuretich, 1984)	see Table DR15	see Table DR15
Rattlesnake Mountains		(Van Houten, 1955; Pekarek et al., 1974; Shive et al., 1977)	(Van Houten, 1955)

Table DR2. Description and stratigraphic position of dated ash beds

Map #	Unit	Location	Description	References
1	Sage Creek Mountain pumice (SCM-1)	N41º 7' 56.5" W110º 8' 11.7"	44 meters above basal E limestone and 14 meters below Bishop conglomerate. Pumice rich sandstone near the base of dominantly fine varegiated alluvial strata of the Turtle Bluffs Member (Bridger E) of the Bridger Formation.	(Evanoff et al., 1998; Murphey, 2001)
2	Tabernacle Butte tuff (TB-1)	N42º 26' 0.6" W109º 22' 31.4"	0.5 meter bentonite in pumice rich upper Bridger formation near the top of Tabernacle Butte	(McGrew, 1959)
3	Henrys Fork tuff (HeF)	N41º 07' 25.3" W110º 09' 27.7"	1 m thick, yellowish gray claystone that weathers to a dark gray band within massive white calcareous marlstone. Base is sharp and top is diffuse. Matrix exhibits bentonite alteration.	(Prothero, 1996; Evanoff et al., 1998; Murphey et al., 1999)
4	Leavitt Creek tuff (LeC)	N41º 14' 13.1" W110º 12' 41.8"	0.5 meter bentonite interbedded with massive gray mudstone of Bridger B	(Evanoff et al., 1998; Murphey, 2001)
5	Church Buttes tuff (ChB)	N41º 28' 34.5" W110º 08' 04.3"	0.7 m thick, olive green claystone that weathers to a dark gray band within massive silty mudstone. Matrix exhibits bentonite alteration.	(Evanoff et al., 1998; Murphey et al., 1999)
6	Continental tuff (CP-1)	N42º 16' 6.2" W108º 43' 07.5"	1 meter thick biotite and pumice rich reworked ash. Caps alluvial strata at the top of Continental Peak and is overlain by Oligocene(?) gravels.	(Clyde et al., 2001)
7	Antelope sand bed (AC-3)	N41º 23' 45.9" W108º 30' 54.2"	60 cm sand bed interbedded with finer alluvial-deltaic strata ~20 m above top of fine mudstone of the upper LaClede Bed of the Laney Member.	Rhodes et al. (2004)
8	Analcite tuff (SB-1)	N41º 21' 1.4" W108º 40' 4.7"	cf. Smith et al. (2003)	Bed 433, Plate 2 of Roehler (1992b) (Ratterman and Surdam, 1981)
8	Sand Butte tuff (SB-3)	N41º 20' 43.7" W108º 40' 13.7"	4 cm tuff interbedded with laminated organic rich mudstone, Basal half is biotite and plagioclase rich and upper half is fine grained. Exhibits zeolite alteration of glassy ash matrix	(O'Neill, 1980)
9	Boar tuff (BT-14)	N41º 57' 48.6" W109º 15' 9.8"	25 cm orange ash bed within laminated mudstone, ~20 m above the base of the Wilkins Peak Member and below "D" sandstone marker bed. North end of White Mountain escarpment.	Boar's tusk section of Pietras et al. (2003a)
10	Firehole tuff (FC-2)	N41º 21' 0.7" W109º 22' 59.9"	cf. Smith et al. (2003)	(Culbertson, 1961, 1998)
11	Rife tuff (BT-18)	N41º 57' 47.2" W109º 15' 8.7"	cf. Smith et al. (2003)	Boar's tusk section of Pietras et al. (2003a)
12	Scheggs tuff (WP-3)	N41º 31' 9.9" W109º 19' 29.8"	35 cm ash bed at the base of the Rife bed of the Tipton Member. Basal ½ contains ~10% biotite, biotite is largely absent in the upper portion of the ash.	Upper ash near Rife-Scheggs contact in Wilkins Peak section of Roehler (1989)
13	K-spar tuff (FQ-1)	N41º 47' 32.2" W110º 42' 39.6"	10 cm orange ash bed in laminated mudstone of Fossil Butte Member	Site G of Grande and Buchheim (1994)
14	Sage tuff (FF)	N41º 46' 44.8" W110º 57' 50.4"	1 m pumiceous reworked ash ~100 m above base of Bulldog Hollow Member of the Fowkes Formation	(Oriel and Tracey, 1970; Nelson, 1973)
15	Yellow tuff (WR-1)	N40º 1' 1.9" W108º 6' 53.2"	3 cm zeolitized ash within laminated mudstone near the base of the Parachute Creek Member, northern Piceance Creek Basin, weathers yellow	"Yellow Tuff bed" of Pipiringos and Johnson (1975)
16	Strawberry tuff (SR-1)	N40º 9' 54.0" W110º 33' 5.6"	0.8 meter tuff from "30m above Tgs-Tgsl contact" in finely bedded siltstone	Sample 20 of Bryant (1989)
17	Oily tuff (IC-6)	N40º 2' 56.8" W110º 31' 42.1"	5-12cm thick zeolitized and oil saturated tuff from uppermost "saline facies"	"tuff from top of Tgs" (Mauger, 1977)
18	Portly tuff (IC-5)	N39º 58' 47.6" W110º 37' 16.3"	~0.6 meters thick zeolitized tuff, uppermost ash at top of "upper tuff zone"	355 meters in Indian Canyon section of Dane (1955)
19	Fat tuff (IC-2)	N39º 58' 46.5" W110º 37' 6.9"	~1m thick biotite-rich ash bed (collected basal 30cm)	Sample 1-69 of Mauger (1977) Sample 22 of Bryant (1989)
20	Blind Canyon tuff (SW-1)	N39º 50' 41.4" W110º 11' 11.8"	30 cm zeolitized, biotite-rich tuff above Blind Canyon	70 meters above Horse Bench sandstone in section 17 of Remy (1992)
21	Wavy tuff (GC-2b)	N39º 50' 59.3" W110º 15' 17.5"	50 cm ash bed within laminated mudstone above Mahogany Zone, Gate Canyon	30 meters above Mahogany zone in section 10 of Remy (1992)
22	Curly tuff (GC-5b)	N39º 50' 33.8" W110º 15' 3.1"	25 cm ash bed in laminated mudstone below the Mahogany zone, Gate Canyon	18 meters in section 10 of Remy (1992)
23	White Lignitic tuff (WB-1)	N42º 42' 54.3" W108º 11' 11.8"	0.5 m thick, tan to white zeolitic tuff interbedded with carbonaceous shale and lignite. Unit 3 of Van Houten (1964). KA 1018 of Evernden et al. (1964).	(Sinclair and Granger, 1911; Evernden et al., 1964; Van Houten, 1964; Love, 1970)
24	Halfway Draw tuff (HD-1)	N42º 51' 52.9" W108º 17' 57.1"	2 m thick, gray claystone containing white pumice clasts up to 5 cm in diameter within massive tan to orange silty mudstone. Matrix exhibits bentonite alteration. White tuff band in Big Sand Draw of Sinclair and Granger (1911). KA 1012 of Evernden et al. (1964).	(Sinclair and Granger, 1911; Hay, 1956; Evernden et al., 1964; Love, 1970)

Locations given according to NAD1927 datum. Positions plotted on map figure on following page.

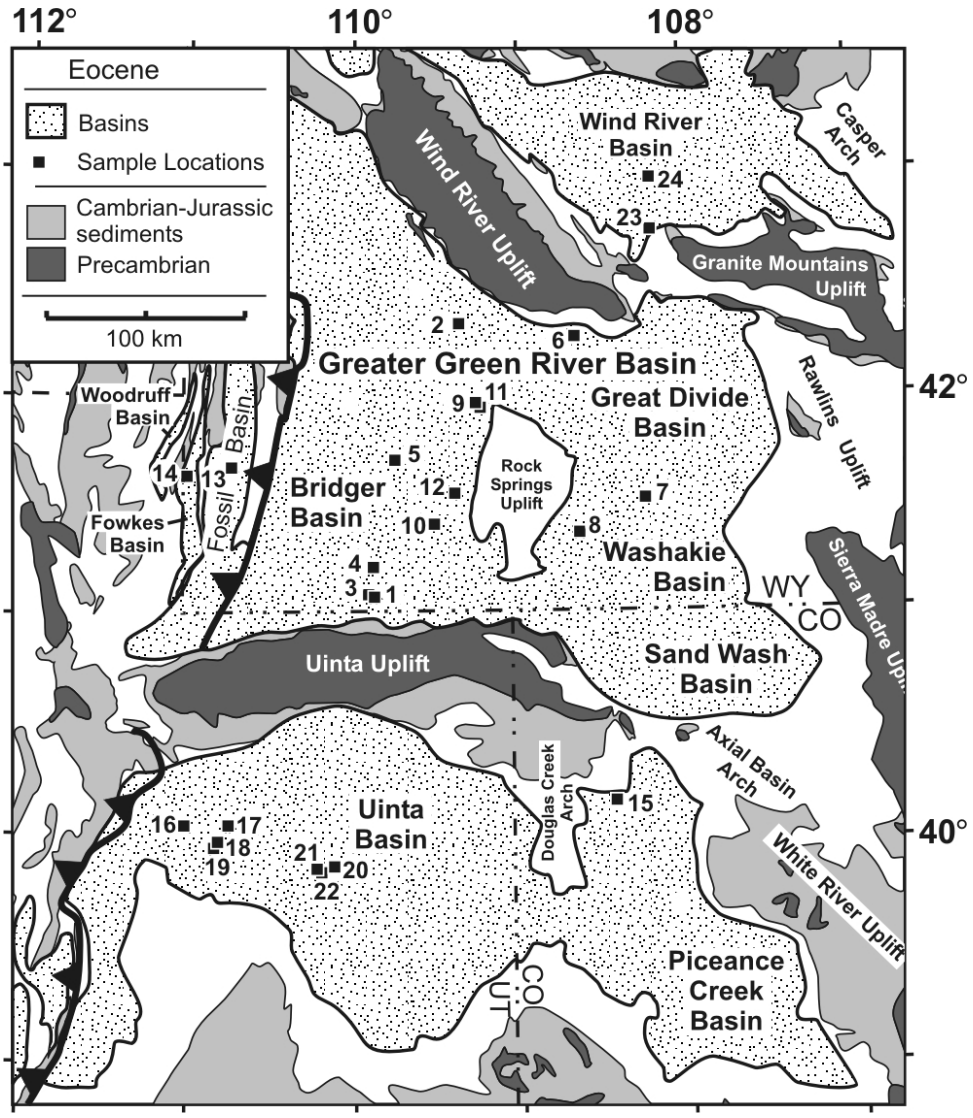

Location map for Table DR2.

Table DR3. Complete $^{40}Ar/^{39}Ar$ results

Sample Experiment	laser power (W)	$^{40}Ar/^{39}Ar$	$^{37}Ar/^{39}Ar$	$^{36}Ar/^{39}Ar$	$^{40}Ar^*$ X10^{-14} mol	$^{40}Ar^*$ %	$^{39}Ar_K$ %	K/Ca	Apparent Age ± 2σ Ma
Scheggs tuff WP-3 sanidine *J* = 0.013405 ± 0.16% μ = 1.0025									
5-20 crystal fusions									
21A6a	1.50	2.156 ± 0.024	0.00769 ± 0.00123	0.000018 ± 0.000139	0.50	99.7		56	51.27 ± 2.23
21A6b	1.50	2.196 ± 0.007	0.04193 ± 0.00081	0.000090 ± 0.000020	2.79	98.9		10	51.76 ± 0.41
21A6c	1.50	2.210 ± 0.009	0.05232 ± 0.00119	0.000118 ± 0.000041	1.72	98.6		8	51.93 ± 0.72
21A6d	1.50	2.200 ± 0.010	0.05806 ± 0.00113	0.000077 ± 0.000047	1.57	99.1		7	51.98 ± 0.80
21A6e	1.50	2.201 ± 0.008	0.07796 ± 0.00149	0.000076 ± 0.000045	1.91	99.2		6	52.07 ± 0.74
21A6f	1.50	2.212 ± 0.007	0.09647 ± 0.00173	0.000101 ± 0.000021	2.85	99.0		4	52.18 ± 0.43
21A6g	1.50	2.186 ± 0.005	0.03057 ± 0.00057	0.000046 ± 0.000023	4.05	99.5		14	51.84 ± 0.40
21A6h	1.50	2.201 ± 0.004	0.03327 ± 0.00075	0.000079 ± 0.000018	4.88	99.0		13	51.96 ± 0.32
6-8 crystal 1 and 2 step fusions *J* = 0.014531 ± 0.10% μ = 1.0035									
32C8a1	0.16	2.010 ± 0.005	0.00590 ± 0.00065	0.000072 ± 0.000073	0.56	98.7	46.4	73	51.42 ± 1.14
32C8a2	1.50	2.041 ± 0.005	0.00606 ± 0.00070	0.000100 ± 0.000074	0.66	98.3	53.6	71	52.02 ± 1.15
32C8b1	0.16	2.007 ± 0.004	0.00469 ± 0.00061	0.000085 ± 0.000076	0.73	98.5	45.7	92	51.27 ± 1.18
32C8b2	1.50	2.027 ± 0.004	0.00455 ± 0.00049	0.000059 ± 0.000049	0.88	98.9	54.3	94	51.96 ± 0.77
32C8c1	0.16	2.020 ± 0.007	0.00791 ± 0.00066	0.000081 ± 0.000075	0.51	98.6	24.4	54	51.62 ± 1.18
32C8c2	1.50	2.025 ± 0.004	0.00681 ± 0.00029	0.000047 ± 0.000035	1.59	99.1	75.6	63	52.00 ± 0.56
32C8d1	0.15	2.024 ± 0.006	0.00438 ± 0.00092	0.000071 ± 0.000156	0.41	98.8	29.7	98	51.80 ± 2.37
32C8d2	1.50	2.053 ± 0.004	0.00522 ± 0.00046	0.000172 ± 0.000047	0.97	97.3	70.3	82	51.78 ± 0.74
32C8e1	0.15	2.119 ± 0.018	0.00223 ± 0.00147	0.000042 ± 0.000294	0.15	99.2	9.5	192	54.43 ± 4.52
32C8e2	1.50	2.029 ± 0.003	0.00544 ± 0.00017	0.000052 ± 0.000031	1.39	99.0	90.5	79	52.06 ± 0.50
32C8f1	0.15	2.055 ± 0.015	0.00328 ± 0.00116	0.000051 ± 0.000241	0.19	99.1	11.5	131	52.73 ± 3.71
32C8f2	1.50	2.023 ± 0.003	0.00432 ± 0.00015	0.000027 ± 0.000026	1.43	99.4	88.5	99	52.10 ± 0.42
32C8g1	0.15	2.042 ± 0.013	0.00395 ± 0.00169	0.000146 ± 0.000377	0.13	97.7	7.8	109	51.69 ± 5.73
32C8g2	1.50	2.017 ± 0.003	0.00381 ± 0.00018	0.000031 ± 0.000031	1.51	99.3	92.2	113	51.92 ± 0.50
32C8h1	0.15	2.051 ± 0.007	0.00483 ± 0.00066	0.000078 ± 0.000104	0.42	98.7	20.7	89	52.42 ± 1.61
32C8h2	1.50	2.012 ± 0.003	0.00439 ± 0.00021	0.000054 ± 0.000027	1.57	99.0	79.3	98	51.62 ± 0.44
32C8i	1.50	2.028 ± 0.003	0.00572 ± 0.00019	0.000057 ± 0.000020	2.53	99.0		75	52.01 ± 0.33
32C8j	1.50	2.027 ± 0.003	0.00589 ± 0.00030	0.000105 ± 0.000048	1.30	98.3		73	51.62 ± 0.74
32C8k	1.50	2.017 ± 0.003	0.00468 ± 0.00023	0.000039 ± 0.000024	1.45	99.2		92	51.85 ± 0.39
32C8l	1.50	2.024 ± 0.003	0.00456 ± 0.00017	0.000069 ± 0.000028	1.55	98.8		94	51.81 ± 0.45
32C8m	1.50	2.035 ± 0.004	0.00570 ± 0.00024	0.000105 ± 0.000034	1.11	98.3		75	51.83 ± 0.54
32C8n	1.50	2.023 ± 0.003	0.00519 ± 0.00023	0.000046 ± 0.000035	1.48	99.1		83	51.97 ± 0.55
32C8o	1.50	2.035 ± 0.004	0.00467 ± 0.00029	0.000071 ± 0.000050	0.90	98.8		92	52.08 ± 0.77
32C8p	1.50	2.025 ± 0.004	0.00374 ± 0.00033	0.000049 ± 0.000055	0.85	99.1		115	51.99 ± 0.85
32C8q	1.50	2.022 ± 0.003	0.00540 ± 0.00021	0.000020 ± 0.000042	1.30	99.5		80	52.14 ± 0.66
32C8r	1.50	2.014 ± 0.003	0.00489 ± 0.00020	0.000042 ± 0.000026	1.68	99.2		88	51.75 ± 0.43
32C8s	1.50	2.035 ± 0.003	0.00467 ± 0.00017	0.000048 ± 0.000045	1.44	99.1		92	52.26 ± 0.70
32C8t	1.50	2.029 ± 0.002	0.00536 ± 0.00018	0.000055 ± 0.000022	1.86	99.0		80	52.04 ± 0.36
32C8u	1.50	2.012 ± 0.003	0.00390 ± 0.00024	0.000059 ± 0.000035	1.29	98.9		110	51.59 ± 0.56
32C8v	1.50	2.020 ± 0.003	0.00417 ± 0.00021	0.000030 ± 0.000026	1.88	99.3		103	51.99 ± 0.43
32C8w	1.50	2.021 ± 0.004	0.00538 ± 0.00032	0.000066 ± 0.000036	1.53	98.8		80	51.77 ± 0.57
32C8x	1.50	2.021 ± 0.003	0.00384 ± 0.00022	0.000047 ± 0.000031	1.39	99.1		112	51.91 ± 0.50
32C8y	1.50	2.019 ± 0.003	0.00552 ± 0.00015	0.000023 ± 0.000016	2.78	99.4		78	52.04 ± 0.28
32C8z	1.50	2.021 ± 0.003	0.00578 ± 0.00022	0.000046 ± 0.000035	1.29	99.1		74	51.92 ± 0.55
32C8aa	1.50	2.013 ± 0.003	0.00463 ± 0.00021	0.000045 ± 0.000048	1.44	99.1		93	51.72 ± 0.75
32C8bb	1.50	2.021 ± 0.004	0.00618 ± 0.00024	0.000007 ± 0.000037	1.22	99.7		70	52.20 ± 0.60
32C8cc	1.50	2.018 ± 0.003	0.00385 ± 0.00026	0.000047 ± 0.000040	1.61	99.1		112	51.82 ± 0.62
32C8dd	1.50	2.011 ± 0.004	0.00440 ± 0.00028	0.000022 ± 0.000048	1.07	99.5		98	51.84 ± 0.74
32C8ee	1.50	2.016 ± 0.004	0.00598 ± 0.00030	0.000051 ± 0.000051	0.90	99.0		72	51.75 ± 0.79
32C8ff	1.50	2.016 ± 0.004	0.00565 ± 0.00032	0.000030 ± 0.000035	1.22	99.4		76	51.91 ± 0.58
32C8gg	1.50	2.015 ± 0.004	0.00576 ± 0.00020	0.000050 ± 0.000024	1.75	99.1		75	51.73 ± 0.41
32C8hh	1.50	2.016 ± 0.004	0.00741 ± 0.00023	0.000039 ± 0.000026	1.77	99.2		58	51.85 ± 0.44
32C8ii	1.50	2.007 ± 0.003	0.00598 ± 0.00022	0.000026 ± 0.000020	2.38	99.4		72	51.71 ± 0.33
32C8jj	1.50	2.027 ± 0.003	0.00424 ± 0.00039	0.000009 ± 0.000067	0.90	99.7		101	52.34 ± 1.03
32C8kk	1.50	2.020 ± 0.003	0.00469 ± 0.00038	0.000056 ± 0.000051	1.23	99.0		92	51.82 ± 0.78
32C8ll	1.50	2.008 ± 0.003	0.00488 ± 0.00017	0.000021 ± 0.000034	1.33	99.5		88	51.76 ± 0.53
32C8mm	1.50	2.011 ± 0.003	0.00534 ± 0.00025	0.000063 ± 0.000033	1.53	98.9		81	51.52 ± 0.52
32C8nn	1.50	2.025 ± 0.003	0.00592 ± 0.00024	0.000064 ± 0.000029	1.94	98.9		73	51.87 ± 0.47
32C8oo	1.50	2.027 ± 0.003	0.00345 ± 0.00017	0.000036 ± 0.000031	1.66	99.3		125	52.13 ± 0.49

Table DR3. Complete $^{40}Ar/^{39}Ar$ results

Sample Experiment	laser power (W)	$^{40}Ar/^{39}Ar$	$^{37}Ar/^{39}Ar$	$^{36}Ar/^{39}Ar$	$^{40}Ar^*$ X10^{-14} mol	$^{40}Ar^*$ %	$^{39}Ar_K$ %	K/Ca	Apparent Age ± 2σ Ma
Scheggs tuff WP-3 sanidine continued									
32C8pp	1.50	2.016 ± 0.004	0.00617 ± 0.00023	0.000072 ± 0.000040	1.10	98.7		70	51.58 ± 0.63
32C8qq	1.50	2.021 ± 0.003	0.00510 ± 0.00020	0.000033 ± 0.000041	1.59	99.3		84	52.00 ± 0.63
32C8rr	1.50	2.017 ± 0.003	0.00391 ± 0.00018	0.000026 ± 0.000041	1.37	99.4		110	51.95 ± 0.63
32C8ss	1.50	2.017 ± 0.003	0.00604 ± 0.00040	0.000029 ± 0.000047	0.88	99.4		71	51.95 ± 0.73
32C8tt	1.50	2.014 ± 0.004	0.00559 ± 0.00039	0.000062 ± 0.000053	0.98	98.9		77	51.61 ± 0.82
Multi-crystal fusion ages									
Inverse isochron age ± 2σ		51.57 ± 0.29						Integrated age ± 2σ	51.90 ± 0.09
$^{40}Ar/^{39}Ar$ intercept ± 2σ		562.1 ± 318.8		MSWD 0.42				Weighted mean age ± 2σ	51.90 ± 0.09
Single crystal fusions									
32C8z	1.50	2.012 ± 0.016	0.00630 ± 0.00170	0.000016 ± 0.000347	0.15	99.6		68	51.89 ± 5.31
32C8aa	1.50	2.021 ± 0.017	0.00329 ± 0.00136	0.000001 ± 0.000281	0.18	99.8		131	52.25 ± 4.33
32C8bb	1.50	2.052 ± 0.016	0.00452 ± 0.00172	0.000002 ± 0.000364	0.15	99.8		95	53.05 ± 5.55
32C8cc	1.50	2.050 ± 0.019	0.00546 ± 0.00205	0.000215 ± 0.000393	0.13	96.7		79	51.37 ± 6.02
32C8dd	1.50	2.046 ± 0.017	0.00677 ± 0.00150	0.000076 ± 0.000297	0.17	98.7		64	52.33 ± 4.56
32C8ee	1.50	2.076 ± 0.031	0.00478 ± 0.00288	0.000173 ± 0.000600	0.08	97.3		90	52.35 ± 9.19
32C8ff	1.50	2.065 ± 0.011	0.00340 ± 0.00087	0.000166 ± 0.000178	0.29	97.4		126	52.12 ± 2.74
32C8gg	1.50	2.051 ± 0.013	0.00392 ± 0.00126	0.000146 ± 0.000216	0.19	97.7		110	51.93 ± 3.34
32C8hh	1.50	2.083 ± 0.019	0.00883 ± 0.00178	0.000541 ± 0.000368	0.15	92.1		49	49.76 ± 5.64
32C8ii	1.50	2.044 ± 0.017	0.00198 ± 0.00142	0.000331 ± 0.000333	0.16	95.0		217	50.34 ± 5.12
32C8jj	1.50	2.037 ± 0.011	0.00427 ± 0.00082	0.000200 ± 0.000136	0.32	96.9		101	51.15 ± 2.13
32C8kk	1.50	2.040 ± 0.016	0.00399 ± 0.00211	0.000147 ± 0.000342	0.16	97.7		108	51.64 ± 5.22
32C8ll	1.50	2.063 ± 0.021	0.00219 ± 0.00242	0.000104 ± 0.000354	0.11	98.3		197	52.54 ± 5.44
32C8mm	1.50	2.048 ± 0.015	0.00441 ± 0.00104	0.000036 ± 0.000212	0.21	99.3		97	52.69 ± 3.29
32C8nn	1.50	2.009 ± 0.016	0.00361 ± 0.00130	0.000067 ± 0.000248	0.17	98.8		119	51.45 ± 3.83
32C8oo	1.50	2.114 ± 0.016	0.00377 ± 0.00141	0.000427 ± 0.000264	0.17	93.8		114	51.40 ± 4.07
32C8pp	1.50	2.026 ± 0.016	0.00114 ± 0.00145	0.000195 ± 0.000215	0.18	96.9		376	50.91 ± 3.35
32C8qq	1.50	2.037 ± 0.018	0.00134 ± 0.00173	0.000038 ± 0.000304	0.14	99.2		320	52.37 ± 4.68
32C8rr	1.50	2.086 ± 0.016	0.00357 ± 0.00111	0.000200 ± 0.000178	0.22	97.0		120	52.41 ± 2.80
32C8ss	1.50	2.070 ± 0.023	0.00328 ± 0.00214	0.000167 ± 0.000428	0.13	97.4		131	52.25 ± 6.56
32C8tt	1.50	2.058 ± 0.022	0.00447 ± 0.00210	0.000195 ± 0.000317	0.14	97.0		96	51.73 ± 4.92
Single crystal fusion ages									
Inverse isochron age ± 2σ		51.52 ± 1.80						Integrated age ± 2σ	51.79 ± 0.94
$^{40}Ar/^{39}Ar$ intercept ± 2σ		356.1 ± 584.6		MSWD 0.13				Weighted mean age ± 2σ	51.77 ± 0.87
Combined fusion ages									
Inverse isochron age ± 2σ		51.63 ± 0.24						Integrated age ± 2σ	51.89 ± 0.10
$^{40}Ar/^{39}Ar$ intercept ± 2σ		507.9 ± 248.3		MSWD 0.34				Weighted mean age ± 2σ	**51.90 ± 0.09**
Rife tuff BT-18 biotite J = 0.014710 ± 0.16% μ = 1.0025									
3 crystal fusions									
11F2a	1.50	2.982 ± 0.008	0.00038 ± 0.00064	0.003427 ± 0.000073	2.04	65.9		1131	51.41 ± 1.16
* 11F2b	1.50	2.621 ± 0.007	0.00058 ± 0.00097	0.002043 ± 0.000031	1.35	76.8		744	52.64 ± 0.56
11F2c	1.50	2.556 ± 0.007	0.00026 ± 0.00045	0.001947 ± 0.000097	0.86	77.3		1628	51.68 ± 1.51
11F2d	1.50	2.516 ± 0.007	0.00036 ± 0.00061	0.001874 ± 0.000042	1.31	77.8		1198	51.21 ± 0.72
* 11F2e	1.50	2.553 ± 0.004	0.00044 ± 0.00080	0.001789 ± 0.000095	1.18	79.1		968	52.83 ± 1.46
11F2f	1.50	2.488 ± 0.008	0.00047 ± 0.00084	0.001881 ± 0.000069	2.24	77.5		920	50.44 ± 1.12
* 11F2g	1.50	2.183 ± 0.005	0.00036 ± 0.00064	0.000422 ± 0.000057	1.35	94.1		1207	53.69 ± 0.91
* 11F2h	1.50	2.647 ± 0.008	0.00045 ± 0.00081	0.002054 ± 0.000063	1.50	76.9		953	53.22 ± 1.02
* 11F2i	1.50	2.607 ± 0.008	0.00047 ± 0.00085	0.001889 ± 0.000071	1.57	78.4		914	53.45 ± 1.16
11F2j	1.50	2.922 ± 0.010	0.00046 ± 0.00083	0.003290 ± 0.000066	1.78	66.6		935	50.89 ± 1.09
11F2k	1.50	2.974 ± 0.010	0.00080 ± 0.00144	0.003516 ± 0.000104	1.61	64.9		538	50.52 ± 1.62
* 11F2l	1.50	2.329 ± 0.008	0.00038 ± 0.00068	0.001047 ± 0.000057	1.30	86.5		1129	52.69 ± 0.95
* 11F2m	1.50	2.903 ± 0.005	0.00071 ± 0.00129	0.002689 ± 0.000130	1.16	72.5		606	54.99 ± 1.99
11F2n	1.50	2.376 ± 0.007	0.00062 ± 0.00113	0.001457 ± 0.000091	1.31	81.7		694	50.79 ± 1.43
11F2o	1.50	3.112 ± 0.009	0.00072 ± 0.00131	0.003959 ± 0.000131	1.08	62.3		599	50.70 ± 2.04
11F2p	1.50	2.546 ± 0.009	0.00071 ± 0.00130	0.001866 ± 0.000141	0.90	78.2		602	52.05 ± 2.20
11F2q	1.50	2.359 ± 0.006	0.00033 ± 0.00060	0.001301 ± 0.000028	2.43	83.5		1312	51.53 ± 0.53
11F2r	1.50	2.398 ± 0.005	0.00074 ± 0.00135	0.001542 ± 0.000102	1.16	80.8		581	50.69 ± 1.58

Table DR3. Complete $^{40}Ar/^{39}Ar$ results

Sample Experiment	laser power (W)	$^{40}Ar/^{39}Ar$	$^{37}Ar/^{39}Ar$	$^{36}Ar/^{39}Ar$	$^{40}Ar^*$ X10^{-14} mol	$^{40}Ar^*$ %	$^{39}Ar_K$ %	K/Ca	Apparent Age ± 2σ Ma
Rife tuff BT-18 biotite continued									
* 11F2s	1.50	2.577 ± 0.005	0.00077 ± 0.00141	0.001866 ± 0.000056	1.34	78.4		562	52.86 ± 0.89
* 11F2t	1.50	2.987 ± 0.011	0.00038 ± 0.00070	0.003257 ± 0.000068	1.58	67.6		1142	52.81 ± 1.14
* 11F2u	1.50	2.234 ± 0.006	0.00034 ± 0.00062	0.000683 ± 0.000030	2.20	90.8		1282	53.01 ± 0.55
Single crystal fusions									
11F2v	1.50	3.605 ± 0.009	0.00060 ± 0.00112	0.005500 ± 0.000114	0.90	54.8		712	51.67 ± 1.77
* 11F2w	1.50	2.364 ± 0.008	0.00030 ± 0.00056	0.001040 ± 0.000070	1.02	86.8		1425	53.66 ± 1.14
11F2x	1.50	2.409 ± 0.006	0.00035 ± 0.00064	0.001440 ± 0.000097	0.80	82.1		1245	51.77 ± 1.52
J = 0.014563 ± 0.10% μ = 1.0035									
* 32C9ba	1.50	2.553 ± 0.019	0.00481 ± 0.00076	0.001546 ± 0.000139	0.43	81.9		89	54.15 ± 2.29
* 32C9bb	1.50	2.752 ± 0.015	0.01371 ± 0.00077	0.002353 ± 0.000089	0.58	74.6		31	53.16 ± 1.54
* 32C9bc	1.50	3.891 ± 0.025	0.07071 ± 0.00176	0.005467 ± 0.000117	0.55	58.5		6	58.84 ± 2.04
* 32C9bd	1.50	2.878 ± 0.020	0.06129 ± 0.00144	0.002478 ± 0.000144	0.50	74.6		7	55.51 ± 2.36
32C9be	1.50	2.140 ± 0.009	0.01067 ± 0.00044	0.000416 ± 0.000070	0.76	94.1		40	52.12 ± 1.15
* 32C9bf	1.50	2.434 ± 0.014	0.03470 ± 0.00106	0.001198 ± 0.000132	0.54	85.4		12	53.79 ± 2.10
Fusion ages									
Inverse isochron age ± 2σ		51.58 ± 0.62				Integrated age ± 2σ			52.28 ± 0.24
$^{40}Ar/^{39}Ar$ intercept ± 2σ		290.1 ± 10.7		MSWD 0.68		Weighted mean age ± 2σ			**51.30 ± 0.30**
						(includes integrated age for UW32C9bg)			
Multi-crystal incremental heating experiments									
* UW32C9bg: 3 crystals									
* 32C9bg1	0.16	3.182 ± 0.005	0.01224 ± 0.00047	0.004562 ± 0.000106	1.06	57.5	48.3	35	47.47 ± 1.62
32C9bg2	0.26	2.422 ± 0.010	0.01270 ± 0.00070	0.000931 ± 0.000182	0.48	88.5	28.9	34	55.45 ± 2.78
32C9bg3	0.39	2.142 ± 0.015	0.03942 ± 0.00178	0.000330 ± 0.000240	0.22	95.4	15.1	11	52.88 ± 3.69
32C9bg4	0.52	2.357 ± 0.019	0.02093 ± 0.00148	0.000361 ± 0.000661	0.10	95.3	6.3	21	58.09 ± 9.99
32C9bg5	1.50	2.505 ± 0.055	0.01397 ± 0.00964	0.001567 ± 0.002810	0.03	81.4	1.4	31	52.76 ± 42.45
Inverse isochron age ± 2σ		51.65 ± 8.44				Integrated age ± 2σ			51.34 ± 1.52
$^{40}Ar/^{39}Ar$ intercept ± 2σ		466.8 ± 469.6		MSWD 0.58		Plateau age ± 2σ			54.68 ± 2.16
UW32C9bh: 3 crystals									
32C9bh1	0.16	2.512 ± 0.027	0.01334 ± 0.00168	0.001336 ± 0.000365	0.14	84.1	8.2	32	54.69 ± 5.66
32C9bh2	0.26	2.132 ± 0.010	0.00655 ± 0.00055	0.000301 ± 0.000110	0.40	95.6	26.9	66	52.79 ± 1.74
32C9bh3	0.39	2.071 ± 0.009	0.02378 ± 0.00076	0.000136 ± 0.000098	0.38	97.9	26.8	18	52.50 ± 1.54
32C9bh4	1.50	2.065 ± 0.007	0.00292 ± 0.00038	0.000134 ± 0.000104	0.54	97.9	38.1	147	52.34 ± 1.61
Inverse isochron age ± 2σ		52.18 ± 1.67				Integrated age ± 2σ			52.70 ± 0.99
$^{40}Ar/^{39}Ar$ intercept ± 2σ		371.4 ± 225.1		MSWD 0.24		Plateau age ± 2σ			52.59 ± 0.93
UW32C9bi: 3 crystals									
32C9bi1	0.16	3.761 ± 0.014	0.02155 ± 0.00102	0.006089 ± 0.000156	0.62	52.1	29.0	20	50.73 ± 2.42
32C9bi2	0.26	2.300 ± 0.010	0.02491 ± 0.00086	0.000731 ± 0.000097	0.44	90.5	33.5	17	53.88 ± 1.53
32C9bi3	0.39	2.184 ± 0.017	0.18560 ± 0.00361	0.000435 ± 0.000202	0.22	94.6	17.7	2	53.47 ± 3.17
32C9bi4	1.50	2.146 ± 0.014	0.07121 ± 0.00189	0.000150 ± 0.000210	0.24	98.0	19.7	6	54.43 ± 3.24
Inverse isochron age ± 2σ		54.23 ± 1.32				Integrated age ± 2σ			53.00 ± 1.22
$^{40}Ar/^{39}Ar$ intercept ± 2σ		273.0 ± 18.0		MSWD 1.85		Plateau age ± 2σ			53.22 ± 1.53
UW32C9bj: 3 crystals									
32C9bj1	0.16	3.138 ± 0.018	0.01244 ± 0.00087	0.003559 ± 0.000225	0.36	66.4	18.7	35	53.90 ± 3.50
32C9bj2	0.26	2.149 ± 0.009	0.01520 ± 0.00089	0.000275 ± 0.000116	0.41	96.1	31.5	28	53.45 ± 1.82
32C9bj3	0.39	2.099 ± 0.008	0.05009 ± 0.00108	0.000222 ± 0.000134	0.40	96.8	31.1	9	52.63 ± 2.06
32C9bj4	1.50	2.106 ± 0.018	0.01041 ± 0.00109	0.000024 ± 0.000238	0.24	99.5	18.7	41	54.23 ± 3.71
Inverse isochron age ± 2σ		53.17 ± 1.42				Integrated age ± 2σ			53.42 ± 1.28
$^{40}Ar/^{39}Ar$ intercept ± 2σ		303.9 ± 44.9		MSWD 0.27		Plateau age ± 2σ			53.30 ± 1.20

Table DR3. Complete $^{40}Ar/^{39}Ar$ results

Sample Experiment	laser power (W)	$^{40}Ar/^{39}Ar$	$^{37}Ar/^{39}Ar$	$^{36}Ar/^{39}Ar$	$^{40}Ar^*$ X10^{-14} mol	$^{40}Ar^*$ %	$^{39}Ar_K$ %	K/Ca	Apparent Age ± 2σ Ma
Rife tuff BT-18 biotite continued									
UW32C9bk: 3 crystals									
32C9bk1	0.16	2.635 ± 0.008	0.03117 ± 0.00111	0.001929 ± 0.000169	0.62	78.3	33.7	14	53.40 ± 2.57
32C9bk2	0.26	2.200 ± 0.009	0.03003 ± 0.00069	0.000416 ± 0.000097	0.48	94.3	31.3	14	53.70 ± 1.52
32C9bk3	0.39	2.099 ± 0.011	0.09785 ± 0.00161	0.000075 ± 0.000120	0.39	99.1	26.6	4	53.83 ± 1.89
32C9bk4	1.50	2.185 ± 0.022	0.02431 ± 0.00260	0.000191 ± 0.000342	0.13	97.3	8.4	18	55.00 ± 5.27
Inverse isochron age ± 2σ		53.87 ± 1.34					Integrated age ± 2σ		53.74 ± 1.20
$^{40}Ar/^{39}Ar$ intercept ± 2σ		285.9 ± 62.7		MSWD 0.10			Plateau age ± 2σ		53.74 ± 1.06
* UW32C9bl: 10 crystals									
* 32C9bl1	0.16	2.708 ± 0.004	0.02176 ± 0.00045	0.002454 ± 0.000041	1.72	73.1	30.9	20	51.29 ± 0.64
32C9bl2	0.26	2.155 ± 0.004	0.01861 ± 0.00039	0.000295 ± 0.000039	1.47	95.8	33.2	23	53.44 ± 0.63
32C9bl3	0.39	2.091 ± 0.003	0.04232 ± 0.00066	0.000175 ± 0.000041	1.20	97.5	27.9	10	52.77 ± 0.64
32C9bl4	1.50	2.172 ± 0.013	0.01748 ± 0.00070	0.000248 ± 0.000145	0.36	96.5	8.0	25	54.24 ± 2.27
Inverse isochron age ± 2σ		51.74 ± 2.98					Integrated age ± 2σ		52.66 ± 0.39
$^{40}Ar/^{39}Ar$ intercept ± 2σ		539.0 ± 506.4		MSWD 1.58			Plateau age ± 2σ		53.16 ± 0.56
* UW32C9bm: 10 crystals									
* 32C9bm1	0.16	3.171 ± 0.006	0.02116 ± 0.00038	0.004152 ± 0.000032	2.86	61.2	39.4	20	50.28 ± 0.53
* 32C9bm2	0.26	2.318 ± 0.004	0.02184 ± 0.00041	0.000628 ± 0.000038	1.62	91.9	30.6	20	55.11 ± 0.61
* 32C9bm3	0.39	2.115 ± 0.004	0.06457 ± 0.00106	0.000256 ± 0.000044	1.09	96.4	22.6	7	52.80 ± 0.69
* 32C9bm4	1.50	2.297 ± 0.014	0.05183 ± 0.00131	0.000514 ± 0.000153	0.39	93.4	7.4	8	55.48 ± 2.41
No isochron							Integrated age ± 2σ		52.71 ± 0.37
* UW32C9bn: 10 crystals									
* 32C9bn1	0.16	3.703 ± 0.006	0.02194 ± 0.00039	0.006008 ± 0.000074	2.03	52.0	24.6	20	49.87 ± 1.13
* 32C9bn2	0.26	2.220 ± 0.004	0.02070 ± 0.00048	0.000381 ± 0.000040	1.60	94.8	32.3	21	54.46 ± 0.63
32C9bn3	0.39	2.096 ± 0.003	0.05223 ± 0.00080	0.000158 ± 0.000038	1.60	97.8	34.3	8	53.05 ± 0.59
32C9bn4	1.50	2.129 ± 0.013	0.01214 ± 0.00083	0.000157 ± 0.000111	0.42	97.7	8.8	35	53.81 ± 1.79
No isochron							Integrated age ± 2σ		52.79 ± 0.43
				MSWD 0.65			Plateau age ± 2σ		53.12 ± 0.57
Combined multi-crystal incremental heating ages									
Inverse isochron age ± 2σ		53.35 ± 0.58					Integrated age ± 2σ		52.76 ± 0.25
$^{40}Ar/^{39}Ar$ intercept ± 2σ		285.5 ± 14.9		MSWD 0.92			Weighted mean: plateau ages ± 2σ		53.15 ± 0.53
Firehole tuff FC-2 sanidine J = 0.022282 ± 0.24% μ = 1.0035									
10-20 crystal fusions									
6-7a	1.50	1.345 ± 0.027	0.00209 ± 0.00110	0.000237 ± 0.000230	0.10	94.7		206	50.50 ± 5.73
6-7b	1.50	1.327 ± 0.058	0.00288 ± 0.00197	0.000082 ± 0.000875	0.05	98.1		149	51.59 ± 20.70
6-7c	1.50	1.303 ± 0.007	0.00771 ± 0.00054	0.000013 ± 0.000140	0.16	99.6		56	51.44 ± 3.28
6-7d	1.50	1.340 ± 0.015	0.00598 ± 0.00161	0.000037 ± 0.000468	0.06	99.1		72	52.61 ± 10.88
6-7e	1.50	1.605 ± 0.008	0.00567 ± 0.00070	0.001011 ± 0.000165	0.27	81.3		76	51.71 ± 3.85
5-20 crystal fusions J = 0.014629 ± 0.15% μ = 1.0025									
11G12a	1.50	7.716 ± 0.033	0.00014 ± 0.00016	0.019617 ± 0.000560	0.77	24.8		3050	49.84 ± 8.49
11G12b	1.50	6.734 ± 0.016	0.00010 ± 0.00012	0.016056 ± 0.000160	3.18	29.5		4192	51.64 ± 2.42
11G12c	1.50	9.625 ± 0.027	0.00010 ± 0.00012	0.025634 ± 0.000304	2.21	21.3		4305	53.19 ± 4.61
11G12d	1.50	5.042 ± 0.008	0.00008 ± 0.00009	0.010363 ± 0.000154	1.43	39.2		5376	51.38 ± 2.33
11G12e	1.50	18.077 ± 0.031	0.00024 ± 0.00027	0.054620 ± 0.000279	4.88	10.7		1828	50.29 ± 4.20
11G12f	1.50	5.270 ± 0.014	0.00011 ± 0.00013	0.011430 ± 0.000128	1.21	35.8		3892	49.15 ± 1.94
11G12g	1.50	2.043 ± 0.005	0.00010 ± 0.00013	0.000372 ± 0.000035	0.59	94.4		4444	50.20 ± 0.60
11G12h	1.50	2.020 ± 0.003	0.00011 ± 0.00015	0.000230 ± 0.000031	2.21	96.4		3748	50.66 ± 0.51
11G12i	1.50	2.091 ± 0.005	0.00015 ± 0.00020	0.000461 ± 0.000028	1.03	93.3		2870	50.74 ± 0.50
11G12j	1.50	2.120 ± 0.006	0.00016 ± 0.00022	0.000459 ± 0.000064	0.53	93.4		2639	51.50 ± 1.01
11G12k	1.50	2.054 ± 0.003	0.00010 ± 0.00013	0.000352 ± 0.000027	2.14	94.7		4495	50.63 ± 0.45
11G12l	1.50	2.041 ± 0.003	0.00012 ± 0.00016	0.000309 ± 0.000023	2.77	95.3		3682	50.61 ± 0.39
11G12m	1.50	2.028 ± 0.003	0.00011 ± 0.00014	0.000266 ± 0.000018	2.60	95.9		4032	50.60 ± 0.32

Table DR3. Complete $^{40}Ar/^{39}Ar$ results

Sample Experiment	laser power (W)	$^{40}Ar/^{39}Ar$	$^{37}Ar/^{39}Ar$	$^{36}Ar/^{39}Ar$	$^{40}Ar^*$ X10^{-14} mol	$^{40}Ar^*$ %	$^{39}Ar_K$ %	K/Ca	Apparent Age ± 2σ Ma
Firehole tuff FC-2 sanidine continued									
11G12n	1.50	2.076 ± 0.003	0.00013 ± 0.00017	0.000405 ± 0.000009	3.00	94.0		3414	50.79 ± 0.23
15 crystal 2 step fusions J = 0.014503 ± 0.10% μ = 1.0035									
32C2a1	0.16	2.093 ± 0.009	0.00609 ± 0.00050	0.000406 ± 0.000081	0.46	94.1	34.8	71	50.80 ± 1.29
32C2a2	1.50	2.013 ± 0.005	0.00569 ± 0.00023	0.000081 ± 0.000051	0.84	98.6	65.2	76	51.20 ± 0.80
32C2b1	0.16	2.094 ± 0.011	0.00545 ± 0.00086	0.000508 ± 0.000194	0.33	92.6	23.8	79	50.05 ± 2.97
32C2b2	1.50	2.019 ± 0.003	0.00577 ± 0.00027	0.000090 ± 0.000057	1.02	98.5	76.2	75	51.30 ± 0.88
32C2c1	0.16	2.083 ± 0.009	0.00577 ± 0.00056	0.000349 ± 0.000116	0.46	94.9	30.5	75	50.97 ± 1.80
32C2c2	1.50	2.007 ± 0.003	0.00570 ± 0.00029	0.000051 ± 0.000046	1.01	99.0	69.5	75	51.27 ± 0.71
32C2d1	0.16	2.050 ± 0.010	0.00609 ± 0.00063	0.000314 ± 0.000156	0.38	95.3	44.3	71	50.39 ± 2.40
32C2d2	1.50	2.068 ± 0.011	0.00554 ± 0.00056	0.000202 ± 0.000117	0.48	96.9	55.7	78	51.68 ± 1.84
32C2e1	0.16	2.033 ± 0.004	0.00622 ± 0.00029	0.000162 ± 0.000038	1.09	97.4	71.5	69	51.10 ± 0.60
32C2e2	1.50	2.028 ± 0.008	0.00531 ± 0.00038	0.000039 ± 0.000159	0.43	99.2	28.5	81	51.89 ± 2.42
32C2f1	0.16	2.051 ± 0.004	0.00755 ± 0.00032	0.000165 ± 0.000067	0.77	97.4	40.2	57	51.54 ± 1.03
32C2f2	1.50	2.021 ± 0.003	0.00604 ± 0.00020	0.000110 ± 0.000054	1.13	98.2	59.8	71	51.18 ± 0.83
32C2g1	0.16	2.035 ± 0.006	0.00611 ± 0.00040	0.000167 ± 0.000091	0.62	97.4	53.9	70	51.12 ± 1.40
32C2g2	1.50	2.040 ± 0.009	0.00585 ± 0.00054	0.000159 ± 0.000073	0.53	97.5	46.1	74	51.29 ± 1.20
32C2h1	0.16	2.040 ± 0.007	0.00632 ± 0.00039	0.000197 ± 0.000096	0.51	96.9	40.5	68	51.00 ± 1.49
32C2h2	1.50	2.011 ± 0.006	0.00572 ± 0.00036	0.000084 ± 0.000052	0.74	98.6	59.5	75	51.12 ± 0.84
32C2i1	0.16	2.070 ± 0.009	0.00542 ± 0.00065	0.000200 ± 0.000138	0.45	96.9	28.7	79	51.75 ± 2.12
32C2i2	1.50	2.004 ± 0.004	0.00573 ± 0.00024	0.000063 ± 0.000046	1.08	98.9	71.3	75	51.11 ± 0.72
32C2j1	0.16	2.092 ± 0.014	0.00758 ± 0.00094	0.000328 ± 0.000132	0.27	95.2	20.9	57	51.35 ± 2.10
32C2j2	1.50	2.033 ± 0.004	0.00636 ± 0.00026	0.000137 ± 0.000043	1.01	97.8	79.1	68	51.30 ± 0.67
32C2k1	0.16	2.077 ± 0.009	0.00616 ± 0.00069	0.000287 ± 0.000122	0.36	95.7	21.8	70	51.28 ± 1.90
32C2k2	1.50	2.001 ± 0.003	0.00560 ± 0.00029	0.000093 ± 0.000041	1.23	98.4	78.2	77	50.82 ± 0.63
Multi-crystal fusion ages									
Inverse isochron age ± 2σ		50.83 ± 0.13					Integrated age ± 2σ		50.96 ± 0.20
$^{40}Ar/^{39}Ar$ intercept ± 2σ		295.3 ± 2.3		MSWD 0.94			Weighted mean age ± 2σ		**50.83 ± 0.13**
Boar tuff BT-14 sanidine J = 0.014664 ± 0.22% μ = 1.0022									
10 crystal fusions									
* 11G1a	1.50	1.984 ± 0.005	0.00015 ± 0.00060	0.000066 ± 0.000016	2.33	98.8		2846	51.12 ± 0.34
11G1b	1.50	1.991 ± 0.003	0.00059 ± 0.00245	0.000242 ± 0.000057	1.00	96.2		731	49.96 ± 0.89
11G1c	1.50	1.981 ± 0.004	0.00015 ± 0.00065	0.000109 ± 0.000041	1.39	98.1		2847	50.71 ± 0.65
11G1d	1.50	1.990 ± 0.004	0.00010 ± 0.00047	0.000147 ± 0.000026	1.76	97.6		4117	50.65 ± 0.44
11G1e	1.50	1.999 ± 0.003	0.00010 ± 0.00045	0.000221 ± 0.000033	1.55	96.5		4398	50.32 ± 0.53
11G1f	1.50	1.998 ± 0.003	0.00015 ± 0.00071	0.000134 ± 0.000062	1.23	97.8		2812	50.95 ± 0.95
11G1g	1.50	2.026 ± 0.003	0.00024 ± 0.00105	0.000362 ± 0.000067	1.08	94.5		1825	49.95 ± 1.03
* 11G1h	1.50	2.022 ± 0.003	0.00022 ± 0.00098	0.000162 ± 0.000042	1.30	97.4		1922	51.37 ± 0.65
11G1i	1.50	1.992 ± 0.005	0.00007 ± 0.00080	0.000164 ± 0.000115	0.61	97.3		6457	50.59 ± 1.76
11G1j	1.50	1.992 ± 0.003	0.00059 ± 0.00242	0.000143 ± 0.000027	2.05	97.6		734	50.74 ± 0.44
* 11G1k	1.50	1.922 ± 0.003	0.00004 ± 0.00053	0.000202 ± 0.000061	0.84	96.7		10968	48.49 ± 0.94
* 11G1l	1.50	1.976 ± 0.003	0.00010 ± 0.00048	0.000019 ± 0.000031	1.72	99.5		4303	51.27 ± 0.50
11G1m	1.50	1.997 ± 0.003	0.00009 ± 0.00046	0.000128 ± 0.000043	1.43	97.9		4970	50.97 ± 0.68
11G1n	1.50	1.986 ± 0.003	0.00028 ± 0.00119	0.000131 ± 0.000035	1.60	97.8		1528	50.66 ± 0.56
Inverse isochron age ± 2σ		51.09 ± 0.41					Integrated age ± 2σ		50.67 ± 0.21
$^{40}Ar/^{39}Ar$ intercept ± 2σ		179.3 ± 104.5		MSWD 0.80			Weighted mean age ± 2σ		**50.61 ± 0.23**
6th tuff TR-5 sanidine J = 0.010632 ± 0.17% μ = 1.0065									
Single crystal fusions									
53F4a	1.50	2.671 ± 0.018	0.00671 ± 0.00122	0.000183 ± 0.000269	0.33	97.9		64	49.49 ± 3.04
53F4b	1.50	2.660 ± 0.014	0.00406 ± 0.00051	0.000099 ± 0.000121	0.68	98.9		106	49.74 ± 1.42
53F4c	1.50	2.683 ± 0.017	0.00587 ± 0.00146	0.000192 ± 0.000402	0.21	97.8		73	49.66 ± 4.48
53F4d	1.50	2.646 ± 0.013	0.00432 ± 0.00112	0.000202 ± 0.000284	0.29	97.7		100	48.90 ± 3.17
53F4e	1.50	2.641 ± 0.014	0.00385 ± 0.00128	0.000333 ± 0.000304	0.24	96.2		112	48.09 ± 3.40
53F4f	1.50	2.723 ± 0.013	0.00595 ± 0.00098	0.000146 ± 0.000311	0.31	98.4		72	50.66 ± 3.46
53F4g	1.50	2.700 ± 0.011	0.00477 ± 0.00182	0.000375 ± 0.000339	0.19	95.8		90	48.97 ± 3.76
53F4h	1.50	2.667 ± 0.013	0.00231 ± 0.00176	0.000373 ± 0.000414	0.21	95.8		186	48.37 ± 4.59

Table DR3. Complete $^{40}Ar/^{39}Ar$ results

Sample Experiment	laser power (W)	$^{40}Ar/^{39}Ar$	$^{37}Ar/^{39}Ar$	$^{36}Ar/^{39}Ar$	$^{40}Ar^*$ X10^{-14} mol	$^{40}Ar^*$ %	$^{39}Ar_K$ %	K/Ca	Apparent Age ± 2σ Ma
6th tuff TR-5 sanidine continued									
53F4i	1.50	2.686 ± 0.014	0.00467 ± 0.00100	0.000298 ± 0.000310	0.30	96.7		92	49.13 ± 3.46
53F4j	1.50	2.697 ± 0.013	0.00317 ± 0.00143	0.000231 ± 0.000411	0.22	97.4		136	49.70 ± 4.55
53F4k	1.50	2.641 ± 0.017	0.00319 ± 0.00156	0.000203 ± 0.000428	0.19	97.7		135	48.82 ± 4.77
53F4l	1.50	2.668 ± 0.016	0.00313 ± 0.00170	0.000184 ± 0.000452	0.22	97.9		138	49.43 ± 5.02
53F4m	1.50	2.824 ± 0.016	0.00516 ± 0.00199	0.000611 ± 0.000582	0.16	93.6		83	49.98 ± 6.44
53F4n	1.50	2.765 ± 0.017	0.00420 ± 0.00205	0.000461 ± 0.000456	0.19	95.0		102	49.71 ± 5.07
53F4o	1.50	2.667 ± 0.020	0.01412 ± 0.00279	0.000355 ± 0.000641	0.15	96.0		30	48.47 ± 7.11
* 53F4p	1.50	4.180 ± 0.023	0.00023 ± 0.00188	0.000071 ± 0.000384	0.29	99.5		1886	78.03 ± 4.25
53F4q	1.50	2.645 ± 0.016	0.00361 ± 0.00178	0.000285 ± 0.000573	0.17	96.8		119	48.43 ± 6.35
53F4r	1.50	2.667 ± 0.015	0.00426 ± 0.00087	0.000081 ± 0.000168	0.40	99.1		101	49.97 ± 1.94
53F4s	1.50	2.684 ± 0.022	0.00616 ± 0.00215	0.000272 ± 0.000447	0.15	97.0		70	49.24 ± 4.99
53F4t	1.50	2.671 ± 0.008	0.00548 ± 0.00108	0.000073 ± 0.000221	0.29	99.1		78	50.09 ± 2.46
53F4u	1.50	2.756 ± 0.018	0.00191 ± 0.00208	0.000433 ± 0.000766	0.16	95.3		225	49.69 ± 8.47
* 53F4v	1.50	4.101 ± 0.024	0.00209 ± 0.00195	0.000297 ± 0.000495	0.24	97.8		205	75.34 ± 5.45
53F4w	1.50	2.658 ± 0.013	0.00512 ± 0.00124	0.000039 ± 0.000293	0.24	99.5		84	50.05 ± 3.27
* 53F4x	1.50	4.100 ± 0.021	0.00286 ± 0.00175	0.000155 ± 0.000341	0.29	98.8		150	76.10 ± 3.78
53F4y	1.50	2.733 ± 0.017	0.01197 ± 0.00168	0.000143 ± 0.000670	0.15	98.4		36	50.88 ± 7.42
53F4z	1.50	2.701 ± 0.015	0.00661 ± 0.00162	0.000118 ± 0.000654	0.16	98.7		65	50.41 ± 7.23
53F4aa	1.50	2.668 ± 0.012	0.00222 ± 0.00134	0.000142 ± 0.000355	0.20	98.4		194	49.65 ± 3.95
53F4bb	1.50	2.808 ± 0.013	0.00365 ± 0.00141	0.000523 ± 0.000530	0.21	94.4		118	50.16 ± 5.87
53F4cc	1.50	2.807 ± 0.022	0.00255 ± 0.00338	0.000560 ± 0.000712	0.12	94.1		169	49.95 ± 7.89
53F4dd	1.50	2.731 ± 0.019	0.00477 ± 0.00191	0.000148 ± 0.000426	0.18	98.4		90	50.80 ± 4.75
53F4ee	1.50	2.689 ± 0.016	0.00256 ± 0.00189	0.000254 ± 0.000714	0.16	97.2		168	49.43 ± 7.90
53F4ff	1.50	2.780 ± 0.026	0.00337 ± 0.00239	0.000426 ± 0.000763	0.13	95.4		128	50.18 ± 8.46
53F4gg	1.50	2.676 ± 0.020	0.00006 ± 0.00208	0.000011 ± 0.000596	0.16	99.8		7516	50.53 ± 6.61
53F4hh	1.50	2.744 ± 0.014	0.00262 ± 0.00192	0.000125 ± 0.000603	0.13	98.6		164	51.17 ± 6.66
53F4ii	1.50	2.712 ± 0.016	0.00258 ± 0.00166	0.000067 ± 0.000612	0.16	99.2		167	50.88 ± 6.77
53F4jj	1.50	2.719 ± 0.014	0.00495 ± 0.00143	0.000227 ± 0.000430	0.22	97.5		87	50.13 ± 4.77
53F4kk	1.50	2.791 ± 0.013	0.00382 ± 0.00184	0.000505 ± 0.000528	0.15	94.6		112	49.94 ± 5.84
53F4ll	1.50	2.671 ± 0.018	0.00671 ± 0.00122	0.000183 ± 0.000269	0.33	97.9		64	49.49 ± 3.04
53F4mm	1.50	2.660 ± 0.014	0.00406 ± 0.00051	0.000099 ± 0.000121	0.68	98.9		106	49.74 ± 1.42
53F4nn	1.50	2.683 ± 0.017	0.00587 ± 0.00146	0.000192 ± 0.000402	0.21	97.8		73	49.66 ± 4.48
Single crystal fusion ages									
Inverse isochron age ± 2σ		49.21 ± 1.48						Integrated age ± 2σ	51.26 ± 0.67
$^{40}Ar/^{39}Ar$ intercept ± 2σ		449.9 ± 613.6		MSWD 0.10				Weighted mean age ± 2σ	49.68 ± 0.59
5 crystal fusions									
53F4oo	1.50	2.640 ± 0.006	0.00381 ± 0.00021	0.000101 ± 0.000081	0.90	98.8		113	49.36 ± 0.92
53F4pp	1.50	2.663 ± 0.011	0.00334 ± 0.00050	0.000104 ± 0.000166	0.54	98.8		129	49.77 ± 1.87
53F4qq	1.50	2.655 ± 0.008	0.00384 ± 0.00038	0.000018 ± 0.000116	0.72	99.7		112	50.09 ± 1.32
* 53F4rr	1.50	2.816 ± 0.005	0.00340 ± 0.00030	0.000130 ± 0.000123	1.09	98.6		127	52.49 ± 1.37
* 53F4ss	1.50	2.837 ± 0.006	0.00608 ± 0.00038	0.000043 ± 0.000093	0.86	99.5		71	53.36 ± 1.05
J = 0.014660 ± 0.18% μ = 1.0025									
* 11F9a	1.50	2.612 ± 0.015	0.00003 ± 0.00006	0.000470 ± 0.000102	0.44	94.5		13111	64.14 ± 1.71
11F9b	1.50	2.348 ± 0.022	0.00021 ± 0.00032	0.001559 ± 0.000344	0.17	80.2		2014	49.12 ± 5.35
* 11F9c	1.50	8.198 ± 0.037	0.00067 ± 0.00099	0.005996 ± 0.000306	0.51	78.3		641	162.31 ± 4.63
* 11F9d	1.50	5.055 ± 0.032	0.00007 ± 0.00036	0.006972 ± 0.000830	0.12	59.2		6603	77.41 ± 12.49
* 11F9e	1.50	3.065 ± 0.030	0.00011 ± 0.00017	0.001312 ± 0.000194	0.27	87.2		3883	69.33 ± 3.29
* 11F9f	1.50	4.580 ± 0.013	0.00010 ± 0.00015	0.008006 ± 0.000332	0.86	48.2		4277	57.51 ± 5.03
11F9g	1.50	3.626 ± 0.057	0.00003 ± 0.00016	0.007330 ± 0.001551	0.08	40.1		16656	38.08 ± 23.87
* 11F9h	1.50	226.013 ± 3.638	0.00209 ± 0.00378	0.680216 ± 0.020623	0.60	11.1		206	563.4 ± 201.9
* 11F9i	1.50	6.057 ± 0.020	0.00008 ± 0.00013	0.011030 ± 0.000485	0.66	46.1		5268	72.40 ± 7.29
11F9j	1.50	3.674 ± 0.029	0.00009 ± 0.00014	0.006424 ± 0.000524	0.27	48.2		4937	46.23 ± 8.07
* 11F9k	1.50	4.713 ± 0.010	0.00008 ± 0.00012	0.006181 ± 0.000192	0.75	61.1		5661	74.65 ± 2.90
* 11F9l	1.50	2.641 ± 0.014	0.00022 ± 0.00032	0.000634 ± 0.000029	0.35	92.7		1999	63.63 ± 0.80
* 11F9m	1.50	3.028 ± 0.012	0.00008 ± 0.00013	0.001866 ± 0.000112	0.43	81.6		5062	64.22 ± 1.77
* 11F9n	1.50	3.079 ± 0.012	0.00004 ± 0.00007	0.001089 ± 0.000117	0.47	89.4		10412	71.37 ± 1.85
* 11F9o	1.50	3.039 ± 0.012	0.00005 ± 0.00008	0.000517 ± 0.000289	0.29	94.8		8653	74.64 ± 4.38
11F9p	1.50	7.254 ± 0.031	0.00018 ± 0.00027	0.018333 ± 0.000505	0.48	25.3		2434	47.81 ± 7.67
* 11F9q	1.50	6.224 ± 0.013	0.00013 ± 0.00019	0.013610 ± 0.000080	1.53	35.3		3420	57.20 ± 1.19

Table DR3. Complete $^{40}Ar/^{39}Ar$ results

Sample Experiment	laser power (W)	$^{40}Ar/^{39}Ar$	$^{37}Ar/^{39}Ar$	$^{36}Ar/^{39}Ar$	$^{40}Ar^*$ X10^{-14} mol	$^{40}Ar^*$ %	$^{39}Ar_K$ %	K/Ca	Apparent Age ± 2σ Ma
6th tuff TR-5 sanidine continued									
11F9r	1.50	2.005 ± 0.019	0.00012 ± 0.00018	0.000487 ± 0.000191	0.20	92.6		3641	48.43 ± 3.06
11F9s	1.50	2.338 ± 0.011	0.00012 ± 0.00019	0.001361 ± 0.000078	0.40	82.6		3470	50.36 ± 1.29
* 11F9t	1.50	2.601 ± 0.006	0.00004 ± 0.00006	0.000347 ± 0.000067	0.72	95.9		11261	64.79 ± 1.06
* 11F9u	1.50	2.465 ± 0.015	0.00014 ± 0.00021	0.000914 ± 0.000054	0.37	88.9		3152	57.01 ± 1.09
11F9v	1.50	2.018 ± 0.012	0.00016 ± 0.00025	0.000380 ± 0.000213	0.26	94.2		2631	49.59 ± 3.31
11F9w	1.50	1.953 ± 0.014	0.00011 ± 0.00017	0.000237 ± 0.000266	0.18	96.2		3975	49.00 ± 4.11
* 11F9x	1.50	2.168 ± 0.007	0.00019 ± 0.00028	0.000175 ± 0.000063	0.43	97.4		2300	55.01 ± 1.02
* 11F9y	1.50	10.275 ± 0.018	0.00009 ± 0.00013	0.025541 ± 0.000237	3.01	26.5		5038	70.62 ± 3.54
Multi-crystal fusion ages									
Inverse isochron age ± 2σ		49.71 ± 0.61					Integrated age ± 2σ		58.74 ± 0.52
$^{40}Ar/^{39}Ar$ intercept ± 2σ		292.8 ± 14.7		MSWD 0.47			Weighted mean age ± 2σ		49.68 ± 0.59
Combined fusion ages									
Inverse isochron age ± 2σ		49.69 ± 0.43					Integrated age ± 2σ		55.22 ± 0.42
$^{40}Ar/^{39}Ar$ intercept ± 2σ		293.1 ± 14.4		MSWD 0.18			Weighted mean age ± 2σ		**49.68 ± 0.42**
Analcite tuff SB-1 sanidine *J* = 0.014374 ± 0.24% μ = 1.0035									
Single crystal fusions									
5B2a	1.50	2.113 ± 0.119	0.02512 ± 0.00049	0.000547 ± 0.000399	0.44	92.2		17	49.85 ± 8.45
5B2b	1.50	1.934 ± 0.100	0.01293 ± 0.00031	0.000106 ± 0.000313	0.48	98.2		33	48.58 ± 6.89
5B2c	1.50	1.973 ± 0.063	0.01514 ± 0.00045	0.000240 ± 0.000178	0.78	96.2		28	48.58 ± 4.16
5B2d	1.50	2.012 ± 0.030	0.01468 ± 0.00022	0.000389 ± 0.000078	1.71	94.1		29	48.45 ± 1.91
5B2e	1.50	1.981 ± 0.095	0.01865 ± 0.00028	0.000217 ± 0.000272	0.52	96.6		23	48.96 ± 6.29
5B2f	1.50	1.925 ± 0.005	0.01302 ± 0.00045	0.000543 ± 0.000224	0.46	91.5		33	45.11 ± 3.35
5B2g	1.50	2.059 ± 0.003	0.01282 ± 0.00037	0.000769 ± 0.000212	0.53	88.8		34	46.80 ± 3.17
5B2h	1.50	1.992 ± 0.006	0.01865 ± 0.00024	0.000206 ± 0.000078	1.62	96.8		23	49.32 ± 1.21
5B2i	1.50	2.587 ± 0.007	0.01301 ± 0.00085	0.002186 ± 0.000252	0.39	74.9		33	49.55 ± 3.77
5B2j	1.50	1.981 ± 0.007	0.01264 ± 0.00042	0.000012 ± 0.000192	0.53	99.6		34	50.48 ± 2.88
5B2k	1.50	1.940 ± 0.006	0.01845 ± 0.00047	0.000171 ± 0.000253	0.48	97.2		23	48.27 ± 3.79
5B2l	1.50	1.983 ± 0.007	0.01366 ± 0.00024	0.000096 ± 0.000111	0.88	98.4		31	49.90 ± 1.69
5B2m	1.50	1.973 ± 0.010	0.01815 ± 0.00093	0.000571 ± 0.000742	0.19	91.3		24	46.10 ± 11.10
5B2n	1.50	1.907 ± 0.010	0.01425 ± 0.00090	0.000448 ± 0.000584	0.24	92.9		30	45.36 ± 8.74
5B2o	1.50	1.906 ± 0.008	0.01546 ± 0.00023	0.000143 ± 0.000266	0.39	97.6		28	47.60 ± 3.99
5B2p	1.50	1.949 ± 0.004	0.01651 ± 0.00037	0.000212 ± 0.000181	0.76	96.6		26	48.18 ± 2.72
5B2q	1.50	1.901 ± 0.006	0.01440 ± 0.00028	0.000294 ± 0.000271	0.43	95.2		30	46.36 ± 4.07
5B2r	1.50	1.987 ± 0.005	0.02141 ± 0.00030	0.000184 ± 0.000176	0.83	97.1		20	49.35 ± 2.64
5B2s	1.50	1.903 ± 0.007	0.02749 ± 0.00068	0.000360 ± 0.000292	0.36	94.3		16	45.93 ± 4.38
5B2t	1.50	2.012 ± 0.004	0.01440 ± 0.00028	0.000200 ± 0.000166	0.66	96.9		30	49.87 ± 2.48
5B2u	1.50	2.000 ± 0.005	0.05487 ± 0.00046	0.000279 ± 0.000080	1.77	95.9		8	49.05 ± 1.22
Single crystal fusion ages									
Inverse isochron age ± 2σ		48.61 ± 0.84					Integrated age ± 2σ		48.57 ± 0.73
$^{40}Ar/^{39}Ar$ intercept ± 2σ		331.5 ± 87.9		MSWD 0.82			Weighted mean age ± 2σ		48.87 ± 0.57
10-15 crystal fusions *J* = 0.022235 ± 0.24% μ = 1.0035									
6-10a	1.50	1.282 ± 0.005	0.02026 ± 0.00020	0.000148 ± 0.000007	6.19	96.6		21	49.02 ± 0.45
6-10b	1.50	1.261 ± 0.003	0.01585 ± 0.00018	0.000078 ± 0.000011	4.30	98.1		27	48.95 ± 0.37
6-10c	1.50	1.256 ± 0.007	0.01789 ± 0.00022	0.000054 ± 0.000010	3.42	98.7		24	49.04 ± 0.62
6-10d	1.50	1.247 ± 0.004	0.01568 ± 0.00016	0.000041 ± 0.000008	4.30	99.0		27	48.85 ± 0.40
6-10e	1.50	1.286 ± 0.006	0.01873 ± 0.00021	0.000139 ± 0.000007	6.19	96.8		23	49.25 ± 0.50
6-10f	1.50	1.279 ± 0.005	0.02542 ± 0.00021	0.000155 ± 0.000008	7.71	96.5		17	48.82 ± 0.44
6-10g	1.50	1.262 ± 0.003	0.01696 ± 0.00014	0.000086 ± 0.000005	6.86	98.0		25	48.94 ± 0.27
6-10h	1.50	1.258 ± 0.004	0.01826 ± 0.00016	0.000050 ± 0.000006	7.26	98.8		24	49.19 ± 0.39
6-10i	1.50	1.272 ± 0.005	0.02063 ± 0.00020	0.000086 ± 0.000009	5.24	98.0		21	49.34 ± 0.48
6-10j	1.50	1.275 ± 0.005	0.02321 ± 0.00024	0.000124 ± 0.000013	3.10	97.1		19	49.01 ± 0.49
J = 0.014549 ± 0.19% μ = 1.0025									
11G10a	1.50	1.918 ± 0.003	0.00026 ± 0.00035	0.000058 ± 0.000027	1.43	98.9		1636	49.09 ± 0.42
11G10b	1.50	1.913 ± 0.005	0.00035 ± 0.00047	0.000149 ± 0.000085	0.79	97.5		1222	48.28 ± 1.30
11G10c	1.50	1.929 ± 0.003	0.00029 ± 0.00038	0.000118 ± 0.000007	3.66	97.9		1501	48.92 ± 0.18

Table DR3. Complete $^{40}Ar/^{39}Ar$ results

Sample Experiment	laser power (W)	$^{40}Ar/^{39}Ar$	$^{37}Ar/^{39}Ar$	$^{36}Ar/^{39}Ar$	$^{40}Ar^*$ X10^{-14} mol	$^{40}Ar^*$ %	$^{39}Ar_K$ %	K/Ca	Apparent Age ± 2σ Ma
Analcite tuff SB-1 sanidine continued									
11G10d	1.50	1.915 ± 0.003	0.00030 ± 0.00041	0.000095 ± 0.000018	3.38	98.3		1418	48.73 ± 0.32
11G10e	1.50	1.939 ± 0.003	0.00032 ± 0.00043	0.000148 ± 0.000008	3.41	97.5		1331	48.94 ± 0.21
11G10f	1.50	1.917 ± 0.002	0.00036 ± 0.00048	0.000070 ± 0.000025	2.49	98.7		1211	48.99 ± 0.39
11G10g	1.50	1.934 ± 0.003	0.00083 ± 0.00111	0.000145 ± 0.000016	3.82	97.6		518	48.85 ± 0.28
11G10h	1.50	1.927 ± 0.003	0.00029 ± 0.00040	0.000088 ± 0.000018	3.15	98.4		1458	49.11 ± 0.30
11G10i	1.50	1.961 ± 0.003	0.00034 ± 0.00045	0.000239 ± 0.000009	4.58	96.2		1270	48.83 ± 0.22
Multi-crystal fusion ages									
Inverse isochron age ± 2σ		49.00 ± 0.22						Integrated age ± 2σ	48.99 ± 0.14
$^{40}Ar/^{39}Ar$ intercept ± 2σ		281.9 ± 52.3		MSWD 0.71				Weighted mean age ± 2σ	48.95 ± 0.12
Combined fusion ages									
Inverse isochron age ± 2σ		48.95 ± 0.19						Integrated age ± 2σ	48.93 ± 0.16
$^{40}Ar/^{39}Ar$ intercept ± 2σ		297.5 ± 42.7		MSWD 0.75				Weighted mean age ± 2σ	**48.95 ± 0.12**
Sand Butte tuff SB-3 feldspar *J* = 0.014354 ± 0.24% μ = 1.0030									
5 crystal fusions									
5B3a	1.50	1.920 ± 0.015	0.01378 ± 0.00032	0.000043 ± 0.000235	0.38	99.1		31	48.64 ± 1.79
5B3b	1.50	1.959 ± 0.007	0.01532 ± 0.00039	0.000123 ± 0.000061	0.59	98.0		28	49.02 ± 0.48
5B3c	1.50	1.930 ± 0.004	0.02695 ± 0.00031	0.000075 ± 0.000286	0.38	98.7		16	48.68 ± 2.13
10-15 crystal fusions *J* = 0.022235 ± 0.24% μ = 1.0035									
6-11a	1.50	1.333 ± 0.008	4.88269 ± 0.04526	0.001920 ± 0.000240	0.14	86.4		0.09	45.79 ± 2.80
6-11b	1.50	1.442 ± 0.009	4.92080 ± 0.04527	0.001942 ± 0.000231	0.19	87.2		0.09	49.92 ± 2.69
6-11c	1.50	1.457 ± 0.007	4.62700 ± 0.03810	0.002328 ± 0.000316	0.17	77.9		0.09	45.10 ± 3.68
6-11d	1.50	1.374 ± 0.008	1.87225 ± 0.01717	0.000937 ± 0.000046	0.50	90.6		0.23	49.29 ± 0.60
6-11e	1.50	1.466 ± 0.004	4.49390 ± 0.03549	0.001999 ± 0.000057	0.77	84.0		0.10	48.85 ± 0.69
6-11f	1.50	1.552 ± 0.007	4.60696 ± 0.04264	0.002330 ± 0.000053	0.86	79.1		0.09	48.73 ± 0.67
Multi crystal fusion ages									
Inverse isochron age ± 2σ		49.05 ± 0.45						Integrated age ± 2σ	48.65 ± 0.43
$^{40}Ar/^{39}Ar$ intercept ± 2σ		290.3 ± 18.5		MSWD 0.38				Weighted mean age ± 2σ	48.94 ± 0.29
Antelope Creek sand AC-3 sanidine and orthoclase *J* = 0.014660 ± 0.12% μ = 1.0025									
Single crystal fusions									
11F3a	1.50	1.880 ± 0.003	0.00015 ± 0.00028	0.000032 ± 0.000055	0.92	99.2		2830	48.67 ± 0.85
11F3b	1.50	1.885 ± 0.008	0.00067 ± 0.00125	0.000096 ± 0.000181	0.52	98.3		638	48.33 ± 2.78
11F3c	1.50	1.870 ± 0.006	0.00026 ± 0.00049	0.000031 ± 0.000125	0.43	99.3		1633	48.44 ± 1.93
11F3d	1.50	1.893 ± 0.010	0.00040 ± 0.00075	0.000105 ± 0.000058	0.60	98.1		1065	48.45 ± 1.02
11F3e	1.50	1.923 ± 0.010	0.00099 ± 0.00184	0.000069 ± 0.000151	0.36	98.7		436	49.51 ± 2.36
11F3f	1.50	1.873 ± 0.007	0.00033 ± 0.00063	0.000095 ± 0.000163	0.32	98.2		1288	48.02 ± 2.51
* 11F3g	1.50	54.262 ± 0.076	0.00001 ± 0.00004	0.000622 ± 0.000043	32.82	99.7		28839	1053.10 ± 2.27
11F3h	1.50	1.870 ± 0.005	0.00091 ± 0.00198	0.000043 ± 0.000080	0.46	99.1		470	48.34 ± 1.26
11F3i	1.50	1.888 ± 0.007	0.00066 ± 0.00143	0.000061 ± 0.000108	0.42	98.8		649	48.68 ± 1.68
11F3j	1.50	1.880 ± 0.005	0.00045 ± 0.00097	0.000021 ± 0.000049	0.67	99.4		961	48.77 ± 0.80
11F3k	1.50	1.873 ± 0.004	0.00018 ± 0.00040	0.000036 ± 0.000060	0.88	99.2		2325	48.49 ± 0.93
* 11F3l	1.50	62.587 ± 0.096	0.00001 ± 0.00003	0.000459 ± 0.000028	45.98	99.8		49546	1172.58 ± 2.65
11F3m	1.50	1.872 ± 0.011	0.00025 ± 0.00054	0.000031 ± 0.000119	0.59	99.3		1716	48.47 ± 1.89
11F3n	1.50	1.875 ± 0.005	0.00079 ± 0.00172	0.000076 ± 0.000123	0.35	98.6		542	48.23 ± 1.88
* 11F3o	1.50	59.058 ± 0.094	0.00003 ± 0.00006	0.000607 ± 0.000024	36.62	99.7		15268	1122.57 ± 2.66
11F3p	1.50	1.868 ± 0.005	0.00015 ± 0.00033	0.000084 ± 0.000108	0.48	98.4		2853	47.98 ± 1.67
11F3q	1.50	1.867 ± 0.007	0.00034 ± 0.00074	0.000135 ± 0.000165	0.37	97.6		1278	47.57 ± 2.54
11F3r	1.50	1.898 ± 0.005	0.00018 ± 0.00040	0.000054 ± 0.000049	0.55	98.9		2366	48.97 ± 0.79
11F3s	1.50	1.879 ± 0.004	0.00013 ± 0.00029	0.000101 ± 0.000062	0.61	98.2		3278	48.14 ± 0.96
11F3t	1.50	1.875 ± 0.004	0.00031 ± 0.00067	0.000039 ± 0.000043	0.69	99.1		1400	48.51 ± 0.68
11F3u	1.50	1.886 ± 0.007	0.00072 ± 0.00156	0.000047 ± 0.000141	0.43	99.0		598	48.73 ± 2.17
11F3v	1.50	1.907 ± 0.005	0.00041 ± 0.00089	0.000020 ± 0.000092	0.39	99.5		1049	49.48 ± 1.42
11F3w	1.50	1.881 ± 0.003	0.00068 ± 0.00149	0.000030 ± 0.000041	0.69	99.3		628	48.73 ± 0.64
11F3x	1.50	1.919 ± 0.007	0.00006 ± 0.00014	0.000080 ± 0.000036	0.93	98.5		6690	49.32 ± 0.65
11F3y	1.50	1.893 ± 0.012	0.00010 ± 0.00021	0.000212 ± 0.000103	0.43	96.5		4488	47.66 ± 1.69

Table DR3. Complete $^{40}Ar/^{39}Ar$ results

Sample Experiment	laser power (W)	$^{40}Ar/^{39}Ar$	$^{37}Ar/^{39}Ar$	$^{36}Ar/^{39}Ar$	$^{40}Ar^*$ X10^{-14} mol	$^{40}Ar^*$ %	$^{39}Ar_K$ %	K/Ca	Apparent Age ± 2σ Ma
Antelope Creek sand AC-3 sanidine and orthoclase continued									
11F3z	1.50	1.861 ± 0.007	0.00086 ± 0.00189	0.000102 ± 0.000138	0.41	98.1		500	47.67 ± 2.14
11F3aa	1.50	1.874 ± 0.010	0.00039 ± 0.00087	0.000104 ± 0.000194	0.34	98.1		1093	48.00 ± 3.00
11F3bb	1.50	1.862 ± 0.010	0.00029 ± 0.00065	0.000023 ± 0.000126	0.36	99.4		1468	48.29 ± 1.98
11F3cc	1.50	1.879 ± 0.004	0.00008 ± 0.00019	0.000000 ± 0.000134	0.59	99.8		5149	48.91 ± 2.05
11F3dd	1.50	1.892 ± 0.004	0.00069 ± 0.00153	0.000032 ± 0.000112	0.69	99.3		619	49.00 ± 1.72
11F3ee	1.50	1.886 ± 0.014	0.00061 ± 0.00135	0.000032 ± 0.000148	0.33	99.3		704	48.84 ± 2.36
11F3ff	1.50	1.924 ± 0.005	0.00056 ± 0.00197	0.000103 ± 0.000066	0.42	98.2		773	49.28 ± 1.03
11F3gg	1.50	1.933 ± 0.007	0.00065 ± 0.00229	0.000185 ± 0.000127	0.36	96.9		664	48.90 ± 1.97
11F3hh	1.50	2.558 ± 0.007	0.00080 ± 0.00282	0.002451 ± 0.000144	0.38	71.5		538	47.74 ± 2.21
* 11F3ii	1.50	2.588 ± 0.003	0.00060 ± 0.00211	0.000602 ± 0.000069	0.82	93.0		716	62.53 ± 1.05
* 11F3jj	1.50	3.070 ± 0.005	0.00040 ± 0.00141	0.000464 ± 0.000052	1.45	95.4		1072	75.84 ± 0.82
11F3kk	1.50	2.183 ± 0.015	0.00101 ± 0.00359	0.000918 ± 0.000271	0.21	87.4		427	49.74 ± 4.18
* 11F3ll	1.50	2.127 ± 0.005	0.00049 ± 0.00175	0.000466 ± 0.000096	0.55	93.3		869	51.75 ± 1.48
11F3mm	1.50	1.908 ± 0.007	0.00110 ± 0.00394	0.000061 ± 0.000267	0.19	98.8		390	49.20 ± 4.08
11F3nn	1.50	1.868 ± 0.006	0.00067 ± 0.00241	0.000086 ± 0.000147	0.30	98.4		638	47.95 ± 2.26
11F3oo	1.50	1.902 ± 0.005	0.00058 ± 0.00209	0.000123 ± 0.000133	0.30	97.8		736	48.57 ± 2.04
11F3pp	1.50	1.892 ± 0.007	0.00051 ± 0.00183	0.000007 ± 0.000099	0.35	99.7		835	49.19 ± 1.55
11F3qq	1.50	1.926 ± 0.009	0.00027 ± 0.00106	0.000243 ± 0.000138	0.29	96.0		1589	48.28 ± 2.15
* 11F3rr	1.50	1.958 ± 0.003	0.00016 ± 0.00059	0.000075 ± 0.000046	0.95	98.6		2653	50.37 ± 0.71
11F3ss	1.50	1.947 ± 0.006	0.00050 ± 0.00177	0.000186 ± 0.000177	0.41	96.9		866	49.24 ± 2.71
* 11F3tt	1.50	75.158 ± 0.114	0.00075 ± 0.00263	0.000203 ± 0.000045	42.64	99.9		573	1339.26 ± 2.90
11F3uu	1.50	1.958 ± 0.015	0.00114 ± 0.00406	0.000368 ± 0.000193	0.17	94.2		376	48.14 ± 3.03
11F3vv	1.50	1.906 ± 0.010	0.00095 ± 0.00340	0.000153 ± 0.000180	0.28	97.4		452	48.43 ± 2.78
11F3ww	1.50	1.897 ± 0.008	0.00093 ± 0.00330	0.000067 ± 0.000143	0.33	98.7		462	48.85 ± 2.21
* 11F3xx	1.50	3.015 ± 0.006	0.00002 ± 0.00024	0.000268 ± 0.000076	0.73	97.2		28146	75.90 ± 1.18
11F3yy	1.50	1.900 ± 0.006	0.00103 ± 0.00364	0.000135 ± 0.000095	0.37	97.7		417	48.41 ± 1.48
11F3zz	1.50	1.891 ± 0.004	0.00020 ± 0.00074	0.000006 ± 0.000074	0.56	99.7		2126	49.18 ± 1.14
* 11F3aaa	1.50	2.398 ± 0.006	0.00010 ± 0.00043	0.000097 ± 0.000110	0.53	98.6		4298	61.47 ± 1.68
* 11F3bbb	1.50	39.612 ± 0.052	0.00008 ± 0.00033	0.000020 ± 0.000062	14.49	100.0		5433	825.86 ± 1.85
11F3ccc	1.50	1.921 ± 0.007	0.00001 ± 0.00050	0.000286 ± 0.000144	0.30	95.4		38798	47.82 ± 2.22
11F3ddd	1.50	2.077 ± 0.007	0.00042 ± 0.00157	0.000812 ± 0.000144	0.41	88.2		1013	47.83 ± 2.21
11F3eee	1.50	1.979 ± 0.004	0.00088 ± 0.00314	0.000340 ± 0.000064	0.63	94.7		487	48.90 ± 0.99
11F3fff	1.50	1.977 ± 0.008	0.00009 ± 0.00057	0.000356 ± 0.000153	0.25	94.4		4851	48.72 ± 2.36
11F3ggg	1.50	1.923 ± 0.006	0.00005 ± 0.00039	0.000176 ± 0.000107	0.45	97.1		8896	48.71 ± 1.66
11F3hhh	1.50	1.905 ± 0.004	0.00056 ± 0.00199	0.000143 ± 0.000071	0.61	97.5		772	48.50 ± 1.09
11F3iii	1.50	1.875 ± 0.008	0.00010 ± 0.00052	0.000023 ± 0.000124	0.37	99.4		4203	48.62 ± 1.93
11F3jjj	1.50	1.880 ± 0.011	0.00093 ± 0.00334	0.000018 ± 0.000136	0.32	99.5		461	48.79 ± 2.14
11F3kkk	1.50	1.919 ± 0.006	0.00032 ± 0.00120	0.000082 ± 0.000181	0.37	98.5		1333	49.32 ± 2.77
11F3lll	1.50	1.902 ± 0.013	0.00026 ± 0.00109	0.000071 ± 0.000388	0.25	98.7		1667	48.97 ± 5.95
11F3mmm	1.50	1.912 ± 0.006	0.00015 ± 0.00058	0.000093 ± 0.000094	0.60	98.3		2930	49.05 ± 1.46
11F3nnn	1.50	1.889 ± 0.004	0.00080 ± 0.00288	0.000052 ± 0.000141	0.36	98.9		535	48.77 ± 2.15
* 11F3ooo	1.50	2.836 ± 0.005	0.00014 ± 0.00053	0.000611 ± 0.000059	0.92	93.5		3110	68.78 ± 0.92
11F3ppp	1.50	1.947 ± 0.013	0.00015 ± 0.00086	0.000306 ± 0.000307	0.23	95.1		2893	48.33 ± 4.71
11F3qqq	1.50	1.907 ± 0.012	0.00053 ± 0.00202	0.000141 ± 0.000210	0.27	97.6		814	48.55 ± 3.25
* 11F3rrr	1.50	88.200 ± 0.074	0.00002 ± 0.00028	0.000134 ± 0.000085	29.57	99.9		17229	1496.64 ± 1.79
11F3sss	1.50	1.893 ± 0.006	0.00050 ± 0.00188	0.000172 ± 0.000179	0.30	97.1		861	47.97 ± 2.74
* 11F3ttt	1.50	2.332 ± 0.007	0.00409 ± 0.01494	0.002162 ± 0.000198	0.38	72.4		105	44.13 ± 3.04
* 11F3uuu	1.50	1.988 ± 0.003	0.00038 ± 0.00144	0.000121 ± 0.000096	0.55	98.0		1117	50.78 ± 1.47
11F3vvv	1.50	1.904 ± 0.004	0.00081 ± 0.00299	0.000245 ± 0.000220	0.29	96.0		530	47.69 ± 3.35
* 11F3www	1.50	2.617 ± 0.003	0.00008 ± 0.00040	0.000014 ± 0.000104	0.78	99.7		5576	67.69 ± 1.58
* 11F3xxx	1.50	31.770 ± 0.057	0.00050 ± 0.00188	0.000564 ± 0.000154	6.50	99.5		853	686.72 ± 2.63
11F3yyy	1.50	1.919 ± 0.010	0.00079 ± 0.00298	0.000019 ± 0.000297	0.18	99.5		542	49.80 ± 4.54
11F3zzz	1.50	1.905 ± 0.008	0.00005 ± 0.00068	0.000028 ± 0.000290	0.22	99.3		9360	49.35 ± 4.42
11F3aaaa	1.50	1.980 ± 0.007	0.00084 ± 0.00314	0.000427 ± 0.000259	0.21	93.4		511	48.27 ± 3.96
* 11F3bbbb	1.50	69.257 ± 0.061	0.00004 ± 0.00032	0.000272 ± 0.000097	27.37	99.9		10573	1263.13 ± 1.76
* 11F3cccc	1.50	83.190 ± 0.117	0.00061 ± 0.00228	0.000030 ± 0.000100	25.89	100.0		708	1438.25 ± 2.87
* 11F3dddd	1.50	59.161 ± 0.085	0.00007 ± 0.00029	0.000675 ± 0.000063	30.53	99.7		6614	1123.74 ± 2.45

Single crystal fusion ages

Inverse isochron age ± 2σ	48.70 ± 0.21			Integrated age ± 2σ	360.51 ± 0.45
$^{40}Ar/^{39}Ar$ intercept ± 2σ	292.8 ± 32.7	MSWD	0.35	Weighted mean age ± 2σ	**48.70 ± 0.19**

Table DR3. Complete $^{40}Ar/^{39}Ar$ results

Sample Experiment	laser power (W)	$^{40}Ar/^{39}Ar$	$^{37}Ar/^{39}Ar$	$^{36}Ar/^{39}Ar$	$^{40}Ar^*$ X10^{-14} mol	$^{40}Ar^*$ %	$^{39}Ar_K$ %	K/Ca	Apparent Age ± 2σ Ma
Continental tuff CP-1 biotite *J* = 0.014651 ± 0.10% μ = 1.0035									
Single crystal incremental heating experiments									
* UW32B5ba: 1 crystal									
* 32B5ba1	0.16	2.682 ± 0.126	0.01351 ± 0.00448	0.005943 ± 0.000992	0.08	34.4	5.1	32	24.22 ± 16.62
32B5ba2	0.26	1.976 ± 0.032	0.00400 ± 0.00121	0.000250 ± 0.000225	0.23	96.0	20.7	107	49.47 ± 3.79
32B5ba3	0.36	1.889 ± 0.023	0.00610 ± 0.00081	0.000088 ± 0.000197	0.31	98.4	29.0	70	48.49 ± 3.23
32B5ba4	0.45	1.969 ± 0.028	0.01348 ± 0.00087	0.000314 ± 0.000189	0.28	95.1	25.0	32	48.82 ± 3.22
32B5ba5	0.58	1.918 ± 0.049	0.00030 ± 0.00131	0.000278 ± 0.000381	0.15	95.5	13.2	1456	47.75 ± 6.33
32B5ba6	1.50	2.129 ± 0.092	0.00037 ± 0.00332	0.001164 ± 0.000628	0.08	83.6	7.0	1153	46.45 ± 10.66
Inverse isochron age ± 2σ		48.77 ± 2.95				Integrated age ± 2σ			47.31 ± 2.02
$^{40}Ar/^{39}Ar$ intercept ± 2σ		285.3 ± 400.0		MSWD 0.11		Plateau age ± 2σ			48.71 ± 1.84
# UW32B5bb: 1 crystal									
32B5bb1	0.16	3.537 ± 0.022	0.00617 ± 0.00185	0.005325 ± 0.000313	0.25	55.4	18.6	70	51.04 ± 4.86
32B5bb2	0.26	2.327 ± 0.013	0.00663 ± 0.00086	0.001355 ± 0.000180	0.25	82.6	28.4	65	50.10 ± 2.81
32B5bb3	0.32	2.310 ± 0.019	0.01144 ± 0.00254	0.000573 ± 0.000574	0.13	92.5	14.7	38	55.62 ± 8.74
32B5bb4	0.52	2.044 ± 0.017	0.01830 ± 0.00097	0.000161 ± 0.000263	0.23	97.5	29.8	23	51.94 ± 4.09
32B5bb5	1.50	2.314 ± 0.030	0.01233 ± 0.00252	0.000981 ± 0.000740	0.08	87.3	8.4	35	52.62 ± 11.34
Inverse isochron age ± 2σ		51.21 ± 2.77				Integrated age ± 2σ			51.85 ± 2.35
$^{40}Ar/^{39}Ar$ intercept ± 2σ		292.2 ± 45.1		MSWD 0.45		Plateau age ± 2σ			51.07 ± 2.00
UW32B5bc: 1 crystal									
32B5bc1	0.16	2.213 ± 0.023	0.01324 ± 0.00192	0.001958 ± 0.000806	0.09	73.7	10.1	32	42.60 ± 12.36
32B5bc2	0.26	2.028 ± 0.014	0.00933 ± 0.00118	0.000560 ± 0.000205	0.19	91.6	23.1	46	48.46 ± 3.20
32B5bc3	0.32	2.085 ± 0.020	0.01338 ± 0.00200	0.000861 ± 0.000357	0.13	87.6	15.6	32	47.64 ± 5.53
32B5bc4	0.52	1.944 ± 0.012	0.10148 ± 0.00263	0.000300 ± 0.000161	0.25	95.6	31.4	4	48.47 ± 2.53
32B5bc5	1.50	1.968 ± 0.015	0.04247 ± 0.00172	0.000078 ± 0.000628	0.16	98.8	19.8	10	50.65 ± 9.57
Inverse isochron age ± 2σ		49.38 ± 2.33				Integrated age ± 2σ			48.18 ± 2.66
$^{40}Ar/^{39}Ar$ intercept ± 2σ		206.4 ± 172.9		MSWD 0.29		Plateau age ± 2σ			48.33 ± 1.82
UW32B5bd: 1 crystal									
32B5bd1	0.16	3.140 ± 0.074	0.01366 ± 0.00929	0.004972 ± 0.001725	0.04	53.1	4.0	31	43.53 ± 26.53
32B5bd2	0.26	2.303 ± 0.023	0.01018 ± 0.00289	0.001467 ± 0.000716	0.10	81.0	12.0	42	48.64 ± 10.94
32B5bd3	0.32	2.053 ± 0.024	0.01312 ± 0.00257	0.000276 ± 0.000405	0.11	95.8	14.7	33	51.28 ± 6.26
32B5bd4	0.52	2.111 ± 0.018	0.03002 ± 0.00096	0.000944 ± 0.000213	0.23	86.7	29.3	14	47.72 ± 3.36
32B5bd5	1.50	2.113 ± 0.011	0.02406 ± 0.00077	0.000694 ± 0.000158	0.31	90.2	40.0	18	49.66 ± 2.45
Inverse isochron age ± 2σ		50.39 ± 3.40				Integrated age ± 2σ			48.96 ± 2.37
$^{40}Ar/^{39}Ar$ intercept ± 2σ		233.4 ± 165.7		MSWD 0.39		Plateau age ± 2σ			49.15 ± 1.86
UW32B5be: 1 crystal									
32B5be1	0.16	2.384 ± 0.018	0.00776 ± 0.00170	0.001960 ± 0.000344	0.16	75.5	8.5	55	46.99 ± 5.31
32B5be2	0.26	2.009 ± 0.011	0.00665 ± 0.00072	0.000368 ± 0.000231	0.25	94.4	15.9	65	49.43 ± 3.55
32B5be3	0.32	2.017 ± 0.013	0.00888 ± 0.00079	0.000511 ± 0.000226	0.26	92.3	16.9	48	48.57 ± 3.50
32B5be4	0.52	1.989 ± 0.007	0.04655 ± 0.00084	0.000494 ± 0.000198	0.48	92.6	31.3	9	48.04 ± 3.03
32B5be5	1.50	1.970 ± 0.007	0.01634 ± 0.00079	0.000297 ± 0.000116	0.41	95.4	27.4	26	48.99 ± 1.80
Inverse isochron age ± 2σ		49.23 ± 1.71				Integrated age ± 2σ			48.52 ± 1.42
$^{40}Ar/^{39}Ar$ intercept ± 2σ		251.4 ± 112.4		MSWD 0.22		Plateau age ± 2σ			48.70 ± 1.28
Combined single crystal incremental heating ages									
Inverse isochron age ± 2σ		48.80 ± 1.12				Integrated age ± 2σ			48.77 ± 0.92
$^{40}Ar/^{39}Ar$ intercept ± 2σ		312.6 ± 38.3		MSWD 1.70		Weighted mean: plateau ages ± 2σ			49.12 ± 1.08

Table DR3. Complete $^{40}Ar/^{39}Ar$ results

Sample Experiment	laser power (W)	$^{40}Ar/^{39}Ar$	$^{37}Ar/^{39}Ar$	$^{36}Ar/^{39}Ar$	$^{40}Ar^*$ X10^{-14} mol	$^{40}Ar^*$ %	$^{39}Ar_K$ %	K/Ca	Apparent Age ± 2σ Ma
Continental tuff CP-1 biotite continued									
Multi-crystal incremental heating experiments									
#* UW32B5bf: 3 crystals									
* 32B5bf1	0.16	2.589 ± 0.010	0.02497 ± 0.00065	0.003567 ± 0.000119	0.53	59.2	19.6	17	40.06 ± 1.85
32B5bf2	0.26	2.065 ± 0.005	0.01165 ± 0.00048	0.000781 ± 0.000071	0.75	88.6	35.1	37	47.75 ± 1.11
32B5bf3	0.32	2.008 ± 0.018	0.04885 ± 0.00120	0.000824 ± 0.000215	0.17	87.8	8.3	9	46.03 ± 3.39
32B5bf4	0.52	1.959 ± 0.007	0.03552 ± 0.00064	0.000225 ± 0.000067	0.66	96.5	32.6	12	49.30 ± 1.07
32B5bf5	1.50	2.613 ± 0.030	0.02382 ± 0.00218	0.002553 ± 0.000522	0.12	71.0	4.4	18	48.41 ± 8.05
Inverse isochron age ± 2σ		49.27 ± 1.58				Integrated age ± 2σ			46.64 ± 0.78
$^{40}Ar/^{39}Ar$ intercept ± 2σ		232.8 ± 102.6		MSWD 2.06		Plateau age ± 2σ			48.43 ± 1.07
* UW32B5bg: 3 crystals									
* 32B5bg1	0.16	3.572 ± 0.011	0.01534 ± 0.00060	0.006914 ± 0.000192	0.67	42.7	17.6	28	39.87 ± 2.96
32B5bg2	0.26	2.199 ± 0.005	0.01141 ± 0.00064	0.001116 ± 0.000076	0.68	84.8	29.0	38	48.64 ± 1.19
32B5bg3	0.32	2.094 ± 0.016	0.02820 ± 0.00123	0.000926 ± 0.000205	0.24	86.8	10.9	15	47.43 ± 3.21
32B5bg4	0.52	1.968 ± 0.004	0.05959 ± 0.00093	0.000301 ± 0.000060	0.75	95.5	35.6	7	49.00 ± 0.93
32B5bg5	1.50	2.049 ± 0.019	0.02835 ± 0.00207	0.000718 ± 0.000298	0.15	89.5	6.9	15	47.86 ± 4.64
Inverse isochron age ± 2σ		49.07 ± 1.24				Integrated age ± 2σ			47.04 ± 0.85
$^{40}Ar/^{39}Ar$ intercept ± 2σ		276.7 ± 65.9		MSWD 0.38		Plateau age ± 2σ			48.77 ± 0.71
UW32B5bh: 3 crystals									
32B5bh1	0.16	8.454 ± 0.061	0.02153 ± 0.00362	0.024898 ± 0.001246	0.21	12.9	3.1	20	28.68 ± 19.26
32B5bh2	0.26	3.208 ± 0.027	0.01274 ± 0.00146	0.004714 ± 0.000382	0.23	56.5	8.9	34	47.26 ± 5.92
32B5bh3	0.32	2.187 ± 0.015	0.01029 ± 0.00106	0.000869 ± 0.000214	0.21	88.1	11.9	42	50.22 ± 3.34
32B5bh4	0.52	2.064 ± 0.008	0.04118 ± 0.00097	0.000628 ± 0.000087	0.49	90.9	29.5	10	48.94 ± 1.38
32B5bh5	1.50	1.960 ± 0.007	0.04469 ± 0.00080	0.000293 ± 0.000066	0.73	95.5	46.6	10	48.83 ± 1.07
Inverse isochron age ± 2σ		49.25 ± 0.83				Integrated age ± 2σ			48.27 ± 1.09
$^{40}Ar/^{39}Ar$ intercept ± 2σ		270.1 ± 24.0		MSWD 1.35		Plateau age ± 2σ			48.88 ± 0.94
* UW32B5bi: 7 crystals									
* 32B5bi1	0.16	3.470 ± 0.009	0.01316 ± 0.00038	0.006404 ± 0.000108	1.33	45.4	13.3	33	41.14 ± 1.66
32B5bi2	0.26	2.220 ± 0.004	0.00872 ± 0.00025	0.001112 ± 0.000028	1.65	85.0	25.9	49	49.22 ± 0.46
32B5bi3	0.39	2.111 ± 0.004	0.03419 ± 0.00048	0.000785 ± 0.000027	1.56	88.9	25.8	13	48.94 ± 0.45
32B5bi4	0.52	1.953 ± 0.004	0.05000 ± 0.00071	0.000253 ± 0.000045	1.48	96.1	26.4	9	48.96 ± 0.71
32B5bi5	1.50	1.955 ± 0.012	0.00941 ± 0.00052	0.000174 ± 0.000103	0.49	97.2	8.7	46	49.53 ± 1.68
Inverse isochron age ± 2σ		48.89 ± 0.81				Integrated age ± 2σ			48.03 ± 0.37
$^{40}Ar/^{39}Ar$ intercept ± 2σ		304.1 ± 36.4		MSWD 0.38		Plateau age ± 2σ			49.07 ± 0.30
UW32B5bj: 3 crystals									
32B5bj1	0.16	6.040 ± 0.071	0.00774 ± 0.00382	0.015620 ± 0.001057	0.18	23.5	3.3	56	37.14 ± 16.45
32B5bj2	0.26	2.516 ± 0.019	0.00670 ± 0.00099	0.002202 ± 0.000215	0.27	74.0	12.4	64	48.53 ± 3.40
32B5bj3	0.39	2.044 ± 0.008	0.00649 ± 0.00041	0.000562 ± 0.000098	0.56	91.7	31.2	66	48.86 ± 1.53
32B5bj4	0.52	1.934 ± 0.014	0.03200 ± 0.00095	0.000247 ± 0.000177	0.29	96.1	16.9	13	48.49 ± 2.78
32B5bj5	1.50	1.926 ± 0.008	0.03150 ± 0.00074	0.000315 ± 0.000082	0.61	95.1	36.1	14	47.75 ± 1.32
Inverse isochron age ± 2σ		48.47 ± 1.00				Integrated age ± 2σ			47.97 ± 1.08
$^{40}Ar/^{39}Ar$ intercept ± 2σ		279.9 ± 34.9		MSWD 0.78		Plateau age ± 2σ			48.24 ± 0.91
UW32B5bk: 3 crystals									
32B5bk1	0.16	2.746 ± 0.068	0.01213 ± 0.00462	0.005221 ± 0.001212	0.06	43.7	2.6	35	31.43 ± 18.91
32B5bk2	0.26	2.039 ± 0.019	0.00512 ± 0.00136	0.000782 ± 0.000239	0.18	88.5	10.6	84	47.06 ± 3.76
32B5bk3	0.39	1.965 ± 0.007	0.00442 ± 0.00046	0.000334 ± 0.000090	0.48	94.8	28.9	97	48.57 ± 1.41
32B5bk4	0.52	1.954 ± 0.014	0.00987 ± 0.00104	0.000230 ± 0.000220	0.24	96.3	14.4	44	49.08 ± 3.41
32B5bk5	1.50	1.917 ± 0.007	0.02363 ± 0.00050	0.000201 ± 0.000055	0.71	96.8	43.5	18	48.37 ± 0.91
Inverse isochron age ± 2σ		49.08 ± 0.78				Integrated age ± 2σ			47.96 ± 0.98
$^{40}Ar/^{39}Ar$ intercept ± 2σ		194.3 ± 87.1		MSWD 1.00		Plateau age ± 2σ			48.38 ± 0.74

Table DR3. Complete $^{40}Ar/^{39}Ar$ results

Sample Experiment	laser power (W)	$^{40}Ar/^{39}Ar$	$^{37}Ar/^{39}Ar$	$^{36}Ar/^{39}Ar$	$^{40}Ar^*$ X10^{-14} mol	$^{40}Ar^*$ %	$^{39}Ar_K$ %	K/Ca	Apparent Age ± 2σ Ma
Continental tuff CP-1 biotite continued									
Combined multi-crystal incremental heating ages									
Inverse isochron age ± 2σ		48.76 ± 0.49							Integrated age ± 2σ 47.71 ± 0.31
$^{40}Ar/^{39}Ar$ intercept ± 2σ		274.0 ± 19.3		MSWD 0.69					Weighted mean: plateau ages ± 2σ 48.54 ± 0.54
Grand combined incremental heating ages									
Inverse isochron age ± 2σ		48.77 ± 0.46							Integrated age ± 2σ 47.97 ± 0.33
$^{40}Ar/^{39}Ar$ intercept ± 2σ		287.0 ± 17.4		MSWD 1.30					Weighted mean: plateau ages ± 2σ 48.64 ± 0.47
				MSWD 1.87					Weighted mean: integrated ages ± 2σ 47.95 ± 0.28
Continental tuff CP-1 sanidine J = 0.010661 ± 0.17% μ = 1.0065									
5 crystal fusions									
* 53F5a	1.50	1.907 ± 0.004	0.00651 ± 0.00021	0.000398 ± 0.000058	1.11	93.8	66		34.09 ± 0.66
53F5b	1.50	2.621 ± 0.010	0.02207 ± 0.00035	0.000266 ± 0.000134	0.84	97.0	19		48.30 ± 1.53
53F5c	1.50	2.600 ± 0.005	0.00871 ± 0.00025	0.000083 ± 0.000063	1.33	99.0	49		48.89 ± 0.73
53F5d	1.50	2.595 ± 0.006	0.00824 ± 0.00038	0.000053 ± 0.000088	0.91	99.4	52		48.97 ± 1.00
53F5e	1.50	2.622 ± 0.007	0.01587 ± 0.00054	0.000161 ± 0.000098	0.90	98.2	27		48.88 ± 1.11
53F5f	1.50	2.648 ± 0.006	0.01626 ± 0.00029	0.000250 ± 0.000096	1.08	97.2	26		48.86 ± 1.09
53F5g	1.50	2.602 ± 0.008	0.00787 ± 0.00034	0.000145 ± 0.000095	0.85	98.3	55		48.58 ± 1.09
53F5h	1.50	2.639 ± 0.007	0.01525 ± 0.00031	0.000182 ± 0.000106	0.77	97.9	28		49.08 ± 1.21
53F5i	1.50	2.634 ± 0.009	0.01658 ± 0.00044	0.000243 ± 0.000086	0.83	97.3	26		48.64 ± 1.01
53F5j	1.50	2.597 ± 0.010	0.02212 ± 0.00038	0.000214 ± 0.000066	1.19	97.6	19		48.13 ± 0.82
* 53F5k	1.50	3.751 ± 0.010	0.01403 ± 0.00031	0.000130 ± 0.000056	1.89	99.0	31		70.06 ± 0.71
* 53F5l	1.50	39.305 ± 0.109	0.00775 ± 0.00061	0.000674 ± 0.000178	23.89	99.5	55		629.06 ± 3.28
53F5m	1.50	2.580 ± 0.004	0.00685 ± 0.00022	0.000093 ± 0.000071	1.18	98.9	63		48.45 ± 0.80
20 crystal 2-step fusions									
53F5n1	0.25	2.636 ± 0.009	0.01082 ± 0.00125	0.000147 ± 0.000360	0.29	98.3	40		49.17 ± 4.00
53F5n2	1.50	2.576 ± 0.004	0.01068 ± 0.00021	0.000041 ± 0.000057	1.42	99.5	40		48.63 ± 0.66
* 53F5o1	0.25	21.158 ± 0.032	0.00669 ± 0.00021	0.000110 ± 0.000051	16.55	99.8	64		366.43 ± 1.37
* 53F5o2	1.50	25.442 ± 0.039	0.00539 ± 0.00137	0.000803 ± 0.000525	2.35	99.1	80		429.35 ± 4.93
53F5p1	0.25	2.594 ± 0.004	0.01183 ± 0.00031	0.000088 ± 0.000078	1.54	99.0	36		48.72 ± 0.88
53F5p2	1.50	2.609 ± 0.008	0.01295 ± 0.00134	0.000160 ± 0.000353	0.32	98.2	33		48.61 ± 3.92
Combined fusion ages									
Inverse isochron age ± 2σ		48.51 ± 0.64							Integrated age ± 2σ 140.63 ± 0.42
$^{40}Ar/^{39}Ar$ intercept ± 2σ		359.5 ± 276.2		MSWD 0.29					Weighted mean age ± 2σ **48.66 ± 0.28**
Church Buttes tuff ChB sanidine J = 0.014605 ± 0.10% μ = 1.0035									
Single crystal fusions									
32B9a	1.50	1.889 ± 0.003	0.00675 ± 0.00006	0.000056 ± 0.000017	2.81	98.9	64		48.57 ± 0.30
32B9b	1.50	1.896 ± 0.002	0.01546 ± 0.00009	0.000048 ± 0.000016	6.97	99.1	28		48.83 ± 0.27
32B9c	1.50	1.889 ± 0.003	0.01347 ± 0.00012	0.000066 ± 0.000033	2.68	98.8	32		48.51 ± 0.52
32B9d	1.50	1.918 ± 0.003	0.00723 ± 0.00013	0.000165 ± 0.000033	1.77	97.2	59		48.49 ± 0.52
32B9e	1.50	1.906 ± 0.002	0.00587 ± 0.00007	0.000081 ± 0.000025	2.88	98.5	73		48.82 ± 0.39
32B9f	1.50	1.899 ± 0.003	0.01274 ± 0.00014	0.000063 ± 0.000033	1.70	98.8	34		48.79 ± 0.53
32B9g	1.50	1.886 ± 0.003	0.00546 ± 0.00007	0.000056 ± 0.000023	1.98	98.9	79		48.49 ± 0.39
32B9h	1.50	1.908 ± 0.004	0.00803 ± 0.00017	0.000051 ± 0.000046	1.14	99.0	54		49.09 ± 0.72
* 32B9i	1.50	2.551 ± 0.004	0.01909 ± 0.00014	0.002735 ± 0.000033	3.15	68.2	23		45.27 ± 0.52
32B9j	1.50	1.907 ± 0.004	0.01195 ± 0.00017	0.000173 ± 0.000049	0.98	97.1	36		48.15 ± 0.77
32B9k	1.50	1.974 ± 0.003	0.03027 ± 0.00022	0.000356 ± 0.000026	1.94	94.6	14		48.54 ± 0.42
32B9l	1.50	1.926 ± 0.003	0.00727 ± 0.00010	0.000189 ± 0.000030	1.74	96.9	59		48.50 ± 0.47
32B9m	1.50	1.930 ± 0.003	0.00638 ± 0.00007	0.000204 ± 0.000013	3.95	96.7	67		48.50 ± 0.26
32B9n	1.50	1.895 ± 0.003	0.01227 ± 0.00009	0.000064 ± 0.000020	3.64	98.8	35		48.67 ± 0.33
32B9o	1.50	1.912 ± 0.006	0.00655 ± 0.00024	0.000207 ± 0.000072	0.80	96.6	66		48.02 ± 1.12
32B9p	1.50	1.888 ± 0.003	0.00488 ± 0.00014	0.000050 ± 0.000043	1.39	99.0	88		48.59 ± 0.68
32B9q	1.50	1.891 ± 0.008	0.00507 ± 0.00030	0.000067 ± 0.000165	0.41	98.7	85		48.53 ± 2.53
32B9r	1.50	1.901 ± 0.003	0.00540 ± 0.00007	0.000020 ± 0.000035	1.88	99.5	80		49.14 ± 0.55
32B9s	1.50	1.890 ± 0.003	0.00483 ± 0.00010	0.000052 ± 0.000034	2.26	99.0	89		48.61 ± 0.54
32B9t	1.50	1.900 ± 0.004	0.01250 ± 0.00010	0.000052 ± 0.000031	1.98	99.0	34		48.90 ± 0.50
32B9u	1.50	1.913 ± 0.004	0.00640 ± 0.00007	0.000048 ± 0.000025	2.90	99.0	67		49.25 ± 0.43
32B9v	1.50	1.897 ± 0.003	0.01422 ± 0.00011	0.000065 ± 0.000024	2.17	98.8	30		48.71 ± 0.40

Table DR3. Complete $^{40}Ar/^{39}Ar$ results

Sample Experiment	laser power (W)	$^{40}Ar/^{39}Ar$	$^{37}Ar/^{39}Ar$	$^{36}Ar/^{39}Ar$	$^{40}Ar^*$ X10^{-14} mol	$^{40}Ar^*$ %	$^{39}Ar_K$ %	K/Ca	Apparent Age ± 2σ Ma
Church Buttes tuff ChB sanidine continued									
* 32B9w	1.50	3.106 ± 0.005	0.00297 ± 0.00009	0.000053 ± 0.000051	2.67	99.4		145	79.53 ± 0.80
32B9x	1.50	1.904 ± 0.003	0.00820 ± 0.00019	0.000123 ± 0.000061	1.00	97.9		52	48.45 ± 0.94
32B9y	1.50	1.887 ± 0.002	0.02607 ± 0.00016	0.000048 ± 0.000020	3.61	99.1		16	48.62 ± 0.33
32B9z	1.50	1.892 ± 0.014	0.02759 ± 0.00035	0.000080 ± 0.000123	0.41	98.6		16	48.50 ± 1.99
* 32B9aa	1.50	2.934 ± 0.004	0.00168 ± 0.00010	0.000060 ± 0.000044	1.85	99.2		255	75.12 ± 0.69
32B9bb	1.50	1.890 ± 0.002	0.02704 ± 0.00019	0.000009 ± 0.000027	2.06	99.7		16	48.99 ± 0.43
32B9cc	1.50	1.900 ± 0.003	0.01126 ± 0.00012	0.000038 ± 0.000031	1.72	99.2		38	48.99 ± 0.50
32B9dd	1.50	1.907 ± 0.003	0.00874 ± 0.00008	0.000070 ± 0.000020	2.29	98.7		49	48.92 ± 0.34
32B9ee	1.50	1.886 ± 0.006	0.00735 ± 0.00016	0.000074 ± 0.000043	1.12	98.6		59	48.36 ± 0.73
32B9ff	1.50	1.887 ± 0.003	0.00764 ± 0.00009	0.000060 ± 0.000036	2.64	98.8		56	48.49 ± 0.56
32B9gg	1.50	1.887 ± 0.003	0.02583 ± 0.00030	0.000113 ± 0.000042	1.13	98.1		17	48.13 ± 0.66
32B9hh	1.50	1.907 ± 0.003	0.00724 ± 0.00007	0.000058 ± 0.000026	2.33	98.9		59	49.01 ± 0.41
32B9ii	1.50	1.898 ± 0.002	0.00508 ± 0.00010	0.000018 ± 0.000031	2.18	99.5		85	49.09 ± 0.49
32B9jj	1.50	1.907 ± 0.003	0.01222 ± 0.00018	0.000118 ± 0.000028	1.60	98.0		35	48.57 ± 0.45
* 32B9kk	1.50	2.261 ± 0.003	0.00803 ± 0.00014	0.000078 ± 0.000021	3.47	98.8		54	57.93 ± 0.35
32B9ll	1.50	1.894 ± 0.005	0.00621 ± 0.00005	0.000037 ± 0.000005	10.72	99.2		69	48.81 ± 0.27
Inverse isochron age ± 2σ		48.77 ± 0.12					Total fusion age ± 2σ		49.87 ± 0.09
$^{40}Ar/^{39}Ar$ intercept ± 2σ		270.3 ± 43.8		MSWD 1.17			Weighted mean age ± 2σ		48.72 ± 0.09
Multi-crystal incremental heating experiments									
UW32B9mm: 10 crystals									
32B9mm1	0.13	1.907 ± 0.002	0.00987 ± 0.00008	0.000058 ± 0.000015	4.65	98.9	40.9	44	49.01 ± 0.25
32B9mm2	0.23	1.890 ± 0.002	0.00817 ± 0.00012	0.000038 ± 0.000020	3.34	99.2	29.6	53	48.73 ± 0.32
32B9mm3	0.32	1.899 ± 0.005	0.00852 ± 0.00024	0.000007 ± 0.000062	0.80	99.7	7.1	50	49.19 ± 0.98
32B9mm4	1.50	1.910 ± 0.004	0.00881 ± 0.00012	0.000067 ± 0.000020	2.55	98.7	22.4	49	49.01 ± 0.37
Inverse isochron age ± 2σ		48.42 ± 1.44					Total fusion age ± 2σ		48.94 ± 0.18
$^{40}Ar/^{39}Ar$ intercept ± 2σ		695.7 ± 1252.1		MSWD 0.81			Weighted mean age ± 2σ		48.94 ± 0.18
UW32B9nn: 10 crystals									
32B9nn1	0.10	1.957 ± 0.011	0.00949 ± 0.00039	0.000233 ± 0.000186	0.38	96.3	4.9	45	48.97 ± 2.87
32B9nn2	0.16	1.880 ± 0.004	0.00967 ± 0.00011	0.000021 ± 0.000011	5.21	99.5	71.1	44	48.59 ± 0.28
32B9nn3	0.36	1.895 ± 0.004	0.01010 ± 0.00014	0.000036 ± 0.000043	1.49	99.2	20.1	43	48.87 ± 0.69
32B9nn4	1.50	1.966 ± 0.015	0.01131 ± 0.00037	0.000302 ± 0.000189	0.30	95.3	3.9	38	48.67 ± 2.96
Inverse isochron age ± 2σ		48.57 ± 0.38					Total fusion age ± 2σ		48.67 ± 0.31
$^{40}Ar/^{39}Ar$ intercept ± 2σ		381.5 ± 434.2		MSWD 0.20			Weighted mean age ± 2σ		48.63 ± 0.26
Combined incremental heating ages									
Inverse isochron age ± 2σ		48.47 ± 0.51					Total fusion age ± 2σ		48.83 ± 0.17
$^{40}Ar/^{39}Ar$ intercept ± 2σ		631.2 ± 474.4		MSWD 0.73			Weighted mean age ± 2σ		48.88 ± 0.15
Grand combined sanidine ages									
Inverse isochron age ± 2σ		48.77 ± 0.11					Total fusion age ± 2σ		49.69 ± 0.09
$^{40}Ar/^{39}Ar$ intercept ± 2σ		279.4 ± 43.4		MSWD 1.30			Weighted mean age ± 2σ		**48.76 ± 0.09**
Leavitt Creek tuff LeC sanidine J = 0.010601 ± 0.18% μ = 1.0065									
Single crystal fusions									
53F1a	1.50	2.625 ± 0.006	0.00799 ± 0.00037	0.000200 ± 0.000078	0.85	97.7		54	48.39 ± 0.89
53F1b	1.50	2.612 ± 0.005	0.01154 ± 0.00026	0.000071 ± 0.000048	1.87	99.2		37	48.87 ± 0.55
53F1c	1.50	2.641 ± 0.006	0.00676 ± 0.00035	0.000176 ± 0.000114	0.67	98.0		64	48.83 ± 1.27
53F1d	1.50	2.595 ± 0.004	0.00548 ± 0.00021	0.000067 ± 0.000040	1.92	99.2		78	48.57 ± 0.47
53F1e	1.50	2.620 ± 0.010	0.00734 ± 0.00036	0.000161 ± 0.000102	0.85	98.1		59	48.52 ± 1.18
53F1f	1.50	2.610 ± 0.005	0.00992 ± 0.00028	0.000127 ± 0.000135	0.93	98.5		43	48.53 ± 1.49
* 53F1g	1.50	3.875 ± 0.012	0.00178 ± 0.00036	0.000073 ± 0.000112	0.87	99.4		241	72.21 ± 1.30
53F1h	1.50	2.599 ± 0.004	0.02406 ± 0.00054	0.000133 ± 0.000083	1.18	98.5		18	48.30 ± 0.92
53F1i	1.50	2.641 ± 0.010	0.02790 ± 0.00063	0.000320 ± 0.000126	0.70	96.4		15	48.07 ± 1.43
53F1j	1.50	2.650 ± 0.006	0.00676 ± 0.00029	0.000154 ± 0.000111	0.80	98.2		64	49.11 ± 1.24
* 53F1k	1.50	4.087 ± 0.010	0.00129 ± 0.00037	0.000214 ± 0.000091	1.39	98.4		333	75.34 ± 1.05
53F1l	1.50	2.639 ± 0.011	0.00482 ± 0.00039	0.000220 ± 0.000117	0.65	97.5		89	48.54 ± 1.36
53F1m	1.50	2.606 ± 0.008	0.00657 ± 0.00046	0.000066 ± 0.000119	0.74	99.2		65	48.79 ± 1.35

Table DR3. Complete $^{40}Ar/^{39}Ar$ results

Sample Experiment	laser power (W)	$^{40}Ar/^{39}Ar$	$^{37}Ar/^{39}Ar$	$^{36}Ar/^{39}Ar$	$^{40}Ar^*$ X10^{-14} mol	$^{40}Ar^*$ %	$^{39}Ar_K$ %	K/Ca	Apparent Age ± 2σ Ma
Leavitt Creek tuff LeC sanidine continued									
53F1n	1.50	2.638 ± 0.010	0.00743 ± 0.00090	0.000182 ± 0.000239	0.38	97.9		58	48.74 ± 2.65
Single crystal fusion ages									
Inverse isochron age ± 2σ		48.55 ± 0.60					Integrated age ± 2σ		51.52 ± 0.30
$^{40}Ar/^{39}Ar$ intercept ± 2σ		333.5 ± 312.4		MSWD 0.28			Weighted mean age ± 2σ		**48.62 ± 0.28**
Henrys Fork tuff HeF sanidine J = 0.014648 ± 0.16% μ = 1.0035									
Single crystal fusions									
32B7a	1.50	1.856 ± 0.003	0.00717 ± 0.00009	0.000031 ± 0.000007	8.33	99.3		60	48.06 ± 0.18
32B7b	1.50	1.860 ± 0.003	0.00749 ± 0.00011	0.000006 ± 0.000021	2.48	99.7		57	48.34 ± 0.36
32B7c	1.50	1.859 ± 0.002	0.00788 ± 0.00012	0.000011 ± 0.000012	5.21	99.6		55	48.27 ± 0.21
32B7d	1.50	1.870 ± 0.003	0.00727 ± 0.00012	0.000052 ± 0.000020	3.17	99.0		59	48.26 ± 0.34
32B7e	1.50	1.859 ± 0.003	0.01005 ± 0.00021	0.000057 ± 0.000017	17.07	98.9		43	47.93 ± 0.29
32B7f	1.50	1.855 ± 0.003	0.00809 ± 0.00010	0.000018 ± 0.000005	9.06	99.5		53	48.11 ± 0.15
32B7g	1.50	1.859 ± 0.002	0.00727 ± 0.00010	0.000018 ± 0.000003	10.99	99.5		59	48.23 ± 0.13
32B7h	1.50	1.859 ± 0.002	0.00640 ± 0.00011	0.000020 ± 0.000012	4.13	99.5		67	48.20 ± 0.22
32B7i	1.50	1.858 ± 0.002	0.00731 ± 0.00008	0.000013 ± 0.000003	13.00	99.6		59	48.24 ± 0.12
32B7j	1.50	1.855 ± 0.002	0.00757 ± 0.00011	0.000024 ± 0.000005	9.25	99.4		57	48.09 ± 0.14
32B7k	1.50	1.870 ± 0.003	0.01208 ± 0.00019	0.000076 ± 0.000018	3.11	98.6		36	48.08 ± 0.31
32B7l	1.50	1.856 ± 0.002	0.00670 ± 0.00008	0.000012 ± 0.000005	11.65	99.6		64	48.19 ± 0.13
32B7m	1.50	1.864 ± 0.002	0.00683 ± 0.00009	0.000042 ± 0.000004	9.60	99.1		63	48.18 ± 0.13
32B7n	1.50	1.856 ± 0.003	0.00793 ± 0.00018	0.000020 ± 0.000014	18.53	99.5		54	48.13 ± 0.26
32B7o	1.50	1.853 ± 0.003	0.00764 ± 0.00016	0.000042 ± 0.000008	15.54	99.1		56	47.89 ± 0.18
32B7p	1.50	1.859 ± 0.003	0.00634 ± 0.00010	0.000031 ± 0.000020	3.21	99.3		68	48.13 ± 0.33
32B7q	1.50	1.860 ± 0.003	0.00710 ± 0.00010	0.000036 ± 0.000010	3.94	99.2		61	48.13 ± 0.22
32B7r	1.50	1.859 ± 0.003	0.00645 ± 0.00012	0.000044 ± 0.000026	2.95	99.1		67	48.02 ± 0.42
32B7s	1.50	1.867 ± 0.002	0.00710 ± 0.00016	0.000062 ± 0.000026	15.62	98.8		61	48.11 ± 0.42
32B7t	1.50	1.856 ± 0.002	0.00676 ± 0.00010	0.000014 ± 0.000008	6.81	99.6		64	48.18 ± 0.16
32B7u	1.50	1.863 ± 0.003	0.00745 ± 0.00015	0.000016 ± 0.000009	2.49	99.5		58	48.35 ± 0.19
32B7v	1.50	1.868 ± 0.003	0.00620 ± 0.00013	0.000034 ± 0.000014	2.97	99.2		69	48.34 ± 0.26
32B7w	1.50	1.862 ± 0.002	0.00646 ± 0.00010	0.000025 ± 0.000015	3.19	99.4		67	48.26 ± 0.26
32B7x	1.50	1.855 ± 0.003	0.00770 ± 0.00015	0.000016 ± 0.000020	2.69	99.5		56	48.14 ± 0.35
32B7y	1.50	1.859 ± 0.003	0.00698 ± 0.00011	0.000035 ± 0.000014	2.74	99.2		62	48.10 ± 0.27
32B7z	1.50	1.858 ± 0.003	0.00725 ± 0.00011	0.000025 ± 0.000009	4.84	99.4		59	48.15 ± 0.19
32B7aa	1.50	1.847 ± 0.002	0.00712 ± 0.00012	0.000014 ± 0.000039	1.81	99.5		60	47.94 ± 0.61
32B7bb	1.50	1.853 ± 0.003	0.00751 ± 0.00010	0.000035 ± 0.000021	3.77	99.2		57	47.95 ± 0.35
32B7cc	1.50	1.859 ± 0.002	0.00788 ± 0.00011	0.000036 ± 0.000035	2.59	99.2		55	48.08 ± 0.55
32B7dd	1.50	1.845 ± 0.004	0.00768 ± 0.00018	0.000029 ± 0.000031	2.52	99.3		56	47.80 ± 0.50
32B7ee	1.50	1.856 ± 0.003	0.00643 ± 0.00013	0.000032 ± 0.000023	2.88	99.3		67	48.04 ± 0.40
32B7ff	1.50	1.859 ± 0.003	0.00616 ± 0.00009	0.000052 ± 0.000014	3.08	98.9		70	47.97 ± 0.26
32B7gg	1.50	1.857 ± 0.003	0.00583 ± 0.00007	0.000018 ± 0.000005	6.93	99.5		74	48.16 ± 0.17
32B7hh	1.50	1.850 ± 0.002	0.00745 ± 0.00016	0.000021 ± 0.000014	3.09	99.4		58	47.98 ± 0.24
32B7ii	1.50	1.858 ± 0.003	0.00698 ± 0.00020	0.000025 ± 0.000023	1.73	99.4		62	48.16 ± 0.38
32B7jj	1.50	1.859 ± 0.003	0.00756 ± 0.00016	0.000069 ± 0.000022	1.87	98.7		57	47.83 ± 0.37
32B7kk	1.50	1.856 ± 0.002	0.00745 ± 0.00011	0.000007 ± 0.000007	4.69	99.7		58	48.24 ± 0.16
32B7ll	1.50	1.861 ± 0.003	0.00851 ± 0.00024	0.000013 ± 0.000016	1.40	99.6		51	48.33 ± 0.30
32B7mm	1.50	1.854 ± 0.002	0.00610 ± 0.00015	0.000048 ± 0.000019	2.84	99.0		70	47.87 ± 0.32
32B7nn	1.50	1.859 ± 0.003	0.00784 ± 0.00023	0.000040 ± 0.000043	1.51	99.1		55	48.05 ± 0.67
32B7oo	1.50	1.850 ± 0.003	0.00773 ± 0.00016	0.000035 ± 0.000041	1.78	99.2		56	47.88 ± 0.64
32B7pp	1.50	1.855 ± 0.002	0.00617 ± 0.00018	0.000033 ± 0.000032	2.53	99.3		70	48.00 ± 0.49
32B7qq	1.50	1.868 ± 0.003	0.00660 ± 0.00018	0.000045 ± 0.000031	1.95	99.1		65	48.26 ± 0.48
32B7rr	1.50	1.861 ± 0.003	0.00984 ± 0.00027	0.000072 ± 0.000024	1.68	98.6		44	47.88 ± 0.39
32B7ss	1.50	1.916 ± 0.003	0.00739 ± 0.00016	0.000236 ± 0.000022	2.55	96.1		58	48.05 ± 0.38
32B7tt	1.50	1.865 ± 0.003	0.00639 ± 0.00016	0.000076 ± 0.000028	1.59	98.6		67	47.93 ± 0.45
32B7uu	1.50	1.879 ± 0.003	0.00750 ± 0.00014	0.000102 ± 0.000021	2.47	98.2		57	48.11 ± 0.36
32B7vv	1.50	1.852 ± 0.003	0.00645 ± 0.00011	0.000030 ± 0.000017	3.41	99.3		67	47.96 ± 0.29
32B7ww	1.50	1.874 ± 0.003	0.00740 ± 0.00016	0.000040 ± 0.000022	2.36	99.2		58	48.45 ± 0.38
32B7xx	1.50	1.861 ± 0.002	0.00766 ± 0.00014	0.000042 ± 0.000021	2.18	99.1		56	48.09 ± 0.33
32B7yy	1.50	1.849 ± 0.003	0.00697 ± 0.00018	0.000049 ± 0.000032	1.51	99.0		62	47.74 ± 0.51
32B7zz	1.50	1.853 ± 0.003	0.00994 ± 0.00016	0.000036 ± 0.000027	1.89	99.2		43	47.94 ± 0.44
32B7aaa	1.50	1.859 ± 0.003	0.00743 ± 0.00015	0.000006 ± 0.000019	1.99	99.7		58	48.32 ± 0.33
32B7bbb	1.50	1.859 ± 0.003	0.00805 ± 0.00013	0.000015 ± 0.000017	3.05	99.5		53	48.24 ± 0.30

Table DR3. Complete $^{40}Ar/^{39}Ar$ results

Sample Experiment	laser power (W)	$^{40}Ar/^{39}Ar$	$^{37}Ar/^{39}Ar$	$^{36}Ar/^{39}Ar$	$^{40}Ar^*$ X10^{-14} mol	$^{40}Ar^*$ %	$^{39}Ar_K$ %	K/Ca	Apparent Age ± 2σ Ma
Henrys Fork tuff HeF sanidine continued									
32B7ccc	1.50	1.843 ± 0.004	0.01717 ± 0.00039	0.000021 ± 0.000052	0.93	99.5		25	47.80 ± 0.82
32B7ddd	1.50	1.862 ± 0.004	0.00663 ± 0.00016	0.000038 ± 0.000019	1.94	99.2		65	48.15 ± 0.34
Single crystal fusion ages									
Inverse isochron age ± 2σ		48.14 ± 0.09				Total fusion age ± 2σ			48.10 ± 0.09
$^{40}Ar/^{39}Ar$ intercept ± 2σ		302.1 ± 59.6		MSWD 1.08		Weighted mean age ± 2σ			48.15 ± 0.08
Multi-crystal incremental heating experiments									
UW32B7eee: 10 crystals									
32B7eee1	0.10	2.127 ± 0.025	0.00963 ± 0.00154	0.000470 ± 0.000392	0.14	93.3	0.6	45	51.69 ± 6.08
32B7eee2	0.13	1.863 ± 0.009	0.00769 ± 0.00041	0.000067 ± 0.000140	0.38	98.7	2.1	56	47.97 ± 2.17
32B7eee3	0.16	1.848 ± 0.004	0.00732 ± 0.00024	0.000049 ± 0.000038	1.12	99.0	6.0	59	47.71 ± 0.62
32B7eee4	0.32	1.853 ± 0.002	0.00740 ± 0.00009	0.000003 ± 0.000003	10.64	99.7	57.1	58	48.18 ± 0.14
32B7eee5	1.50	1.864 ± 0.002	0.00740 ± 0.00010	0.000043 ± 0.000008	6.40	99.1	34.1	58	48.17 ± 0.17
Inverse isochron age ± 2σ		48.14 ± 0.16				Total fusion age ± 2σ			48.17 ± 0.14
$^{40}Ar/^{39}Ar$ intercept ± 2σ		367.1 ± 235.3		MSWD 0.91		Weighted mean age ± 2σ			48.17 ± 0.13
UW32B7fff: 10 crystals									
32B7fff1	0.10	1.992 ± 0.017	0.00951 ± 0.00118	0.000353 ± 0.000200	0.23	94.6	0.8	45	49.11 ± 3.16
32B7fff2	0.12	1.862 ± 0.007	0.00657 ± 0.00061	0.000088 ± 0.000074	0.49	98.4	1.9	65	47.78 ± 1.18
32B7fff3	0.15	1.845 ± 0.004	0.00654 ± 0.00025	0.000052 ± 0.000037	0.95	98.9	3.7	66	47.61 ± 0.59
32B7fff4	0.26	1.845 ± 0.003	0.00712 ± 0.00013	0.000004 ± 0.000012	19.97	99.7	78.1	60	47.97 ± 0.25
32B7fff5	1.50	1.867 ± 0.003	0.00679 ± 0.00013	0.000046 ± 0.000010	4.00	99.1	15.5	63	48.21 ± 0.20
Inverse isochron age ± 2σ		47.90 ± 0.36				Total fusion age ± 2σ			48.00 ± 0.22
$^{40}Ar/^{39}Ar$ intercept ± 2σ		533.4 ± 392.8		MSWD 1.41		Weighted mean age ± 2σ			48.08 ± 0.20
UW32B7ggg: 10 crystals									
32B7ggg1	0.10	1.872 ± 0.004	0.01580 ± 0.00042	0.000086 ± 0.000050	0.99	98.5	6.1	27	48.06 ± 0.80
32B7ggg2	0.12	1.851 ± 0.003	0.01459 ± 0.00023	0.000015 ± 0.000014	2.49	99.6	15.5	29	48.05 ± 0.26
32B7ggg3	0.15	1.854 ± 0.002	0.01013 ± 0.00013	0.000008 ± 0.000006	8.14	99.7	50.5	42	48.17 ± 0.15
32B7ggg4	0.26	1.855 ± 0.002	0.01237 ± 0.00025	0.000038 ± 0.000018	1.79	99.2	11.1	35	47.99 ± 0.30
32B7ggg5	1.50	1.866 ± 0.002	0.00898 ± 0.00014	0.000007 ± 0.000015	2.74	99.7	16.9	48	48.50 ± 0.26
Inverse isochron age ± 2σ		47.79 ± 0.78				Total fusion age ± 2σ			48.18 ± 0.14
$^{40}Ar/^{39}Ar$ intercept ± 2σ		1887 ± 9751		MSWD 2.20		Weighted mean age ± 2σ			48.18 ± 0.18
Combined multi-crystal incremental heating ages									
Inverse isochron age ± 2σ		48.10 ± 0.13				Total fusion age ± 2σ			48.10 ± 0.12
$^{40}Ar/^{39}Ar$ intercept ± 2σ		451.0 ± 206.7		MSWD 0.35		Weighted mean age ± 2σ			48.15 ± 0.11
Grand combined sanidine ages									
Inverse isochron age ± 2σ		48.13 ± 0.09				Total fusion age ± 2σ			48.10 ± 0.09
$^{40}Ar/^{39}Ar$ intercept ± 2σ		330.6 ± 60.4		MSWD 1.04		Weighted mean age ± 2σ			**48.15 ± 0.08**
Tabernacle Butte tuff TB-1 sanidine J = 0.010572 ± 0.13% μ = 1.0065									
Single crystal fusions									
53F3a	1.50	2.571 ± 0.004	0.00640 ± 0.00009	0.000054 ± 0.000021	4.94	99.3		67	48.07 ± 0.27
53F3b	1.50	2.573 ± 0.004	0.00602 ± 0.00009	0.000057 ± 0.000014	5.65	99.3		71	48.08 ± 0.21
53F3c	1.50	2.606 ± 0.004	0.00727 ± 0.00010	0.000162 ± 0.000022	3.64	98.1		59	48.13 ± 0.28
53F3d	1.50	2.586 ± 0.004	0.01805 ± 0.00026	0.000077 ± 0.000023	3.52	99.1		24	48.24 ± 0.29
53F3e	1.50	2.565 ± 0.003	0.00654 ± 0.00011	0.000033 ± 0.000010	6.99	99.6		66	48.06 ± 0.17
53F3f	1.50	2.566 ± 0.003	0.00750 ± 0.00012	0.000061 ± 0.000020	4.74	99.3		57	47.93 ± 0.26
53F3g	1.50	2.570 ± 0.004	0.00589 ± 0.00009	0.000032 ± 0.000020	7.26	99.6		73	48.17 ± 0.26
53F3h	1.50	2.569 ± 0.004	0.00739 ± 0.00010	0.000027 ± 0.000022	3.74	99.6		58	48.18 ± 0.28
53F3i	1.50	2.570 ± 0.004	0.00663 ± 0.00008	0.000033 ± 0.000014	8.06	99.6		65	48.17 ± 0.21
53F3j	1.50	2.568 ± 0.005	0.00586 ± 0.00007	0.000046 ± 0.000016	5.97	99.4		73	48.05 ± 0.25
53F3k	1.50	2.588 ± 0.004	0.00952 ± 0.00022	0.000104 ± 0.000044	1.88	98.8		45	48.11 ± 0.51
53F3l	1.50	2.584 ± 0.004	0.00676 ± 0.00016	0.000125 ± 0.000052	2.34	98.5		64	47.91 ± 0.60
53F3m	1.50	2.561 ± 0.009	0.00661 ± 0.00017	0.000062 ± 0.000023	2.47	99.2		65	47.84 ± 0.42
53F3n	1.50	2.592 ± 0.007	0.01525 ± 0.00018	0.000075 ± 0.000036	3.47	99.1		28	48.35 ± 0.48

Table DR3. Complete $^{40}Ar/^{39}Ar$ results

Sample Experiment	laser power (W)	$^{40}Ar/^{39}Ar$	$^{37}Ar/^{39}Ar$	$^{36}Ar/^{39}Ar$	$^{40}Ar^*$ X10^{-14} mol	$^{40}Ar^*$ %	$^{39}Ar_K$ %	K/Ca	Apparent Age ± 2σ Ma
Tabernacle Butte tuff TB-1 sanidine continued									
53F3o	1.50	2.569 ± 0.005	0.00710 ± 0.00024	0.000069 ± 0.000037	1.83	99.2		61	47.94 ± 0.45
53F3p	1.50	2.598 ± 0.006	0.00723 ± 0.00012	0.000100 ± 0.000017	3.72	98.8		59	48.31 ± 0.28
53F3q	1.50	2.612 ± 0.005	0.00724 ± 0.00016	0.000225 ± 0.000043	1.85	97.4		59	47.88 ± 0.50
53F3r	1.50	2.726 ± 0.004	0.00628 ± 0.00015	0.000570 ± 0.000027	2.69	93.8		69	48.11 ± 0.33
53F3s	1.50	2.582 ± 0.004	0.00711 ± 0.00010	0.000053 ± 0.000012	5.23	99.3		60	48.27 ± 0.21
53F3t	1.50	2.588 ± 0.004	0.00648 ± 0.00019	0.000049 ± 0.000030	2.67	99.4		66	48.41 ± 0.36
53F3u	1.50	2.573 ± 0.004	0.00636 ± 0.00018	0.000111 ± 0.000031	1.96	98.7		68	47.79 ± 0.37
53F3v	1.50	2.584 ± 0.005	0.00673 ± 0.00014	0.000088 ± 0.000024	2.75	98.9		64	48.12 ± 0.33
53F3w	1.50	2.573 ± 0.003	0.00734 ± 0.00015	0.000076 ± 0.000038	3.73	99.1		59	47.99 ± 0.44
53F3x	1.50	2.584 ± 0.003	0.00637 ± 0.00023	0.000125 ± 0.000051	1.89	98.5		68	47.92 ± 0.58
53F3y	1.50	2.582 ± 0.004	0.00635 ± 0.00015	0.000106 ± 0.000037	2.45	98.7		68	47.99 ± 0.43
53F3z	1.50	2.580 ± 0.005	0.00634 ± 0.00017	0.000022 ± 0.000036	1.70	99.7		68	48.41 ± 0.43
53F3aa	1.50	2.586 ± 0.006	0.00566 ± 0.00025	0.000099 ± 0.000052	1.62	98.8		76	48.10 ± 0.61
53F3bb	1.50	2.573 ± 0.005	0.00699 ± 0.00021	0.000071 ± 0.000049	1.55	99.1		61	48.01 ± 0.57
53F3cc	1.50	2.569 ± 0.005	0.01072 ± 0.00020	0.000084 ± 0.000037	1.79	99.0		40	47.87 ± 0.44
53F3dd	1.50	2.572 ± 0.004	0.00717 ± 0.00013	0.000062 ± 0.000031	2.95	99.2		60	48.03 ± 0.36
Single crystal fusion ages									
Inverse isochron age ± 2σ		48.10 ± 0.10						Integrated age ± 2σ	48.10 ± 0.09
$^{40}Ar/^{39}Ar$ intercept ± 2σ		302.8 ± 33.6		MSWD 0.81				Weighted mean age ± 2σ	48.11 ± 0.08
Multi-crystal incremental heating experiments									
UW53Fee: 5 crystals									
53F3ee1	0.06	2.771 ± 0.011	0.01957 ± 0.00109	0.000174 ± 0.000577	0.20	98.1	1.3	22	51.14 ± 6.33
53F3ee2	0.10	2.588 ± 0.010	0.01478 ± 0.00045	0.000106 ± 0.000152	0.59	98.8	4.1	29	48.10 ± 1.71
53F3ee3	0.20	2.563 ± 0.004	0.00851 ± 0.00011	0.000017 ± 0.000018	5.28	99.8	37.4	51	48.11 ± 0.24
53F3ee4	0.26	2.565 ± 0.004	0.00744 ± 0.00012	0.000033 ± 0.000016	4.95	99.6	35.0	58	48.08 ± 0.23
53F3ee5	1.50	2.578 ± 0.004	0.00738 ± 0.00015	0.000021 ± 0.000032	3.16	99.7	22.2	58	48.39 ± 0.38
Inverse isochron age ± 2σ		47.46 ± 1.92						Integrated age ± 2σ	48.20 ± 0.19
$^{40}Ar/^{39}Ar$ intercept ± 2σ		1829 ± 11460		MSWD 0.74				Plateau age ± 2σ	48.14 ± 0.16
UW53Fff: 5 crystals									
53F3ff1	0.06	2.571 ± 0.008	0.00805 ± 0.00023	0.000042 ± 0.000036	1.91	99.5	13.0	53	48.13 ± 0.50
53F3ff2	0.10	2.557 ± 0.004	0.00647 ± 0.00010	0.000011 ± 0.000010	6.43	99.8	44.1	66	48.03 ± 0.20
53F3ff3	0.20	2.562 ± 0.006	0.00638 ± 0.00017	0.000054 ± 0.000029	2.89	99.3	19.8	67	47.90 ± 0.39
53F3ff4	0.26	2.564 ± 0.032	0.00649 ± 0.00083	0.000144 ± 0.000158	0.49	98.3	3.3	66	47.43 ± 2.09
53F3ff5	1.50	2.580 ± 0.007	0.00652 ± 0.00013	0.000047 ± 0.000029	2.91	99.4	19.8	66	48.27 ± 0.40
Inverse isochron age ± 2σ		47.96 ± 0.32						Integrated age ± 2σ	48.05 ± 0.18
$^{40}Ar/^{39}Ar$ intercept ± 2σ		503.2 ± 708.9		MSWD 0.55				Plateau age ± 2σ	48.05 ± 0.17
Grand combinend sanidine ages									
Inverse isochron age ± 2σ		48.09 ± 0.09						Integrated age ± 2σ	48.11 ± 0.08
$^{40}Ar/^{39}Ar$ intercept ± 2σ		303.7 ± 32.8		MSWD 0.78				Weighted mean age ± 2σ	**48.11 ± 0.08**

Table DR3. Complete $^{40}Ar/^{39}Ar$ results

Sample Experiment	laser power (W)	$^{40}Ar/^{39}Ar$	$^{37}Ar/^{39}Ar$	$^{36}Ar/^{39}Ar$	$^{40}Ar^*$ X10^{-14} mol	$^{40}Ar^*$ %	$^{39}Ar_K$ %	K/Ca	Apparent Age ± 2σ Ma
Sage Creek Mountain pumice SCM sanidine *J* = 0.010549 ± 0.15% μ = 1.0065									
Single crystal fusions									
53F2a	1.50	2.527 ± 0.004	0.00684 ± 0.00010	0.000044 ± 0.000011	6.25	99.4		63	47.21 ± 0.19
53F2b	1.50	2.523 ± 0.004	0.00698 ± 0.00008	0.000033 ± 0.000013	6.29	99.6		62	47.18 ± 0.20
53F2c	1.50	2.521 ± 0.003	0.00511 ± 0.00009	0.000040 ± 0.000012	5.00	99.5		84	47.11 ± 0.18
53F2d	1.50	2.528 ± 0.004	0.00557 ± 0.00009	0.000043 ± 0.000013	4.70	99.5		77	47.23 ± 0.20
53F2e	1.50	2.527 ± 0.004	0.00528 ± 0.00008	0.000063 ± 0.000022	5.55	99.2		81	47.10 ± 0.28
53F2f	1.50	2.536 ± 0.004	0.00570 ± 0.00018	0.000103 ± 0.000035	2.65	98.8		75	47.04 ± 0.41
53F2g	1.50	2.535 ± 0.003	0.00643 ± 0.00011	0.000059 ± 0.000017	4.00	99.3		67	47.26 ± 0.23
53F2h	1.50	2.536 ± 0.004	0.00687 ± 0.00021	0.000088 ± 0.000043	2.52	98.9		63	47.12 ± 0.50
53F2i	1.50	2.530 ± 0.003	0.00654 ± 0.00014	0.000008 ± 0.000035	1.91	99.9		66	47.46 ± 0.41
53F2j	1.50	2.531 ± 0.004	0.00668 ± 0.00009	0.000065 ± 0.000022	3.49	99.2		64	47.16 ± 0.28
53F2k	1.50	2.520 ± 0.004	0.00536 ± 0.00011	0.000021 ± 0.000022	4.45	99.7		80	47.20 ± 0.28
53F2l	1.50	2.532 ± 0.004	0.00739 ± 0.00011	0.000043 ± 0.000026	3.40	99.5		58	47.29 ± 0.32
53F2m	1.50	2.521 ± 0.004	0.00604 ± 0.00014	0.000051 ± 0.000028	3.24	99.4		71	47.05 ± 0.35
53F2n	1.50	2.535 ± 0.004	0.00482 ± 0.00014	0.000112 ± 0.000036	1.84	98.6		89	46.97 ± 0.43
53F2o	1.50	2.526 ± 0.003	0.00560 ± 0.00012	0.000032 ± 0.000019	3.25	99.6		77	47.24 ± 0.25
53F2p	1.50	2.523 ± 0.004	0.00550 ± 0.00015	0.000081 ± 0.000028	2.67	99.0		78	46.93 ± 0.34
53F2q	1.50	2.528 ± 0.005	0.00550 ± 0.00010	0.000028 ± 0.000015	4.20	99.6		78	47.30 ± 0.24
53F2r	1.50	2.524 ± 0.004	0.00599 ± 0.00008	0.000014 ± 0.000013	5.72	99.8		72	47.30 ± 0.20
53F2s	1.50	2.551 ± 0.003	0.00538 ± 0.00009	0.000130 ± 0.000022	6.06	98.5		80	47.18 ± 0.26
53F2t	1.50	2.524 ± 0.004	0.00657 ± 0.00009	0.000026 ± 0.000008	7.72	99.6		65	47.24 ± 0.16
53F2u	1.50	2.551 ± 0.004	0.00488 ± 0.00010	0.000148 ± 0.000029	2.87	98.2		88	47.06 ± 0.35
53F2v	1.50	2.539 ± 0.004	0.00590 ± 0.00011	0.000121 ± 0.000021	3.22	98.5		73	47.00 ± 0.27
53F2w	1.50	2.572 ± 0.007	0.00880 ± 0.00042	0.000193 ± 0.000070	1.21	97.7		49	47.22 ± 0.81
53F2x	1.50	2.513 ± 0.004	0.00538 ± 0.00010	0.000026 ± 0.000012	5.91	99.6		80	47.03 ± 0.19
53F2y	1.50	2.520 ± 0.004	0.00563 ± 0.00012	0.000061 ± 0.000023	2.88	99.2		76	46.98 ± 0.29
53F2z	1.50	2.516 ± 0.003	0.00484 ± 0.00010	0.000024 ± 0.000012	5.10	99.7		89	47.11 ± 0.18
53F2aa	1.50	2.520 ± 0.003	0.00534 ± 0.00011	0.000033 ± 0.000022	3.60	99.6		81	47.12 ± 0.27
53F2bb	1.50	2.539 ± 0.004	0.00645 ± 0.00015	0.000041 ± 0.000025	2.19	99.5		67	47.44 ± 0.31
53F2cc	1.50	2.518 ± 0.005	0.00501 ± 0.00016	0.000013 ± 0.000047	1.39	99.8		86	47.21 ± 0.54
53F2dd	1.50	2.526 ± 0.004	0.00688 ± 0.00015	0.000040 ± 0.000018	3.42	99.5		62	47.20 ± 0.25
53F2ee	1.50	2.515 ± 0.006	0.00582 ± 0.00015	0.000055 ± 0.000035	1.70	99.3		74	46.91 ± 0.44
53F2ff	1.50	2.528 ± 0.004	0.00491 ± 0.00011	0.000073 ± 0.000065	1.90	99.1		88	47.07 ± 0.72
53F2gg	1.50	2.521 ± 0.004	0.00570 ± 0.00013	0.000052 ± 0.000045	2.37	99.3		75	47.04 ± 0.52
53F2hh	1.50	2.560 ± 0.009	0.04693 ± 0.00102	0.000089 ± 0.000089	0.80	99.0		9	47.63 ± 1.03
53F2ii	1.50	2.535 ± 0.006	0.00682 ± 0.00018	0.000068 ± 0.000051	1.73	99.2		63	47.23 ± 0.60
Single crystal fusion ages									
Inverse isochron age ± 2σ		50.69 ± 0.42						Integrated age ± 2σ	47.17 ± 0.09
$^{40}Ar/^{39}Ar$ intercept ± 2σ		161.3 ± 74.5		MSWD 0.72				Weighted mean age ± 2σ	47.16 ± 0.08
Multi-crystal incremental heating experiments									
UW53Fjj: 5 crystals									
53F2jj1	0.06	2.616 ± 0.005	0.02648 ± 0.00037	0.000277 ± 0.000095	1.16	96.9	7.8	16	47.60 ± 1.06
53F2jj2	0.10	2.532 ± 0.004	0.00955 ± 0.00028	0.000053 ± 0.000035	2.30	99.3	16.1	45	47.25 ± 0.41
53F2jj3	0.20	2.515 ± 0.004	0.00540 ± 0.00009	0.000009 ± 0.000014	6.13	99.8	43.1	80	47.17 ± 0.20
53F2jj4	0.26	2.523 ± 0.004	0.00543 ± 0.00019	0.000025 ± 0.000036	1.79	99.7	12.6	79	47.23 ± 0.42
53F2jj5	1.50	2.522 ± 0.004	0.00519 ± 0.00011	0.000017 ± 0.000028	2.90	99.8	20.3	83	47.25 ± 0.33
Inverse isochron age ± 2σ		47.17 ± 0.22						Integrated age ± 2σ	47.24 ± 0.18
$^{40}Ar/^{39}Ar$ intercept ± 2σ		387.6 ± 273.6		MSWD 0.21				Plateau age ± 2σ	47.21 ± 0.16
UW53Fjj: 5 crystals									
53F2kk1	0.06	2.563 ± 0.005	0.02837 ± 0.00050	0.000122 ± 0.000072	1.30	98.6	7.4	15	47.48 ± 0.80
53F2kk2	0.10	2.518 ± 0.004	0.00708 ± 0.00015	0.000036 ± 0.000042	1.80	99.5	10.5	61	47.08 ± 0.49
53F2kk3	0.20	2.514 ± 0.004	0.00656 ± 0.00009	0.000022 ± 0.000009	9.18	99.7	53.8	66	47.08 ± 0.18
53F2kk4	0.26	2.531 ± 0.008	0.00653 ± 0.00034	0.000067 ± 0.000102	0.83	99.2	4.8	66	47.14 ± 1.15
53F2kk5	1.50	2.525 ± 0.003	0.00664 ± 0.00014	0.000012 ± 0.000032	4.01	99.8	23.4	65	47.33 ± 0.38
Inverse isochron age ± 2σ		46.97 ± 0.44						Integrated age ± 2σ	47.17 ± 0.18
$^{40}Ar/^{39}Ar$ intercept ± 2σ		644.4 ± 1101		MSWD 0.57				Plateau age ± 2σ	47.13 ± 0.16

Table DR3. Complete $^{40}Ar/^{39}Ar$ results

Sample Experiment	laser power (W)	$^{40}Ar/^{39}Ar$	$^{37}Ar/^{39}Ar$	$^{36}Ar/^{39}Ar$	$^{40}Ar^*$ X10^{-14} mol	$^{40}Ar^*$ %	$^{39}Ar_K$ %	K/Ca	Apparent Age ± 2σ Ma
Sage Creek Mountain pumice sand SCM sanidine continued									
Grand combinend sanidine ages									
Inverse isochron age ± 2σ		47.14 ± 0.10					Integrated age ± 2σ		47.17 ± 0.08
$^{40}Ar/^{39}Ar$ intercept ± 2σ		336.9 ± 84.9		MSWD 0.69			Weighted mean age ± 2σ		**47.17 ± 0.08**
Curly tuff GC-5b biotite *J* = 0.014647 ± 0.14% μ = 1.0022									
Single crystal incremental heating experiments									
* UW11F6a: 1 crystal (initial step yielded no measurable gas)									
11F6a	1.50	1.914 ± 0.004	0.00016 ± 0.00058	0.000135 ± 0.000075	0.59	97.7		2676	48.75 ± 1.16
* UW11F6b: 1 crystal (initial step yielded no measurable gas)									
11F6b	1.75	1.891 ± 0.016	0.00069 ± 0.00243	0.000081 ± 0.000143	0.25	98.5		621	48.55 ± 2.32
* UW11F6c: 1 crystal									
* 11F6c1	0.25	2.087 ± 0.019	0.00115 ± 0.00408	0.001225 ± 0.000416	0.12	82.4	20.5	375	44.90 ± 6.40
* 11F6c2	0.37	2.193 ± 0.014	0.00483 ± 0.01661	0.000379 ± 0.000311	0.19	94.7	32.0	89	54.07 ± 4.77
* 11F6c3	1.50	1.963 ± 0.008	0.00074 ± 0.00260	0.000185 ± 0.000213	0.25	97.0	47.4	580	49.61 ± 3.26
No isochron							Integrated age ± 2σ		50.07 ± 2.54
* UW11F6d: 1 crystal									
* 11F6d1	0.37	1.998 ± 0.010	0.00173 ± 0.00605	0.001286 ± 0.000305	0.16	80.7	13.1	248	42.12 ± 4.68
* 11F6d2	1.50	1.973 ± 0.003	0.00135 ± 0.00465	0.000217 ± 0.000064	1.02	96.5	86.9	318	49.64 ± 0.99
No isochron							Integrated age ± 2σ		48.66 ± 1.06
UW11F6e: 1 crystal									
11F6e1	0.40	2.079 ± 0.016	0.00061 ± 0.00203	0.001130 ± 0.000205	0.22	83.7	6.6	708	45.40 ± 3.24
11F6e2	0.55	1.972 ± 0.009	0.00010 ± 0.00044	0.000295 ± 0.000151	0.35	95.3	10.8	4351	49.01 ± 2.34
11F6e3	1.50	1.928 ± 0.004	0.00056 ± 0.00184	0.000136 ± 0.000024	2.60	97.7	82.5	768	49.08 ± 0.42
Inverse isochron age ± 2σ		50.69 ± 0.42					Integrated age ± 2σ		48.83 ± 0.48
$^{40}Ar/^{39}Ar$ intercept ± 2σ		161.3 ± 74.5		MSWD 2.55			Plateau age ± 2σ		49.02 ± 0.66
* UW11F6f: 1 crystal									
* 11F6f1	0.24	3.399 ± 0.020	0.00225 ± 0.00757	0.007637 ± 0.000263	0.34	33.5	18.2	191	29.81 ± 4.15
11F6f2	0.37	2.482 ± 0.021	0.00097 ± 0.00331	0.001700 ± 0.000295	0.24	79.6	17.7	445	51.46 ± 4.59
11F6f3	0.50	2.531 ± 0.020	0.00063 ± 0.00217	0.002086 ± 0.000510	0.25	75.5	18.0	683	49.77 ± 7.81
11F6f4	0.80	2.325 ± 0.013	0.00159 ± 0.00534	0.001397 ± 0.000139	0.39	82.1	30.7	271	49.71 ± 2.20
11F6f5	1.50	2.121 ± 0.022	0.00075 ± 0.00262	0.000479 ± 0.000292	0.18	93.1	15.4	577	51.44 ± 4.57
Inverse isochron age ± 2σ		50.69 ± 5.82					Integrated age ± 2σ		46.70 ± 2.04
$^{40}Ar/^{39}Ar$ intercept ± 2σ		282.3 ± 169.1		MSWD 0.27			Plateau age ± 2σ		50.24 ± 1.77
* UW11F6g: 1 crystal									
* 11F6g1	0.24	2.314 ± 0.014	0.00028 ± 0.00105	0.002041 ± 0.000172	0.32	73.7	15.8	1540	44.55 ± 2.71
11F6g2	0.37	1.972 ± 0.009	0.00029 ± 0.00099	0.000220 ± 0.000101	0.49	96.5	28.7	1496	49.59 ± 1.60
11F6g3	1.50	1.888 ± 0.005	0.00084 ± 0.00281	0.000083 ± 0.000049	0.90	98.5	55.5	514	48.46 ± 0.78
No isochron							Integrated age ± 2σ		48.16 ± 0.77
				MSWD 1.63			Plateau age ± 2σ		48.68 ± 0.90
UW11F6h: 1 crystal									
11F6h1	0.25	2.232 ± 0.012	0.00121 ± 0.00423	0.001896 ± 0.000352	0.20	74.7	16.8	357	43.54 ± 5.40
11F6h2	0.37	1.956 ± 0.005	0.00053 ± 0.00188	0.000357 ± 0.000146	0.32	94.4	30.6	816	48.13 ± 2.23
11F6h3	1.50	1.931 ± 0.005	0.00143 ± 0.00492	0.000135 ± 0.000132	0.54	97.7	52.6	301	49.17 ± 2.03
Inverse isochron age ± 2σ		49.45 ± 1.10					Integrated age ± 2σ		47.91 ± 1.56
$^{40}Ar/^{39}Ar$ intercept ± 2σ		172.4 ± 75.3		MSWD 1.94			Plateau age ± 2σ		48.33 ± 2.01

Table DR3. Complete $^{40}Ar/^{39}Ar$ results

Sample Experiment	laser power (W)	$^{40}Ar/^{39}Ar$	$^{37}Ar/^{39}Ar$	$^{36}Ar/^{39}Ar$	$^{40}Ar^*$ X10^{-14} mol	$^{40}Ar^*$ %	$^{39}Ar_K$ %	K/Ca	Apparent Age ± 2σ Ma
Curly tuff GC-5b biotite continued									
UW11F6i: 1 crystal									
11F6i1	0.37	1.957 ± 0.044	0.00200 ± 0.00704	0.000778 ± 0.000544	0.10	88.0	5.2	215	44.95 ± 8.58
11F6i2	1.50	1.941 ± 0.005	0.00047 ± 0.00163	0.000215 ± 0.000036	1.42	96.5	77.0	914	48.83 ± 0.59
11F6i3	1.75	1.949 ± 0.013	0.00203 ± 0.00706	0.000196 ± 0.000149	0.33	96.8	17.8	212	49.18 ± 2.37
Inverse isochron age ± 2σ		50.33 ± 0.94					Integrated age ± 2σ		48.69 ± 0.77
$^{40}Ar/^{39}Ar$ intercept ± 2σ		27.8 ± 89.9		MSWD 0.45			Plateau age ± 2σ		48.84 ± 0.58
UW11F6j: 1 crystal									
11F6j1	0.45	2.058 ± 0.031	0.00105 0.00370	0.000320 0.000320	0.14	95.2	13.4	410	51.02 ± 5.11
11F6j2	1.75	1.967 ± 0.006	0.00055 0.00193	0.000229 0.000045	0.85	96.3	86.6	775	49.39 ± 0.76
No isochron							Integrated age ± 2σ		49.61 ± 0.95
				MSWD 0.40			Plateau age ± 2σ		49.43 ± 0.75
Combined single crystal incremental heating ages									
Inverse isochron age ± 2σ		49.51 ± 0.37					Integrated age ± 2σ		48.55 ± 0.35
$^{40}Ar/^{39}Ar$ intercept ± 2σ		194.5 ± 59.4		MSWD 0.68			Weighted mean: plateau ages ± 2σ		**49.02 ± 0.30**
Multi-crystal incremental heating experiments									
* UW11F6k: 8 crystals									
* 11F6k1	0.12	2.262 ± 0.006	0.00061 ± 0.00239	0.002028 ± 0.000075	1.19	73.3	11.7	711	43.30 ± 1.17
11F6k2	0.20	1.991 ± 0.006	0.00011 ± 0.00044	0.000303 ± 0.000018	2.11	95.3	23.5	3899	49.44 ± 0.40
11F6k3	0.25	1.961 ± 0.006	0.00029 ± 0.00116	0.000176 ± 0.000033	1.54	97.1	17.5	1467	49.63 ± 0.60
11F6k4	0.30	1.931 ± 0.006	0.00094 ± 0.00371	0.000086 ± 0.000035	1.33	98.4	15.3	456	49.56 ± 0.62
11F6k5	0.40	1.915 ± 0.003	0.00089 ± 0.00350	0.000066 ± 0.000019	2.14	98.7	24.9	483	49.30 ± 0.33
11F6k6	0.50	1.896 ± 0.005	0.00106 ± 0.00421	0.000083 ± 0.000143	0.37	98.5	4.3	405	48.68 ± 2.19
11F6k7	1.50	1.931 ± 0.005	0.00003 ± 0.00091	0.000202 ± 0.000212	0.25	96.7	2.9	12537	48.66 ± 3.23
Inverse isochron age ± 2σ		49.30 ± 0.42					Integrated age ± 2σ		48.68 ± 0.28
$^{40}Ar/^{39}Ar$ intercept ± 2σ		321.3 ± 86.2		MSWD 0.38			Plateau age ± 2σ		49.40 ± 0.23
* UW11F6l: 5 crystals									
* 11F6l1	0.12	2.275 ± 0.008	0.00002 ± 0.00020	0.002191 ± 0.000041	1.47	71.3	18.9	17538	42.39 ± 0.73
* 11F6l2	0.20	2.048 ± 0.006	0.00027 ± 0.00108	0.000380 ± 0.000025	1.69	94.3	24.2	1578	50.33 ± 0.49
11F6l3	0.25	2.012 ± 0.006	0.00037 ± 0.00148	0.000315 ± 0.000040	1.15	95.1	16.6	1150	49.88 ± 0.68
11F6l4	0.30	1.946 ± 0.005	0.00124 ± 0.00488	0.000215 ± 0.000053	0.74	96.5	11.2	348	48.96 ± 0.85
11F6l5	1.50	1.928 ± 0.003	0.00062 ± 0.00245	0.000094 ± 0.000029	1.92	98.3	29.1	692	49.40 ± 0.47
Inverse isochron age ± 2σ		49.03 ± 1.11					Integrated age ± 2σ		48.45 ± 0.44
$^{40}Ar/^{39}Ar$ intercept ± 2σ		390.1 ± 224.3		MSWD 1.54			Plateau age ± 2σ		49.33 ± 0.28
* UW11F6m: 5 crystals									
* 11F6m1	0.12	2.418 ± 0.008	0.00116 ± 0.00461	0.002985 ± 0.000152	0.34	63.3	6.0	371	40.01 ± 2.34
11F6m2	0.16	2.021 ± 0.005	0.00087 ± 0.00347	0.000512 ± 0.000100	0.42	92.3	8.9	495	48.62 ± 1.54
11F6m3	0.22	1.996 ± 0.007	0.00003 ± 0.00028	0.000277 ± 0.000046	0.93	95.7	20.1	13190	49.77 ± 0.78
11F6m4	0.28	1.936 ± 0.006	0.00197 ± 0.00777	0.000210 ± 0.000043	0.76	96.6	17.1	218	48.74 ± 0.72
11F6m5	0.40	1.912 ± 0.005	0.00070 ± 0.00277	0.000102 ± 0.000018	1.95	98.2	44.0	612	48.93 ± 0.39
11F6m6	1.50	1.934 ± 0.008	0.00164 ± 0.00657	0.000055 ± 0.000354	0.18	98.9	4.0	262	49.85 ± 5.39
Inverse isochron age ± 2σ		48.67 ± 0.75					Integrated age ± 2σ		48.54 ± 0.40
$^{40}Ar/^{39}Ar$ intercept ± 2σ		379.6 ± 167.6		MSWD 1.10			Plateau age ± 2σ		49.02 ± 0.35

Table DR3. Complete $^{40}Ar/^{39}Ar$ results

Sample Experiment	laser power (W)	$^{40}Ar/^{39}Ar$	$^{37}Ar/^{39}Ar$	$^{36}Ar/^{39}Ar$	$^{40}Ar^*$ X10^{-14} mol	$^{40}Ar^*$ %	$^{39}Ar_K$ %	K/Ca	Apparent Age ± 2σ Ma
Curly tuff GC-5b biotite continued									
* UW11F6n: 5 crystals									
* 11F6n1	0.08	3.716 ± 0.029	0.00160 ± 0.00697	0.009729 ± 0.000577	0.13	22.5	1.8	269	21.96 ± 8.96
11F6n2	0.16	2.189 ± 0.005	0.00031 ± 0.00158	0.001137 ± 0.000135	0.32	84.4	7.3	1372	48.19 ± 2.07
11F6n3	0.22	1.984 ± 0.006	0.00029 ± 0.00118	0.000205 ± 0.000056	0.73	96.7	18.4	1478	50.00 ± 0.91
11F6n4	0.30	1.931 ± 0.004	0.00052 ± 0.00207	0.000103 ± 0.000042	0.97	98.2	25.2	827	49.41 ± 0.67
11F6n5	0.40	1.916 ± 0.004	0.00112 ± 0.00444	0.000132 ± 0.000052	0.73	97.7	19.1	383	48.80 ± 0.82
11F6n6	1.50	1.901 ± 0.003	0.00030 ± 0.00119	0.000006 ± 0.000034	1.06	99.7	28.1	1444	49.39 ± 0.55
Inverse isochron age ± 2σ		49.38 ± 0.51					Integrated age ± 2σ		48.82 ± 0.40
$^{40}Ar/^{39}Ar$ intercept ± 2σ		283.3 ± 92.5		MSWD 1.30			Plateau age ± 2σ		49.35 ± 0.40
* UW11F6o: 7 crystals									
* 11F6o1	0.08	3.147 ± 0.020	0.00092 ± 0.00398	0.008085 ± 0.000538	0.22	23.9	1.5	466	19.81 ± 8.31
* 11F6o2	0.16	2.457 ± 0.010	0.00068 ± 0.00272	0.002651 ± 0.000111	0.64	67.9	5.7	636	43.58 ± 1.75
11F6o3	0.20	2.114 ± 0.007	0.00013 ± 0.00065	0.000698 ± 0.000073	0.84	90.0	8.7	3254	49.61 ± 1.15
11F6o4	0.28	2.031 ± 0.005	0.00033 ± 0.00131	0.000388 ± 0.000030	1.67	94.1	18.1	1297	49.82 ± 0.52
11F6o5	0.35	1.967 ± 0.005	0.00056 ± 0.00223	0.000218 ± 0.000024	1.69	96.5	18.9	764	49.46 ± 0.44
11F6o6	0.43	1.939 ± 0.004	0.00067 ± 0.00263	0.000155 ± 0.000033	1.75	97.4	19.8	645	49.22 ± 0.54
11F6o7	0.50	1.928 ± 0.005	0.00036 ± 0.00143	0.000120 ± 0.000028	1.39	97.9	15.9	1194	49.20 ± 0.50
11F6o8	1.50	1.925 ± 0.004	0.00018 ± 0.00073	0.000126 ± 0.000040	1.00	97.8	11.4	2431	49.09 ± 0.64
Inverse isochron age ± 2σ		49.02 ± 0.53					Integrated age ± 2σ		48.63 ± 0.28
$^{40}Ar/^{39}Ar$ intercept ± 2σ		359.5 ± 78.4		MSWD 0.97			Plateau age ± 2σ		49.39 ± 0.24
Combined incremental heating ages				MSWD 1.00			Weighted mean: integrated ages ± 2σ		48.65 ± 0.14
Wavy tuff GC-2b biotite J = 0.014356 ± 0.24% μ = 1.0035									
5 crystal fusions									
5A6a	1.50	2.277 0.004	0.01698 0.00043	0.001286 0.000015	13.53	83.2		25	48.38 ± 0.29
5A6b	1.50	2.276 0.003	0.01610 0.00040	0.001297 0.000017	11.98	83.0		27	48.29 ± 0.28
5A6c	1.50	2.171 0.003	0.01255 0.00033	0.000927 0.000027	13.27	87.2		34	48.38 ± 0.43
5A6d	1.50	2.172 0.006	0.01805 0.00047	0.000924 0.000025	12.03	87.3		24	48.45 ± 0.46
5A6e	1.50	2.145 0.003	0.02639 0.00058	0.000845 0.000015	10.88	88.2		16	48.38 ± 0.25
5A6f	1.50	2.233 0.005	0.01575 0.00043	0.001093 0.000019	9.54	85.4		27	48.73 ± 0.37
5A6g	1.50	2.150 0.004	0.01549 0.00037	0.000808 0.000014	14.17	88.7		28	48.76 ± 0.29
* 5A6h	1.50	2.187 0.006	0.01064 0.00030	0.000930 0.000017	8.89	87.3		40	48.77 ± 0.38
* 5A6i	1.50	2.127 0.006	0.01640 0.00045	0.000709 0.000025	7.78	90.0		26	48.90 ± 0.48
Inverse isochron age ± 2σ		48.83 ± 0.71					Integrated age ± 2σ		48.54 ± 0.17
$^{40}Ar/^{39}Ar$ intercept ± 2σ		281.6 ± 26.6		MSWD 1.45			Weighted mean age ± 2σ		48.47 ± 0.18
Single crystal fusions J = 0.022229 ± 0.12% μ = 1.0035									
6-6a	1.50	1.335 ± 0.003	0.01245 ± 0.00013	0.000321 ± 0.000006	6.75	92.6		35	48.91 ± 0.25
* 6-6b	1.50	1.291 ± 0.006	0.03774 ± 0.00049	0.000056 ± 0.000025	1.48	98.6		11	50.34 ± 0.72
6-6c	1.50	1.334 ± 0.005	0.01972 ± 0.00025	0.000319 ± 0.000026	1.74	92.7		22	48.91 ± 0.72
6-6d	1.50	1.265 ± 0.003	0.01189 ± 0.00016	0.000157 ± 0.000023	2.21	96.0		36	48.07 ± 0.58
6-6e	1.50	1.261 ± 0.005	0.00509 ± 0.00008	0.000121 ± 0.000018	2.00	96.8		84	48.30 ± 0.56
6-6f	1.50	1.412 ± 0.003	0.03643 ± 0.00036	0.000596 ± 0.000020	2.57	87.4		12	48.81 ± 0.50
6-6g	1.50	1.288 ± 0.003	0.01605 ± 0.00016	0.000198 ± 0.000014	3.16	95.2		27	48.53 ± 0.38
6-6h	1.50	1.275 ± 0.006	0.01400 ± 0.00015	0.000123 ± 0.000015	2.65	96.9		31	48.85 ± 0.57
6-6i	1.50	1.274 ± 0.002	0.01862 ± 0.00026	0.000141 ± 0.000065	1.05	96.5		23	48.65 ± 1.52
6-6j	1.50	1.269 ± 0.005	0.01586 ± 0.00016	0.000110 ± 0.000021	2.25	97.2		27	48.80 ± 0.64
* 6-6k	1.50	1.326 ± 0.002	0.00371 ± 0.00007	0.000252 ± 0.000016	3.02	94.1		116	49.33 ± 0.39
6-6l	1.50	1.326 ± 0.006	0.04157 ± 0.00040	0.000337 ± 0.000018	2.91	92.4		10	48.47 ± 0.63
* 6-6m	1.50	1.291 ± 0.004	0.00680 ± 0.00028	0.000533 ± 0.000080	0.49	87.5		63	44.74 ± 1.88
6-6n	1.50	1.288 ± 0.004	0.03766 ± 0.00063	0.000182 ± 0.000036	1.13	95.7		11	48.76 ± 0.88
6-6o	1.50	1.279 ± 0.004	0.00524 ± 0.00039	0.000222 ± 0.000110	0.43	94.5		82	47.85 ± 2.56
6-6p	1.50	1.261 ± 0.005	0.00271 ± 0.00010	0.000166 ± 0.000032	1.37	95.8		159	47.78 ± 0.83
6-6q	1.50	1.310 ± 0.005	0.00045 ± 0.00023	0.000216 ± 0.000084	0.60	94.8		959	49.12 ± 1.96
6-6r	1.50	1.246 ± 0.002	0.00142 ± 0.00019	0.000086 ± 0.000062	0.77	97.6		303	48.12 ± 1.45
6-6s	1.50	1.263 ± 0.007	0.01012 ± 0.00021	0.000130 ± 0.000050	0.77	96.7		42	48.31 ± 1.26

Table DR3. Complete $^{40}Ar/^{39}Ar$ results

Sample Experiment	laser power (W)	$^{40}Ar/^{39}Ar$	$^{37}Ar/^{39}Ar$	$^{36}Ar/^{39}Ar$	$^{40}Ar^*$ X10^{-14} mol	$^{40}Ar^*$ %	$^{39}Ar_K$ %	K/Ca	Apparent Age ± 2σ Ma
Wavy tuff GC-2b biotite continued									
6-6t	1.50	1.252 ± 0.005	0.00080 ± 0.00022	0.000006 ± 0.000092	0.53	99.5		534	49.28 ± 2.15
6-6u	1.50	1.271 ± 0.002	0.01078 ± 0.00016	0.000183 ± 0.000037	1.57	95.4		40	48.01 ± 0.87
6-6v	1.50	1.395 ± 0.003	0.01064 ± 0.00032	0.000583 ± 0.000097	0.52	87.4		40	48.21 ± 2.25
6-6w	1.50	1.341 ± 0.002	0.00549 ± 0.00032	0.000331 ± 0.000071	0.81	92.4		78	49.02 ± 1.65
6-6x	1.50	1.282 ± 0.002	0.00226 ± 0.00016	0.000199 ± 0.000060	0.75	95.1		190	48.23 ± 1.40
6-6y	1.50	1.276 ± 0.003	0.00336 ± 0.00026	0.000310 ± 0.000060	0.66	92.5		128	46.72 ± 1.40
6-6z	1.50	1.297 ± 0.003	0.00356 ± 0.00015	0.000194 ± 0.000069	0.82	95.2		121	48.87 ± 1.60
6-6aa	1.50	1.445 ± 0.003	0.01177 ± 0.00028	0.000832 ± 0.000032	1.49	82.7		37	47.34 ± 0.77
6-6bb	1.50	1.319 ± 0.003	0.00449 ± 0.00031	0.000277 ± 0.000135	0.49	93.5		96	48.77 ± 3.12
6-6cc	1.50	1.271 ± 0.003	0.00332 ± 0.00020	0.000141 ± 0.000058	0.91	96.4		129	48.46 ± 1.37
6-6dd	1.50	1.380 ± 0.004	0.00370 ± 0.00041	0.000507 ± 0.000138	0.41	88.8		116	48.51 ± 3.19
6-6ee	1.50	1.288 ± 0.003	0.00765 ± 0.00020	0.000215 ± 0.000032	1.16	94.8		56	48.31 ± 0.76
6-6ff	1.50	1.371 ± 0.003	0.00567 ± 0.00040	0.000442 ± 0.000141	0.36	90.2		76	48.89 ± 3.27
6-6gg	1.50	1.262 ± 0.002	0.00265 ± 0.00015	0.000131 ± 0.000046	1.20	96.6		162	48.21 ± 1.08
6-6hh	1.50	1.275 ± 0.003	0.01222 ± 0.00024	0.000191 ± 0.000058	0.94	95.3		35	48.08 ± 1.36
6-6ii	1.50	1.379 ± 0.005	0.00448 ± 0.00013	0.000455 ± 0.000041	1.44	89.9		96	49.04 ± 1.01
6-6jj	1.50	1.257 ± 0.002	0.00720 ± 0.00012	0.000059 ± 0.000024	2.07	98.3		60	48.86 ± 0.57
6-6kk	1.50	1.308 ± 0.003	0.01650 ± 0.00023	0.000211 ± 0.000039	1.38	95.0		26	49.14 ± 0.93
6-6ll	1.50	1.283 ± 0.003	0.00531 ± 0.00012	0.000188 ± 0.000023	2.13	95.4		81	48.41 ± 0.57
6-6mm	1.50	1.468 ± 0.004	0.00227 ± 0.00017	0.000754 ± 0.000063	0.95	84.5		189	49.08 ± 1.49
6-6nn	1.50	1.325 ± 0.002	0.03246 ± 0.00046	0.000383 ± 0.000029	1.65	91.3		13	47.87 ± 0.70
6-6oo	1.50	1.268 ± 0.003	0.00563 ± 0.00020	0.000202 ± 0.000035	1.37	95.0		76	47.65 ± 0.84
6-6pp	1.50	1.318 ± 0.003	0.00457 ± 0.00013	0.000300 ± 0.000037	1.44	93.0		94	48.47 ± 0.88
6-6qq	1.50	1.276 ± 0.002	0.00286 ± 0.00009	0.000176 ± 0.000022	2.14	95.6		150	48.24 ± 0.54
6-6rr	1.50	1.413 ± 0.007	0.00666 ± 0.00026	0.000573 ± 0.000108	0.53	87.7		65	49.04 ± 2.55
6-6ss	1.50	1.359 ± 0.003	0.00830 ± 0.00013	0.000458 ± 0.000027	2.22	89.7		52	48.26 ± 0.67
* 6-6tt	1.50	1.880 ± 0.004	0.00780 ± 0.00016	0.002560 ± 0.000037	2.76	59.5		55	44.33 ± 0.86
6-6uu	1.50	1.379 ± 0.003	0.01552 ± 0.00035	0.000462 ± 0.000042	1.60	89.9		28	49.03 ± 1.00
6-6vv	1.50	1.392 ± 0.002	0.01536 ± 0.00020	0.000565 ± 0.000029	2.60	87.8		28	48.34 ± 0.68
6-6ww	1.50	1.372 ± 0.003	0.01027 ± 0.00022	0.000447 ± 0.000043	1.43	90.1		42	48.88 ± 1.02
6-6xx	1.50	1.357 ± 0.003	0.01246 ± 0.00024	0.000379 ± 0.000049	1.27	91.5		35	49.11 ± 1.15
6-6yy	1.50	1.387 ± 0.005	0.03095 ± 0.00044	0.000535 ± 0.000043	1.74	88.4		14	48.55 ± 1.05
6-6zz	1.50	1.391 ± 0.003	0.00502 ± 0.00014	0.000516 ± 0.000046	1.35	88.7		86	48.83 ± 1.08
6-6aaa	1.50	1.272 ± 0.003	0.02947 ± 0.00045	0.000166 ± 0.000036	1.71	96.0		15	48.29 ± 0.86
6-6bbb	1.50	1.790 ± 0.005	0.00518 ± 0.00011	0.002003 ± 0.000055	1.76	66.7		83	47.24 ± 1.32
Single crystal fusion ages									
Inverse isochron age ± 2σ		48.56 ± 0.24				Integrated age ± 2σ			48.44 ± 0.16
$^{40}Ar/^{39}Ar$ intercept ± 2σ		293.4 ± 14.9		MSWD 1.31		Weighted mean age ± 2σ			48.53 ± 0.17
Single crystal incremental heating experiments J = 0.009489 ± 0.16% μ = 1.0050									
* UW39E4ba: 1 crystal									
* 39E4ba1	0.10	11.203 ± 0.047	0.01675 ± 0.00130	0.030285 ± 0.000889	0.58	20.1	1.0	26	38.19 ± 8.88
39E4ba2	0.15	3.821 ± 0.019	0.00897 ± 0.00074	0.003705 ± 0.000366	0.43	71.3	2.1	48	46.08 ± 3.65
39E4ba3	0.20	3.459 ± 0.014	0.00738 ± 0.00049	0.001960 ± 0.000192	0.76	83.2	4.0	58	48.63 ± 1.94
39E4ba4	0.36	3.066 ± 0.005	0.03114 ± 0.00031	0.000553 ± 0.000027	5.07	94.7	30.5	14	49.04 ± 0.30
39E4ba5	0.64	2.925 ± 0.005	0.07901 ± 0.00066	0.000248 ± 0.000013	9.81	97.7	61.8	5	48.27 ± 0.20
39E4ba6	1.50	3.179 ± 0.027	0.64223 ± 0.00899	0.001483 ± 0.001386	0.10	87.8	0.6	1	47.16 ± 13.70
Inverse isochron age ± 2σ		48.17 ± 0.67							
$^{40}Ar/^{39}Ar$ intercept ± 2σ		351.7 ± 99.8				Integrated age ± 2σ			48.37 ± 0.23
* UW39E4bb: 1 crystal									
* 39E4bb1	0.13	9.948 ± 0.069	0.33249 ± 0.00512	0.030066 ± 0.000915	0.45	10.9	2.3	1	18.55 ± 9.12
39E4bb2	0.26	3.745 ± 0.017	0.03610 ± 0.00092	0.003223 ± 0.000168	0.65	74.6	8.7	12	47.22 ± 1.71
39E4bb3	0.36	3.218 ± 0.008	0.00861 ± 0.00037	0.001104 ± 0.000135	0.89	89.9	13.9	50	48.83 ± 1.35
39E4bb4	0.45	3.146 ± 0.010	0.00797 ± 0.00034	0.000803 ± 0.000140	0.95	92.4	15.0	54	49.12 ± 1.41
39E4bb5	0.56	3.033 ± 0.010	0.02015 ± 0.00041	0.000696 ± 0.000114	0.87	93.2	14.4	21	47.77 ± 1.17
39E4bb6	1.50	2.983 ± 0.005	0.02232 ± 0.00030	0.000321 ± 0.000036	2.72	96.8	45.7	19	48.79 ± 0.40
Inverse isochron age ± 2σ		48.90 ± 0.48				Integrated age ± 2σ			47.88 ± 0.46
$^{40}Ar/^{39}Ar$ intercept ± 2σ		268.9 ± 35.7		MSWD 1.51		Plateau age ± 2σ			48.66 ± 0.43

Table DR3. Complete $^{40}Ar/^{39}Ar$ results

Sample Experiment	laser power (W)	$^{40}Ar/^{39}Ar$	$^{37}Ar/^{39}Ar$	$^{36}Ar/^{39}Ar$	$^{40}Ar^*$ X10^{-14} mol	$^{40}Ar^*$ %	$^{39}Ar_K$ %	K/Ca	Apparent Age ± 2σ Ma
Wavy tuff GC-2b biotite continued									
#* UW39E4bc: 1 crystal									
* 39E4bc1	0.13	6.630 ± 0.017	0.00808 ± 0.00099	0.015815 ± 0.000342	0.88	29.5	7.4	53	33.19 ± 3.40
39E4bc2	0.26	3.726 ± 0.009	0.00589 ± 0.00035	0.003104 ± 0.000106	1.40	75.4	21.0	73	47.45 ± 1.07
39E4bc3	0.36	3.374 ± 0.011	0.00571 ± 0.00062	0.001831 ± 0.000157	0.82	84.0	13.5	75	47.85 ± 1.58
39E4bc4	0.48	3.623 ± 0.009	0.01136 ± 0.00044	0.002629 ± 0.000119	1.20	78.6	18.5	38	48.07 ± 1.19
39E4bc5	0.59	3.414 ± 0.011	0.05299 ± 0.00075	0.002080 ± 0.000088	1.68	82.1	27.4	8	47.36 ± 0.92
39E4bc6	1.50	3.334 ± 0.013	0.12653 ± 0.00172	0.001839 ± 0.000174	0.73	84.0	12.3	3	47.30 ± 1.77
Inverse isochron age ± 2σ		47.20 ± 2.74				Integrated age ± 2σ			46.53 ± 0.57
$^{40}Ar/^{39}Ar$ intercept ± 2σ		305.1 ± 67.9		MSWD 0.30		Plateau age ± 2σ			47.58 ± 0.54
#* UW39E4bd: 1 crystal									
* 39E4bd1	0.13	6.319 ± 0.054	0.01029 ± 0.00299	0.015600 ± 0.000726	0.39	27.0	2.0	42	29.02 ± 7.28
* 39E4bd2	0.26	3.375 ± 0.007	0.00471 ± 0.00046	0.002067 ± 0.000096	1.22	81.9	11.9	91	46.69 ± 0.97
39E4bd3	0.36	3.015 ± 0.007	0.00341 ± 0.00033	0.000449 ± 0.000061	1.56	95.6	17.0	126	48.67 ± 0.64
39E4bd4	0.48	3.098 ± 0.006	0.00610 ± 0.00034	0.000832 ± 0.000069	1.61	92.1	17.2	70	48.17 ± 0.71
39E4bd5	0.59	2.985 ± 0.011	0.01170 ± 0.00047	0.000605 ± 0.000116	0.85	94.0	9.4	37	47.41 ± 1.19
39E4bd6	1.50	2.965 ± 0.007	0.03597 ± 0.00050	0.000403 ± 0.000029	3.82	96.0	42.5	12	48.10 ± 0.36
Inverse isochron age ± 2σ		47.96 ± 1.37				Integrated age ± 2σ			47.59 ± 0.32
$^{40}Ar/^{39}Ar$ intercept ± 2σ		322.7 ± 172.3		MSWD 1.40		Plateau age ± 2σ			48.18 ± 0.34
UW39E4be: 1 crystal									
39E4be1	0.13	9.542 ± 0.229	0.20691 ± 0.01640	0.027134 ± 0.003415	0.11	16.1	0.8	2	26.16 ± 34.41
39E4be2	0.26	3.941 ± 0.026	0.01289 ± 0.00146	0.003801 ± 0.000344	0.45	71.5	7.5	33	47.61 ± 3.48
39E4be3	0.36	3.032 ± 0.014	0.00531 ± 0.00089	0.000502 ± 0.000171	0.63	95.1	13.6	81	48.69 ± 1.75
39E4be4	0.48	3.033 ± 0.014	0.00820 ± 0.00057	0.000642 ± 0.000203	0.69	93.7	14.9	52	48.03 ± 2.06
39E4be5	0.59	2.981 ± 0.017	0.01164 ± 0.00134	0.000592 ± 0.000183	0.51	94.1	11.2	37	47.41 ± 1.89
39E4be6	1.50	2.944 ± 0.005	0.01627 ± 0.00034	0.000296 ± 0.000051	2.32	97.0	52.0	26	48.25 ± 0.52
Inverse isochron age ± 2σ		48.36 ± 0.53				Integrated age ± 2σ			47.97 ± 0.64
$^{40}Ar/^{39}Ar$ intercept ± 2σ		271.9 ± 43.6		MSWD 0.57		Plateau age ± 2σ			48.20 ± 0.47
UW39E4bf: 1 crystal									
* 39E4bf1	0.13	14.024 ± 0.132	0.18811 ± 0.00672	0.042003 ± 0.001439	0.40	11.6	1.5	2	27.63 ± 14.30
39E4bf2	0.26	4.510 ± 0.028	0.01913 ± 0.00158	0.006053 ± 0.000353	0.37	60.4	4.2	22	46.00 ± 3.58
39E4bf3	0.36	3.629 ± 0.021	0.00976 ± 0.00091	0.002589 ± 0.000259	0.51	78.9	7.2	44	48.37 ± 2.62
39E4bf4	0.48	3.170 ± 0.012	0.00848 ± 0.00107	0.000852 ± 0.000200	0.64	92.0	10.4	51	49.27 ± 2.01
39E4bf5	0.59	3.113 ± 0.016	0.01069 ± 0.00059	0.000791 ± 0.000123	0.78	92.5	12.9	40	48.64 ± 1.31
39E4bf6	1.50	2.939 ± 0.007	0.03848 ± 0.00054	0.000327 ± 0.000023	3.67	96.8	63.9	11	48.05 ± 0.32
Inverse isochron age ± 2σ		48.15 ± 0.40				Integrated age ± 2σ			47.89 ± 0.47
$^{40}Ar/^{39}Ar$ intercept ± 2σ		388.6 ± 34.0		MSWD 0.89		Plateau age ± 2σ			48.10 ± 0.31
* UW39E4bg: 1 crystal									
* 39E4bg1	0.13	11.384 ± 0.154	0.05522 ± 0.00864	0.033967 ± 0.001573	0.21	11.9	1.2	8	22.98 ± 15.84
39E4bg2	0.26	4.754 ± 0.041	0.01081 ± 0.00121	0.006877 ± 0.000527	0.42	57.3	5.9	40	46.00 ± 5.32
39E4bg3	0.36	3.269 ± 0.018	0.00577 ± 0.00111	0.001369 ± 0.000192	0.54	87.6	10.9	74	48.37 ± 1.97
39E4bg4	0.48	3.146 ± 0.010	0.00462 ± 0.00054	0.000790 ± 0.000154	0.84	92.6	17.7	93	49.17 ± 1.54
39E4bg5	0.59	3.082 ± 0.018	0.00679 ± 0.00124	0.000909 ± 0.000191	0.49	91.3	10.5	63	47.53 ± 1.98
39E4bg6	1.50	2.951 ± 0.007	0.01310 ± 0.00041	0.000328 ± 0.000044	2.41	96.7	53.8	33	48.22 ± 0.48
Inverse isochron age ± 2σ		48.34 ± 0.55				Integrated age ± 2σ			47.89 ± 0.61
$^{40}Ar/^{39}Ar$ intercept ± 2σ		285.6 ± 43.2		MSWD 0.67		Plateau age ± 2σ			48.25 ± 0.44

Table DR3. Complete $^{40}Ar/^{39}Ar$ results

Sample Experiment	laser power (W)	$^{40}Ar/^{39}Ar$	$^{37}Ar/^{39}Ar$	$^{36}Ar/^{39}Ar$	$^{40}Ar^*$ X10^{-14} mol	$^{40}Ar^*$ %	$^{39}Ar_K$ %	K/Ca	Apparent Age ± 2σ Ma
Wavy tuff GC-2b biotite continued									
#* UW39E4bh: 1 crystal									
* 39E4bh1	0.13	7.128 ± 0.037	0.00865 ± 0.00217	0.017399 ± 0.000478	0.54	27.9	4.0	50	33.69 ± 4.80
* 39E4bh2	0.26	4.088 ± 0.014	0.00806 ± 0.00046	0.004786 ± 0.000133	1.16	65.4	15.0	53	45.19 ± 1.36
39E4bh3	0.36	3.533 ± 0.011	0.01010 ± 0.00051	0.002307 ± 0.000179	0.89	80.7	13.3	43	48.16 ± 1.80
39E4bh4	0.48	3.711 ± 0.012	0.01401 ± 0.00045	0.003061 ± 0.000102	1.05	75.6	14.9	31	47.41 ± 1.07
39E4bh5	0.59	3.549 ± 0.017	0.03401 ± 0.00119	0.002479 ± 0.000227	0.79	79.4	11.8	13	47.61 ± 2.29
39E4bh6	1.50	3.451 ± 0.008	0.13128 ± 0.00166	0.002300 ± 0.000064	2.68	80.6	41.1	3	46.99 ± 0.66
Inverse isochron age ± 2σ		45.84 ± 4.25				Integrated age ± 2σ			46.48 ± 0.56
$^{40}Ar/^{39}Ar$ intercept ± 2σ		329.0 ± 104.9		MSWD 0.60		Plateau age ± 2σ			47.22 ± 0.53
* UW39E4bi: 1 crystal									
* 39E4bi1	0.13	9.099 ± 0.094	0.22826 ± 0.00754	0.024025 ± 0.001640	0.28	22.2	1.6	2	34.21 ± 16.39
* 39E4bi2	0.26	4.484 ± 0.015	0.02878 ± 0.00108	0.005883 ± 0.000206	0.78	61.3	9.2	15	46.42 ± 2.08
39E4bi3	0.36	3.597 ± 0.010	0.00907 ± 0.00060	0.002474 ± 0.000101	1.28	79.7	18.7	47	48.41 ± 1.04
39E4bi4	0.48	3.424 ± 0.009	0.01117 ± 0.00050	0.001779 ± 0.000076	1.15	84.6	17.7	38	48.95 ± 0.80
39E4bi5	0.59	3.230 ± 0.018	0.03051 ± 0.00116	0.001161 ± 0.000172	0.53	89.4	8.6	14	48.78 ± 1.78
39E4bi6	1.50	3.073 ± 0.006	0.05949 ± 0.00082	0.000730 ± 0.000040	2.58	93.1	44.2	7	48.32 ± 0.44
Inverse isochron age ± 2σ		48.19 ± 0.76				Integrated age ± 2σ			48.09 ± 0.48
$^{40}Ar/^{39}Ar$ intercept ± 2σ		330.5 ± 35.1		MSWD 0.68		Plateau age ± 2σ			48.47 ± 0.36
UW39E4bj: 1 crystal									
39E4bj1	0.13	12.453 ± 0.153	0.02136 ± 0.00826	0.033702 ± 0.001823	0.20	20.0	0.8	20	42.22 ± 18.39
39E4bj2	0.26	3.974 ± 0.023	0.00725 ± 0.00103	0.003584 ± 0.000292	0.51	73.3	6.6	59	49.21 ± 2.95
39E4bj3	0.36	3.067 ± 0.012	0.00602 ± 0.00061	0.000536 ± 0.000109	0.95	94.8	15.9	71	49.11 ± 1.14
39E4bj4	0.48	3.047 ± 0.008	0.00590 ± 0.00042	0.000519 ± 0.000095	1.21	95.0	20.5	73	48.87 ± 0.96
39E4bj5	0.59	2.973 ± 0.013	0.02753 ± 0.00072	0.000373 ± 0.000178	0.65	96.3	11.3	16	48.37 ± 1.81
39E4bj6	1.50	2.950 ± 0.006	0.04907 ± 0.00073	0.000298 ± 0.000038	2.58	97.1	44.9	9	48.39 ± 0.42
Inverse isochron age ± 2σ		48.54 ± 0.41				Integrated age ± 2σ			48.60 ± 0.46
$^{40}Ar/^{39}Ar$ intercept ± 2σ		294.8 ± 28.1		MSWD 0.54		Plateau age ± 2σ			48.53 ± 0.36
#* UW39E4bk: 1 crystal									
* 39E4bk1	0.13	8.666 ± 0.032	0.17869 ± 0.00289	0.022604 ± 0.000479	0.96	23.1	3.7	2	33.92 ± 4.78
* 39E4bk2	0.26	3.697 ± 0.008	0.02253 ± 0.00048	0.003041 ± 0.000107	1.57	75.7	14.2	19	47.29 ± 1.08
39E4bk3	0.36	3.236 ± 0.006	0.00842 ± 0.00028	0.001214 ± 0.000041	2.22	88.9	22.9	51	48.59 ± 0.45
39E4bk4	0.48	3.104 ± 0.007	0.02417 ± 0.00041	0.000929 ± 0.000075	1.87	91.2	20.1	18	47.81 ± 0.76
39E4bk5	0.59	3.040 ± 0.007	0.04519 ± 0.00060	0.000620 ± 0.000037	2.71	94.1	29.7	9	48.29 ± 0.42
39E4bk6	1.50	2.976 ± 0.012	0.03855 ± 0.00082	0.000529 ± 0.000109	0.84	94.8	9.4	11	47.68 ± 1.15
Inverse isochron age ± 2σ		47.70 ± 1.09				Integrated age ± 2σ			47.54 ± 0.35
$^{40}Ar/^{39}Ar$ intercept ± 2σ		337.2 ± 71.7		MSWD 1.48		Plateau age ± 2σ			48.31 ± 0.35
#* UW39E4bl: 1 crystal									
* 39E4bl1	0.13	5.454 ± 0.024	0.09131 ± 0.00164	0.011287 ± 0.000328	0.88	39.0	9.4	5	36.02 ± 3.34
39E4bl2	0.26	3.573 ± 0.014	0.01379 ± 0.00059	0.002506 ± 0.000120	1.20	79.3	19.5	31	47.86 ± 1.25
39E4bl3	0.36	3.301 ± 0.015	0.00967 ± 0.00055	0.001530 ± 0.000103	1.26	86.3	22.1	44	48.12 ± 1.12
39E4bl4	0.48	3.118 ± 0.008	0.01317 ± 0.00029	0.001052 ± 0.000079	1.82	90.0	33.8	33	47.44 ± 0.83
39E4bl5	0.59	3.075 ± 0.024	0.00818 ± 0.00096	0.000742 ± 0.000246	0.52	92.9	9.8	52	48.23 ± 2.56
39E4bl6	1.50	3.142 ± 0.040	0.02039 ± 0.00164	0.000775 ± 0.000486	0.29	92.7	5.3	21	49.20 ± 4.96
Inverse isochron age ± 2σ		47.42 ± 1.60				Integrated age ± 2σ			46.77 ± 0.66
$^{40}Ar/^{39}Ar$ intercept ± 2σ		309.7 ± 61.6		MSWD 0.38		Plateau age ± 2σ			47.76 ± 0.57

Table DR3. Complete $^{40}Ar/^{39}Ar$ results

Sample Experiment	laser power (W)	$^{40}Ar/^{39}Ar$	$^{37}Ar/^{39}Ar$	$^{36}Ar/^{39}Ar$	$^{40}Ar^*$ X10^{-14} mol	$^{40}Ar^*$ %	$^{39}Ar_K$ %	K/Ca	Apparent Age ± 2σ Ma
Wavy tuff GC-2b biotite continued									
#* UW39E4bm: 1 crystal									
* 39E4bm1	0.13	6.144 ± 0.041	0.02611 ± 0.00238	0.012963 ± 0.000371	0.60	37.7	8.6	16	39.19 ± 3.84
39E4bm2	0.26	3.425 ± 0.021	0.00737 ± 0.00080	0.001780 ± 0.000213	0.70	84.6	18.0	58	48.96 ± 2.21
39E4bm3	0.36	3.286 ± 0.018	0.00832 ± 0.00076	0.001403 ± 0.000198	0.78	87.4	21.1	52	48.50 ± 2.03
39E4bm4	0.48	3.110 ± 0.017	0.03454 ± 0.00105	0.000893 ± 0.000208	0.65	91.6	18.5	12	48.11 ± 2.12
39E4bm5	0.59	3.060 ± 0.014	0.02612 ± 0.00089	0.000831 ± 0.000145	0.90	92.0	26.0	16	47.57 ± 1.50
39E4bm6	1.50	3.027 ± 0.043	0.01439 ± 0.00179	0.000763 ± 0.000400	0.26	92.6	7.7	30	47.35 ± 4.19
Inverse isochron age ± 2σ		46.52 ± 3.65				Integrated age ± 2σ			47.38 ± 0.93
$^{40}Ar/^{39}Ar$ intercept ± 2σ		379.9 ± 185.9		MSWD 0.35		Plateau age ± 2σ			48.10 ± 0.93
* UW39E4bn: 1 crystal									
* 39E4bn1	0.13	4.542 ± 0.052	0.01192 ± 0.01186	0.008446 ± 0.001079	0.14	45.0	1.7	36	34.69 ± 10.78
39E4bn2	0.26	3.244 ± 0.010	0.00714 ± 0.00203	0.001566 ± 0.000166	0.60	85.7	9.9	60	46.99 ± 1.67
39E4bn3	0.35	3.003 ± 0.010	0.01017 ± 0.00229	0.000447 ± 0.000168	0.76	95.6	13.6	42	48.48 ± 1.69
39E4bn4	0.47	2.974 ± 0.004	0.05756 ± 0.00164	0.000395 ± 0.000025	3.73	96.2	67.0	7	48.33 ± 0.28
39E4bn5	0.58	2.964 ± 0.018	0.10993 ± 0.00528	0.000341 ± 0.000389	0.30	96.9	5.4	4	48.49 ± 3.88
39E4bn6	1.50	3.098 ± 0.031	0.10384 ± 0.00941	0.000951 ± 0.000728	0.14	91.2	2.4	4	47.72 ± 7.25
Inverse isochron age ± 2σ		48.76 ± 0.52				Integrated age ± 2σ			47.98 ± 0.48
$^{40}Ar/^{39}Ar$ intercept ± 2σ		228.4 ± 66.8		MSWD 0.65		Plateau age ± 2σ			48.30 ± 0.28
UW39E4bo: 1 crystal									
39E4bo1	0.14	3.843 ± 0.010	0.00782 ± 0.00193	0.003590 ± 0.000150	0.84	72.4	17.4	55	47.00 ± 1.50
39E4bo2	0.27	3.093 ± 0.006	0.00952 ± 0.00128	0.000650 ± 0.000081	1.38	93.8	35.5	45	48.99 ± 0.82
39E4bo3	0.37	2.986 ± 0.006	0.04407 ± 0.00180	0.000473 ± 0.000054	1.41	95.4	37.7	10	48.12 ± 0.56
39E4bo4	0.46	2.976 ± 0.011	0.04986 ± 0.00729	0.000541 ± 0.000417	0.21	94.7	5.5	9	47.63 ± 4.13
39E4bo5	0.55	2.945 ± 0.030	0.01480 ± 0.01853	0.000556 ± 0.001096	0.09	94.4	2.3	29	47.00 ± 10.85
39E4bo6	1.50	3.091 ± 0.033	0.00105 ± 0.03417	0.001118 ± 0.001345	0.06	89.3	1.6	408	46.64 ± 13.30
Inverse isochron age ± 2σ		48.54 ± 0.60				Integrated age ± 2σ			48.16 ± 0.60
$^{40}Ar/^{39}Ar$ intercept ± 2σ		274.3 ± 30.3		MSWD 1.30		Plateau age ± 2σ			48.26 ± 0.51
UW39E4bp: 1 crystal									
39E4bp1	0.14	3.482 ± 0.010	0.00217 ± 0.00159	0.002387 ± 0.000180	0.76	79.7	24.7	198	46.91 ± 1.80
39E4bp2	0.27	3.036 ± 0.006	0.01296 ± 0.00121	0.000519 ± 0.000067	1.16	95.0	43.2	33	48.68 ± 0.70
39E4bp3	0.37	2.945 ± 0.009	0.05820 ± 0.00261	0.000399 ± 0.000132	0.69	96.1	26.4	7	47.82 ± 1.34
39E4bp4	0.47	2.974 ± 0.039	0.17396 ± 0.01838	0.000714 ± 0.000930	0.09	93.3	3.4	2	46.90 ± 9.26
39E4bp5	1.50	3.052 ± 0.058	0.14398 ± 0.02125	0.001149 ± 0.001641	0.06	89.2	2.3	3	46.03 ± 16.30
Inverse isochron age ± 2σ		48.79 ± 0.79				Integrated age ± 2σ			47.90 ± 0.81
$^{40}Ar/^{39}Ar$ intercept ± 2σ		254.4 ± 52.3		MSWD 1.06		Plateau age ± 2σ			48.32 ± 0.61
#* UW39E4bq: 1 crystal									
* 39E4bq1	0.13	3.442 ± 0.010	0.00470 ± 0.00246	0.002596 ± 0.000123	0.66	77.7	11.8	92	45.21 ± 1.25
39E4bq2	0.26	2.987 ± 0.007	0.00422 ± 0.00067	0.000413 ± 0.000038	1.70	95.9	35.0	102	48.38 ± 0.43
39E4bq3	0.36	2.950 ± 0.007	0.02031 ± 0.00145	0.000382 ± 0.000051	1.58	96.2	33.0	21	47.94 ± 0.55
39E4bq4	0.42	2.943 ± 0.010	0.02895 ± 0.00270	0.000490 ± 0.000148	0.55	95.1	11.5	15	47.30 ± 1.49
39E4bq5	0.50	2.918 ± 0.018	0.02847 ± 0.00570	0.000325 ± 0.000335	0.20	96.8	4.2	15	47.69 ± 3.36
39E4bq6	1.50	2.931 ± 0.018	0.00952 ± 0.00546	0.000328 ± 0.000347	0.22	96.7	4.5	45	47.87 ± 3.46
Inverse isochron age ± 2σ		39.98 ± 20.17				Integrated age ± 2σ			47.68 ± 0.40
$^{40}Ar/^{39}Ar$ intercept ± 2σ		1519.5 ± 7106.2		MSWD 0.79		Plateau age ± 2σ			48.16 ± 0.34

Table DR3. Complete $^{40}Ar/^{39}Ar$ results

Sample Experiment	laser power (W)	$^{40}Ar/^{39}Ar$	$^{37}Ar/^{39}Ar$	$^{36}Ar/^{39}Ar$	$^{40}Ar^*$ X10^{-14} mol	$^{40}Ar^*$ %	$^{39}Ar_K$ %	K/Ca	Apparent Age ± 2σ Ma
Wavy tuff GC-2b biotite continued									
#* UW39E4br: 1 crystal									
* 39E4br1	0.13	4.313 ± 0.012	0.00717 ± 0.00294	0.006254 ± 0.000150	0.81	57.1	15.9	60	41.71 ± 1.50
* 39E4br2	0.26	3.219 ± 0.010	0.00767 ± 0.00168	0.001021 ± 0.000082	0.91	90.6	24.1	56	49.25 ± 0.87
39E4br3	0.36	3.109 ± 0.008	0.02230 ± 0.00188	0.000864 ± 0.000055	1.32	91.8	36.2	19	48.22 ± 0.60
39E4br4	0.42	3.078 ± 0.013	0.04826 ± 0.00304	0.000840 ± 0.000128	0.55	92.0	15.1	9	47.86 ± 1.32
39E4br5	0.50	3.057 ± 0.022	0.04072 ± 0.00656	0.000582 ± 0.000338	0.18	94.4	5.1	11	48.77 ± 3.40
39E4br6	1.50	3.082 ± 0.021	0.04389 ± 0.01296	0.000860 ± 0.000636	0.13	91.8	3.7	10	47.82 ± 6.30
Inverse isochron age ± 2σ		46.51 ± 13.51					Integrated age ± 2σ		47.40 ± 0.53
$^{40}Ar/^{39}Ar$ intercept ± 2σ		413.8 ± 1326.8		MSWD 0.13			Plateau age ± 2σ		48.17 ± 0.54
Combined single crystal incremental heating ages									
Inverse isochron age ± 2σ		48.49 ± 0.27					Integrated age ± 2σ		47.74 ± 0.13
$^{40}Ar/^{39}Ar$ intercept ± 2σ		281.1 ± 16.8		MSWD 0.51			Weighted mean: plateau ages ± 2σ		**48.37 ± 0.23**
				MSWD 1.30			Weighted mean: integrated ages ± 2σ		48.18 ± 0.18
Blind Canyon tuff SW-1b biotite *J* = 0.014663 ± 0.12% μ = 1.0022									
Single crystal incremental heating experiments									
#* UW11F8a: 1 crystal									
* 11F8a1	0.22	1.958 ± 0.004	0.00028 ± 0.00103	0.000727 ± 0.000062	1.47	88.8	49.9	1563	45.42 ± 0.97
11F8a2	0.32	1.924 ± 0.005	0.00094 ± 0.00349	0.000501 ± 0.000126	0.48	92.1	16.7	459	46.26 ± 1.93
11F8a3	1.50	1.867 ± 0.004	0.00137 ± 0.00508	0.000156 ± 0.000057	0.94	97.3	33.4	314	47.41 ± 0.89
No isochron							Integrated age ± 2σ		46.23 ± 0.66
				MSWD 1.17			Plateau age ± 2σ		47.21 ± 0.88
#* UW11F8b: 1 crystal									
* 11F8b1	0.15	2.256 ± 0.007	0.00069 ± 0.00267	0.002213 ± 0.000146	0.39	70.8	18.0	620	41.77 ± 2.25
11F8b2	0.22	1.940 ± 0.005	0.00019 ± 0.00082	0.000327 ± 0.000125	0.36	94.8	19.7	2252	47.99 ± 1.92
11F8b3	0.35	1.894 ± 0.005	0.00128 ± 0.00477	0.000346 ± 0.000080	0.49	94.4	27.0	335	46.68 ± 1.25
11F8b4	1.50	1.838 ± 0.004	0.00054 ± 0.00202	0.000056 ± 0.000074	0.62	98.9	35.3	798	47.43 ± 1.15
Inverse isochron age ± 2σ		47.23 ± 1.71					Integrated age ± 2σ		46.32 ± 0.77
$^{40}Ar/^{39}Ar$ intercept ± 2σ		296.8 ± 290.2		MSWD 0.76			Plateau age ± 2σ		47.23 ± 0.78
UW11F8c: 1 crystal									
11F8c1	0.15	2.258 ± 0.030	0.00080 ± 0.00303	0.001731 ± 0.000162	0.38	77.1	7.4	538	45.50 ± 2.92
11F8c2	0.22	1.871 ± 0.015	0.00072 ± 0.00269	0.000270 ± 0.000079	0.65	95.5	15.4	600	46.66 ± 1.45
11F8c3	1.50	1.849 ± 0.004	0.00075 ± 0.00282	0.000147 ± 0.000027	3.21	97.4	77.3	570	47.03 ± 0.46
Inverse isochron age ± 2σ		47.15 ± 0.51					Integrated age ± 2σ		46.86 ± 0.48
$^{40}Ar/^{39}Ar$ intercept ± 2σ		257.2 ± 65.4		MSWD 0.63			Plateau age ± 2σ		46.96 ± 0.44
#* UW11F8d: 1 crystal									
* 11F8d1	0.15	2.226 ± 0.006	0.00032 ± 0.00121	0.002029 ± 0.000051	1.93	72.9	23.5	1342	42.39 ± 0.83
11F8d2	0.22	1.940 ± 0.004	0.00009 ± 0.00037	0.000441 ± 0.000051	1.40	93.0	19.6	4645	47.13 ± 0.80
11F8d3	0.30	1.887 ± 0.004	0.00125 ± 0.00470	0.000294 ± 0.000036	1.92	95.2	27.6	343	46.87 ± 0.58
11F8d4	1.50	1.838 ± 0.003	0.00141 ± 0.00527	0.000104 ± 0.000031	1.98	98.1	29.3	306	47.06 ± 0.50
Inverse isochron age ± 2σ		47.01 ± 0.70					Integrated age ± 2σ		45.93 ± 0.35
$^{40}Ar/^{39}Ar$ intercept ± 2σ		294.8 ± 102.3		MSWD 0.18			Plateau age ± 2σ		47.01 ± 0.35
UW11F8e: 1 crystal									
11F8e1	0.15	2.122 ± 0.007	0.00045 ± 0.00174	0.001280 ± 0.000129	0.47	81.9	11.3	950	45.42 ± 2.00
11F8e2	0.22	1.864 ± 0.005	0.00005 ± 0.00036	0.000297 ± 0.000086	0.54	95.0	14.7	7827	46.26 ± 1.34
11F8e3	0.30	1.865 ± 0.004	0.00079 ± 0.00298	0.000234 ± 0.000059	0.78	96.0	21.3	543	46.77 ± 0.92
11F8e4	1.50	1.839 ± 0.003	0.00111 ± 0.00416	0.000094 ± 0.000019	1.91	98.2	52.7	388	47.16 ± 0.33
Inverse isochron age ± 2σ		47.26 ± 0.32					Integrated age ± 2σ		46.75 ± 0.40
$^{40}Ar/^{39}Ar$ intercept ± 2σ		234.8 ± 51.6		MSWD 1.62			Plateau age ± 2σ		47.03 ± 0.38

Table DR3. Complete $^{40}Ar/^{39}Ar$ results

Sample Experiment	laser power (W)	$^{40}Ar/^{39}Ar$	$^{37}Ar/^{39}Ar$	$^{36}Ar/^{39}Ar$	$^{40}Ar^*$ X10^{-14} mol	$^{40}Ar^*$ %	$^{39}Ar_K$ %	K/Ca	Apparent Age ± 2σ Ma
Blind Canyon tuff SW-1b biotite continued									
* UW11F8f: 1 crystal									
* 11F8f1	0.12	3.181 ± 0.010	0.00054 ± 0.00225	0.005466 ± 0.000326	0.36	49.1	4.3	801	40.83 ± 5.00
11F8f2	0.20	1.977 ± 0.004	0.00015 ± 0.00067	0.000611 ± 0.000051	0.90	90.6	17.7	2792	46.79 ± 0.81
11F8f3	0.30	1.891 ± 0.004	0.00006 ± 0.00028	0.000241 ± 0.000030	1.14	96.0	23.5	7004	47.39 ± 0.50
11F8f4	0.40	1.863 ± 0.005	0.00079 ± 0.00312	0.000108 ± 0.000032	1.15	98.0	24.0	542	47.67 ± 0.56
11F8f5	0.50	1.832 ± 0.004	0.00074 ± 0.00291	0.000136 ± 0.000026	1.15	97.6	24.4	580	46.67 ± 0.45
11F8f6	1.50	1.850 ± 0.008	0.00000 ± 0.00070	0.000018 ± 0.000157	0.29	99.5	6.2	117068	48.04 ± 2.43
Inverse isochron age ± 2σ		47.10 ± 0.87				Integrated age ± 2σ			46.93 ± 0.37
$^{40}Ar/^{39}Ar$ intercept ± 2σ		303.6 ± 136.0		MSWD 2.57		Plateau age ± 2σ			47.14 ± 0.43
Combined incremental heating ages				MSWD 1.20	Weighted mean: integrated ages ± 2σ				46.74 ± 0.33
Multi-crystal incremental heating experiments									
UW11F8g: 5 crystals									
11F8g1	0.13	2.361 ± 0.010	0.00194 ± 0.00731	0.002238 ± 0.000234	0.30	71.8	3.4	222	44.28 ± 3.61
11F8g2	0.20	1.996 ± 0.007	0.00006 ± 0.00056	0.000601 ± 0.000099	0.57	90.9	7.8	6959	47.35 ± 1.54
11F8g3	0.25	1.858 ± 0.005	0.00008 ± 0.00033	0.000123 ± 0.000042	1.07	97.8	15.7	5514	47.44 ± 0.70
11F8g4	0.33	1.840 ± 0.007	0.00045 ± 0.00171	0.000113 ± 0.000036	1.46	97.9	21.5	947	47.06 ± 0.65
11F8g5	0.43	1.827 ± 0.003	0.00067 ± 0.00251	0.000078 ± 0.000015	2.60	98.5	38.5	644	46.99 ± 0.28
11F8g6	0.57	1.845 ± 0.004	0.00077 ± 0.00288	0.000086 ± 0.000059	0.89	98.4	13.1	562	47.38 ± 0.93
Inverse isochron age ± 2σ		47.13 ± 0.27				Integrated age ± 2σ			47.06 ± 0.30
$^{40}Ar/^{39}Ar$ intercept ± 2σ		273.3 ± 53.5		MSWD 0.88		Plateau age ± 2σ			47.07 ± 0.24
* UW11F8h: 5 crystals									
* 11F8h1	0.12	2.334 ± 0.009	0.00046 ± 0.00175	0.002714 ± 0.000068	0.87	65.5	6.0	937	39.97 ± 1.12
11F8h2	0.20	1.966 ± 0.008	0.00011 ± 0.00042	0.000514 ± 0.000033	1.43	92.0	11.7	4023	47.26 ± 0.65
11F8h3	0.25	1.898 ± 0.006	0.00020 ± 0.00077	0.000245 ± 0.000027	2.01	95.9	17.0	2119	47.54 ± 0.50
11F8h4	0.33	1.860 ± 0.006	0.00042 ± 0.00157	0.000122 ± 0.000023	2.01	97.8	17.3	1032	47.51 ± 0.47
11F8h5	0.40	1.836 ± 0.003	0.00080 ± 0.00300	0.000092 ± 0.000015	3.17	98.3	27.7	537	47.10 ± 0.28
11F8h6	1.50	1.842 ± 0.003	0.00063 ± 0.00236	0.000087 ± 0.000035	2.33	98.3	20.3	685	47.31 ± 0.55
Inverse isochron age ± 2σ		47.19 ± 0.33				Integrated age ± 2σ			46.88 ± 0.21
$^{40}Ar/^{39}Ar$ intercept ± 2σ		318.1 ± 64.4		MSWD 0.89		Plateau age ± 2σ			47.28 ± 0.20
#* UW11F8i: 5 crystals									
* 11F8i1	0.12	2.510 ± 0.009	0.00104 ± 0.00391	0.004114 ± 0.000053	1.43	51.4	14.1	413	33.80 ± 0.88
* 11F8i2	0.20	2.283 ± 0.007	0.00148 ± 0.00556	0.001337 ± 0.000073	0.74	82.5	8.0	291	49.14 ± 1.17
* 11F8i3	0.25	2.050 ± 0.005	0.00069 ± 0.00262	0.000576 ± 0.000063	0.79	91.5	9.6	621	48.95 ± 1.00
11F8i4	0.30	1.930 ± 0.010	0.00213 ± 0.00806	0.000486 ± 0.000148	0.26	92.3	3.3	201	46.54 ± 2.31
11F8i5	0.35	1.872 ± 0.004	0.00072 ± 0.00271	0.000204 ± 0.000074	0.66	96.5	8.7	599	47.19 ± 1.14
11F8i6	0.40	1.843 ± 0.004	0.00107 ± 0.00404	0.000214 ± 0.000045	1.13	96.3	15.3	401	46.36 ± 0.73
11F8i7	0.60	1.846 ± 0.003	0.00130 ± 0.00488	0.000097 ± 0.000016	2.88	98.2	38.8	331	47.32 ± 0.29
11F8i8	1.50	1.931 ± 0.014	0.00154 ± 0.00588	0.000221 ± 0.000230	0.16	96.4	2.1	279	48.58 ± 3.57
Inverse isochron age ± 2σ		47.24 ± 0.85				Integrated age ± 2σ			45.56 ± 0.29
$^{40}Ar/^{39}Ar$ intercept ± 2σ		278.1 ± 318.8		MSWD 1.74		Plateau age ± 2σ			47.18 ± 0.35
* UW11F8j: 4 crystals									
* 11F8j1	0.12	2.778 ± 0.008	0.00062 ± 0.00235	0.004251 ± 0.000090	1.01	54.6	7.6	695	39.70 ± 1.43
11F8j2	0.20	1.974 ± 0.004	0.00008 ± 0.00033	0.000483 ± 0.000035	1.37	92.5	14.5	5568	47.69 ± 0.58
11F8j3	0.25	1.890 ± 0.004	0.00046 ± 0.00174	0.000262 ± 0.000030	1.33	95.7	14.8	932	47.21 ± 0.51
11F8j4	0.33	1.863 ± 0.004	0.00055 ± 0.00208	0.000179 ± 0.000027	2.18	96.9	24.5	779	47.14 ± 0.47
11F8j5	0.40	1.848 ± 0.004	0.00079 ± 0.00297	0.000129 ± 0.000026	2.19	97.7	24.9	545	47.14 ± 0.43
11F8j6	0.60	1.843 ± 0.005	0.00150 ± 0.00566	0.000124 ± 0.000050	1.12	97.8	12.7	286	47.05 ± 0.79
11F8j7	1.50	1.883 ± 0.041	0.00373 ± 0.01417	0.000267 ± 0.000646	0.08	95.6	1.0	115	46.98 ± 10.07
Inverse isochron age ± 2σ		46.87 ± 0.58				Integrated age ± 2σ			46.65 ± 0.27
$^{40}Ar/^{39}Ar$ intercept ± 2σ		357.7 ± 86.5		MSWD 0.61		Plateau age ± 2σ			47.24 ± 0.24

Table DR3. Complete $^{40}Ar/^{39}Ar$ results

Sample Experiment	laser power (W)	$^{40}Ar/^{39}Ar$	$^{37}Ar/^{39}Ar$	$^{36}Ar/^{39}Ar$	$^{40}Ar^*$ X10^{-14} mol	$^{40}Ar^*$ %	$^{39}Ar_K$ %	K/Ca	Apparent Age ± 2σ Ma
Blind Canyon tuff SW-1b biotite continued									
#* UW11F8k: 4 crystals									
* 11F8k1	0.12	2.479 ± 0.006	0.00063 ± 0.00237	0.003659 ± 0.000075	0.87	56.2	6.2	686	36.49 ± 1.18
11F8k2	0.20	2.001 ± 0.006	0.00011 ± 0.00046	0.000677 ± 0.000041	1.20	89.8	10.6	3791	46.91 ± 0.69
11F8k3	0.25	1.932 ± 0.005	0.00037 ± 0.00138	0.000402 ± 0.000039	1.69	93.6	15.6	1178	47.21 ± 0.64
11F8k4	0.33	1.881 ± 0.005	0.00023 ± 0.00086	0.000303 ± 0.000029	1.61	95.0	15.2	1909	46.65 ± 0.51
11F8k5	0.40	1.838 ± 0.003	0.00098 ± 0.00368	0.000126 ± 0.000015	2.82	97.7	27.3	441	46.91 ± 0.27
11F8k6	0.50	1.838 ± 0.003	0.00098 ± 0.00370	0.000125 ± 0.000032	2.16	97.7	20.9	438	46.92 ± 0.52
11F8k7	1.50	1.885 ± 0.005	0.00205 ± 0.00776	0.000117 ± 0.000101	0.45	97.9	4.2	209	48.18 ± 1.55
Inverse isochron age ± 2σ		46.88 ± 0.36				Integrated age ± 2σ			46.33 ± 0.23
$^{40}Ar/^{39}Ar$ intercept ± 2σ		302.7 ± 50.5		MSWD 0.91		Plateau age ± 2σ			46.92 ± 0.20
* UW11F8l: 4 crystals									
* 11F8l1	0.12	2.358 ± 0.009	0.00008 ± 0.00055	0.003111 ± 0.000166	0.36	60.8	3.6	5681	37.54 ± 2.56
11F8l2	0.20	1.949 ± 0.004	0.00028 ± 0.00110	0.000531 ± 0.000063	0.87	91.7	10.5	1538	46.67 ± 0.98
11F8l3	0.25	1.879 ± 0.004	0.00021 ± 0.00080	0.000212 ± 0.000034	1.44	96.4	18.2	2068	47.30 ± 0.54
11F8l4	0.33	1.852 ± 0.004	0.00042 ± 0.00161	0.000148 ± 0.000040	1.35	97.4	17.3	1018	47.08 ± 0.64
11F8l5	0.40	1.840 ± 0.004	0.00091 ± 0.00346	0.000108 ± 0.000041	1.72	98.0	22.2	472	47.09 ± 0.65
11F8l6	1.50	1.832 ± 0.004	0.00052 ± 0.00198	0.000105 ± 0.000026	2.19	98.1	28.2	826	46.91 ± 0.44
Inverse isochron age ± 2σ		47.06 ± 0.48				Integrated age ± 2σ			46.69 ± 0.28
$^{40}Ar/^{39}Ar$ intercept ± 2σ		292.0 ± 93.4		MSWD 0.46		Plateau age ± 2σ			47.04 ± 0.27
* UW11F8m: 2 crystals									
* 11F8m1	0.12	2.505 ± 0.008	0.00027 ± 0.00110	0.003263 ± 0.000120	0.74	61.3	4.7	1611	40.19 ± 1.86
* 11F8m2	0.20	1.969 ± 0.005	0.00018 ± 0.00071	0.000424 ± 0.000039	1.30	93.4	10.6	2451	47.99 ± 0.64
11F8m3	0.25	1.896 ± 0.003	0.00006 ± 0.00027	0.000262 ± 0.000037	2.00	95.7	16.9	7176	47.36 ± 0.58
11F8m4	0.30	1.852 ± 0.003	0.00034 ± 0.00132	0.000167 ± 0.000025	1.90	97.1	16.4	1283	46.94 ± 0.41
11F8m5	0.40	1.836 ± 0.003	0.00086 ± 0.00339	0.000106 ± 0.000015	3.60	98.0	31.3	498	46.99 ± 0.28
11F8m6	0.55	1.831 ± 0.004	0.00055 ± 0.00216	0.000084 ± 0.000025	2.16	98.4	18.9	781	47.04 ± 0.43
11F8m7	1.50	1.906 ± 0.013	0.00130 ± 0.00542	0.000131 ± 0.000425	0.15	97.7	1.3	330	48.62 ± 6.51
Inverse isochron age ± 2σ		46.79 ± 0.61				Integrated age ± 2σ			46.86 ± 0.22
$^{40}Ar/^{39}Ar$ intercept ± 2σ		367.7 ± 171.3		MSWD 0.46		Plateau age ± 2σ			47.03 ± 0.20
Combined multi-crystal incremental heating ages				MSWD 1.40		Weighted mean: integrated ages ± 2σ			46.83 ± 0.18
Grand combined incremental heating ages									
Inverse isochron age ± 2σ		47.18 ± 0.20				Integrated age ± 2σ			46.57 ± 0.10
$^{40}Ar/^{39}Ar$ intercept ± 2σ		256.7 ± 32.1		MSWD 0.10		Weighted mean: plateau age ± 2σ			**47.04 ± 0.18**
				MSWD 1.20		Weighted mean: integrated ages ± 2σ			46.81 ± 0.12
Fat tuff IC-2 biotite J = 0.014515 ± 0.10% μ = 1.0035									
Single crystal incremental heating experiments									
# UW32C3a: 1 crystal									
32C3a1	0.16	5.042 ± 0.064	0.01126 ± 0.00198	0.010903 ± 0.000787	0.14	36.1	0.6	38	47.04 ± 12.13
32C3a2	0.26	2.156 ± 0.010	0.00452 ± 0.00027	0.001198 ± 0.000094	0.49	83.5	5.1	95	46.53 ± 1.50
32C3a3	0.39	1.867 ± 0.004	0.00314 ± 0.00008	0.000264 ± 0.000043	1.36	95.7	16.3	137	46.21 ± 0.68
32C3a4	0.58	1.829 ± 0.004	0.01058 ± 0.00008	0.000136 ± 0.000015	2.56	97.8	31.4	41	46.23 ± 0.29
32C3a5	1.50	1.821 ± 0.002	0.02582 ± 0.00016	0.000114 ± 0.000012	3.77	98.2	46.6	17	46.21 ± 0.22
Inverse isochron age ± 2σ		46.20 ± 0.21				Integrated age ± 2σ			46.24 ± 0.21
$^{40}Ar/^{39}Ar$ intercept ± 2σ		301.7 ± 34.5		MSWD 0.05		Plateau age ± 2σ			46.22 ± 0.17

Table DR3. Complete $^{40}Ar/^{39}Ar$ results

Sample Experiment	laser power (W)	$^{40}Ar/^{39}Ar$	$^{37}Ar/^{39}Ar$	$^{36}Ar/^{39}Ar$	$^{40}Ar^*$ X10^{-14} mol	$^{40}Ar^*$ %	$^{39}Ar_K$ %	K/Ca	Apparent Age ± 2σ Ma
Fat tuff IC-2 biotite continued									
#* UW32C3b: 1 crystal									
* 32C3b1	0.19	3.708 ± 0.018	0.01105 ± 0.00044	0.008987 ± 0.000173	0.55	28.3	5.3	39	27.26 ± 2.73
32C3b2	0.39	2.315 ± 0.004	0.00771 ± 0.00010	0.001750 ± 0.000037	1.87	77.5	28.6	56	46.38 ± 0.59
32C3b3	0.65	2.058 ± 0.004	0.01718 ± 0.00018	0.000897 ± 0.000031	1.75	87.0	30.1	25	46.27 ± 0.50
32C3b4	0.90	1.913 ± 0.004	0.02107 ± 0.00017	0.000380 ± 0.000034	1.68	94.0	31.1	20	46.49 ± 0.54
32C3b5	1.50	2.115 ± 0.021	0.00739 ± 0.00050	0.001202 ± 0.000182	0.29	83.0	4.9	58	45.40 ± 2.93
Inverse isochron age ± 2σ		46.42 ± 0.63				Integrated age ± 2σ			45.32 ± 0.35
$^{40}Ar/^{39}Ar$ intercept ± 2σ		293.1 ± 22.5		MSWD 0.26		Plateau age ± 2σ			46.36 ± 0.31
#* UW32C3c: 1 crystal									
* 32C3c1	0.16	4.406 ± 0.017	0.02598 ± 0.00047	0.011906 ± 0.000202	0.80	20.1	1.8	17	23.04 ± 3.13
* 32C3c2	0.32	1.991 ± 0.003	0.00672 ± 0.00009	0.000870 ± 0.000016	3.77	86.9	18.5	64	44.74 ± 0.29
32C3c3	0.61	1.892 ± 0.003	0.00837 ± 0.00008	0.000370 ± 0.000006	9.53	94.0	49.1	51	45.98 ± 0.17
32C3c4	0.84	1.830 ± 0.002	0.01342 ± 0.00009	0.000123 ± 0.000011	5.38	97.8	28.7	32	46.28 ± 0.20
32C3c5	1.50	1.844 ± 0.016	0.00356 ± 0.00023	0.000222 ± 0.000116	0.39	96.2	2.1	121	45.87 ± 1.92
Inverse isochron age ± 2σ		46.42 ± 0.28				Integrated age ± 2σ			45.43 ± 0.14
$^{40}Ar/^{39}Ar$ intercept ± 2σ		249.1 ± 38.2		MSWD 2.59		Plateau age ± 2σ			46.10 ± 0.21
#* UW32C3d: 1 crystal									
* 32C3d1	0.19	3.803 ± 0.012	0.00890 ± 0.00025	0.008084 ± 0.000106	1.09	37.1	3.8	48	36.57 ± 1.68
* 32C3d2	0.32	2.050 ± 0.004	0.00433 ± 0.00014	0.001054 ± 0.000028	1.89	84.6	12.3	99	44.86 ± 0.46
32C3d3	0.45	1.884 ± 0.003	0.00446 ± 0.00008	0.000287 ± 0.000016	3.77	95.3	26.7	96	46.39 ± 0.27
32C3d4	0.65	1.847 ± 0.003	0.01697 ± 0.00015	0.000133 ± 0.000011	3.86	97.7	27.9	25	46.65 ± 0.21
32C3d5	0.84	1.831 ± 0.002	0.00863 ± 0.00010	0.000108 ± 0.000019	3.33	98.0	24.3	50	46.40 ± 0.31
32C3d6	1.50	1.840 ± 0.007	0.00171 ± 0.00022	0.000124 ± 0.000077	0.68	97.8	4.9	251	46.51 ± 1.21
Inverse isochron age ± 2σ		46.64 ± 0.37				Integrated age ± 2σ			45.91 ± 0.16
$^{40}Ar/^{39}Ar$ intercept ± 2σ		267.3 ± 77.5		MSWD 0.97		Plateau age ± 2σ			46.52 ± 0.15
* UW32C3e: 1 crystal									
* 32C3e1	0.19	2.783 ± 0.053	0.04029 ± 0.00280	0.001541 ± 0.000818	0.09	83.6	1.6	11	59.90 ± 12.53
32C3e2	0.39	1.916 ± 0.007	0.01116 ± 0.00017	0.000378 ± 0.000100	0.60	94.0	16.3	39	46.54 ± 1.54
32C3e3	0.65	1.842 ± 0.004	0.02414 ± 0.00037	0.000155 ± 0.000040	1.22	97.4	34.4	18	46.36 ± 0.64
32C3e4	0.78	1.830 ± 0.006	0.04305 ± 0.00041	0.000091 ± 0.000084	0.74	98.5	21.0	10	46.57 ± 1.29
32C3e5	1.50	1.816 ± 0.005	0.03105 ± 0.00025	0.000072 ± 0.000054	0.93	98.7	26.6	14	46.33 ± 0.85
Inverse isochron age ± 2σ		46.32 ± 0.93				Integrated age ± 2σ			46.64 ± 0.53
$^{40}Ar/^{39}Ar$ intercept ± 2σ		316.0 ± 229.8		MSWD 0.05		Plateau age ± 2σ			46.39 ± 0.46
#* UW32C3f: 1 crystal									
* 32C3f1	0.23	2.540 ± 0.027	0.00918 ± 0.00080	0.004757 ± 0.000401	0.18	44.5	1.8	47	29.36 ± 6.24
32C3f2	0.32	2.226 ± 0.012	0.00555 ± 0.00025	0.001493 ± 0.000175	0.36	80.0	4.1	77	46.02 ± 2.70
32C3f3	0.45	1.884 ± 0.006	0.00297 ± 0.00021	0.000348 ± 0.000086	0.71	94.3	9.7	145	45.94 ± 1.33
32C3f4	0.71	1.844 ± 0.003	0.00515 ± 0.00013	0.000124 ± 0.000030	2.17	97.8	30.1	83	46.61 ± 0.47
32C3f5	1.50	1.820 ± 0.003	0.02837 ± 0.00021	0.000060 ± 0.000013	3.85	98.9	54.2	15	46.52 ± 0.24
Inverse isochron age ± 2σ		46.56 ± 0.25				Integrated age ± 2σ			46.16 ± 0.28
$^{40}Ar/^{39}Ar$ intercept ± 2σ		278.8 ± 64.5		MSWD 0.35		Plateau age ± 2σ			46.52 ± 0.21
UW32C3g: 1 crystal									
32C3g1	0.16	5.486 ± 0.056	0.01069 ± 0.00129	0.013881 ± 0.001043	0.19	25.2	0.5	40	35.79 ± 15.95
32C3g2	0.26	2.404 ± 0.008	0.00346 ± 0.00031	0.002077 ± 0.000098	0.58	74.3	3.7	124	46.17 ± 1.51
32C3g3	0.45	1.906 ± 0.002	0.00240 ± 0.00007	0.000350 ± 0.000033	2.75	94.3	22.1	179	46.47 ± 0.52
32C3g4	0.61	1.838 ± 0.003	0.00253 ± 0.00005	0.000112 ± 0.000024	2.53	98.0	21.1	170	46.54 ± 0.39
32C3g5	0.78	1.825 ± 0.002	0.00614 ± 0.00008	0.000084 ± 0.000016	2.77	98.4	23.3	70	46.42 ± 0.27
32C3g6	1.50	1.829 ± 0.003	0.00303 ± 0.00004	0.000082 ± 0.000017	3.50	98.4	29.3	142	46.53 ± 0.29
Inverse isochron age ± 2σ		46.52 ± 0.19				Integrated age ± 2σ			46.42 ± 0.21
$^{40}Ar/^{39}Ar$ intercept ± 2σ		283.5 ± 23.2		MSWD 0.47		Plateau age ± 2σ			46.48 ± 0.17

Table DR3. Complete $^{40}Ar/^{39}Ar$ results

Sample Experiment	laser power (W)	$^{40}Ar/^{39}Ar$	$^{37}Ar/^{39}Ar$	$^{36}Ar/^{39}Ar$	$^{40}Ar^*$ X10^{-14} mol	$^{40}Ar^*$ %	$^{39}Ar_K$ %	K/Ca	Apparent Age ± 2σ Ma
Fat tuff IC-2 biotite continued									
* UW32C3h: 1 crystal									
* 32C3h1	0.19	4.567 ± 0.013	0.01417 ± 0.00031	0.009647 ± 0.000168	0.85	37.5	1.2	30	44.30 ± 2.57
* 32C3h2	0.39	1.985 ± 0.003	0.00656 ± 0.00006	0.000555 ± 0.000008	7.75	91.5	25.4	66	46.95 ± 0.18
32C3h3	0.65	1.837 ± 0.002	0.03307 ± 0.00020	0.000135 ± 0.000005	13.68	97.7	48.4	13	46.42 ± 0.13
32C3h4	0.84	1.815 ± 0.002	0.01792 ± 0.00012	0.000066 ± 0.000008	6.12	98.7	21.9	24	46.33 ± 0.16
32C3h5	1.50	1.845 ± 0.004	0.00365 ± 0.00021	0.000204 ± 0.000065	0.85	96.5	3.0	118	46.02 ± 0.99
Inverse isochron age ± 2σ		46.26 ± 0.36					Integrated age ± 2σ		46.50 ± 0.11
$^{40}Ar/^{39}Ar$ intercept ± 2σ		342.2 ± 132.9		MSWD 0.62			Plateau age ± 2σ		46.38 ± 0.11
#* UW32C3i: 1 crystal									
* 32C3i1	0.23	3.111 ± 0.005	0.00801 ± 0.00007	0.005033 ± 0.000041	4.90	52.1	24.9	54	41.92 ± 0.63
* 32C3i2	0.39	2.064 ± 0.004	0.00750 ± 0.00009	0.000803 ± 0.000012	5.08	88.3	39.0	57	47.11 ± 0.25
32C3i3	0.52	1.872 ± 0.003	0.01718 ± 0.00014	0.000267 ± 0.000017	3.11	95.6	26.2	25	46.28 ± 0.29
32C3i4	0.68	1.883 ± 0.003	0.01233 ± 0.00017	0.000202 ± 0.000057	1.11	96.6	9.3	35	47.04 ± 0.87
32C3i5	1.50	1.888 ± 0.036	0.01719 ± 0.00225	0.000631 ± 0.000689	0.07	89.9	0.6	25	43.93 ± 10.57
Inverse isochron age ± 2σ		49.45 ± 2.06					Integrated age ± 2σ		45.58 ± 0.23
$^{40}Ar/^{39}Ar$ intercept ± 2σ		-177.3 ± 365.4		MSWD 1.49			Plateau age ± 2σ		46.35 ± 0.33
UW32C3j: 1 crystal									
32C3j1	0.19	4.601 ± 0.028	0.02411 ± 0.00055	0.009576 ± 0.000299	0.38	38.4	1.6	18	45.72 ± 4.56
32C3j2	0.39	1.969 ± 0.003	0.00721 ± 0.00008	0.000533 ± 0.000022	2.93	91.8	29.6	60	46.71 ± 0.36
32C3j3	0.71	1.853 ± 0.002	0.02039 ± 0.00015	0.000186 ± 0.000013	5.80	96.9	62.2	21	46.40 ± 0.23
32C3j4	1.50	1.886 ± 0.008	0.00159 ± 0.00020	0.000097 ± 0.000078	0.63	98.2	6.6	271	47.87 ± 1.23
Inverse isochron age ± 2σ		46.50 ± 0.45					Integrated age ± 2σ		46.58 ± 0.21
$^{40}Ar/^{39}Ar$ intercept ± 2σ		297.9 ± 33.9		MSWD 2.39			Plateau age ± 2σ		46.52 ± 0.30
UW32C3k: 1 crystal									
32C3k1	0.23	3.797 ± 0.039	0.01473 ± 0.00105	0.006782 ± 0.000631	0.14	47.1	0.5	29	46.27 ± 9.66
32C3k2	0.45	1.911 ± 0.002	0.00381 ± 0.00009	0.000368 ± 0.000023	2.16	94.1	14.3	113	46.47 ± 0.36
32C3k3	0.65	1.813 ± 0.002	0.00218 ± 0.00004	0.000067 ± 0.000011	4.32	98.7	30.2	197	46.24 ± 0.20
32C3k4	1.50	1.816 ± 0.002	0.03784 ± 0.00025	0.000075 ± 0.000007	7.88	98.7	55.0	11	46.32 ± 0.15
Inverse isochron age ± 2σ		46.27 ± 0.16					Integrated age ± 2σ		46.32 ± 0.13
$^{40}Ar/^{39}Ar$ intercept ± 2σ		309.8 ± 38.9		MSWD 0.46			Plateau age ± 2σ		46.31 ± 0.12
* UW32C3l: 1 crystal									
* 32C3l1	0.23	3.226 ± 0.015	0.00532 ± 0.00068	0.005204 ± 0.000097	0.60	52.2	3.6	81	43.57 ± 1.57
32C3l2	0.36	2.055 ± 0.006	0.00416 ± 0.00040	0.000839 ± 0.000040	0.92	87.7	8.6	103	46.60 ± 0.68
32C3l3	0.52	1.868 ± 0.003	0.00218 ± 0.00008	0.000194 ± 0.000017	2.46	96.7	25.3	197	46.68 ± 0.31
32C3l4	0.65	1.827 ± 0.004	0.00554 ± 0.00021	0.000094 ± 0.000032	1.49	98.3	15.7	78	46.40 ± 0.51
32C3l5	1.50	1.811 ± 0.003	0.00845 ± 0.00013	0.000047 ± 0.000007	4.39	99.0	46.7	51	46.36 ± 0.19
Inverse isochron age ± 2σ		46.39 ± 0.20					Integrated age ± 2σ		46.37 ± 0.17
$^{40}Ar/^{39}Ar$ intercept ± 2σ		315.0 ± 36.6		MSWD 1.14			Plateau age ± 2σ		46.45 ± 0.17
#* UW32C3m: 1 crystal									
32C3m1	0.23	2.885 ± 0.004	0.00234 ± 0.00011	0.003625 ± 0.000058	2.68	62.7	20.9	184	46.77 ± 0.89
32C3m2	0.36	2.073 ± 0.004	0.00354 ± 0.00016	0.000843 ± 0.000018	2.50	87.8	27.1	121	47.03 ± 0.33
32C3m3	0.52	1.886 ± 0.003	0.01269 ± 0.00021	0.000262 ± 0.000021	2.55	95.7	30.4	34	46.65 ± 0.36
32C3m4	0.65	1.850 ± 0.003	0.00923 ± 0.00027	0.000170 ± 0.000031	1.59	97.1	19.4	47	46.43 ± 0.50
* 32C3m5	1.50	0.895 ± 0.010	0.00296 ± 0.00128	0.000103 ± 0.000217	0.09	96.1	2.3	145	22.38 ± 3.35
Inverse isochron age ± 2σ		46.70 ± 0.41					Integrated age ± 2σ		46.19 ± 0.27
$^{40}Ar/^{39}Ar$ intercept ± 2σ		300.1 ± 15.4		MSWD 1.61			Plateau age ± 2σ		46.77 ± 0.27
Combined single crystal incremental heating ages									
Inverse isochron age ± 2σ		46.34 ± 0.10					Integrated age ± 2σ		46.13 ± 0.07
$^{40}Ar/^{39}Ar$ intercept ± 2σ		300.1 ± 12.9		MSWD 2.10			Weighted mean: plateau ages ± 2σ		**46.34 ± 0.13**
				MSWD 1.50			Weighted mean: integrated ages ± 2σ		46.44 ± 0.10

Table DR3. Complete $^{40}Ar/^{39}Ar$ results

Sample Experiment	laser power (W)	$^{40}Ar/^{39}Ar$	$^{37}Ar/^{39}Ar$	$^{36}Ar/^{39}Ar$	$^{40}Ar^*$ X10^{-14} mol	$^{40}Ar^*$ %	$^{39}Ar_K$ %	K/Ca	Apparent Age ± 2σ Ma
Portly tuff IC-5 biotite *J* = 0.014547 ± 0.10% μ = 1.0035									
Single crystal incremental heating experiments									
UW32C5ba: 1 crystal									
32C5ba1	0.16	2.880 ± 0.033	0.00887 ± 0.00445	0.003798 ± 0.000933	0.08	60.9	7.2	48	45.44 ± 14.19
32C5ba2	0.26	2.315 ± 0.026	0.00411 ± 0.00189	0.001481 ± 0.000543	0.12	80.9	13.4	105	48.50 ± 8.29
32C5ba3	0.39	1.778 ± 0.011	0.00627 ± 0.00088	0.000071 ± 0.000229	0.19	98.6	28.2	69	45.42 ± 3.51
32C5ba4	0.52	1.787 ± 0.011	0.00080 ± 0.00086	0.000091 ± 0.000169	0.24	98.2	35.9	537	45.49 ± 2.61
32C5ba5	1.50	1.798 ± 0.016	0.00146 ± 0.00197	0.000020 ± 0.000405	0.10	99.4	15.3	294	46.30 ± 6.19
Inverse isochron age ± 2σ		45.55 ± 2.23				Integrated age ± 2σ			45.99 ± 2.24
$^{40}Ar/^{39}Ar$ intercept ± 2σ		322.8 ± 141.9		MSWD 0.14		Plateau age ± 2σ			45.71 ± 1.91
UW32C5bb: 1 crystal									
32C5bb1	0.16	2.149 ± 0.047	0.00588 ± 0.00589	0.001459 ± 0.001125	0.05	79.7	2.6	73	44.42 ± 17.20
32C5bb2	0.26	1.869 ± 0.011	0.00324 ± 0.00067	0.000252 ± 0.000202	0.27	95.8	14.9	133	46.38 ± 3.10
32C5bb3	0.39	1.790 ± 0.005	0.00117 ± 0.00031	0.000089 ± 0.000064	0.64	98.3	36.4	367	45.59 ± 1.00
32C5bb4	0.52	1.787 ± 0.007	0.00063 ± 0.00033	0.000084 ± 0.000087	0.59	98.4	33.7	678	45.54 ± 1.37
32C5bb5	1.50	1.807 ± 0.014	0.00011 ± 0.00124	0.000227 ± 0.000194	0.22	96.0	12.4	3742	44.98 ± 3.02
Inverse isochron age ± 2σ		45.45 ± 1.50				Integrated age ± 2σ			45.59 ± 0.95
$^{40}Ar/^{39}Ar$ intercept ± 2σ		345.1 ± 480.7		MSWD 0.11		Plateau age ± 2σ			45.58 ± 0.76
UW32C5bc: 1 crystal									
32C5bc1	0.16	1.950 ± 0.043	0.00112 ± 0.00449	0.001158 ± 0.000987	0.06	82.2	2.7	385	41.60 ± 15.12
32C5bc2	0.26	1.816 ± 0.011	0.00139 ± 0.00073	0.000328 ± 0.000140	0.27	94.4	14.1	308	44.44 ± 2.19
32C5bc3	0.39	1.791 ± 0.008	0.00546 ± 0.00039	0.000081 ± 0.000082	0.59	98.4	30.9	79	45.67 ± 1.29
32C5bc4	0.52	1.783 ± 0.005	0.00064 ± 0.00026	0.000054 ± 0.000059	0.84	98.8	43.8	670	45.66 ± 0.94
32C5bc5	1.50	1.789 ± 0.015	0.00010 ± 0.00146	0.000166 ± 0.000226	0.16	97.0	8.4	4135	44.98 ± 3.51
Inverse isochron age ± 2σ		45.91 ± 0.51				Integrated age ± 2σ			45.32 ± 0.83
$^{40}Ar/^{39}Ar$ intercept ± 2σ		131.5 ± 142.0		MSWD 0.37		Plateau age ± 2σ			45.50 ± 0.70
UW32C5bd: 1 crystal									
32C5bd1	0.16	2.600 ± 0.096	0.01138 ± 0.00679	0.003873 ± 0.002119	0.03	55.8	2.7	38	37.69 ± 32.55
32C5bd2	0.26	1.809 ± 0.020	0.00278 ± 0.00133	0.000193 ± 0.000319	0.13	96.6	15.5	155	45.29 ± 4.93
32C5bd3	0.39	1.793 ± 0.011	0.00889 ± 0.00070	0.000071 ± 0.000141	0.31	98.6	38.4	48	45.82 ± 2.22
32C5bd4	0.52	1.800 ± 0.013	0.00151 ± 0.00061	0.000157 ± 0.000164	0.26	97.2	31.7	284	45.33 ± 2.57
32C5bd5	1.50	1.804 ± 0.024	0.00154 ± 0.00214	0.000079 ± 0.000451	0.10	98.5	11.7	279	46.02 ± 6.93
Inverse isochron age ± 2σ		45.85 ± 1.35				Integrated age ± 2σ			45.39 ± 1.84
$^{40}Ar/^{39}Ar$ intercept ± 2σ		210.4 ± 237.2		MSWD 0.09		Plateau age ± 2σ			45.58 ± 1.55
UW32C5be: 1 crystal									
32C5be1	0.16	3.025 ± 0.155	0.01053 ± 0.01347	0.004320 ± 0.002777	0.03	57.7	3.9	41	45.22 ± 42.71
32C5be2	0.26	1.850 ± 0.030	0.00392 ± 0.00219	0.000407 ± 0.000799	0.07	93.3	19.5	110	44.71 ± 12.19
32C5be3	0.39	1.876 ± 0.018	0.00159 ± 0.00155	0.000108 ± 0.000330	0.14	98.1	37.4	270	47.63 ± 5.07
32C5be4	0.52	1.828 ± 0.032	0.00289 ± 0.00241	0.000311 ± 0.000697	0.08	94.7	20.7	149	44.89 ± 10.67
32C5be5	1.50	1.791 ± 0.033	0.00382 ± 0.00286	0.000267 ± 0.000595	0.07	95.3	18.4	113	44.28 ± 9.16
Inverse isochron age ± 2σ		46.17 ± 4.92				Integrated age ± 2σ			45.78 ± 4.45
$^{40}Ar/^{39}Ar$ intercept ± 2σ		328.9 ± 498.8		MSWD 0.15		Plateau age ± 2σ			46.36 ± 3.87
UW32C5bf: 1 crystal									
32C5bf1	0.16	2.175 ± 0.074	0.00384 ± 0.01048	0.001328 ± 0.002159	0.03	81.8	6.1	112	46.07 ± 32.86
32C5bf2	0.26	1.819 ± 0.020	0.00097 ± 0.00184	0.000196 ± 0.000391	0.11	96.6	24.2	443	45.52 ± 6.00
32C5bf3	0.39	1.769 ± 0.016	0.00434 ± 0.00091	0.000126 ± 0.000185	0.19	97.7	40.2	99	44.77 ± 2.92
32C5bf4	0.52	1.866 ± 0.032	0.01065 ± 0.00250	0.000401 ± 0.000566	0.07	93.5	15.0	40	45.20 ± 8.72
32C5bf5	1.50	1.811 ± 0.031	0.00152 ± 0.00265	0.000139 ± 0.000553	0.07	97.5	14.5	283	45.75 ± 8.52
Inverse isochron age ± 2σ		44.63 ± 5.48				Integrated age ± 2σ			45.24 ± 3.28
$^{40}Ar/^{39}Ar$ intercept ± 2σ		386.2 ± 1139		MSWD 0.02		Plateau age ± 2σ			45.01 ± 2.40

Table DR3. Complete $^{40}Ar/^{39}Ar$ results

Sample Experiment	laser power (W)	$^{40}Ar/^{39}Ar$	$^{37}Ar/^{39}Ar$	$^{36}Ar/^{39}Ar$	$^{40}Ar^*$ X10^{-14} mol	$^{40}Ar^*$ %	$^{39}Ar_K$ %	K/Ca	Apparent Age ± 2σ Ma
Portly tuff IC-5 biotite continued									
UW32C5bg: 1 crystal									
32C5bg1	0.16	2.563 ± 0.043	0.00567 ± 0.00506	0.002808 ± 0.000899	0.07	67.5	2.9	76	44.81 ± 13.76
32C5bg2	0.26	1.832 ± 0.013	0.00207 ± 0.00105	0.000227 ± 0.000216	0.22	96.1	12.5	208	45.61 ± 3.34
32C5bg3	0.39	1.791 ± 0.008	0.00335 ± 0.00041	0.000078 ± 0.000076	0.53	98.5	31.1	128	45.71 ± 1.22
32C5bg4	0.52	1.796 ± 0.007	0.00153 ± 0.00029	0.000054 ± 0.000071	0.62	98.9	35.7	281	46.00 ± 1.13
32C5bg5	1.50	1.808 ± 0.009	0.00030 ± 0.00088	0.000082 ± 0.000126	0.31	98.4	17.8	1441	46.10 ± 1.96
Inverse isochron age ± 2σ		45.91 ± 0.81					Integrated age ± 2σ		45.84 ± 0.87
$^{40}Ar/^{39}Ar$ intercept ± 2σ		281.3 ± 184.0		MSWD 0.06			Plateau age ± 2σ		45.88 ± 0.75
UW32C5bh: 1 crystal									
32C5bh1	0.16	2.349 ± 0.021	0.01075 ± 0.00213	0.002414 ± 0.000378	0.14	69.5	8.3	40	42.32 ± 5.82
32C5bh2	0.26	1.836 ± 0.008	0.00308 ± 0.00043	0.000222 ± 0.000099	0.42	96.2	31.1	140	45.77 ± 1.54
32C5bh3	0.39	1.803 ± 0.005	0.00147 ± 0.00032	0.000090 ± 0.000062	0.60	98.3	46.0	292	45.90 ± 0.97
32C5bh4	0.52	1.804 ± 0.015	0.00074 ± 0.00130	0.000059 ± 0.000242	0.17	98.8	13.0	583	46.17 ± 3.74
32C5bh5	1.50	1.763 ± 0.098	0.01117 ± 0.01038	0.000231 ± 0.002240	0.02	95.9	1.6	39	43.85 ± 34.28
Inverse isochron age ± 2σ		46.06 ± 0.73					Integrated age ± 2σ		45.56 ± 1.09
$^{40}Ar/^{39}Ar$ intercept ± 2σ		235.5 ± 79.3		MSWD 0.38			Plateau age ± 2σ		45.81 ± 0.80
UW32C5bi: 1 crystal									
32C5bi1	0.16	2.365 ± 0.013	0.01268 ± 0.00076	0.002350 ± 0.000145	0.34	70.5	10.7	34	43.22 ± 2.26
32C5bi2	0.26	1.841 ± 0.005	0.00601 ± 0.00035	0.000262 ± 0.000073	0.62	95.6	24.9	72	45.60 ± 1.14
32C5bi3	0.39	1.814 ± 0.003	0.03674 ± 0.00062	0.000112 ± 0.000046	0.99	98.1	40.1	12	46.09 ± 0.72
32C5bi4	0.52	1.797 ± 0.008	0.00138 ± 0.00070	0.000181 ± 0.000115	0.34	96.8	14.1	313	45.08 ± 1.79
32C5bi5	1.50	1.818 ± 0.011	0.00379 ± 0.00098	0.000057 ± 0.000166	0.25	98.8	10.3	113	46.56 ± 2.57
Inverse isochron age ± 2σ		46.06 ± 0.53					Integrated age ± 2σ		45.57 ± 0.60
$^{40}Ar/^{39}Ar$ intercept ± 2σ		248.0 ± 35.0		MSWD 1.75			Plateau age ± 2σ		45.74 ± 0.72
UW32C5bj: 1 crystal									
32C5bj1	0.16	2.477 ± 0.064	0.00934 ± 0.00664	0.002764 ± 0.001659	0.05	66.9	3.1	46	42.96 ± 25.32
32C5bj2	0.26	1.843 ± 0.015	0.00621 ± 0.00118	0.000149 ± 0.000262	0.17	97.4	14.9	69	46.51 ± 4.03
32C5bj3	0.39	1.802 ± 0.007	0.01765 ± 0.00072	0.000134 ± 0.000145	0.40	97.6	34.7	24	45.58 ± 2.23
32C5bj4	0.52	1.832 ± 0.009	0.03124 ± 0.00125	0.000236 ± 0.000131	0.29	96.1	24.6	14	45.61 ± 2.04
32C5bj5	1.50	1.817 ± 0.012	0.00384 ± 0.00076	0.000119 ± 0.000178	0.26	97.8	22.8	112	46.07 ± 2.75
Inverse isochron age ± 2σ		45.88 ± 1.85					Integrated age ± 2σ		45.76 ± 1.48
$^{40}Ar/^{39}Ar$ intercept ± 2σ		271.8 ± 344.1		MSWD 0.07			Plateau age ± 2σ		45.78 ± 1.25
UW32C5bk: 1 crystal									
32C5bk1	0.16	2.292 ± 0.031	0.00640 ± 0.00317	0.002314 ± 0.000544	0.09	70.0	4.1	67	41.62 ± 8.38
32C5bk2	0.26	1.836 ± 0.010	0.00222 ± 0.00062	0.000246 ± 0.000171	0.28	95.8	15.5	193	45.58 ± 2.65
32C5bk3	0.39	1.788 ± 0.004	0.00605 ± 0.00019	0.000084 ± 0.000039	1.06	98.4	59.9	71	45.59 ± 0.62
32C5bk4	0.52	1.800 ± 0.015	0.00011 ± 0.00076	0.000074 ± 0.000183	0.24	98.5	13.4	3745	45.96 ± 2.87
32C5bk5	1.50	1.820 ± 0.017	0.00021 ± 0.00159	0.000248 ± 0.000329	0.13	95.7	7.1	2065	45.15 ± 5.05
Inverse isochron age ± 2σ		45.76 ± 0.56					Integrated age ± 2σ		45.45 ± 0.84
$^{40}Ar/^{39}Ar$ intercept ± 2σ		229.8 ± 112.8		MSWD 0.25			Plateau age ± 2σ		45.58 ± 0.58
Combined single crystal incremental heating ages									
Inverse isochron age ± 2σ		45.81 ± 0.26					Integrated age ± 2σ		45.57 ± 0.36
$^{40}Ar/^{39}Ar$ intercept ± 2σ		259.9 ± 29.5		MSWD 0.13			Weighted mean: plateau ages ± 2σ		45.67 ± 0.27
				MSWD 0.11			Weighted mean: integrated ages ± 2σ		45.56 ± 0.32

Table DR3. Complete $^{40}Ar/^{39}Ar$ results

Sample Experiment	laser power (W)	$^{40}Ar/^{39}Ar$	$^{37}Ar/^{39}Ar$	$^{36}Ar/^{39}Ar$	$^{40}Ar^*$ X10^{-14} mol	$^{40}Ar^*$ %	$^{39}Ar_K$ %	K/Ca	Apparent Age ± 2σ Ma
Portly tuff IC-5 biotite continued									
Multi-crystal incremental heating experiments									
UW32C5bl: 3 crystals									
32C5bl1	0.13	2.745 ± 0.025	0.00047 ± 0.02295	0.003247 ± 0.000514	0.18	64.9	1.9	916	46.14 ± 7.85
32C5bl2	0.20	1.922 ± 0.007	0.00293 ± 0.00498	0.000361 ± 0.000163	0.46	94.2	7.0	147	46.92 ± 2.48
32C5bl3	0.29	1.807 ± 0.003	0.00341 ± 0.00167	0.000156 ± 0.000036	1.33	97.2	21.5	126	45.52 ± 0.57
32C5bl4	0.38	1.795 ± 0.003	0.01717 ± 0.00143	0.000130 ± 0.000026	1.99	97.7	32.4	25	45.43 ± 0.43
32C5bl5	0.47	1.794 ± 0.002	0.00049 ± 0.00094	0.000064 ± 0.000029	2.05	98.7	33.4	886	45.87 ± 0.45
32C5bl6	1.50	1.860 ± 0.020	0.00786 ± 0.00844	0.000414 ± 0.000196	0.24	93.2	3.8	55	44.94 ± 3.13
Inverse isochron age ± 2σ		45.57 ± 0.40				Integrated age ± 2σ			45.69 ± 0.35
$^{40}Ar/^{39}Ar$ intercept ± 2σ		311.3 ± 96.0		MSWD 0.69		Plateau age ± 2σ			45.62 ± 0.28
UW32C5bm: 3 crystals									
32C5bm1	0.13	3.245 ± 0.018	0.02203 ± 0.01121	0.005286 ± 0.000333	0.38	51.8	3.5	20	43.56 ± 5.09
32C5bm2	0.20	1.866 ± 0.006	0.00159 ± 0.00404	0.000404 ± 0.000099	0.57	93.4	8.9	270	45.15 ± 1.53
32C5bm3	0.29	1.813 ± 0.004	0.00721 ± 0.00152	0.000166 ± 0.000061	1.25	97.1	20.1	60	45.61 ± 0.95
32C5bm4	0.38	1.801 ± 0.003	0.00820 ± 0.00136	0.000092 ± 0.000026	1.69	98.3	27.3	52	45.85 ± 0.43
32C5bm5	0.47	1.792 ± 0.003	0.00204 ± 0.00094	0.000114 ± 0.000019	2.46	97.9	40.0	211	45.45 ± 0.34
32C5bm6	1.50	1.870 ± 0.107	0.17733 ± 0.10081	0.001331 ± 0.002294	0.02	79.5	0.3	2	38.59 ± 35.26
Inverse isochron age ± 2σ		45.64 ± 0.28				Integrated age ± 2σ			45.48 ± 0.36
$^{40}Ar/^{39}Ar$ intercept ± 2σ		279.8 ± 35.9		MSWD 0.64		Plateau age ± 2σ			45.58 ± 0.26
UW32C5bn: 3 crystals									
32C5bn1	0.13	4.197 ± 0.032	0.02030 ± 0.01728	0.008953 ± 0.000634	0.28	36.9	3.0	21	40.19 ± 9.66
32C5bn2	0.20	1.896 ± 0.014	0.01443 ± 0.00518	0.000337 ± 0.000155	0.35	94.6	8.4	30	46.45 ± 2.45
32C5bn3	0.29	1.817 ± 0.006	0.01329 ± 0.00193	0.000183 ± 0.000048	0.86	96.8	21.3	32	45.58 ± 0.79
32C5bn4	0.38	1.795 ± 0.003	0.00281 ± 0.00106	0.000119 ± 0.000042	1.54	97.8	38.7	153	45.48 ± 0.65
32C5bn5	0.47	1.794 ± 0.004	0.00058 ± 0.00204	0.000165 ± 0.000056	0.92	97.0	23.0	744	45.13 ± 0.87
32C5bn6	1.50	1.896 ± 0.019	0.00037 ± 0.01038	0.000426 ± 0.000285	0.24	93.1	5.6	1157	45.75 ± 4.41
Inverse isochron age ± 2σ		45.53 ± 0.44				Integrated age ± 2σ			45.36 ± 0.57
$^{40}Ar/^{39}Ar$ intercept ± 2σ		276.2 ± 40.0		MSWD 0.51		Plateau age ± 2σ			45.45 ± 0.43
UW32C5bo: 3 crystals									
32C5bo1	0.13	2.299 ± 0.014	0.02371 ± 0.00695	0.002665 ± 0.000266	0.33	65.6	6.7	18	39.16 ± 4.08
32C5bo2	0.20	1.854 ± 0.009	0.00576 ± 0.00525	0.000477 ± 0.000142	0.42	92.2	10.5	75	44.29 ± 2.18
32C5bo3	0.29	1.848 ± 0.005	0.00435 ± 0.00279	0.000326 ± 0.000066	0.87	94.5	21.6	99	45.28 ± 1.03
32C5bo4	0.38	1.822 ± 0.005	0.00738 ± 0.00267	0.000174 ± 0.000070	0.86	97.0	21.8	58	45.78 ± 1.09
32C5bo5	0.47	1.839 ± 0.006	0.00837 ± 0.00280	0.000234 ± 0.000074	0.89	96.0	22.4	51	45.76 ± 1.17
32C5bo6	1.50	1.851 ± 0.008	0.00687 ± 0.00289	0.000233 ± 0.000069	0.69	96.1	17.0	63	46.08 ± 1.12
Inverse isochron age ± 2σ		46.30 ± 0.49				Integrated age ± 2σ			45.12 ± 0.58
$^{40}Ar/^{39}Ar$ intercept ± 2σ		190.2 ± 42.9		MSWD 2.53		Plateau age ± 2σ			45.51 ± 0.84
UW32C5bp: 3 crystals									
32C5bp1	0.13	4.020 ± 0.028	0.00106 ± 0.01187	0.007586 ± 0.000482	0.37	44.1	4.6	405	45.96 ± 7.36
32C5bp2	0.20	1.844 ± 0.007	0.00249 ± 0.00436	0.000132 ± 0.000104	0.48	97.6	13.2	173	46.64 ± 1.60
32C5bp3	0.29	1.809 ± 0.004	0.02384 ± 0.00233	0.000209 ± 0.000037	1.08	96.4	30.4	18	45.21 ± 0.59
32C5bp4	0.38	1.797 ± 0.003	0.01352 ± 0.00182	0.000134 ± 0.000037	1.49	97.6	42.2	32	45.45 ± 0.58
32C5bp5	1.50	1.867 ± 0.015	0.02320 ± 0.00674	0.000153 ± 0.000179	0.35	97.4	9.5	19	47.12 ± 2.81
Inverse isochron age ± 2σ		45.42 ± 0.53				Integrated age ± 2σ			45.72 ± 0.57
$^{40}Ar/^{39}Ar$ intercept ± 2σ		301.5 ± 46.9		MSWD 1.07		Plateau age ± 2σ			45.45 ± 0.41
Combined multi-crystal incremental heating ages									
Inverse isochron age ± 2σ		45.61 ± 0.17				Integrated age ± 2σ			45.49 ± 0.21
$^{40}Ar/^{39}Ar$ intercept ± 2σ		280.9 ± 19.9	MSWD 0.19			Weighted mean: plateau ages ± 2σ			45.55 ± 0.16
			MSWD 0.93			Weighted mean: integrated ages ± 2σ			45.52 ± 0.20

Table DR3. Complete $^{40}Ar/^{39}Ar$ results

Sample Experiment	laser power (W)	$^{40}Ar/^{39}Ar$	$^{37}Ar/^{39}Ar$	$^{36}Ar/^{39}Ar$	$^{40}Ar^*$ X10^{-14} mol	$^{40}Ar^*$ %	$^{39}Ar_K$ %	K/Ca	Apparent Age ± 2σ Ma
Portly tuff IC-5 biotite continued									
Grand combined incremental heating ages									
Inverse isochron age ± 2σ		45.63 ± 0.15						Integrated age ± 2σ	45.52 ± 0.19
$^{40}Ar/^{39}Ar$ intercept ± 2σ		286.4 ± 20.0		MSWD 0.17				Weighted mean: plateau ages ± 2σ	**45.58 ± 0.14**
				MSWD 0.33				Weighted mean: integrated ages ± 2σ	45.53 ± 0.17
Oily tuff IC-6 biotite J = 0.014572 ± 0.10% μ = 1.0035									
Single crystal incremental heating experiments									
UW32C7ba: 1 crystal									
32C7ba1	0.16	2.510 ± 0.040	0.03223 ± 0.00103	0.002792 ± 0.000266	0.24	67.0	4.3	13	43.70 ± 4.50
32C7ba2	0.32	1.794 ± 0.006	0.00923 ± 0.00015	0.000148 ± 0.000040	1.26	97.3	31.4	47	45.34 ± 0.68
32C7ba3	0.65	1.760 ± 0.003	0.03950 ± 0.00026	0.000034 ± 0.000035	2.52	99.3	63.9	11	45.38 ± 0.56
32C7ba4	1.50	1.389 ± 0.428	0.00701 ± 0.00777	0.000190 ± 0.003204	0.01	95.7	0.4	61	34.59 ± 53.60
Inverse isochron age ± 2σ		45.40 ± 0.43						Integrated age ± 2σ	45.25 ± 0.50
$^{40}Ar/^{39}Ar$ intercept ± 2σ		272.6 ± 59.5		MSWD 0.24				Plateau age ± 2σ	45.25 ± 0.43
UW32C7bb: 1 crystal									
32C7bb1	0.23	1.992 ± 0.014	0.00241 ± 0.00046	0.001046 ± 0.000171	0.31	84.3	38.4	179	43.60 ± 2.68
32C7bb2	0.42	1.793 ± 0.010	0.01726 ± 0.00031	0.000265 ± 0.000102	0.40	95.5	55.6	25	44.44 ± 1.63
32C7bb3	0.52	2.162 ± 0.122	0.00434 ± 0.00419	0.001189 ± 0.001727	0.04	83.6	4.4	99	46.89 ± 26.82
32C7bb4	1.50	1.539 ± 0.307	0.01227 ± 0.00938	0.001067 ± 0.003367	0.01	79.3	1.6	35	31.80 ± 53.63
Inverse isochron age ± 2σ		44.65 ± 2.08						Integrated age ± 2σ	44.02 ± 2.01
$^{40}Ar/^{39}Ar$ intercept ± 2σ		259.4 ± 138.7		MSWD 0.18				Plateau age ± 2σ	44.21 ± 1.39
UW32C7bc: 1 crystal									
32C7bc1	0.19	1.937 ± 0.003	0.00273 ± 0.00007	0.000692 ± 0.000016	3.34	89.2	31.6	158	44.87 ± 0.29
32C7bc2	0.29	1.775 ± 0.003	0.00657 ± 0.00010	0.000110 ± 0.000015	2.90	97.9	29.9	65	45.13 ± 0.26
32C7bc3	0.39	1.785 ± 0.006	0.03225 ± 0.00028	0.000117 ± 0.000015	3.16	97.9	32.4	13	45.38 ± 0.39
32C7bc4	0.52	1.867 ± 0.009	0.00464 ± 0.00023	0.000399 ± 0.000071	0.59	93.5	5.8	93	45.30 ± 1.16
32C7bc5	1.50	1.804 ± 0.088	0.00860 ± 0.00317	0.000139 ± 0.001082	0.04	97.5	0.4	50	45.67 ± 16.98
Inverse isochron age ± 2σ		45.27 ± 0.26						Integrated age ± 2σ	45.09 ± 0.14
$^{40}Ar/^{39}Ar$ intercept ± 2σ		273.8 ± 22.9		MSWD 1.18				Plateau age ± 2σ	45.14 ± 0.19
UW32C7bd: 1 crystal									
32C7bd1	0.19	2.018 ± 0.007	0.00282 ± 0.00009	0.000916 ± 0.000029	1.53	86.4	20.2	152	45.24 ± 0.56
32C7bd2	0.32	1.760 ± 0.003	0.00422 ± 0.00007	0.000038 ± 0.000015	3.65	99.1	55.2	102	45.28 ± 0.28
32C7bd3	0.45	1.760 ± 0.007	0.00209 ± 0.00009	0.000110 ± 0.000038	1.27	97.9	19.2	206	44.74 ± 0.68
32C7bd4	1.50	1.761 ± 0.025	0.00091 ± 0.00026	0.000108 ± 0.000148	0.36	97.9	5.4	474	44.78 ± 2.57
Inverse isochron age ± 2σ		45.19 ± 0.30						Integrated age ± 2σ	45.14 ± 0.28
$^{40}Ar/^{39}Ar$ intercept ± 2σ		297.2 ± 29.8		MSWD 0.77				Plateau age ± 2σ	45.20 ± 0.24
UW32C7be: 1 crystal									
32C7be1	0.16	1.985 ± 0.004	0.00693 ± 0.00032	0.000973 ± 0.000070	0.60	85.3	7.9	62	43.97 ± 1.08
32C7be2	0.23	1.782 ± 0.003	0.00182 ± 0.00009	0.000100 ± 0.000028	1.47	98.1	21.3	236	45.37 ± 0.45
32C7be3	0.36	1.765 ± 0.002	0.01698 ± 0.00015	0.000073 ± 0.000015	3.79	98.6	55.5	25	45.17 ± 0.24
32C7be4	0.39	1.780 ± 0.004	0.00579 ± 0.00021	0.000109 ± 0.000065	0.62	98.0	9.0	74	45.27 ± 1.02
32C7be5	1.50	1.785 ± 0.008	0.00133 ± 0.00027	0.000160 ± 0.000127	0.44	97.1	6.3	322	45.00 ± 1.96
Inverse isochron age ± 2σ		45.31 ± 0.21						Integrated age ± 2σ	45.11 ± 0.25
$^{40}Ar/^{39}Ar$ intercept ± 2σ		245.0 ± 40.2		MSWD 1.43				Plateau age ± 2σ	45.17 ± 0.25

Table DR3. Complete $^{40}Ar/^{39}Ar$ results

Sample Experiment	laser power (W)	$^{40}Ar/^{39}Ar$	$^{37}Ar/^{39}Ar$	$^{36}Ar/^{39}Ar$	$^{40}Ar^*$ X10^{-14} mol	$^{40}Ar^*$ %	$^{39}Ar_K$ %	K/Ca	Apparent Age ± 2σ Ma
Oily tuff IC-6 biotite continued									
UW32C7bf: 1 crystal									
32C7bf1	0.18	1.931 ± 0.003	0.00346 ± 0.00016	0.000807 ± 0.000052	1.13	87.4	20.9	124	43.84 ± 0.81
32C7bf2	0.24	1.795 ± 0.003	0.00181 ± 0.00011	0.000174 ± 0.000036	1.53	96.9	30.4	238	45.14 ± 0.57
32C7bf3	0.37	1.741 ± 0.002	0.02093 ± 0.00021	0.000042 ± 0.000021	2.30	99.1	47.1	21	44.80 ± 0.34
32C7bf4	0.40	1.027 ± 0.016	0.03964 ± 0.00367	0.000076 ± 0.001849	0.02	97.7	0.6	11	26.17 ± 28.32
32C7bf5	1.50	1.653 ± 0.010	0.11686 ± 0.00299	0.000232 ± 0.000826	0.05	96.1	1.1	4	41.31 ± 12.56
Inverse isochron age ± 2σ		44.92 ± 0.42					Integrated age ± 2σ		44.55 ± 0.37
$^{40}Ar/^{39}Ar$ intercept ± 2σ		256.7 ± 56.6		MSWD 2.28			Plateau age ± 2σ		44.77 ± 0.42
UW32C7bg: 1 crystal									
32C7bg1	0.16	2.884 ± 0.006	0.00506 ± 0.00034	0.003759 ± 0.000229	0.47	61.3	12.2	85	45.91 ± 3.47
32C7bg2	0.21	1.802 ± 0.003	0.00226 ± 0.00017	0.000078 ± 0.000106	0.58	98.5	24.2	190	46.06 ± 1.61
32C7bg3	0.26	1.789 ± 0.004	0.00131 ± 0.00024	0.000062 ± 0.000143	0.55	98.7	23.0	328	45.85 ± 2.17
32C7bg4	0.32	1.773 ± 0.005	0.00319 ± 0.00032	0.000059 ± 0.000119	0.45	98.8	19.2	135	45.46 ± 1.81
32C7bg5	0.39	1.754 ± 0.006	0.00141 ± 0.00028	0.000004 ± 0.000136	0.43	99.7	18.5	306	45.38 ± 2.08
32C7bg6	1.50	1.657 ± 0.016	0.00214 ± 0.00207	0.000326 ± 0.000687	0.06	93.9	2.9	201	40.45 ± 10.47
Inverse isochron age ± 2σ		45.66 ± 0.96					Integrated age ± 2σ		45.59 ± 0.97
$^{40}Ar/^{39}Ar$ intercept ± 2σ		299.3 ± 38.5		MSWD 0.28			Plateau age ± 2σ		45.69 ± 0.90
* UW32C7bh: 1 crystal									
* 32C7bh1	0.16	1.978 ± 0.003	0.01339 ± 0.00010	0.000860 ± 0.000022	3.24	87.0	13.4	32	44.67 ± 0.36
32C7bh2	0.23	1.777 ± 0.002	0.00443 ± 0.00004	0.000087 ± 0.000010	5.05	98.3	23.2	97	45.35 ± 0.19
32C7bh3	0.29	1.758 ± 0.002	0.02136 ± 0.00015	0.000055 ± 0.000005	9.49	98.9	44.0	20	45.15 ± 0.12
32C7bh4	0.36	1.762 ± 0.002	0.13873 ± 0.00093	0.000048 ± 0.000013	3.47	99.5	16.0	3	45.55 ± 0.23
32C7bh5	0.45	1.774 ± 0.004	0.22428 ± 0.00176	0.000160 ± 0.000060	0.60	98.1	2.8	2	45.17 ± 0.93
32C7bh6	1.50	1.888 ± 0.013	0.89253 ± 0.00822	0.000448 ± 0.000340	0.14	96.5	0.6	0.5	47.29 ± 5.19
Inverse isochron age ± 2σ		45.06 ± 0.53					Integrated age ± 2σ		45.21 ± 0.11
$^{40}Ar/^{39}Ar$ intercept ± 2σ		435.6 ± 451.3		MSWD 2.76			Plateau age ± 2σ		45.26 ± 0.16
UW32C7bi: 1 crystal									
32C7bi1	0.17	3.366 ± 0.023	0.02487 ± 0.00140	0.006091 ± 0.000516	0.21	46.5	2.1	17	40.65 ± 7.90
32C7bi2	0.24	1.956 ± 0.014	0.01148 ± 0.00115	0.001030 ± 0.000228	0.23	84.2	4.1	37	42.80 ± 3.52
32C7bi3	0.36	1.793 ± 0.003	0.00437 ± 0.00026	0.000134 ± 0.000041	1.18	97.5	22.9	98	45.40 ± 0.64
32C7bi4	0.42	1.766 ± 0.003	0.00521 ± 0.00016	0.000058 ± 0.000025	1.80	98.8	35.5	83	45.29 ± 0.40
32C7bi5	1.50	1.764 ± 0.003	0.11410 ± 0.00171	0.000110 ± 0.000027	1.78	98.4	35.3	4	45.07 ± 0.43
Inverse isochron age ± 2σ		45.28 ± 0.26					Integrated age ± 2σ		45.04 ± 0.34
$^{40}Ar/^{39}Ar$ intercept ± 2σ		263.5 ± 43.2		MSWD 1.04			Plateau age ± 2σ		45.20 ± 0.27
UW32C7bj: 1 crystal									
32C7bj1	0.17	2.281 ± 0.011	0.01216 ± 0.00104	0.001998 ± 0.000148	0.31	74.0	3.3	35	43.82 ± 2.30
32C7bj2	0.24	1.823 ± 0.005	0.00719 ± 0.00059	0.000305 ± 0.000085	0.45	94.8	6.1	60	44.90 ± 1.31
32C7bj3	0.36	1.774 ± 0.003	0.00371 ± 0.00021	0.000083 ± 0.000034	1.42	98.4	19.8	116	45.30 ± 0.53
32C7bj4	0.42	1.769 ± 0.003	0.00326 ± 0.00016	0.000100 ± 0.000015	2.51	98.1	35.2	132	45.05 ± 0.26
32C7bj5	1.50	1.772 ± 0.003	0.09467 ± 0.00136	0.000127 ± 0.000027	2.55	98.0	35.6	5	45.10 ± 0.43
Inverse isochron age ± 2σ		45.16 ± 0.23					Integrated age ± 2σ		45.07 ± 0.24
$^{40}Ar/^{39}Ar$ intercept ± 2σ		269.2 ± 42.8		MSWD 0.51			Plateau age ± 2σ		45.08 ± 0.21
Combined single crystal incremental heating ages									
Inverse isochron age ± 2σ		45.18 ± 0.11					Integrated age ± 2σ		45.11 ± 0.10
$^{40}Ar/^{39}Ar$ intercept ± 2σ		280.4 ± 11.9		MSWD 0.93			Weighted mean: plateau ages ± 2σ		**45.14 ± 0.10**
				MSWD 1.70			Weighted mean: integrated ages ± 2σ		45.13 ± 0.10
Strawberry tuff SR-1 sanidine J = 0.014656 ± 0.16% μ = 1.0035									
6-8 crystal 1 and 2 step fusions									
* 32B6a	1.50	1.803 ± 0.003	0.00564 ± 0.00017	0.000081 ± 0.000022	1.48	98.4		76	46.33 ± 0.38
* 32B6b	1.50	2.039 ± 0.003	0.00296 ± 0.00017	0.000053 ± 0.000034	1.49	99.0		145	52.61 ± 0.53

Table DR3. Complete $^{40}Ar/^{39}Ar$ results

Sample Experiment	laser power (W)	$^{40}Ar/^{39}Ar$	$^{37}Ar/^{39}Ar$	$^{36}Ar/^{39}Ar$	$^{40}Ar^*$ X10^{-14} mol	$^{40}Ar^*$ %	$^{39}Ar_K$ %	K/Ca	Apparent Age ± 2σ Ma
Strawberry tuff SR-1 sanidine continued									
* 32B6c	1.50	1.785 ± 0.004	0.00480 ± 0.00028	0.000072 ± 0.000044	1.44	98.6		90	45.93 ± 0.69
32B6d	1.50	1.722 ± 0.007	0.00517 ± 0.00051	0.000059 ± 0.000078	0.43	98.7		83	44.42 ± 1.23
32B6e	1.50	1.702 ± 0.007	0.00502 ± 0.00038	0.000094 ± 0.000116	0.51	98.1		86	43.63 ± 1.80
* 32B6f	1.50	1.883 ± 0.005	0.00399 ± 0.00038	0.000051 ± 0.000084	0.73	99.0		108	48.62 ± 1.30
* 32B6g	1.50	1.930 ± 0.012	0.00424 ± 0.00051	0.000060 ± 0.000114	0.52	98.9		101	49.77 ± 1.83
* 32B6h1	0.16	1.867 ± 0.016	0.00026 ± 0.00231	0.000041 ± 0.000694	0.08	99.1	13.1	1669	48.27 ± 10.58
* 32B6h2	1.50	1.977 ± 0.006	0.00276 ± 0.00041	0.000113 ± 0.000080	0.56	98.1	86.9	156	50.56 ± 1.25
* 32B6i1	0.13	1.935 ± 0.024	0.00129 ± 0.00377	0.000637 ± 0.000948	0.06	90.0	10.2	332	45.50 ± 14.50
* 32B6i2	1.50	2.018 ± 0.005	0.00328 ± 0.00036	0.000123 ± 0.000092	0.60	98.0	89.8	131	51.54 ± 1.41
* 32B6j1	0.16	2.022 ± 0.022	0.00277 ± 0.00261	0.000189 ± 0.000594	0.09	97.0	11.9	155	51.14 ± 9.10
* 32B6j2	1.50	2.150 ± 0.007	0.00278 ± 0.00046	0.000087 ± 0.000085	0.71	98.6	88.1	155	55.19 ± 1.34
* 32B6k1	0.17	4.281 ± 0.028	0.00238 ± 0.00152	0.000666 ± 0.000302	0.40	95.3	16.9	181	104.78 ± 4.65
* 32B6k2	1.50	4.397 ± 0.008	0.00332 ± 0.00021	0.000112 ± 0.000054	2.02	99.1	83.1	130	111.74 ± 0.88
* 32B6l1	0.19	1.854 ± 0.010	0.00378 ± 0.00060	0.000131 ± 0.000144	0.31	97.7	43.1	114	47.26 ± 2.25
* 32B6l2	1.50	1.906 ± 0.011	0.00386 ± 0.00069	0.000049 ± 0.000107	0.42	99.0	56.9	112	49.22 ± 1.73
* 32B6m1	0.16	2.225 ± 0.026	0.00255 ± 0.00111	0.000380 ± 0.000312	0.18	94.7	39.7	168	54.89 ± 4.91
* 32B6m2	1.50	2.041 ± 0.016	0.00514 ± 0.00070	0.000167 ± 0.000250	0.25	97.4	60.3	84	51.81 ± 3.88
* 32B6n1	0.16	2.006 ± 0.008	0.00240 ± 0.00058	0.000130 ± 0.000131	0.38	97.9	48.0	179	51.18 ± 2.04
* 32B6n2	1.50	2.059 ± 0.010	0.00242 ± 0.00051	0.000122 ± 0.000111	0.43	98.0	52.0	178	52.60 ± 1.75
* 32B6o1	0.16	1.952 ± 0.012	0.00364 ± 0.00060	0.000122 ± 0.000192	0.35	97.9	32.7	118	49.85 ± 2.99
* 32B6o2	1.50	2.166 ± 0.006	0.00313 ± 0.00028	0.000075 ± 0.000074	0.79	98.8	67.3	137	55.69 ± 1.16
* 32B6p1	0.16	1.954 ± 0.019	0.00146 ± 0.00121	0.000224 ± 0.000333	0.18	96.4	17.3	294	49.11 ± 5.16
* 32B6p2	1.50	2.061 ± 0.006	0.00344 ± 0.00035	0.000131 ± 0.000067	0.89	97.9	82.7	125	52.59 ± 1.07
* 32B6q1	0.16	1.856 ± 0.021	0.00550 ± 0.00202	0.000287 ± 0.000540	0.09	95.2	13.6	78	46.12 ± 8.30
* 32B6q2	1.50	1.882 ± 0.009	0.00431 ± 0.00035	0.000079 ± 0.000095	0.57	98.5	86.4	100	48.37 ± 1.51
* 32B6r1	0.16	2.084 ± 0.021	0.00066 ± 0.00177	0.000402 ± 0.000479	0.12	94.1	9.3	651	51.11 ± 7.35
* 32B6r2	1.50	2.026 ± 0.003	0.00387 ± 0.00020	0.000026 ± 0.000049	1.13	99.4	90.7	111	52.49 ± 0.77
* 32B6s1	0.16	1.733 ± 0.032	0.00713 ± 0.00421	0.000243 ± 0.000967	0.05	95.6	4.7	60	43.29 ± 14.83
* 32B6s2	1.50	1.806 ± 0.004	0.00456 ± 0.00017	0.000141 ± 0.000047	1.02	97.5	95.3	94	45.96 ± 0.73
* 32B6t1	0.16	2.434 ± 0.106	0.00474 ± 0.01477	0.000882 ± 0.003319	0.02	89.1	1.8	91	56.45 ± 50.56
* 32B6t2	1.50	1.848 ± 0.006	0.01188 ± 0.00030	0.000167 ± 0.000092	0.66	97.1	98.2	36	46.85 ± 1.44
* 32B6u1	0.16	2.033 ± 0.015	0.00172 ± 0.00090	0.000177 ± 0.000235	0.22	97.2	15.9	250	51.51 ± 3.66
* 32B6u2	1.50	2.128 ± 0.003	0.00280 ± 0.00018	0.000033 ± 0.000042	1.25	99.3	84.1	153	55.03 ± 0.66
* 32B6v1	0.16	1.951 ± 0.014	0.00148 ± 0.00066	0.000080 ± 0.000155	0.33	98.6	30.7	291	50.13 ± 2.45
* 32B6v2	1.50	2.022 ± 0.005	0.00340 ± 0.00026	0.000070 ± 0.000088	0.76	98.8	69.3	126	52.03 ± 1.36
* 32B6w1	0.16	1.843 ± 0.011	0.00323 ± 0.00100	0.000145 ± 0.000172	0.25	97.4	27.4	133	46.86 ± 2.68
* 32B6w2	1.50	2.200 ± 0.005	0.00341 ± 0.00026	0.000063 ± 0.000072	0.79	99.0	72.6	126	56.66 ± 1.12
* 32B6x	1.50	1.840 ± 0.003	0.00339 ± 0.00021	0.000033 ± 0.000053	0.93	99.2		127	47.65 ± 0.82
* 32B6y	1.50	1.830 ± 0.006	0.00417 ± 0.00024	0.000064 ± 0.000071	0.67	98.7		103	47.15 ± 1.13
* 32B6z	1.50	1.782 ± 0.005	0.00486 ± 0.00045	0.000011 ± 0.000054	0.74	99.6		88	46.31 ± 0.85
* 32B6aa	1.50	1.785 ± 0.008	0.00455 ± 0.00051	0.000059 ± 0.000115	0.39	98.8		95	46.04 ± 1.80
	No isochron						Integrated age ± 2σ		52.45 ± 0.24
				MSWD 0.53			Weighted mean age ± 2σ		44.17 ± 1.02
Single crystal fusions									
* 32B6bb	1.50	1.760 ± 0.032	0.02279 ± 0.04251	0.001208 ± 0.000649	0.07	79.6		19	36.65 ± 10.07
32B6cc	1.50	1.726 ± 0.025	0.08567 ± 0.03917	0.000266 ± 0.000944	0.07	95.6		5	43.08 ± 14.47
* 32B6dd	1.50	2.092 ± 0.022	0.01667 ± 0.01940	0.000716 ± 0.000433	0.16	89.7		26	48.96 ± 6.68
32B6ee	1.50	1.678 ± 0.026	0.02048 ± 0.03732	0.000049 ± 0.000875	0.08	99.0		21	43.38 ± 13.41
32B6ff	1.50	1.689 ± 0.038	0.00059 ± 0.05564	0.000272 ± 0.001182	0.05	95.0		723	41.93 ± 18.15
32B6gg	1.50	1.728 ± 0.034	0.06098 ± 0.05067	0.000876 ± 0.000821	0.06	85.0		7	38.45 ± 12.69
32B6hh	1.50	1.705 ± 0.038	0.00882 ± 0.05786	0.000030 ± 0.001207	0.05	99.3		49	44.19 ± 18.51
32B6ii	1.50	1.707 ± 0.057	0.00314 ± 0.09823	0.000803 ± 0.002162	0.03	85.8		137	38.32 ± 33.20
32B6jj	1.50	1.745 ± 0.021	0.00039 ± 0.02774	0.000208 ± 0.000350	0.13	96.2		1093	43.86 ± 5.45
32B6kk	1.50	1.752 ± 0.056	0.02260 ± 0.08646	0.000301 ± 0.001872	0.03	94.8		19	43.37 ± 28.71
32B6ll	1.50	1.732 ± 0.019	0.00058 ± 0.02145	0.000097 ± 0.000488	0.13	98.1		740	44.36 ± 7.50
32B6mm	1.50	1.746 ± 0.037	0.11140 ± 0.06540	0.000262 ± 0.001237	0.04	95.8		4	43.69 ± 18.97
* 32B6nn	1.50	2.003 ± 0.036	0.09093 ± 0.05853	0.000290 ± 0.001607	0.06	95.8		5	50.06 ± 24.50
32B6oo	1.50	1.760 ± 0.032	0.01899 ± 0.06534	0.000640 ± 0.001386	0.04	89.1		23	40.98 ± 21.24
32B6pp	1.50	1.771 ± 0.028	0.00175 ± 0.03976	0.000015 ± 0.000811	0.07	99.5		246	46.00 ± 12.44
32B6qq	1.50	1.745 ± 0.022	0.03504 ± 0.03224	0.000124 ± 0.000615	0.10	97.8		12	44.57 ± 9.44

Table DR3. Complete $^{40}Ar/^{39}Ar$ results

Sample Experiment	laser power (W)	$^{40}Ar/^{39}Ar$	$^{37}Ar/^{39}Ar$	$^{36}Ar/^{39}Ar$	$^{40}Ar^*$ X10^{-14} mol	$^{40}Ar^*$ %	$^{39}Ar_K$ %	K/Ca	Apparent Age ± 2σ Ma
Strawberry tuff SR-1 sanidine continued									
* 32B6rr	1.50	2.533 ± 0.028	0.04588 ± 0.03278	0.000191 ± 0.000794	0.11	97.7		9	64.29 ± 12.06
32B6ss	1.50	1.799 ± 0.023	0.00134 ± 0.04818	0.000020 ± 0.001098	0.07	99.4		321	46.69 ± 16.77
32B6tt	1.50	1.700 ± 0.068	0.09878 ± 0.11547	0.001019 ± 0.002624	0.02	82.5		4	36.69 ± 40.34
32B6uu	1.50	1.767 ± 0.048	0.00662 ± 0.07723	0.000731 ± 0.002479	0.03	87.5		65	40.43 ± 37.96
32B6vv	1.50	1.747 ± 0.012	0.00058 ± 0.01756	0.000290 ± 0.000388	0.15	94.8		747	43.28 ± 5.94
32B6ww	1.50	1.732 ± 0.027	0.01206 ± 0.04732	0.000837 ± 0.000864	0.05	85.5		36	38.74 ± 13.28
32B6xx	1.50	1.739 ± 0.011	0.00053 ± 0.02042	0.000269 ± 0.000300	0.17	95.2		818	43.25 ± 4.62
* 32B6yy	1.50	1.727 ± 0.014	0.00514 ± 0.02250	0.001322 ± 0.000321	0.12	77.1		84	34.87 ± 4.98
32B6zz	1.50	1.732 ± 0.014	0.00357 ± 0.01969	0.000265 ± 0.000335	0.13	95.2		120	43.08 ± 5.16
Inverse isochron age ± 2σ		50.44 ± 10.87					Integrated age ± 2σ		43.80 ± 2.31
$^{40}Ar/^{39}Ar$ intercept ± 2σ		-775.4 ± 9986.5		MSWD 0.10			Weighted mean age ± 2σ		43.29 ± 2.12
Combined fusion ages									
Inverse isochron age ± 2σ		43.77 ± 1.61					Integrated age ± 2σ		51.73 ± 0.29
$^{40}Ar/^{39}Ar$ intercept ± 2σ		383.1 ± 1247.6		MSWD 0.14			Weighted mean age ± 2σ		**44.00 ± 0.92**
Strawberry tuff SR-1b biotite J = 0.014656 ± 0.16% μ = 1.0035									
Multi-crystal incremental heating experiments									
* UW32B6ba: 3 crystals									
* 32B6ba	0.16	2.820 ± 0.010	0.01913 ± 0.00064	0.004949 ± 0.000157	0.52	48.0	33.9	22	35.46 ± 2.44
32B6ba	0.26	2.468 ± 0.015	0.02067 ± 0.00103	0.002202 ± 0.000286	0.33	73.5	24.6	21	47.36 ± 4.40
32B6ba	0.36	2.427 ± 0.017	0.03763 ± 0.00162	0.002618 ± 0.000216	0.25	68.1	18.8	11	43.15 ± 3.38
32B6ba	0.45	3.011 ± 0.021	0.06977 ± 0.00326	0.005177 ± 0.000327	0.18	49.2	11.3	6	38.77 ± 5.05
32B6ba	0.58	2.044 ± 0.024	0.07864 ± 0.00379	0.000899 ± 0.000715	0.07	87.1	6.2	5	46.46 ± 10.95
32B6ba	1.50	2.152 ± 0.022	0.03101 ± 0.00385	0.001371 ± 0.000895	0.06	81.1	5.2	14	45.55 ± 13.67
Inverse isochron age ± 2σ		49.32 ± 4.38					Integrated age ± 2σ		41.42 ± 1.89
$^{40}Ar/^{39}Ar$ intercept ± 2σ		219.4 ± 56.1		MSWD 1.75			Plateau age ± 2σ		43.59 ± 3.02
* UW32B6bb: 3 crystals									
* 32B6bb	0.16	2.886 ± 0.011	0.01754 ± 0.00076	0.005738 ± 0.000156	0.45	41.1	18.7	25	31.12 ± 2.41
* 32B6bb	0.26	2.148 ± 0.010	0.01392 ± 0.00058	0.001305 ± 0.000151	0.40	81.9	22.4	31	45.90 ± 2.34
32B6bb	0.32	2.218 ± 0.013	0.02113 ± 0.00102	0.001636 ± 0.000154	0.27	78.1	14.9	20	45.21 ± 2.43
32B6bb	0.52	2.092 ± 0.005	0.08186 ± 0.00142	0.001551 ± 0.000118	0.45	78.2	26.1	5	42.73 ± 1.82
32B6bb	1.50	2.227 ± 0.008	0.08956 ± 0.00158	0.002363 ± 0.000181	0.33	68.8	17.8	5	40.04 ± 2.80
Inverse isochron age ± 2σ		43.23 ± 16.57					Integrated age ± 2σ		41.17 ± 1.04
$^{40}Ar/^{39}Ar$ intercept ± 2σ		287.2 ± 602.1		MSWD 3.92			Plateau age ± 2σ		42.86 ± 2.56
#* UW32B6bc: 3 crystals									
* 32B6bc	0.16	3.613 ± 0.012	0.03196 ± 0.00080	0.009305 ± 0.000124	0.69	23.8	22.7	13	22.63 ± 1.95
32B6bc	0.26	2.964 ± 0.018	0.03413 ± 0.00191	0.004343 ± 0.000175	0.39	56.6	15.8	13	43.84 ± 2.75
32B6bc	0.32	3.022 ± 0.022	0.03496 ± 0.00112	0.005051 ± 0.000318	0.31	50.5	12.0	12	39.91 ± 4.96
32B6bc	0.52	2.661 ± 0.018	0.04197 ± 0.00097	0.003610 ± 0.000128	0.63	59.9	28.5	10	41.61 ± 2.14
32B6bc	1.50	2.462 ± 0.023	0.12625 ± 0.00215	0.003096 ± 0.000212	0.43	63.1	21.0	3	40.57 ± 3.45
Inverse isochron age ± 2σ		36.60 ± 11.19					Integrated age ± 2σ		37.25 ± 1.28
$^{40}Ar/^{39}Ar$ intercept ± 2σ		349.0 ± 124.1		MSWD 1.10			Plateau age ± 2σ		41.90 ± 1.52
#* UW32B6bd: 3 crystals									
* 32B6bd	0.16	3.041 ± 0.019	0.02695 ± 0.00101	0.006714 ± 0.000183	0.49	34.7	30.0	16	27.65 ± 2.90
32B6bd	0.26	2.683 ± 0.039	0.02982 ± 0.00148	0.003757 ± 0.000263	0.27	58.5	19.2	14	41.03 ± 4.47
32B6bd	0.32	2.808 ± 0.036	0.03488 ± 0.00144	0.003959 ± 0.000390	0.18	58.3	12.0	12	42.72 ± 6.22
32B6bd	0.52	2.491 ± 0.021	0.04854 ± 0.00104	0.003038 ± 0.000306	0.30	63.9	22.3	9	41.60 ± 4.78
32B6bd	1.50	2.723 ± 0.031	0.07424 ± 0.00202	0.003675 ± 0.000390	0.24	60.2	16.5	6	42.77 ± 6.13
Inverse isochron age ± 2σ		38.52 ± 27.68					Integrated age ± 2σ		37.65 ± 2.05
$^{40}Ar/^{39}Ar$ intercept ± 2σ		331.3 ± 324.4		MSWD 0.11			Plateau age ± 2σ		41.82 ± 2.61

Table DR3. Complete $^{40}Ar/^{39}Ar$ results

Sample Experiment	laser power (W)	$^{40}Ar/^{39}Ar$	$^{37}Ar/^{39}Ar$	$^{36}Ar/^{39}Ar$	$^{40}Ar^*$ X10^{-14} mol	$^{40}Ar^*$ %	$^{39}Ar_K$ %	K/Ca	Apparent Age ± 2σ Ma
Strawberry tuff SR-1b biotite continued									
* UW32B6be: 3 crystals									
* 32B6be	0.16	3.162 ± 0.014	0.02440 ± 0.00108	0.006736 ± 0.000216	0.42	37.0	20.9	18	30.62 ± 3.35
32B6be	0.26	2.364 ± 0.015	0.02285 ± 0.00127	0.001995 ± 0.000256	0.29	74.9	19.1	19	46.23 ± 3.96
32B6be	0.32	2.278 ± 0.013	0.02115 ± 0.00115	0.001666 ± 0.000258	0.20	78.3	13.9	20	46.51 ± 3.97
32B6be	0.52	2.214 ± 0.008	0.06020 ± 0.00171	0.001428 ± 0.000256	0.31	80.9	22.0	7	46.75 ± 3.92
32B6be	1.50	1.983 ± 0.010	0.08253 ± 0.00156	0.000755 ± 0.000148	0.30	88.8	24.1	5	45.97 ± 2.31
Inverse isochron age ± 2σ		45.73 ± 4.45				Integrated age ± 2σ			43.07 ± 1.56
$^{40}Ar/^{39}Ar$ intercept ± 2σ		311.8 ± 131.5		MSWD 0.05		Plateau age ± 2σ			46.24 ± 1.62
* UW32B6bf: 3 crystals									
* 32B6bf	0.16	3.893 ± 0.013	0.04140 ± 0.00106	0.008829 ± 0.000263	0.41	32.9	26.0	10	33.57 ± 4.05
32B6bf	0.26	2.941 ± 0.017	0.03819 ± 0.00112	0.004493 ± 0.000322	0.25	54.8	20.5	11	42.09 ± 4.95
32B6bf	0.32	3.039 ± 0.016	0.05287 ± 0.00226	0.004031 ± 0.000646	0.16	60.8	12.8	8	48.17 ± 9.85
32B6bf	0.52	2.687 ± 0.014	0.05927 ± 0.00164	0.003558 ± 0.000266	0.29	60.9	26.4	7	42.72 ± 4.09
32B6bf	1.50	2.320 ± 0.016	0.07650 ± 0.00274	0.002992 ± 0.000438	0.13	62.0	14.3	6	37.60 ± 6.72
Inverse isochron age ± 2σ		27.20 ± 21.48				Integrated age ± 2σ			40.18 ± 2.42
$^{40}Ar/^{39}Ar$ intercept ± 2σ		447.8 ± 321.6		MSWD 1.13		Plateau age ± 2σ			42.09 ± 2.92
#* UW32B6bg: 3 crystals									
* 32B6bg	0.16	3.050 ± 0.008	0.02418 ± 0.00068	0.006855 ± 0.000173	0.58	33.5	20.9	18	26.78 ± 2.66
32B6bg	0.26	2.430 ± 0.007	0.02227 ± 0.00073	0.002598 ± 0.000162	0.41	68.3	18.3	19	43.33 ± 2.48
32B6bg	0.32	2.470 ± 0.015	0.02461 ± 0.00130	0.002557 ± 0.000241	0.27	69.3	12.2	17	44.68 ± 3.74
32B6bg	0.52	2.379 ± 0.007	0.04691 ± 0.00083	0.002592 ± 0.000232	0.59	67.8	27.3	9	42.11 ± 3.55
32B6bg	1.50	2.052 ± 0.010	0.08475 ± 0.00146	0.001217 ± 0.000182	0.40	82.6	21.3	5	44.24 ± 2.81
Inverse isochron age ± 2σ		44.63 ± 5.07				Integrated age ± 2σ			39.91 ± 1.42
$^{40}Ar/^{39}Ar$ intercept ± 2σ		277.0 ± 88.7		MSWD 0.43		Plateau age ± 2σ			43.59 ± 1.51
#* UW32B6bh: 5 crystals									
* 32B6bh	0.16	2.768 ± 0.005	0.01948 ± 0.00036	0.005215 ± 0.000074	1.50	44.2	43.1	22	32.04 ± 1.15
32B6bh	0.26	2.280 ± 0.006	0.02165 ± 0.00047	0.002254 ± 0.000097	0.75	70.7	26.3	20	42.07 ± 1.51
32B6bh	0.32	2.225 ± 0.018	0.04721 ± 0.00131	0.002324 ± 0.000269	0.26	69.1	9.4	9	40.17 ± 4.19
32B6bh	0.52	2.019 ± 0.010	0.17879 ± 0.00240	0.001499 ± 0.000140	0.36	78.5	14.0	2	41.42 ± 2.19
32B6bh	1.50	2.024 ± 0.018	0.04993 ± 0.00154	0.001720 ± 0.000304	0.18	74.8	7.2	9	39.60 ± 4.72
Inverse isochron age ± 2σ		39.34 ± 7.17				Integrated age ± 2σ			37.30 ± 0.88
$^{40}Ar/^{39}Ar$ intercept ± 2σ		339.3 ± 143.2		MSWD 0.53		Plateau age ± 2σ			41.60 ± 1.15
#* UW32B6bi: 5 crystals									
* 32B6bi	0.16	3.380 ± 0.007	0.03212 ± 0.00062	0.007549 ± 0.000087	1.03	33.9	41.2	13	30.07 ± 1.35
32B6bi	0.26	2.778 ± 0.011	0.03370 ± 0.00100	0.003617 ± 0.000134	0.51	61.5	24.9	13	44.56 ± 2.09
32B6bi	0.32	2.710 ± 0.020	0.04312 ± 0.00175	0.003565 ± 0.000227	0.23	61.1	11.5	10	43.22 ± 3.59
32B6bi	0.52	2.276 ± 0.016	0.11200 ± 0.00251	0.002348 ± 0.000231	0.23	69.7	13.8	4	41.45 ± 3.60
32B6bi	1.50	2.307 ± 0.020	0.04476 ± 0.00187	0.001869 ± 0.000420	0.15	76.0	8.6	10	45.77 ± 6.47
Inverse isochron age ± 2σ		39.19 ± 9.66				Integrated age ± 2σ			38.13 ± 1.14
$^{40}Ar/^{39}Ar$ intercept ± 2σ		350.3 ± 120.6		MSWD 0.90		Plateau age ± 2σ			43.79 ± 1.57
* UW32B6bj: 5 crystals									
* 32B6bj	0.16	3.002 ± 0.007	0.02632 ± 0.00068	0.005995 ± 0.000117	0.84	40.9	29.3	16	32.16 ± 1.80
32B6bj	0.26	2.492 ± 0.009	0.02863 ± 0.00101	0.002662 ± 0.000135	0.55	68.3	22.8	15	44.45 ± 2.09
32B6bj	0.32	2.622 ± 0.013	0.03356 ± 0.00097	0.002942 ± 0.000263	0.34	66.8	13.5	13	45.68 ± 4.05
32B6bj	0.52	2.273 ± 0.013	0.06824 ± 0.00118	0.002119 ± 0.000163	0.46	72.5	20.9	6	43.01 ± 2.55
32B6bj	1.50	2.052 ± 0.015	0.11233 ± 0.00235	0.001201 ± 0.000199	0.27	82.9	13.6	4	44.41 ± 3.12
Inverse isochron age ± 2σ		42.66 ± 5.73				Integrated age ± 2σ			40.72 ± 1.13
$^{40}Ar/^{39}Ar$ intercept ± 2σ		321.7 ± 97.8		MSWD 0.49		Plateau age ± 2σ			44.18 ± 1.35

Table DR3. Complete $^{40}Ar/^{39}Ar$ results

Sample Experiment	laser power (W)	$^{40}Ar/^{39}Ar$	$^{37}Ar/^{39}Ar$	$^{36}Ar/^{39}Ar$	$^{40}Ar^*$ X10^{-14} mol	$^{40}Ar^*$ %	$^{39}Ar_K$ %	K/Ca	Apparent Age ± 2σ Ma
Strawberry tuff SR-1b biotite continued									
#* UW32B6bk: 5 crystals									
* 32B6bk	0.16	3.381 ± 0.011	0.02805 ± 0.00085	0.008152 ± 0.000169	0.66	28.7	24.6	15	25.44 ± 2.62
32B6bk	0.26	2.811 ± 0.012	0.03093 ± 0.00101	0.003511 ± 0.000241	0.48	63.0	21.3	14	46.22 ± 3.70
32B6bk	0.32	2.672 ± 0.016	0.03187 ± 0.00116	0.003257 ± 0.000224	0.27	63.9	12.8	13	44.56 ± 3.50
32B6bk	0.52	2.397 ± 0.011	0.05960 ± 0.00133	0.002553 ± 0.000171	0.52	68.5	27.0	7	42.90 ± 2.65
32B6bk	1.50	2.135 ± 0.015	0.08092 ± 0.00147	0.001504 ± 0.000240	0.25	79.3	14.4	5	44.18 ± 3.73
Inverse isochron age ± 2σ		41.06 ± 7.31						Integrated age ± 2σ	39.73 ± 1.43
$^{40}Ar/^{39}Ar$ intercept ± 2σ		340.5 ± 105.8		MSWD 0.73				Plateau age ± 2σ	44.17 ± 1.65
#* UW32B6bl: 5 crystals									
* 32B6bl	0.16	3.981 ± 0.012	0.03824 ± 0.00095	0.010498 ± 0.000212	0.80	22.0	21.7	11	23.05 ± 3.27
* 32B6bl	0.26	3.313 ± 0.015	0.03804 ± 0.00127	0.006221 ± 0.000146	0.53	44.5	17.2	11	38.51 ± 2.27
32B6bl	0.32	2.937 ± 0.018	0.03665 ± 0.00103	0.004304 ± 0.000256	0.35	56.6	13.0	12	43.43 ± 3.98
32B6bl	0.52	2.732 ± 0.007	0.05388 ± 0.00104	0.003787 ± 0.000183	0.71	59.0	28.3	8	42.11 ± 2.81
32B6bl	1.50	2.195 ± 0.014	0.10146 ± 0.00196	0.001829 ± 0.000152	0.40	75.5	19.7	4	43.29 ± 2.40
Inverse isochron age ± 2σ		43.60 ± 4.61						Integrated age ± 2σ	37.78 ± 1.34
$^{40}Ar/^{39}Ar$ intercept ± 2σ		286.3 ± 57.5		MSWD 0.24				Plateau age ± 2σ	42.90 ± 1.66
Combined incremental heating ages								Integrated age ± 2σ	39.34 ± 0.40
				MSWD 1.80				Weighted mean: integrated ages ± 2σ	41.30 ± 1.20
Yellow tuff WR-1 sanidine J = 0.009489 ± 0.16% μ = 1.0050									
20 crystal fusions									
* 39E4a	1.50	3.341 ± 0.006	0.00451 ± 0.00045	0.000450 ± 0.000092	1.16	96.0		95	54.09 ± 0.93
39E4b	1.50	3.159 ± 0.006	0.00529 ± 0.00057	0.000552 ± 0.000082	1.18	94.8		81	50.57 ± 0.84
* 39E4c	1.50	3.682 ± 0.006	0.00478 ± 0.00050	0.001136 ± 0.000134	1.17	90.9		90	56.39 ± 1.33
* 39E4d	1.50	4.266 ± 0.010	0.00355 ± 0.00035	0.001729 ± 0.000114	1.37	88.0		121	63.16 ± 1.15
* 39E4e	1.50	3.791 ± 0.009	0.00484 ± 0.00049	0.001044 ± 0.000135	1.17	91.9		89	58.64 ± 1.35
39E4f	1.50	3.124 ± 0.007	0.00650 ± 0.00034	0.000205 ± 0.000066	1.11	98.1		66	51.68 ± 0.70
* 39E4g	1.50	3.491 ± 0.009	0.00477 ± 0.00056	0.000790 ± 0.000112	0.87	93.3		90	54.91 ± 1.14
* 39E4h	1.50	3.917 ± 0.010	0.00484 ± 0.00077	0.001132 ± 0.000106	1.03	91.4		89	60.30 ± 1.09
* 39E4i	1.50	3.470 ± 0.006	0.00511 ± 0.00027	0.000991 ± 0.000103	1.20	91.5		84	53.58 ± 1.02
* 39E4j	1.50	12.088 ± 0.025	0.00409 ± 0.00039	0.001218 ± 0.000115	4.58	97.0		105	190.36 ± 1.29
* 39E4k	1.50	4.690 ± 0.010	0.00345 ± 0.00037	0.000229 ± 0.000108	1.67	98.5		124	77.44 ± 1.10
No isochron								Integrated age ± 2σ	72.40 ± 0.35
				MSWD 4.18				Weighted mean age ± 2σ	51.23 ± 1.10
3 crystal fusions									
39E4l	1.50	3.047 ± 0.032	0.00022 ± 0.00380	0.000478 ± 0.000814	0.13	95.3		1941	49.05 ± 8.08
39E4m	1.50	3.079 ± 0.042	0.00967 ± 0.00555	0.000346 ± 0.000933	0.10	96.7		44	50.25 ± 9.28
39E4n	1.50	3.088 ± 0.038	0.00061 ± 0.00283	0.000458 ± 0.000903	0.15	95.6		706	49.84 ± 8.97
* 39E4o	1.50	3.802 ± 0.032	0.01331 ± 0.00615	0.001097 ± 0.000680	0.17	91.5		32	58.59 ± 6.74
* 39E4p	1.50	3.964 ± 0.047	0.00946 ± 0.00404	0.000196 ± 0.000999	0.13	98.5		45	65.66 ± 9.87
39E4q	1.50	3.103 ± 0.042	0.00133 ± 0.00414	0.000342 ± 0.000854	0.13	96.7		324	50.65 ± 8.51
* 39E4r	1.50	6.122 ± 0.030	0.00773 ± 0.00295	0.000452 ± 0.000684	0.33	97.8		56	99.70 ± 6.62
39E4s	1.50	3.097 ± 0.039	0.00789 ± 0.00362	0.000224 ± 0.000964	0.13	97.9		55	51.15 ± 9.57
* 39E4t	1.50	4.646 ± 0.042	0.00509 ± 0.00405	0.001947 ± 0.000859	0.19	87.6		84	68.36 ± 8.47
* 39E4u	1.50	4.582 ± 0.052	0.00490 ± 0.00567	0.000517 ± 0.001273	0.15	96.7		88	74.27 ± 12.48
39E4v	1.50	3.159 ± 0.036	0.00624 ± 0.00300	0.000054 ± 0.000706	0.15	99.5		69	53.01 ± 7.04
39E4w	1.50	3.069 ± 0.045	0.00536 ± 0.00321	0.000038 ± 0.000800	0.14	99.6		80	51.59 ± 8.01
39E4x	1.50	3.146 ± 0.046	0.00012 ± 0.00443	0.000431 ± 0.001346	0.11	95.9		3553	50.94 ± 13.33
* 39E4y	1.50	5.580 ± 0.036	0.00008 ± 0.00377	0.000431 ± 0.000680	0.28	97.7		5267	91.00 ± 6.65
* 39E4z	1.50	3.606 ± 0.046	0.00735 ± 0.00363	0.000270 ± 0.000683	0.18	97.8		58	59.37 ± 6.86
39E4aa	1.50	3.194 ± 0.045	0.00553 ± 0.00428	0.000012 ± 0.000940	0.12	99.9		78	53.79 ± 9.35
* 39E4bb	1.50	4.094 ± 0.042	0.00009 ± 0.00251	0.000267 ± 0.000542	0.26	98.0		4927	67.44 ± 5.45
* 39E4cc	1.50	9.161 ± 0.051	0.00576 ± 0.00272	0.000426 ± 0.000520	0.49	98.6		75	148.39 ± 5.10
39E4dd	1.50	3.153 ± 0.061	0.01060 ± 0.01058	0.001061 ± 0.001704	0.06	90.1		41	47.97 ± 16.91
* 39E4ee	1.50	4.042 ± 0.027	0.00010 ± 0.00321	0.000140 ± 0.000490	0.23	99.0		4356	67.21 ± 4.85
* 39E4ff	1.50	4.126 ± 0.051	0.00012 ± 0.00450	0.000495 ± 0.000907	0.14	96.4		3570	66.85 ± 9.00

Table DR3. Complete $^{40}Ar/^{39}Ar$ results

Sample Experiment	laser power (W)	$^{40}Ar/^{39}Ar$	$^{37}Ar/^{39}Ar$	$^{36}Ar/^{39}Ar$	$^{40}Ar^*$ X10^{-14} mol	$^{40}Ar^*$ %	$^{39}Ar_K$ %	K/Ca	Apparent Age ± 2σ Ma
Yellow tuff WR-1 sanidine continued									
39E4gg	1.50	3.107 ± 0.032	0.00007 ± 0.00246	0.000389 ± 0.000486	0.17	96.3		5965	50.50 ± 4.90
* 39E4hh	1.50	4.349 ± 0.044	0.00014 ± 0.00435	0.000348 ± 0.000782	0.18	97.6		3171	71.25 ± 7.74
39E4ii	1.50	3.063 ± 0.038	0.00046 ± 0.00257	0.000086 ± 0.000689	0.14	99.1		935	51.25 ± 6.89
39E4jj	1.50	3.348 ± 0.038	0.00428 ± 0.00373	0.000032 ± 0.000791	0.12	99.7		100	56.26 ± 7.86
39E4kk	1.50	3.085 ± 0.041	0.00462 ± 0.00281	0.000186 ± 0.000648	0.13	98.2		93	51.13 ± 6.52
39E4ll	1.50	3.125 ± 0.041	0.00805 ± 0.00385	0.000162 ± 0.000749	0.14	98.5		53	51.92 ± 7.48
39E4mm	1.50	3.125 ± 0.030	0.00424 ± 0.00273	0.000520 ± 0.000596	0.17	95.1		101	50.16 ± 5.94
39E4nn	1.50	3.132 ± 0.036	0.00723 ± 0.00305	0.000356 ± 0.000551	0.15	96.6		60	51.08 ± 5.54
* 39E4oo	1.50	14.888 ± 0.043	0.20075 ± 0.00465	0.000706 ± 0.000378	0.93	98.7		2	235.51 ± 3.59
* 39E4pp	1.50	3.873 ± 0.031	0.00015 ± 0.00223	0.000353 ± 0.000568	0.23	97.3		2839	63.38 ± 5.64
* 39E4qq	1.50	3.779 ± 0.031	0.08940 ± 0.00322	0.000375 ± 0.000430	0.26	97.2		5	61.84 ± 4.33
* 39E4rr	1.50	3.806 ± 0.022	0.00013 ± 0.00270	0.000166 ± 0.000498	0.25	98.7		3343	63.18 ± 4.91
* 39E4ss	1.50	4.221 ± 0.033	0.00010 ± 0.00248	0.000104 ± 0.000645	0.21	99.3		4159	70.34 ± 6.37
39E4tt	1.50	3.049 ± 0.037	0.00016 ± 0.00445	0.000616 ± 0.001032	0.08	94.0		2614	48.42 ± 10.24
* 39E4uu	1.50	4.596 ± 0.033	0.00219 ± 0.00327	0.000221 ± 0.000564	0.24	98.6		196	75.92 ± 5.58
* 39E4vv	1.50	3.996 ± 0.034	0.00014 ± 0.00294	0.000363 ± 0.000633	0.20	97.3		3107	65.35 ± 6.27
39E4ww	1.50	3.162 ± 0.026	0.00636 ± 0.00787	0.000285 ± 0.000781	0.12	97.3		68	51.93 ± 7.72
* 39E4xx	1.50	3.705 ± 0.041	0.00467 ± 0.00464	0.000226 ± 0.000595	0.14	98.2		92	61.22 ± 5.97
39E4yy	1.50	3.368 ± 0.045	0.00388 ± 0.00424	0.000893 ± 0.000941	0.10	92.1		111	52.36 ± 9.36
* 39E4zz	1.50	4.747 ± 0.054	0.00879 ± 0.00776	0.000322 ± 0.000947	0.14	98.0		49	77.92 ± 9.34
39E4aaa	1.50	6.213 ± 0.067	0.00029 ± 0.00686	0.009474 ± 0.001166	0.15	54.9		1498	57.50 ± 11.57
Inverse isochron age ± 2σ		50.98 ± 2.10						Integrated age ± 2σ	69.72 ± 1.12
$^{40}Ar/^{39}Ar$ intercept ± 2σ		345.1 ± 90.6		MSWD 0.23				Weighted mean age ± 2σ	51.39 ± 1.70
Combined fusion ages									
Inverse isochron age ± 2σ		51.03 ± 0.74						Integrated age ± 2σ	71.49 ± 0.45
$^{40}Ar/^{39}Ar$ intercept ± 2σ		331.8 ± 82.5		MSWD 0.40				Weighted mean age ± 2σ	**51.24 ± 0.52**
K-spar tuff FQ-1 sanidine *J* = 0.014548 ± 0.14% μ = 1.0025									
10 crystal fusions									
11G4a	1.50	2.029 ± 0.008	0.00004 ± 0.00010	0.000218 ± 0.000129	0.52	96.6		12252	50.71 ± 1.99
11G4b	1.50	2.038 ± 0.004	0.00009 ± 0.00020	0.000138 ± 0.000026	2.10	97.8		4639	51.54 ± 0.43
11G4c	1.50	2.053 ± 0.003	0.00012 ± 0.00026	0.000144 ± 0.000036	1.61	97.7		3607	51.90 ± 0.56
11G4d	1.50	2.017 ± 0.005	0.00008 ± 0.00019	0.000191 ± 0.000152	0.64	97.0		5107	50.62 ± 2.30
11G4e	1.50	2.121 ± 0.005	0.00018 ± 0.00041	0.000435 ± 0.000109	0.54	93.7		2338	51.44 ± 1.65
* 11G4f	1.50	2.308 ± 0.004	0.00011 ± 0.00036	0.000287 ± 0.000036	1.36	96.1		3935	57.30 ± 0.57
11G4g	1.50	2.019 ± 0.003	0.00051 ± 0.00165	0.000090 ± 0.000049	0.95	98.5		847	51.42 ± 0.75
11G4h	1.50	2.020 ± 0.003	0.00059 ± 0.00192	0.000094 ± 0.000053	0.78	98.4		728	51.44 ± 0.82
11G4i	1.50	2.032 ± 0.004	0.00015 ± 0.00050	0.000163 ± 0.000051	1.01	97.4		2868	51.21 ± 0.80
10 crystal 1 and 2 step fusions *J* = 0.014562 ± 0.10% μ = 1.0035									
32C6a1	0.16	2.018 ± 0.009	0.00641 ± 0.00069	0.000075 ± 0.000172	0.36	98.7	21.7	67	51.59 ± 2.64
32C6a2	1.50	2.020 ± 0.004	0.00572 ± 0.00022	0.000039 ± 0.000037	1.30	99.2	78.3	75	51.91 ± 0.59
32C6b1	0.16	2.071 ± 0.014	0.00296 ± 0.00124	0.000173 ± 0.000320	0.16	97.3	7.7	145	52.19 ± 4.88
32C6b2	1.50	2.012 ± 0.003	0.00539 ± 0.00017	0.000057 ± 0.000031	1.86	99.0	92.3	80	51.55 ± 0.49
32C6c1	0.16	2.015 ± 0.003	0.00583 ± 0.00019	0.000043 ± 0.000034	1.54	99.2	56.2	74	51.75 ± 0.54
32C6c2	1.50	2.032 ± 0.003	0.00544 ± 0.00022	0.000077 ± 0.000046	1.21	98.7	43.8	79	51.93 ± 0.71
32C6d1	0.16	2.010 ± 0.004	0.00511 ± 0.00041	0.000072 ± 0.000079	0.73	98.7	30.3	84	51.39 ± 1.21
32C6d2	1.50	2.013 ± 0.003	0.00509 ± 0.00019	0.000063 ± 0.000030	1.69	98.9	69.7	85	51.55 ± 0.48
32C6e1	0.16	2.052 ± 0.013	0.00597 ± 0.00084	0.000224 ± 0.000227	0.20	96.6	19.8	72	51.31 ± 3.49
11G4e2	1.50	2.030 ± 0.004	0.00543 ± 0.00031	0.000098 ± 0.000068	0.81	98.4	80.2	79	51.71 ± 1.04
11G4f1	0.16	2.025 ± 0.008	0.00424 ± 0.00043	0.000084 ± 0.000094	0.49	98.6	28.1	101	51.68 ± 1.48
11G4f2	1.50	2.018 ± 0.003	0.00518 ± 0.00021	0.000045 ± 0.000031	1.25	99.1	71.9	83	51.81 ± 0.49
32C6g1	0.16	1.994 ± 0.006	0.00590 ± 0.00035	0.000081 ± 0.000070	0.60	98.6	36.8	73	50.92 ± 1.11
32C6g2	1.50	1.996 ± 0.004	0.00629 ± 0.00034	0.000046 ± 0.000047	1.04	99.1	63.2	68	51.24 ± 0.74
32C6h1	0.16	2.014 ± 0.007	0.04882 ± 0.00085	0.000064 ± 0.000091	0.60	99.0	55.6	9	51.64 ± 1.41
32C6h2	1.50	2.024 ± 0.007	0.04628 ± 0.00078	0.000134 ± 0.000103	0.48	98.0	44.4	9	51.37 ± 1.60
32C6i1	0.16	2.018 ± 0.004	0.00515 ± 0.00019	0.000032 ± 0.000025	2.06	99.3	89.8	84	51.89 ± 0.42
32C6i2	1.50	2.043 ± 0.013	0.00498 ± 0.00097	0.000047 ± 0.000157	0.24	99.1	10.2	86	52.42 ± 2.46
32C6j1	0.16	2.013 ± 0.004	0.00911 ± 0.00021	0.000091 ± 0.000051	1.49	98.5	51.9	47	51.33 ± 0.79

Table DR3. Complete $^{40}Ar/^{39}Ar$ results

Sample Experiment	laser power (W)	$^{40}Ar/^{39}Ar$	$^{37}Ar/^{39}Ar$	$^{36}Ar/^{39}Ar$	$^{40}Ar^*$ X10^{-14} mol	$^{40}Ar^*$ %	$^{39}Ar_K$ %	K/Ca	Apparent Age ± 2σ Ma
K-spar tuff FQ-1 sanidine continued									
32C6j2	1.50	2.011 ± 0.003	0.00680 ± 0.00031	0.000026 ± 0.000039	1.37	99.4	48.1	63	51.78 ± 0.61
32C6k1	0.16	2.015 ± 0.005	0.00546 ± 0.00045	0.000117 ± 0.000070	0.64	98.1	46.2	79	51.19 ± 1.09
32C6k2	1.50	2.015 ± 0.005	0.00558 ± 0.00042	0.000008 ± 0.000058	0.75	99.7	53.8	77	52.00 ± 0.91
32C6l1	0.16	2.017 ± 0.003	0.00581 ± 0.00013	0.000040 ± 0.000019	2.52	99.2	85.3	74	51.82 ± 0.33
32C6l2	1.50	2.038 ± 0.012	0.00468 ± 0.00053	0.000069 ± 0.000115	0.44	98.8	14.7	92	52.12 ± 1.84
32C6m1	0.16	2.029 ± 0.003	0.00590 ± 0.00016	0.000099 ± 0.000025	1.79	98.4	66.1	73	51.69 ± 0.40
32C6m2	1.50	2.033 ± 0.003	0.00610 ± 0.00035	0.000145 ± 0.000038	0.92	97.7	33.9	70	51.42 ± 0.60
32C6n1	0.16	2.017 ± 0.004	0.01373 ± 0.00035	0.000068 ± 0.000038	1.31	98.8	87.2	31	51.62 ± 0.60
32C6n2	1.50	2.081 ± 0.014	0.02205 ± 0.00142	0.000101 ± 0.000247	0.20	98.4	12.8	20	53.03 ± 3.80
32C6o1	0.16	2.009 ± 0.003	0.00597 ± 0.00029	0.000039 ± 0.000033	1.37	99.2	82.3	72	51.62 ± 0.52
32C6o2	1.50	2.051 ± 0.014	0.00515 ± 0.00088	0.000020 ± 0.000196	0.30	99.5	17.7	84	52.82 ± 3.03
32C61	1.50	2.000 ± 0.003	0.00515 ± 0.00020	0.000032 ± 0.000027	2.02	99.3		84	51.45 ± 0.43
32C6q	1.50	2.025 ± 0.003	0.00539 ± 0.00033	0.000073 ± 0.000029	1.55	98.7		80	51.77 ± 0.46
32C6r	1.50	2.026 ± 0.003	0.00600 ± 0.00021	0.000074 ± 0.000032	1.58	98.7		72	51.78 ± 0.51
32C6s	1.50	2.016 ± 0.003	0.00536 ± 0.00016	0.000062 ± 0.000023	2.17	98.9		80	51.63 ± 0.39
32C6t	1.50	1.994 ± 0.003	0.00510 ± 0.00018	0.000022 ± 0.000021	2.21	99.5		84	51.36 ± 0.36
32C6u	1.50	2.016 ± 0.003	0.00502 ± 0.00022	0.000059 ± 0.000024	1.99	98.9		86	51.64 ± 0.39
32C6v	1.50	2.018 ± 0.003	0.00615 ± 0.00021	0.000065 ± 0.000027	2.09	98.8		70	51.66 ± 0.44
32C6w	1.50	2.015 ± 0.003	0.00533 ± 0.00018	0.000062 ± 0.000026	1.82	98.9		81	51.60 ± 0.41
32C6x	1.50	2.015 ± 0.003	0.00512 ± 0.00028	0.000058 ± 0.000023	2.23	98.9		84	51.62 ± 0.38
32C6y	1.50	2.028 ± 0.003	0.00775 ± 0.00021	0.000065 ± 0.000028	1.50	98.9		55	51.92 ± 0.45
32C6z	1.50	2.019 ± 0.003	0.00384 ± 0.00015	0.000061 ± 0.000020	2.13	98.9		112	51.71 ± 0.33
32C6aa	1.50	2.018 ± 0.002	0.00599 ± 0.00020	0.000067 ± 0.000030	1.83	98.8		72	51.64 ± 0.46
32C6bb	1.50	2.015 ± 0.003	0.00455 ± 0.00012	0.000041 ± 0.000016	2.99	99.2		94	51.75 ± 0.29
32C6cc	1.50	2.022 ± 0.003	0.00564 ± 0.00028	0.000083 ± 0.000041	1.42	98.6		76	51.62 ± 0.64
32C6dd	1.50	2.018 ± 0.003	0.00475 ± 0.00022	0.000048 ± 0.000035	1.56	99.1		91	51.79 ± 0.56
32C6ee	1.50	2.018 ± 0.003	0.00466 ± 0.00024	0.000061 ± 0.000040	1.56	98.9		92	51.67 ± 0.62
32C6ff	1.50	2.019 ± 0.003	0.00620 ± 0.00021	0.000060 ± 0.000019	1.95	98.9		69	51.71 ± 0.33
Multi-crystal fusion ages									
Inverse isochron age ± 2σ		51.51 ± 0.20					Integrated age ± 2σ		51.73 ± 0.10
$^{40}Ar/^{39}Ar$ intercept ± 2σ		389.4 ± 133.2		MSWD 0.44			Weighted mean age ± 2σ		**51.66 ± 0.09**
Fowkes ash FF sanidine *J* = 0.014547 ± 0.10% μ = 1.0035									
5 crystal 1 and 2 step fusions									
* 32C5a	0.16	2.105 ± 0.008	0.01048 ± 0.00051	0.000138 ± 0.000076	0.68	97.9		41	53.28 ± 1.21
* 32C5b	1.50	1.927 ± 0.004	0.00729 ± 0.00033	0.000076 ± 0.000050	1.25	98.6		59	49.21 ± 0.78
32C5c	0.16	1.933 ± 0.025	0.00798 ± 0.00285	0.000217 ± 0.000780	0.07	96.5		54	48.28 ± 11.85
32C5d	1.50	1.853 ± 0.003	0.00679 ± 0.00016	0.000026 ± 0.000030	1.33	99.4		63	47.67 ± 0.48
32C5e	0.16	1.928 ± 0.013	0.00839 ± 0.00112	0.000297 ± 0.000270	0.21	95.2		51	47.56 ± 4.13
32C5f	1.50	1.875 ± 0.003	0.00995 ± 0.00026	0.000029 ± 0.000035	1.41	99.3		43	48.24 ± 0.56
* 32C5g	0.16	2.108 ± 0.004	0.00730 ± 0.00025	0.000035 ± 0.000042	1.06	99.3		59	54.13 ± 0.67
* 32C5h	1.50	2.043 ± 0.003	0.00684 ± 0.00031	0.000085 ± 0.000063	0.85	98.6		63	52.10 ± 0.96
32C5i	0.16	1.860 ± 0.004	0.00889 ± 0.00042	0.000074 ± 0.000056	0.75	98.6		48	47.52 ± 0.88
32C5j	1.50	1.882 ± 0.007	0.00935 ± 0.00031	0.000075 ± 0.000081	0.66	98.6		46	48.06 ± 1.26
32C5k	0.16	1.897 ± 0.010	0.00925 ± 0.00073	0.000142 ± 0.000207	0.23	97.6		46	47.94 ± 3.18
32C5l	1.50	1.869 ± 0.003	0.00679 ± 0.00016	0.000049 ± 0.000039	1.35	99.0		63	47.93 ± 0.61
32C5m	0.16	1.861 ± 0.004	0.00778 ± 0.00037	0.000038 ± 0.000070	0.65	99.2		55	47.80 ± 1.09
32C5n	1.50	1.864 ± 0.003	0.00930 ± 0.00022	0.000028 ± 0.000038	1.30	99.3		46	47.96 ± 0.59
32C5o	0.16	1.874 ± 0.007	0.01311 ± 0.00039	0.000030 ± 0.000092	0.58	99.3		33	48.21 ± 1.43
32C5p	1.50	1.859 ± 0.005	0.01003 ± 0.00048	0.000016 ± 0.000058	0.71	99.5		43	47.92 ± 0.90
32C5q	0.16	1.868 ± 0.003	0.00717 ± 0.00028	0.000053 ± 0.000057	1.09	98.9		60	47.86 ± 0.88
32C5r	1.50	1.869 ± 0.005	0.00714 ± 0.00027	0.000056 ± 0.000087	0.61	98.9		60	47.86 ± 1.33
* 32C5s	0.16	2.017 ± 0.007	0.01685 ± 0.00048	0.000117 ± 0.000108	0.62	98.1		26	51.20 ± 1.66
* 32C5t	1.50	1.969 ± 0.003	0.00982 ± 0.00027	0.000071 ± 0.000062	1.02	98.7		44	50.33 ± 0.94
32C5u	1.50	1.867 ± 0.003	0.00736 ± 0.00021	0.000026 ± 0.000029	1.78	99.4		58	48.03 ± 0.46
32C5v	1.50	1.880 ± 0.003	0.00904 ± 0.00027	0.000013 ± 0.000039	1.31	99.6		48	48.47 ± 0.62
32C5w	1.50	1.873 ± 0.004	0.03810 ± 0.00055	0.000092 ± 0.000045	1.09	98.5		11	47.77 ± 0.71
32C5x	1.50	1.868 ± 0.003	0.01027 ± 0.00026	0.000069 ± 0.000045	1.12	98.7		42	47.75 ± 0.69
32C5y	1.50	1.870 ± 0.003	0.00755 ± 0.00017	0.000058 ± 0.000028	1.65	98.9		57	47.88 ± 0.45

Table DR3. Complete $^{40}Ar/^{39}Ar$ results

Sample Experiment	laser power (W)	$^{40}Ar/^{39}Ar$	$^{37}Ar/^{39}Ar$	$^{36}Ar/^{39}Ar$	$^{40}Ar^*$ X10^{-14} mol	$^{40}Ar^*$ %	$^{39}Ar_K$ %	K/Ca	Apparent Age ± 2σ Ma
Fowkes ash FF sanidine continued									
Inverse isochron age ± 2σ		47.18 ± 1.09					Integrated age ± 2σ		48.73 ± 0.18
$^{40}Ar/^{39}Ar$ intercept ± 2σ		1041 ± 2845		MSWD 0.41			Weighted mean age ± 2σ		**47.94 ± 0.17**
Halfway Draw tuff HD-1 sanidine *J* = 0.014499 ± 0.10% μ = 1.0035									
Single crystal fusions									
32C1a	1.50	2.037 ± 0.003	0.00407 ± 0.00005	0.000089 ± 0.000016	4.07	98.5	106		51.73 ± 0.29
32C1b	1.50	2.028 ± 0.003	0.00341 ± 0.00006	0.000052 ± 0.000007	31.90	99.0	126		51.79 ± 0.20
32C1c	1.50	2.329 ± 0.005	0.00589 ± 0.00012	0.001458 ± 0.000054	1.03	81.3	73		48.88 ± 0.84
32C1d	1.50	2.108 ± 0.003	0.00383 ± 0.00009	0.000378 ± 0.000025	2.26	94.5	112		51.35 ± 0.39
32C1e	1.50	2.040 ± 0.003	0.00386 ± 0.00010	0.000140 ± 0.000080	1.01	97.8	111		51.42 ± 1.21
32C1f	1.50	2.043 ± 0.003	0.00440 ± 0.00010	0.000129 ± 0.000055	0.98	97.9	98		51.58 ± 0.84
32C1g	1.50	2.034 ± 0.005	0.00424 ± 0.00027	0.000122 ± 0.000071	0.67	98.0	101		51.41 ± 1.09
32C1h	1.50	2.027 ± 0.003	0.00322 ± 0.00004	0.000066 ± 0.000015	2.94	98.8	134		51.65 ± 0.27
32C1i	1.50	2.043 ± 0.003	0.00399 ± 0.00009	0.000052 ± 0.000047	1.06	99.0	108		52.17 ± 0.73
32C1j	1.50	2.090 ± 0.003	0.00371 ± 0.00012	0.000232 ± 0.000052	1.46	96.5	116		52.00 ± 0.80
32C1k	1.50	2.858 ± 0.011	0.00394 ± 0.00015	0.002748 ± 0.000048	2.43	71.4	109		52.62 ± 0.85
* 32C1l	1.50	2.857 ± 0.009	0.00366 ± 0.00036	0.002429 ± 0.000130	0.76	74.7	118		54.99 ± 1.99
32C1m	1.50	2.075 ± 0.004	0.00582 ± 0.00031	0.000189 ± 0.000063	0.96	97.1	74		51.94 ± 0.97
32C1n	1.50	2.083 ± 0.004	0.00387 ± 0.00018	0.000269 ± 0.000050	1.24	96.0	111		51.54 ± 0.77
32C1o	1.50	2.131 ± 0.004	0.00289 ± 0.00023	0.000360 ± 0.000064	0.89	94.8	149		52.09 ± 0.99
32C1p	1.50	2.325 ± 0.004	0.00386 ± 0.00020	0.001011 ± 0.000056	1.19	87.0	111		52.13 ± 0.86
32C1q	1.50	4.953 ± 0.007	0.00606 ± 0.00045	0.009865 ± 0.000209	1.31	41.1	71		52.42 ± 3.14
32C1r	1.50	3.324 ± 0.007	0.00375 ± 0.00032	0.004540 ± 0.000093	0.96	59.5	115		51.02 ± 1.42
32C1s	1.50	2.684 ± 0.006	0.00402 ± 0.00035	0.002100 ± 0.000131	0.84	76.7	107		53.07 ± 1.97
32C1t	1.50	2.209 ± 0.004	0.00349 ± 0.00019	0.000621 ± 0.000043	1.20	91.5	123		52.11 ± 0.67
32C1u	1.50	2.055 ± 0.004	0.00298 ± 0.00035	0.000096 ± 0.000086	0.68	98.4	144		52.14 ± 1.31
32C1v	1.50	2.045 ± 0.003	0.00328 ± 0.00016	0.000085 ± 0.000052	1.16	98.6	131		51.97 ± 0.79
32C1w	1.50	2.029 ± 0.002	0.01019 ± 0.00016	0.000096 ± 0.000040	1.87	98.4	42		51.50 ± 0.62
32C1x	1.50	2.066 ± 0.003	0.00297 ± 0.00020	0.000163 ± 0.000051	1.06	97.5	145		51.93 ± 0.79
32C1y	1.50	2.029 ± 0.004	0.00368 ± 0.00034	0.000010 ± 0.000069	0.94	99.6	117		52.13 ± 1.05
32C1z	1.50	2.049 ± 0.004	0.00246 ± 0.00028	0.000054 ± 0.000096	0.73	99.0	175		52.30 ± 1.45
32C1aa	1.50	2.032 ± 0.004	0.00367 ± 0.00030	0.000074 ± 0.000056	0.96	98.7	117		51.71 ± 0.86
32C1bb	1.50	2.082 ± 0.010	0.00536 ± 0.00047	0.000285 ± 0.000157	0.45	95.8	80		51.40 ± 2.41
32C1cc	1.50	2.080 ± 0.008	0.00524 ± 0.00039	0.000171 ± 0.000080	0.62	97.4	82		52.20 ± 1.27
32C1dd	1.50	2.045 ± 0.004	0.00329 ± 0.00022	0.000097 ± 0.000055	1.01	98.4	131		51.87 ± 0.85
32C1ee	1.50	2.028 ± 0.009	0.00474 ± 0.00058	0.000050 ± 0.000138	0.37	99.1	91		51.79 ± 2.13
32C1ff	1.50	2.049 ± 0.004	0.00748 ± 0.00038	0.000205 ± 0.000103	0.71	96.8	57		51.16 ± 1.55
32C1gg	1.50	2.028 ± 0.004	0.00329 ± 0.00044	0.000123 ± 0.000063	0.73	98.0	131		51.25 ± 0.96
* 32C1hh	1.50	2.151 ± 0.004	0.00357 ± 0.00029	0.000057 ± 0.000059	0.82	99.0	120		54.88 ± 0.91
32C1ii	1.50	2.032 ± 0.004	0.00512 ± 0.00029	0.000069 ± 0.000052	1.15	98.8	84		51.76 ± 0.80
32C1jj	1.50	2.032 ± 0.005	0.00339 ± 0.00036	0.000061 ± 0.000053	0.79	98.9	127		51.81 ± 0.83
32C1kk	1.50	2.022 ± 0.004	0.00286 ± 0.00033	0.000040 ± 0.000058	0.97	99.2	151		51.72 ± 0.89
32C1ll	1.50	2.029 ± 0.003	0.00335 ± 0.00024	0.000043 ± 0.000037	1.43	99.2	128		51.86 ± 0.57
32C1mm	1.50	2.051 ± 0.007	0.00421 ± 0.00071	0.000060 ± 0.000119	0.47	98.9	102		52.30 ± 1.81
32C1nn	1.50	2.026 ± 0.007	0.00420 ± 0.00043	0.000115 ± 0.000071	0.66	98.1	102		51.26 ± 1.12
32C1oo	1.50	2.054 ± 0.006	0.00299 ± 0.00041	0.000193 ± 0.000068	0.68	97.0	144		51.38 ± 1.07
* 32C1pp	1.50	2.173 ± 0.003	0.00382 ± 0.00012	0.000003 ± 0.000020	2.79	99.8	112		55.83 ± 0.34
32C1qq	1.50	2.045 ± 0.005	0.00387 ± 0.00050	0.000079 ± 0.000096	0.62	98.7	111		52.00 ± 1.47
32C1rr	1.50	2.032 ± 0.003	0.00375 ± 0.00026	0.000034 ± 0.000053	1.04	99.3	115		52.02 ± 0.81
32C1ss	1.50	2.035 ± 0.004	0.00284 ± 0.00021	0.000089 ± 0.000061	0.77	98.5	151		51.67 ± 0.94
32C1tt	1.50	2.030 ± 0.003	0.00486 ± 0.00022	0.000072 ± 0.000041	1.03	98.7	88		51.69 ± 0.64
32C1uu	1.50	2.033 ± 0.004	0.00378 ± 0.00020	0.000037 ± 0.000040	1.18	99.2	114		52.03 ± 0.63
32C1vv	1.50	2.035 ± 0.007	0.00291 ± 0.00031	0.000104 ± 0.000074	0.62	98.3	148		51.57 ± 1.16
32C1ww	1.50	2.054 ± 0.006	0.00345 ± 0.00044	0.000133 ± 0.000056	0.70	97.9	124		51.83 ± 0.89
32C1xx	1.50	2.063 ± 0.003	0.00427 ± 0.00015	0.000182 ± 0.000025	2.17	97.2	101		51.69 ± 0.40
32C1yy	1.50	2.028 ± 0.005	0.00469 ± 0.00038	0.000122 ± 0.000060	0.79	98.0	92		51.27 ± 0.94
32C1zz	1.50	2.024 ± 0.004	0.00411 ± 0.00029	0.000084 ± 0.000047	0.96	98.6	105		51.45 ± 0.72
32C1aaa	1.50	2.034 ± 0.004	0.00279 ± 0.00024	0.000057 ± 0.000052	1.00	99.0	154		51.89 ± 0.82
32C1bbb	1.50	2.086 ± 0.002	0.00402 ± 0.00012	0.000245 ± 0.000027	1.79	96.3	107		51.80 ± 0.43
Combined single crystal fusion ages									
Inverse isochron age ± 2σ		51.73 ± 0.11					Total fusion age ± 2σ		51.93 ± 0.12
$^{40}Ar/^{39}Ar$ intercept ± 2σ		300.2 ± 7.1		MSWD 0.57			Weighted mean age ± 2σ		51.75 ± 0.10

Table DR3. Complete $^{40}Ar/^{39}Ar$ results

Sample Experiment	laser power (W)	$^{40}Ar/^{39}Ar$	$^{37}Ar/^{39}Ar$	$^{36}Ar/^{39}Ar$	$^{40}Ar^*$ X10^{-14} mol	$^{40}Ar^*$ %	$^{39}Ar_K$ %	K/Ca	Apparent Age ± 2σ Ma
Halfway Draw tuff HD-1 sanidine continued									
Multi-crystal incremental heating experiments									
UW32C1ccc: 5 crystals									
32C1ccc1	0.10	2.029 ± 0.007	0.00379 ± 0.00046	0.000079 ± 0.000126	0.44	98.6		113	51.60 ± 1.92
32C1ccc2	0.12	2.025 ± 0.007	0.00571 ± 0.00039	0.000123 ± 0.000076	0.63	98.0		75	51.17 ± 1.19
32C1ccc3	0.17	2.036 ± 0.003	0.00363 ± 0.00014	0.000052 ± 0.000035	1.53	99.0		118	51.98 ± 0.56
32C1ccc4	1.50	2.054 ± 0.003	0.00393 ± 0.00024	0.000111 ± 0.000025	1.70	98.2		109	52.00 ± 0.40
Inverse isochron age ± 2σ		51.26 ± 2.01						Total fusion age ± 2σ	51.83 ± 0.37
$^{40}Ar/^{39}Ar$ intercept ± 2σ		581.4 ± 1287		MSWD 0.63				Weighted mean age ± 2σ	51.93 ± 0.31
UW32C1ddd: 5 crystals									
32C1ddd1	0.12	2.051 ± 0.006	0.00507 ± 0.00040	0.000124 ± 0.000090	0.50	98.0		85	51.82 ± 1.39
32C1ddd2	0.17	2.026 ± 0.003	0.00390 ± 0.00016	0.000043 ± 0.000031	1.65	99.2		110	51.81 ± 0.48
32C1ddd3	1.50	2.051 ± 0.008	0.00375 ± 0.00077	0.000073 ± 0.000143	0.48	98.7		115	52.21 ± 2.18
Inverse isochron age ± 2σ		51.73 ± 1.25						Total fusion age ± 2σ	51.88 ± 0.56
$^{40}Ar/^{39}Ar$ intercept ± 2σ		366.4 ± 924.0		MSWD 0.06				Weighted mean age ± 2σ	51.83 ± 0.45
UW32C1eee: 5 crystals									
32C1eee1	0.12	2.046 ± 0.005	0.01188 ± 0.00044	0.000094 ± 0.000123	0.62	98.5		36	51.93 ± 1.86
32C1eee2	0.17	2.019 ± 0.003	0.00849 ± 0.00023	0.000048 ± 0.000033	1.87	99.1		51	51.59 ± 0.51
32C1eee3	1.50	2.027 ± 0.006	0.00579 ± 0.00032	0.000012 ± 0.000088	0.60	99.6		74	52.06 ± 1.36
Inverse isochron age ± 2σ		50.92 ± 4.16						Total fusion age ± 2σ	51.75 ± 0.55
$^{40}Ar/^{39}Ar$ intercept ± 2σ		966.1 ± 8509		MSWD 0.25				Weighted mean age ± 2σ	51.67 ± 0.47
UW32C1fff: 5 crystals									
32C1fff1	0.12	2.007 ± 0.007	0.00365 ± 0.00047	0.000186 ± 0.000142	0.41	97.0		118	50.24 ± 2.17
32C1fff2	0.17	2.012 ± 0.003	0.00353 ± 0.00029	0.000028 ± 0.000042	1.04	99.4		122	51.54 ± 0.65
32C1fff3	1.50	2.020 ± 0.003	0.00400 ± 0.00016	0.000042 ± 0.000028	1.83	99.2		108	51.65 ± 0.45
Inverse isochron age ± 2σ		52.76 ± 2.06						Total fusion age ± 2σ	51.44 ± 0.43
$^{40}Ar/^{39}Ar$ intercept ± 2σ		-855.6 ± 8923		MSWD 0.81				Weighted mean age ± 2σ	51.57 ± 0.37
UW32C1ggg: 5 crystals									
32C1ggg1	0.12	2.061 ± 0.010	0.00389 ± 0.00076	0.000170 ± 0.000135	0.35	97.4		110	51.73 ± 2.09
32C1ggg2	0.17	2.015 ± 0.003	0.00399 ± 0.00021	0.000032 ± 0.000051	1.01	99.3		108	51.60 ± 0.77
32C1ggg3	1.50	2.038 ± 0.004	0.00393 ± 0.00020	0.000101 ± 0.000024	1.68	98.3		109	51.66 ± 0.41
Inverse isochron age ± 2σ		51.57 ± 1.18						Total fusion age ± 2σ	51.65 ± 0.42
$^{40}Ar/^{39}Ar$ intercept ± 2σ		329.2 ± 497.4		MSWD 0.01				Weighted mean age ± 2σ	51.65 ± 0.36
UW32C1hhh: 5 crystals									
32C1hhh1	0.12	2.018 ± 0.012	0.01163 ± 0.00063	0.000199 ± 0.000103	0.40	96.9		37	50.44 ± 1.65
32C1hhh2	0.17	2.035 ± 0.003	0.00436 ± 0.00025	0.000086 ± 0.000045	1.37	98.5		99	51.71 ± 0.69
32C1hhh3	1.50	2.044 ± 0.003	0.00404 ± 0.00018	0.000088 ± 0.000031	1.83	98.5		107	51.92 ± 0.49
Inverse isochron age ± 2σ		53.26 ± 1.69						Total fusion age ± 2σ	51.67 ± 0.41
$^{40}Ar/^{39}Ar$ intercept ± 2σ		-338.5 ± 871.6		MSWD 1.51				Weighted mean age ± 2σ	51.77 ± 0.48
Combined incremental heating ages									
Inverse isochron age ± 2σ		51.32 ± 0.61						Total fusion age ± 2σ	51.70 ± 0.19
$^{40}Ar/^{39}Ar$ intercept ± 2σ		529.5 ± 411.4		MSWD 0.38				Weighted mean age ± 2σ	51.72 ± 0.16
Grand combined sanidine ages									
Inverse isochron age ± 2σ		51.73 ± 0.10						Total fusion age ± 2σ	51.89 ± 0.10
$^{40}Ar/^{39}Ar$ intercept ± 2σ		300.5 ± 7.0		MSWD 0.54				Weighted mean age ± 2σ	**51.74 ± 0.09**
White Lignitic tuff WL-1 sanidine J = 0.009489 ± 0.16% μ = 1.0050									
Single crystal fusions									
39E3a	1.50	2.910 ± 0.054	0.01209 ± 0.00311	0.000107 ± 0.001118	0.11	98.9		36	48.61 ±11.16
39E3b	1.50	2.948 ± 0.026	0.01284 ± 0.00119	0.000417 ± 0.000445	0.24	95.8		33	47.73 ± 4.46

Table DR3. Complete $^{40}Ar/^{39}Ar$ results

Sample Experiment	laser power (W)	$^{40}Ar/^{39}Ar$	$^{37}Ar/^{39}Ar$	$^{36}Ar/^{39}Ar$	$^{40}Ar^*$ X10^{-14} mol	$^{40}Ar^*$ %	$^{39}Ar_K$ %	K/Ca	Apparent Age ± 2σ Ma
White Lignitic tuff WL-1 sanidine continued									
39E3c	1.50	2.930 ± 0.029	0.01360 ± 0.00183	0.000315 ± 0.000436	0.23	96.8		32	47.93 ± 4.41
39E3d	1.50	2.962 ± 0.033	0.01330 ± 0.00202	0.000305 ± 0.000891	0.19	97.0		32	48.51 ± 8.85
39E3e	1.50	2.926 ± 0.025	0.01445 ± 0.00129	0.000169 ± 0.000422	0.28	98.3		30	48.58 ± 4.24
39E3f	1.50	2.950 ± 0.033	0.02174 ± 0.00218	0.000098 ± 0.000587	0.19	99.0		20	49.34 ± 5.88
39E3g	1.50	2.949 ± 0.034	0.01627 ± 0.00230	0.000659 ± 0.000677	0.18	93.4		26	46.56 ± 6.77
39E3h	1.50	2.945 ± 0.054	0.02156 ± 0.00292	0.000170 ± 0.000839	0.12	98.3		20	48.89 ± 8.45
39E3i	1.50	2.889 ± 0.021	0.01271 ± 0.00096	0.000076 ± 0.000326	0.30	99.2		34	48.42 ± 3.29
39E3j	1.50	2.865 ± 0.014	0.01288 ± 0.00077	0.000186 ± 0.000244	0.50	98.1		33	47.47 ± 2.45
39E3k	1.50	2.861 ± 0.018	0.01311 ± 0.00068	0.000232 ± 0.000344	0.35	97.6		33	47.19 ± 3.44
Single crystal fusion ages									
Inverse isochron age ± 2σ		46.70 ± 5.13					Total fusion age ± 2σ		47.97 ± 1.46
$^{40}Ar/^{39}Ar$ intercept ± 2σ		622.8 ± 2831.3		MSWD 0.10			Weighted mean age ± 2σ		47.88 ± 1.31
10 crystal fusions									
39E3l	1.50	2.894 ± 0.006	0.19141 ± 0.00219	0.000255 ± 0.000079	1.77	97.9		2	47.85 ± 0.81
39E3m	1.50	2.846 ± 0.005	0.15491 ± 0.00168	0.000109 ± 0.000031	3.04	99.3		3	47.73 ± 0.34
39E3n	1.50	2.859 ± 0.007	0.07941 ± 0.00085	0.000089 ± 0.000035	2.59	99.3		5	47.94 ± 0.41
39E3o	1.50	2.854 ± 0.006	0.07713 ± 0.00089	0.000142 ± 0.000024	2.74	98.7		6	47.60 ± 0.32
39E3p	1.50	2.853 ± 0.010	0.11695 ± 0.00158	0.000142 ± 0.000053	1.72	98.8		4	47.63 ± 0.63
39E3q	1.50	2.852 ± 0.005	0.09546 ± 0.00108	0.000063 ± 0.000023	4.15	99.6		5	47.98 ± 0.28
39E3r	1.50	2.884 ± 0.005	0.09815 ± 0.00109	0.000213 ± 0.000022	3.63	98.1		4	47.78 ± 0.28
39E3s	1.50	2.846 ± 0.006	0.11873 ± 0.00134	0.000142 ± 0.000038	2.51	98.8		4	47.52 ± 0.43
39E3t	1.50	2.851 ± 0.006	0.10649 ± 0.00117	0.000111 ± 0.000033	3.21	99.1		4	47.74 ± 0.37
39E3u	1.50	2.856 ± 0.009	0.13758 ± 0.00155	0.000136 ± 0.000053	1.64	98.9		3	47.73 ± 0.61
* 39E3v	1.50	2.858 ± 0.006	0.12615 ± 0.00144	0.000088 ± 0.000039	2.99	99.4		3	48.00 ± 0.44
39E3w	1.50	2.951 ± 0.007	0.06977 ± 0.00080	0.000123 ± 0.000042	2.96	98.9		6	49.30 ± 0.48
39E3x	1.50	2.872 ± 0.008	0.21294 ± 0.00239	0.000180 ± 0.000039	2.10	98.7		2	47.88 ± 0.47
39E3y	1.50	2.868 ± 0.007	0.03962 ± 0.00048	0.000048 ± 0.000041	2.51	99.6		11	48.24 ± 0.47
39E3z	1.50	2.830 ± 0.006	0.09631 ± 0.00140	0.000174 ± 0.000036	2.52	98.4		4	47.07 ± 0.40
39E3aa	1.50	2.859 ± 0.007	0.11935 ± 0.00185	0.000199 ± 0.000061	1.91	98.2		4	47.46 ± 0.65
39E3bb	1.50	2.905 ± 0.008	0.11474 ± 0.00180	0.000315 ± 0.000101	0.97	97.1		4	47.64 ± 1.04
39E3cc	1.50	2.860 ± 0.008	0.11628 ± 0.00181	0.000186 ± 0.000055	1.99	98.4		4	47.54 ± 0.60
39E3dd	1.50	2.838 ± 0.006	0.03081 ± 0.00056	0.000081 ± 0.000034	2.77	99.2		14	47.58 ± 0.39
39E3ee	1.50	2.853 ± 0.008	0.11127 ± 0.00189	0.000158 ± 0.000056	1.73	98.6		4	47.54 ± 0.62
39E3ff	1.50	2.847 ± 0.006	0.10257 ± 0.00160	0.000197 ± 0.000091	1.30	98.2		4	47.25 ± 0.91
39E3gg	1.50	2.878 ± 0.007	0.07619 ± 0.00117	0.000164 ± 0.000057	2.08	98.5		6	47.89 ± 0.60
39E3hh	1.50	2.833 ± 0.006	0.08590 ± 0.00141	0.000109 ± 0.000049	1.90	99.1		5	47.42 ± 0.53
39E3ii	1.50	2.834 ± 0.006	0.12568 ± 0.00186	0.000138 ± 0.000039	2.23	98.9		3	47.35 ± 0.44
39E3jj	1.50	2.839 ± 0.007	0.15024 ± 0.00231	0.000172 ± 0.000071	1.28	98.6		3	47.30 ± 0.73
Multi-crystal fusion ages									
Inverse isochron age ± 2σ		47.33 ± 0.37					Total fusion age ± 2σ		47.77 ± 0.12
$^{40}Ar/^{39}Ar$ intercept ± 2σ		510.3 ± 304.6		MSWD 1.42			Weighted mean age ± 2σ		47.70 ± 0.13
Combined fusion ages									
Inverse isochron age ± 2σ		47.33 ± 0.33					Total fusion age ± 2σ		47.78 ± 0.13
$^{40}Ar/^{39}Ar$ intercept ± 2σ		507.3 ± 263.6		MSWD 0.99			Weighted mean age ± 2σ		**47.70 ± 0.12**

Note: All ages calculated relative to 28.34 Ma for the Taylor Creek rhyolite sanidine (Renne at al., 1998); using the decay constants of Steiger and Jäger (1977); uncertainties in Ar isotope ratios reported at 1σ analytical precision, uncertainties in ages reported at 2σ analytical precision. Corrected for ^{37}Ar and ^{39}Ar decay, half lives of 35.2 days and 269 years, respectively. Preferred ages are emboldened.

* indicates analyses or experiments that have been excluded from plateau age calculations

# indicates experiments that have been excluded from calculation of integrated age weighted means.

Table DR4. Summary of average major element compositions of biotite phenocrysts from nine tuff beds

	Rife		Continental		Curly		Wavy		Blind Canyon		Fat		Portly		Oily		Strawberry	
Element	biotite n=14	lowest K_20	biotite n=9	lowest K_20	biotite n=19	lowest K_20	biotite n=18	lowest K_20	biotite n=18	biotite n=16	lowest K_20	biotite n=19	lowest K_20	biotite n=18	lowest K_20	biotite n=18	biotite n=14	lowest K_20
SiO_2	35.5	35.2	35.9	37.0	34.9	33.0	35.7	35.8	35.7	35.5	33.9	34.9	33.0	35.7	35.8	35.7	35.5	35.2
Al_2O_3	13.9	13.6	13.7	13.7	13.4	13.0	13.3	13.3	14.1	13.6	13.0	13.4	13.0	13.3	13.3	14.1	13.9	13.6
FeO	17.0	16.9	18.9	19.1	22.1	21.4	19.3	18.2	17.4	19.1	18.2	22.1	21.4	19.3	18.2	17.4	17.0	16.9
MgO	13.2	13.3	11.5	11.7	9.51	9.98	11.4	12.0	12.9	11.3	11.0	9.51	9.98	11.4	12.0	12.9	13.2	13.3
MnO	0.14	0.13	0.13	0.09	0.21	0.35	0.25	0.20	0.17	0.18	0.15	0.21	0.35	0.25	0.20	0.17	0.14	0.13
CaO	0.20	0.45	0.09	0.25	0.18	1.90	BDL	BDL	0.05	0.05	0.07	0.18	1.90	BDL	BDL	0.05	0.20	0.45
Na_2O	0.43	0.54	0.45	0.41	0.38	0.37	0.37	0.31	0.51	0.41	0.49	0.38	0.37	0.37	0.31	0.51	0.43	0.54
K_2O	7.40	5.52	8.42	7.93	8.36	7.36	8.92	8.49	8.43	8.56	8.22	8.36	7.36	8.92	8.49	8.43	7.40	5.52
TiO_2	4.33	4.31	5.06	5.03	4.83	4.44	4.94	4.72	4.88	5.05	4.88	4.83	4.44	4.94	4.72	4.88	4.33	4.31
BaO	0.44	0.32	0.66	0.46	0.80	0.61	0.73	0.52	0.85	0.77	0.73	0.80	0.61	0.73	0.52	0.85	0.44	0.32
F	0.40	0.27	0.39	0.21	0.45	0.49	0.33	0.29	0.41	0.41	0.53	0.45	0.49	0.33	0.29	0.41	0.40	0.27
Excess O	5.48	5.73	4.09	4.71	3.32	7.13	3.73	4.17	3.38	4.51	6.46	3.32	7.13	3.73	4.17	3.38	5.48	5.73
Total	98.6	96.3	99.5	100.7	98.6	100.2	99.1	98.1	98.9	99.5	97.7	98.6	100.2	99.1	98.1	98.9	98.6	96.3

Notes: Electron microprobe wavelength dispersive spectrometer measurements made with 15 keV, 10 nA, 2-5 um defocused beam, with 10 sec peak and 10 sec background counting times, and F Ka with a thallium acid phtalate crystal and O Ka with 60Å layered dispersive element crystal using Cameca SX51. Characterized Wards biotite used as standard for Si, Al, Mg and O, and natural and synthetic standards used for other elements. "Excess O" is unaccounted for in stoichometric apportionments: most is assumed to be structural water and ferric iron but some, especially in "lowest K_2O" analyses, is likely introduced OH/H_2O. Low totals of "lowest K_2O" phases (~vermiculite) presumed to be due to loss of O by beam damage. P_2O_5, Ce_2O_3, and La_2O_3 were below detection limits in all analyses. Compilation includes 272 individual electron microprobe analyses. n-number of analyses, BDL-below detection limit.

Table DR5. Recalibrated $^{40}Ar/^{39}Ar$ ages from the Eocene of the northern Rocky Mountains

Location Sample	Stratigraphy	Dated Material	Method	flux monitor	Age (Ma)	± 2σ†	± 2σ‡	± 2σ§	References
Plateau province									
ET-8	Tg	bio & hbd	ih	Mmhb	43.67	1.29	1.29	1.49	Sheliga (1980)
ST-2	Tg	feld	ih		43.92	0.99	0.99	1.24	
WCT-1	Tg	bio	ih		46.70	2.26	2.26	2.39	
Uinta Basin									
Sample 14	Tg	bio	?	?	45.31	0.34	0.35	0.84	Constenius et al. (2003)
Bighorn Basin									
Willwood Ash	Twi	san	combo	TCs	52.59	0.12	0.19	0.91	Smith et al. (2004)
Absaroka Volcanic Province-Intrusions									
AR76-121	Dunrud Pk rhyolite	san	dih	FCs	43.95	0.18	0.20	0.77	Hiza (1999)
AR76-120	Kirwin dacite (Mt Burwell)	hbld	dih		45.10	1.71	1.71	1.88	
AR77-184	Rampart banackite	bio	ih		46.84	0.22	0.24	0.83	
70-0-4	Ishawooa banackite	bio	ih		47.04	0.22	0.24	0.83	
HMD4-96	Sunlight (White Mt) monzogabbro	bio	dih		48.51	0.16	0.19	0.84	
HM1-94	Crandall banakite	hbld	ih		49.42	0.18	0.21	0.86	
YFP7-93	S. Gallatin Range dacite	bio	ih		50.31	0.18	0.21	0.88	
PR2-93	Golmeyer Cr andesite dike	bio	dih		51.88	0.40	0.42	0.97	
YGDC1-96	Bighorn Peak dacite	hbld			53.97	0.60	0.61	1.10	
Absaroka Volcanic Province-Extrusive									
70-0-13	Pinnacle Butte ash	san	ih		47.26	0.18	0.21	0.83	
68-0-51	Blue point ash (Irish Rock)	hbld	ih		48.00	0.20	0.22	0.84	
3497	Blue point ash (Two Ocean)	feld	ih		48.10	0.14	0.17	0.83	
P-348	Lost Creek tuff	san	ih		49.08	0.16	0.19	0.85	
P-306	Pacific Creek tuff	bio	ih		49.19	0.24	0.26	0.87	
YCS-5-95	Slough Creek tuff Aslan Member	san	ih		49.93	0.16	0.19	0.86	
YCS-3-95	Slough Creek tuff upper rhyolitic unit	bio	dih		50.10	0.20	0.23	0.88	
HHM17B-95	Crandall trachyte ash-flow tuff	bio	ih		50.32	0.28	0.30	0.90	
YRL1-93	Sepulcher Mtn ash-flow	bio	dih		53.69	0.60	0.61	1.09	
Independence Volcano									
2085	Independence stock	bio	ih	Mmhb	48.77	0.12	0.16	0.84	Harlan et al. (1996)
1054	"	"	ih		48.80	0.12	0.16	0.84	
IN8	"	"	ih		48.90	0.15	0.18	0.85	
2117	"	"	ih		49.35	0.11	0.15	0.85	
1077	dacite sill	bio	ih		50.24	0.17	0.20	0.87	
91IN2	basal dacite breccia above Paleozoic	hbld	ih		51.82	0.14	0.18	0.89	
Washburn Volcano									
MW9743	andesite	gm	ih iso	Mmhb	52.19	0.80	0.81	1.20	Feeley et al. (2002)
MW9746	sulphur creek stock	bio	ih iso		52.89	0.20	0.23	0.92	
MW97-01	dacitic lava flow at base of sequence	gm	ih iso		55.51	0.60	0.62	1.12	
Sunlight Volcano									
SV97-02	upper Trout Peak Trachyandesite	gm	ih	Mmhb	48.37	0.10	0.15	0.83	Feeley and Cosca (2003)
SV97-37	trachytic core of Copper Lakes stock	bio	ih		48.41	0.08	0.13	0.83	
SV97-07	base of Trout Peak Trachyandesite	gm	ih		48.62	0.10	0.15	0.83	
SV97-14	top of lower Trout Peak Trachyandesite	gm	ih		48.76	0.10	0.15	0.84	
SV97-33	trachyte dike on Black Mtn	bio	ih		49.47	0.10	0.15	0.85	

Table DR5. Recalibrated $^{40}Ar/^{39}Ar$ ages from the Eocene of the northern Rocky Mountains

Location Sample	Stratigraphy	Dated Material	Method	flux monitor	Age (Ma)	± 2σ†	± 2σ‡	± 2σ§	References
Sunlight Volcano									
SV97-03	base of Jim Mountain Mb. of Wapiti Fm.	plag	ih		49.78	0.16	0.19	0.86	
SV97-29	"Langford Fm." on Black Mtn.	amph	ih		49.83	0.16	0.19	0.86	
Crazy Mountains									
diorite and gabbro	Big Timber Stock	bio	?	Mmhb	49.47	0.14	0.18	0.85	S.S. Harlan, in Wilson and Elliot (1997)
	"	bio	?		49.60	0.22	0.25	0.87	
quartz monzodiorite	"	bio	?		49.50	0.20	0.23	0.87	
	"	bio	?		49.60	0.24	0.26	0.88	
SE Challis Volcanics									
DG-711-88	porphyritic rhyolite intrusion (Trpi: Navarre Creek Dome)	bio	ih	Mmhb	47.73	0.26	0.28	0.85	Snider (1995)
	"	bio	ih		48.05	0.28	0.30	0.87	
MD-620-88	rhyolite dike (Trpi)	bio	ih		48.09	0.26	0.28	0.86	
JDB-422-87	rhyolite intrusion Porphyry Peak (Tri)	bio	ih		48.57	0.26	0.28	0.87	
KK-345-89	Garfield stock (Tg)	bio	dih		48.78	0.26	0.28	0.87	
LS-369-89	upper dacite flow/dome (Tdu)	bio	ih		47.57	0.26	0.28	0.85	
LS-659-89	tuff of Stoddard Gulch (Ts)	bio	ih		47.63	0.30	0.32	0.87	
FJM-72B-87	ryolite flow/dome complex at The Needles (Tru)	san	ih		47.70	0.32	0.34	0.87	
LS-392-89	lower rhyolite lavas (Tri)	bio	ih		48.37	0.56	0.57	1.00	
JDB-462-87	lower latite lavas (Tll)	bio	ih		49.07	0.34	0.36	0.90	
LS-616c-87	lower dacite flow/dome (Tdl)	bio	ih		49.13	0.48	0.49	0.97	
Tru	rhyolite flow	san	ih	Mmhb	47.70	0.32	0.34	0.87	Snider and Moye (1989)
Tll	tuff breccia	bio	ih		49.07	0.34	0.36	0.90	
Tri	Boone Creek stock	bio	ih		49.13	0.26	0.28	0.88	
Tch	tuff of Cherry Creek	san	ih		49.14	1.03	1.03	1.32	
Tdl	tuff breccia	bio	ih		49.20	0.52	0.53	0.99	
E Challis Volcanics									
88-141	tuff in Wet Creek cglm	san	ih	Mmhb	45.65	0.20	0.22	0.80	Janecke and Snee (1993)
88-136	Tuff of Challis Creek	san	ih		45.95	0.20	0.22	0.81	
88-100	rhyolite tuff	san	ih		46.36	0.40	0.41	0.89	
88-134	tuff of mud lake	bio	dih		47.97	0.40	0.42	0.91	
88-222	tuff in andesite flows	hbld	ih		48.47	0.80	0.81	1.15	
88-138	dacite of Warren Mt	hbld	ih		48.67	0.60	0.61	1.03	
88-146	andesite lava flow	hbld	dih		48.77	0.20	0.23	0.86	
88-133	dacite of Crow's Nest Canyon	hbld	ih		48.87	0.20	0.23	0.86	
88-139	dacite of Warren Mt.	hbld	ih		49.07	0.40	0.42	0.93	
88-88	tuff in andesite flows	bio	ih		49.27	0.40	0.42	0.93	
88-143	dacite lava flow	hbld	ih		49.47	0.60	0.61	1.04	
8 (Tc 1)	vitric tuff above (5) Lehmi Pass, Beaverhead Mtns	san	fus	TCs	48.64	0.24	0.28	0.87	M'Gonigle and Dalrymple (1996)
7 (88-100)	basal lithic tuff Tendoy Mtns	san	fus		48.88	0.34	0.37	0.91	
6 (87-64)	basal lithic tuff Tendoy Mtns	san	fus		49.31	0.37	0.39	0.92	
5 (Tcq)	basal rhyolite tuff Lehmi Pass, Beaverhead Mtns	san	fus		49.34	0.24	0.28	0.88	
Panther Creek Basin									
6-22-4	Tck - Tuffs of Castle Rock	san	ih	Mmhb	45.61	0.20	0.22	0.80	Janecke et al. (1997)
93-1	Tuffs of Challis Creek	san	ih		45.95	0.16	0.19	0.80	
6-18-10	Tvl1 -Fractured ash flow tuff	san	ih		45.99	0.20	0.22	0.81	

Table DR5. Recalibrated $^{40}Ar/^{39}Ar$ ages from the Eocene of the northern Rocky Mountains

Location Sample	Stratigraphy	Dated Material	Method	flux monitor	Age (Ma)	± 2σ†	± 2σ‡	± 2σ§	References
Horse Prairie Basin									
8	aphanitic mafic lava flow overlying Bloody Dick fault	gm	ih	FCs	47.80	0.85	0.85	1.17	Vandenburg et al. (1998)
5	top of undivided Challis volcanics	san	fus		47.82	0.26	0.28	0.86	
7	volcanic breccia within Ts1	gm	dih		47.85	1.19	1.19	1.44	
4	base of undivided Challis volcanics	san	fus		49.24	0.34	0.36	0.91	
3	base of undivided Challis volcanics	san	fus		49.68	1.33	1.33	1.57	
13 (82-322)	rhyolitic ash-flow tuff, top of CVG	san	fus	TCs	46.59	0.34	0.37	0.87	M'Gonigle and Dalrymple (1996)
11 (88-59)	rhyolitic welded ash-flow tuff in basal volcanics	san	fus		46.75	0.41	0.43	0.90	
3 (82-528)	basal crystal-lithic tuff	san	fus		49.46	0.34	0.37	0.91	
Muddy Creek Basin									
4	10 cm tephra in tuffaceous shale	san	fus	FCs	45.45	0.44	0.45	0.89	Janecke et al. (1999)
2	biotitic ash flow tuff in facies A	san	fus		47.36	0.52	0.53	0.96	
1	quartzite bearing ash flow tuff - basal unit	san	fus		49.78	0.10	0.14	0.85	
9 (91-171)	crystal-lithic tuff base of tuffaceous facies	san	fus	TCs	47.75	0.26	0.30	0.86	M'Gonigle and Dalrymple (1996)
Sage Creek Basin									
17 (91-170)	crystal tuff	san	fus	TCs	46.20	0.22	0.26	0.82	M'Gonigle and Dalrymple (1996)
Medicine Lodge Basin									
18 (91-104)	lithic tuff, overlying Proterozoic	san	fus	TCs	45.69	0.26	0.29	0.83	M'Gonigle and Dalrymple (1996)
16 (87-63)	rhyolitic welded ash-flow tuff overlies Archean	san	fus		46.36	0.28	0.31	0.84	
15 (89-135-4)	crystal-lithic tuff, overlies (10), base of lake deposits	san	fus		46.38	0.32	0.35	0.86	
14 (82-551)	crystal-lithic tuff, base of sediments	san	fus		46.45	0.28	0.31	0.85	
12 (81-189)	rhyolitic welded ash-flow tuff in ss above CVG beds	san	fus		46.70	0.30	0.33	0.86	
10 (89-135-3)	crystal-lithic tuff above 700 m andesite-basalt flows below (15)	san	fus		47.04	0.37	0.39	0.88	
4 (82-504)	basal rhyolite	san	fus		49.39	0.37	0.39	0.92	
Lowland Creek Volcanics									
LVC-32	intrusive rhyolite	san	ih	Mmhb	48.79	0.48	0.50	0.96	Ispolatov (1997)
LVC-15	dacite porphyry	hbld			50.06	0.46	0.48	0.97	
LVC-18	andesite porphyry	plag			50.56	2.14	2.14	2.30	
LVC-6	rhyodacite porphyry clast in rhyolite tuff	bio			51.78	0.40	0.42	0.97	
95LVC-9	rhyodacite porphyry flow	hbld			52.59	0.38	0.40	0.97	
95LVC-10A	rhyolite tuff	bio			52.79	0.48	0.50	1.02	
LVC-19-3	andesite porphyry	plag			52.99	1.91	1.92	2.12	
95LVC-7	intrusive rhyolite porphyry	hbld			53.03	0.24	0.27	0.93	
Anaconda Core Complex									
ME-1	mylonite below main detachment in Anaconda Range	musc	ih	FCs	47.58	0.28	0.30	0.86	O'Neill et al. (2004)

Table DR5. Recalibrated $^{40}Ar/^{39}Ar$ ages from the Eocene of the northern Rocky Mountains

Location Sample	Stratigraphy	Dated Material	Method	flux monitor	Age (Ma)	± 2σ†	± 2σ‡	± 2σ§	References
Bitterroot Core Complex									
B85	Whistling Pig pluton	kspar	iso	Mmhb	48.07	0.60	0.61	1.02	House et al. (2002)
B85	"	bio	iso		48.87	0.80	0.81	1.16	
EM3b	Spruce Creek mylonite zone	musc	iso		48.97	0.60	0.61	1.03	
EM3c	"	bio	iso		49.57	1.01	1.01	1.31	
NB12-11	Skookum Butte stock	bio	iso		50.48	1.01	1.01	1.32	
NB12-11	"	kspar	iso		52.69	2.01	2.01	2.20	
EM3b	Spruce Creek mylonite zone	kspar	iso		53.60	1.01	1.01	1.36	
EM3d	"	bio	iso		54.10	2.01	2.01	2.21	
EM6	"	bio	iso		54.50	0.60	0.61	1.11	
EM3d	"	hbld	iso		55.91	2.11	2.12	2.32	

Notes: All ages have been converted to the standard values of Renne et al. (1998) and are presented with 2σ uncertainties. san-sanidine, bio-biotite, hbld-hornblende, amph-amphibole, musc-muscovite, gm-groundmass, plag-plagioclase, feld-feldspar, ih-plateau age from incremental heating experiment, dih-discordant plateau age from incremental heating experiment, iso-inverse isochron from incremental heating experiment, fus-fusion age, combo-combined fusion and incremental heating age, TCs-Taylor Creek Rhyolite sanidine, FCs-Fish Canyon Tuff sanidine, Mmhb-McClue Mountain hornblende.

†Analytical uncertainty

‡Analytical and intercalibration uncertainty for preferred age

§Fully propagated uncertainty for preferred age

Table DR6. Paleocurrent indicator and provenance references for Figure 13

Number	Location	References
1	NW GGRB	(Steidtmann, 1969; West, 1973; Anderson and Picard, 1974; Dorr et al., 1977)
2	N GGRB	(Love, 1970; McGee, 1983; Steidtmann et al., 1986; Groll and Steidtmann, 1987; Steidtmann and Middleton, 1991)
3	NNE GGRB	(Knight, 1937; Pipiringos, 1955, 1961; Dickey, 1962; Masursky, 1962; Stephens and Healey, 1964; Love, 1970; Pipringos and Denson, 1970)
4	NE GGRB	(Sklenar and Anderson, 1985)
5	SE GGRB	(Roehler, 1969; Sklenar and Anderson, 1985; Roehler, 1990)
6	S GGRB	(Hansen, 1965; Culbertson, 1969; Sullivan, 1980; Crews and Ethridge, 1993; Roehler, 1993)
7	SW GGRB & FB	(Oriel, 1961, 1962; Lawrence, 1963; Rubey et al., 1975; Zonneveld et al., 2003)
8	N PCB	(Trudell et al., 1970; Duncan et al., 1974; O'Sullivan, 1974; Roehler, 1974; Trudell et al., 1974; O'Sullivan, 1975; Surdam and Stanley, 1980a; Johnson, 1981; Donnell, 1982; Johnson, 1984; Hail, 1987; O'Sullivan, 1987)
9	NE PCB	(Duncan and Belser, 1950; Donnell, 1961a; Ritzma, 1965; Snow, 1970; Lundell, 1977; Johnson, 1984)
10	SE PCB	(Donnell, 1961b)
11	Douglas Creek Arch	(Moncure, 1979; Moncure and Surdam, 1980; Cole, 1985)
12	S UB	(Spieker, 1946; Cashion, 1967; Marcantel and Weiss, 1968; Peterson, 1976; Pitman et al., 1982; Bruhn et al., 1983; Smith, 1984; Dickinson et al., 1986; Franczyk et al., 1991; Pusca, 2003)
13	SW UB	(Spieker, 1949; Zawiskie et al., 1982)
14	Plateau Province	(Muessig, 1951; Goldstrand, 1991, 1994; Weiss and Warner, 2001)
15	NW UB	(Stagner, 1941; Stanley and Collinson, 1979; Bruhn et al., 1986)
16	NE UB	(Chatfield, 1965; Sanborn and Goodwin, 1965; Picard, 1967; Pitman et al., 1982; Dickinson et al., 1986)
17	W Central GGRB	(Culbertson, 1962; Ebens, 1963; McGrew and Sullivan, 1970; Kistner, 1973; Gustav, 1974; Wolfbauer and Surdam, 1974; Surdam and Stanley, 1980a)
18	E Central GGRB	(Oriel, 1961, 1962; Roehler, 1969, 1970, 1973a, b; Braunagel and Stanley, 1977; Mauger, 1977; Stanley and Surdam, 1978; Surdam and Stanley, 1979, 1980a; Roehler, 1988; Roehler et al., 1990; Stucky et al., 1996)
19	Fowkes Basin	
20	Wind River Basin	(Bauer, 1934; Love, 1939; Van Houten, 1955; Keefer, 1957; Van Houten, 1964; Keefer, 1965; Rohrer, 1966a; Soister, 1968; Love, 1970; MacGinitie, 1974; Emry, 1975; Love, 1978; Seeland, 1978a, b; Boles and Surdam, 1979; Korth, 1982; Stucky, 1982, 1984a)
21	Gros Ventre Basin	(Love, 1947, 1956; Rohrer, 1968, 1969; MacGinitie, 1974; Love et al., 1978)

Notes: GGRB-Greater Green River Basin, PCB-Piceance Creek Basin, UB-Uinta Basin, FB-Fossil Basin

Table DR7. References for segments of Figure 2

Segment	Location	References
	Fossil Basin	(Oriel and Tracey, 1970; Buchheim, 1994; Buchheim and Eugster, 1998)
1	NW Bridger Basin	(Bradley, 1926; McGrew, 1959; Bradley, 1964; West, 1973; Dorr et al., 1977; Groll and Steidtmann, 1987; Roehler, 1992a)
2	Central Bridger Basin	(Matthew, 1909; Culbertson, 1961, 1962; Bradley, 1964; Culbertson, 1965; McGrew and Sullivan, 1970; Kistner, 1973; Wolfbauer and Surdam, 1974; Eugster and Hardie, 1975; Smoot, 1983; Sullivan, 1985; Roehler, 1992a; Evanoff et al., 1998; Murphey, 2001)
3	South Rock Springs Uplift	(Ritzma, 1961; Bradley, 1964; Bradley and Eugster, 1969; Roehler, 1992a)
4	Sand Wash Basin	(Sears and Bradley, 1924; Ritzma, 1955; Bradley, 1964; Roehler, 1973b; Trudell et al., 1973; Stanley and Surdam, 1978; Surdam and Stanley, 1979, 1980b; Roehler, 1991a, 1992a; McCarroll et al., 1996a; Stucky et al., 1996)
5	Axial Basin Arch	no strata
6	Piceance Creek Basin	(Bradley, 1931; Donnell, 1961a; Trudell et al., 1970; Brobst and Tucker, 1973; Cashion and Donnell, 1974; Roehler, 1974; Trudell et al., 1974; Lundell and Surdam, 1975; Lundell, 1977; Dyni, 1981; Johnson, 1981; Kihm, 1984; Johnson, 1985; Hail, 1987; O'Sullivan, 1987; Johnson and Johnson, 1991)
7	Douglas Creek Arch – E Uinta Basin	(Bradley, 1931; Cashion, 1967; Cashion and Donnell, 1972, 1974; O'Sullivan, 1974; Moncure and Surdam, 1980; Cole, 1985; Johnson, 1985; Johnson et al., 1988; Johnson and Johnson, 1991)
8	Central Uinta Basin	(Bradley, 1931; Dane, 1954, 1955; Picard, 1955; Ray et al., 1956; Ryder et al., 1976; Johnson, 1985; Johnson and Johnson, 1991; Remy, 1992; Pusca, 2003)
9	Western Uinta Basin	(Dane, 1954, 1955; Ray et al., 1956; Picard, 1957a)
	Wasatch Plateau	(Sheliga, 1980; Weiss and Warner, 2001)

Table DR8. Physical and temporal constraints: Absaroka Volcanic Province sites in Figure 5

Site	Location	Lithostratigraphy	Biostratigraphy	Magnetostratigraphy	Radioisotopic ages
1	Golmeyer Creek area	(Chadwick, 1969)			(Chadwick, 1969; Hiza, 1999)
2	Independence Volcano	(Pierce, 1963; Rubel, 1971; Pierce, 1997)		(Harlan et al., 1996)	(Pierce, 1963; Harlan et al., 1996)
3	Lamar River	(Smedes and Prostka, 1972; Prostka et al., 1975; Wedow et al., 1975; Fritz, 1982; Hickenlooper and Gutmann, 1982)		(Hickenlooper and Gutmann, 1982)	(Hiza, 1999)
4	Sunlight Volcanic Center	(Nelson and Pierce, 1968; Nelson et al., 1980b; Pierce, 1997)			(Feeley and Cosca, 2003)
5	Jim Mountain	(Torres and Gingerich, 1983; Torres, 1985; Malone, 1995, 1996)	(Torres, 1985; Gunnell et al., 1992)	(Pruss, 1975; Shive and Pruss, 1977)	(Feeley and Cosca, 2003)
6	Ptarmigan Mountain	(Nelson and Pierce, 1968)	(Jepson, 1939; Bown, 1982)	(Pruss, 1975; Shive and Pruss, 1977)	
7	Carter Mountain	(Bown, 1979; Eaton, 1982)	(Eaton, 1982)	(Lee and Shive, 1983; Isbell, 1989)	
8	Phelps Mountain	(Bown, 1979)		(Lee and Shive, 1983)	
9	North Fork – Owl Creek	(Sundell, 1982; Sundell et al., 1984)	(Bown, 1982; Sundell et al., 1984; Eaton, 1985)	(Lee and Shive, 1983; Sundell et al., 1984)	
10	East Fork – Wind River	(Love, 1939)	(Wood et al., 1936; Love, 1939; MacFadden, 1980; Winterfield, 1990)	(Flynn, 1986) (Lee and Shive, 1983)	
11	Togwotee Pass	(Love, 1947; Love et al., 1951; Love, 1956; Rohrer, 1966a, 1968, 1969; MacGinitie, 1974)	(McKenna, 1972, 1980)		(Rohrer and Obradovich, 1969)

REFERENCES CITED IN DATA REPOSITORY

Abbott, W., 1957, Tertiary of the Uinta Basin, *in* Seal, O.G., ed., Guidebook to the Geology of the Uinta Basin: Salt Lake City, Utah, Intermountain Association of Petroleum Geologists, 8th Annual Field Conference, p. 102-109.

Ambrose, P., Bartels, W.S., Gunnell, G.F., and Williams, E.M., 1997, Stratigraphy and vertebrate paleontology of the Wasatch Formation, Fossil Butte National Monument, Wyoming: Journal of Vertebrate Paleontology, v. 17, no. 3, suppl., p. 29.

Anderman, G.G., 1955, Tertiary deformational history of a portion of the north flank of the Uinta Mountains in the vicinity of Manila, Utah, *in* Anderman, G.G., ed., Green River Basin: Casper, Wyoming Geological Association, 10th Annual Field Conference, Guidebook, p. 130-134.

Anderson, D.W., and Picard, M.D., 1972, Stratigraphy of the Duchesne River Formation (Eocene-Oligocene?), northern Uinta Basin, northeastern Utah: Utah Geological and Mineralogical Survey Bulletin 97, 29 p.

—, 1974, Evolution of synorogenic clastic deposits in the intermontane Uinta Basin of Utah, *in* Dickinson, W.R., ed., Tectonics and Sedimentation: Society of Economic Paleontologists and Mineralogists Special Publication 22, p. 167-189.

Anderson, J.J., and Rowley, P.D., 1975, Cenozoic stratigraphy of southwestern high plateaus of Utah, *in* Anderson, J.J., Rowley, P.D., Fleck, R.J., and Nairn, A.E.M., eds., Cenozoic Geology of Southwestern High Plateaus of Utah: Geological Society of America Special Paper 160, p. 1-51.

Anemone, R.L., 2001, New paleogene faunas from the Great Divide Basin of southwestern Wyoming [abs.], *in* Ash, A.W., and Wing, S.L., eds., Climate and biota of the early Paleogene: International Meeting and Field Conference, Powell, Wyoming, 3-8 July, 2001: Washington, D.C., National Museum of Natural History, p. 2.

Anemone, R.L., Over, D.J., Nachman, B.A., and Harris, J., 2000, A new late Wasatchian mammalian fauna from the Great Basin, Sweetwater County, Wyoming [abs.]: Journal of Vertebrate Paleontology, v. 20, no. 3, suppl., p. 26.

Antweiler, J.C., Love, J.D., Prostka, H.J., Kulik, D.M., Anderson, L.A., Williams, E.M., Jinks, J.E., and Light, T.D., 1989, Mineral resources of the Teton Wilderness and adjacent areas, Teton, Fremont, and Park Counties: U.S. Geological Survey Bulletin 1781, 105 p.

Axelrod, D.I., 1968, Tertiary floras and topographic history of the Snake River Basin, Idaho: Geological Society of America Bulletin, v. 79, p. 713-734.

Bauer, C.M., 1934, Wind River Basin: Geological Society of America Bulletin, v. 45, p. 665-696.

Bay, K.W., 1969, Stratigraphy of Eocene sedimentary rocks in the Lysite Mountain area, Hot Springs, Fremont, and Washakie Counties, Wyoming [PhD thesis]: Laramie, University of Wyoming, 179 p.

Berggren, W.A., Kent, D.V., Swisher, C.C., III, and Aubry, M.-P., 1995, A revised Cenozoic geochronology and chronostratigraphy, *in* Berggren, W.A., Kent, D.V., Aubry, M.-P., and Hardenbol, J., eds., Geochronology, Time Scales, and Global Stratigraphic Correlation: SEPM (Society for Sedimentary Geology) Special Publication 54, p. 129-212.

Berner, R., and Briggs, L.I., 1958, Continental Eocene sedimentation in Huerfano Park, Colorado: Geological Society of America Bulletin, v. 69, p. 1533.

Berry, E.W., 1930, A flora of Green River Age in the Wind River Basin of Wyoming: U.S. Geological Survey Professional Paper 165, p. 55-81.

Blackstone, D.L., Jr., 1975, Late Cretaceous and Cenozoic history of Laramie Basin region, Southeast Wyoming, *in* Curtis, B.F., ed., Cenozoic History of the Southern Rocky Mountains: Geological Society of America Memoir 144, p. 249-279.

Boles, J.R., and Surdam, R.C., 1979, Diagenesis of volcanogenic sediments in a Tertiary saline lake; Wagon Bed Formation, Wyoming: American Journal of Science, v. 279, p. 832-853.

Bowers, W.E., 1990, Geologic map of Bryce Canyon National Park and vicinity, southwestern Utah: U.S. Geological Survey Miscellaneous Investigations Series Map I-2108, Scale 1:24 000, 1 Sheet and 1 Pamphlet.

Bown, T.M., 1979, Correlation of Eocene volcaniclastic rocks, southeastern Absaroka Range in northwestern Wyoming: U.S. Geological Survey Professional Paper 1150, p. 68-69.

—, 1982, Geology, paleontology, and correlation of Eocene volcaniclastic rocks, southeast Absaroka range, Hot Springs County, Wyoming: U.S. Geological Survey Professional Paper 1201-A, 75 p.

Bown, T.M., Rose, K.D., Simons, E.L., and Wing, S.L., 1994, Distribution and stratigraphic correlation of upper Paleocene and lower Eocene fossil mammal and plant localities of the Fort Union, Willwood, and Tatman Formations, southern Bighorn Basin, Wyoming: U.S. Geological Survey Professional Paper 1540, 103 p.

Bradley, W.H., 1926, Shore phases of the Green River Formation in northern Sweetwater County, Wyoming: U.S. Geological Survey Professional Paper 140-D, 121-131 p.

—, 1929, The varves and climate of the Green River epoch: U.S. Geological Survey Professional Paper 158-E, 110 p.

—, 1931, Origin and microfossils of the oil shale of the Green River Formation of Colorado and Utah: U.S. Geological Survey Professional Paper 168, 58 p.

—, 1959, Revision of stratigraphic nomenclature of Green River Formation of Wyoming: American Association of Petroleum Geologists Bulletin, v. 43, p. 1072-1075.

—, 1964, The geology of the Green River Formation and associated Eocene rocks in southwestern Wyoming and adjacent parts of Colorado and Utah: U.S. Geological Survey Professional Paper 496-A, 86 p.

Bradley, W.H., and Eugster, H.P., 1969, Geochemistry and Paleolimnology of the trona deposits and associated authigenic minerals of the Green River Formation of Wyoming: U.S. Geological Survey Professional Paper 496-B, 71 p.

Braunagel, L.H., and Stanley, K.O., 1977, Origin of variegated redbeds in the Cathedral Bluffs Tongue of the Wasatch Formation (Eocene), Wyoming: Journal of Sedimentary Petrology, v. 47, p. 1201-1219.

Brobst, D.A., and Tucker, J.D., 1973, X-ray minerology of the Parachute Creek Member, Green River Formation, in the northern Piceance Creek Basin, Colorado: U.S. Geological Survey Professional Paper 803, 53 p.

Brokaw, A.L., 1967, Geologic map and sections of the Ely quadrangle White Pine County, Nevada: U.S. Geological Survey Geologic Quadrangle Map GQ-697, Scale 1:24 000, 1 Sheet.

Brown, P.L., 1950, Occurrence and origin of the known trona deposits in Sweetwater and Uinta Counties, Wyoming [M.A. thesis]: Laramie, University of Wyoming, 82 p.

Brown, R.W., 1929, Additions to the flora of the Green River Formation: U.S. Geological Survey Professional Paper 154-J, p. 279-293.

—, 1934, The recognizable species of the Green River flora: U.S. Geological Survey Professional Paper 185-C, p. 45-77.

—, 1948, Age of the Kingsbury conglomerate [Wyoming] is Eocene: Geological Society of America Bulletin, v. 59, p. 1165-1172.

Bruhn, R.L., Picard, M.D., and Beck, S.L., 1983, Mesozoic and early Tertiary structure and sedimentology of the central Wasatch Mountains, Uinta Mountains and Uinta Basin, *in* Gurgel, K.D., ed., Geologic excursions in the Overthrust Belt and metamorphic core complexes of the Intermountain region; Guidebook, Part I: Utah Geological and Mineralogical Survey Special Studies 59, p. 63-105.

Bruhn, R.L., Picard, M.D., and Isby, J.S., 1986, Tectonics and sedimentology of Uinta Arch, Western Uinta Mountains, and Uinta Basin, *in* Peterson, J.A., ed., Paleotectonics and Sedimentation in the Rocky Mountain Region, United States: American Association of Petroleum Geologists Memoir 41, p. 333-352.

Bryant, B., 1992, Geologic and structure maps of the Salt Lake City 1° x 2° quadrangle, Utah and Wyoming: U.S. Geological Survey Miscellaneous Investigations Series Map I-1997, Scale 1:125 000, 3 Sheets.

Bryant, B., McGrew, L.W., and Wobus, R.A., 1981, Geologic map of the Denver 1° by 2° quadrangle, North-central Colorado; Sheet 1, Geology; Sheet 2, Structure [modified]: U.S. Geological Survey Miscellaneous Investigations Series Map I-1163, Scale Scale 1:250 000, 2 Sheets.

Bryant, B., Naeser, C.W., Marvin, R.F., and Mehnert, H.H., 1989, Upper Cretaceous and Paleogene rocks and isotopic ages of Paleogene tuffs, Uinta Basin, Utah: U.S. Geological Survey Bulletin 1787-J, 22 p.

Buchheim, H.P., 1978, Paleolimnology of the Laney Member of the Eocene Green River Formation [PhD thesis]: Laramie, University of Wyoming, 101 p.

—, 1994, Eocene fossil lake, Green River Formation, Wyoming: A history of fluctuating salinity, *in* Renaut, R.W., and Last, W.M., eds., Sedimentology and Geochemistry of Modern and Ancient Saline Lakes: SEPM (Society for Sedimentary Geology) Special Publication 50, p. 239-247.
Buchheim, H.P., Brand, L.R., and Goodwin, H.T., 2000, Lacustrine to fluvial deposition in the Eocene Bridger Formation: Palaeogeography, Palaeoclimatology, Palaeoecology, v. 162, p. 191-209.
Buchheim, H.P., and Eugster, H.P., 1998, Eocene Fossil Lake: the Green River Formation of Fossil Basin, southwestern Wyoming, *in* Pitman, J.K., and Carroll, A.R., eds., Modern & ancient lake systems; new problems and perspectives: Salt Lake City, Utah Geological Association, Publication 26, p. 191-208.
Burnside, M.J., and Culbertson, W.C., 1979, Trona deposits in the Green River Formation, Sweetwater, Uinta, and Lincoln Counties, Wyoming: U.S. Geological Survey Open-File Report 79-737, 10 p.
Cashion, W.B., 1967, Geology and fuel resources of the Green River Formation Southeastern Uinta Basin Utah and Colorado: U.S. Geological Survey Professional Paper 548, 48 p.
—, 1974, Geologic map of the Southam Canyon quadrangle, Uintah County, Utah: U.S. Geological Survey Miscellaneous Field Studies Map MF-579, Scale 1:24 000, 1 Sheet.
—, 1986, Geologic map of the Bonanza quadrangle, Uintah County, Utah: U.S. Geological Survey Miscellaneous Field Studies Map MF-1865, Scale 1:24 000, 1 Sheet.
Cashion, W.B., and Donnell, J.R., 1972, Chart showing correlation of key units in the organic-rich sequence of the Green River Formation, Piceance Creek basin, Colorado, and Uinta basin, Utah: U.S. Geological Survey Oil and Gas Investigations Chart, Scale OC-65, 1 Sheet.
—, 1974, Revision of the nomenclature of the upper part of the Green River Formation, Piceance Creek Basin, Colorado, and Eastern Uinta Basin, Utah: U.S. Geological Survey Bulletin 1394-G, 9 p.
Chadwick, R.A., 1969, The northern Gallatin Range, Montana: northwestern part of the Absaroka-Gallatin Volcanic Field: University of Wyoming Contributions to Geology, v. 8, no. 2, pt. 2, p. 150-166.
Chatfield, J., 1965, Petroleum Geology of the greater Red Wash area, Uintah County, Utah: The Mountain Geologist, v. 2, p. 115-121.
Clyde, W.C., Sheldon, N.D., Koch, P.L., Gunnell, G.F., and Bartels, W.S., 2001, Linking the Wasatchian/ Bridgerian boundary to the Cenozoic global climate optimum: new magnetostratigraphic and isotopic results from South Pass, Wyoming: Palaeogeography, Palaeoclimatology, Palaeoecology, v. 167, p. 175-199.
Clyde, W.C., Stamatakos, J., and Gingerich, P.D., 1994, Chronology of the Wasatchian Land-Mammal Age (Early Eocene): Magnetostratigraphic results from the McCullough Peaks Section. Northern Bighorn Basin, Wyoming: The Journal of Geology, v. 102, p. 367-377.
Clyde, W.C., Zonneveld, J.-P., Stamatakos, J., Gunnell, G.F., and Bartels, W.S., 1997, Magnetostratigraphy across the Wasatchian/Bridgerian NALMA boundary (early to middle Eocene) in the western Green River Basin, Wyoming: The Journal of Geology, v. 105, p. 657-669.
Cole, R.D., 1985, Depositional environments of oil shale in the Green River Formation, Douglas Creek Arch, Colorado and Utah, *in* Picard, M.D., ed., Geology and Energy Resources, Uinta Basin of Utah: Salt Lake City, Utah Geological Association, Publication 12, p. 211-224.
Comstock, T.B., 1875, Geological Report, *in* Jones, W.A., ed., Report upon the reconnaissance of northwestern Wyoming, including Yellostone Park, made in the summer of 1873: Washington, D.C., Government Printing Office, p. 85-292.
Constenius, K.N., Esser, R.P., and Layer, P.W., 2003, Extensional collapse of the Charleston-Nebo salient and its relationship to space-time variations in Cordilleran orogenic belt tectonism and continental stratigraphy, *in* Raynolds, R.G., and Flores, R.M., eds., Cenozoic Systems of the Rocky Mountain Region: Denver, Colorado, Rocky Mountain Section, SEPM (Society for Sedimentary Geology), p. 303-353.
Covert, H.H., Robinson, P., and Harris, J.R., 1998, Evidence for two lineages of *Notharctus* during the Bridger C and D [abs.]: Journal of Vertebrate Paleontology, v. 18, no. 3, suppl., p. 36.
Crews, S.G., and Ethridge, F.G., 1993, Laramide tectonics and humid alluvial fan sedimentation, NE Uinta Uplift, Utah and Wyoming: Journal of Sedimentary Petrology, v. 63, p. 420-436.
Culbertson, W.C., 1961, Stratigraphy of the Wilkins Peak Member of the Green River Formation, Firehole Basin quadrangle, Wyoming: U.S. Geological Survey Professional Paper 424-D, p. 170-173.
—, 1962, Laney Shale Member and Tower Sandstone Lentil of the Green River Formation, Green River Area, Wyoming: U.S. Geological Survey Professional Paper 449-C, p. 54-57.

—, 1965, Tongues of the Green River and Wasatch Formations in southeastern part of the Green River Basin, Wyoming, *in* De Voto, R.H., and Bitter, R.K., eds., Sedimentation of Late Cretaceous and Tertiary Outcrops, Rock Springs Uplift: Casper, Wyoming Geological Association, 19th Annual Field Conference, Guidebook, p. 151-155.
—, 1966, Trona in the Wilkins Peak Member of the Green River Formation, southwestern Wyoming: U.S. Geological Survey Professional Paper 550-B, p. 159-164.
—, 1969, Facies changes in the Eocene rocks in the south-eastern part of the Green River Basin, Wyoming, *in* Lindsay, J.B., ed., Geologic Guidebook of the Uinta Mountains, Utah's Maverick Range: Salt Lake City, Utah, Intermountain Association of Petroleum Geologists, 16th Annual Field Conference, p. 205-211.
—, 1971, Stratigraphy of the trona deposits in the Green River Formation, southwest Wyoming: University of Wyoming Contributions to Geology, v. 10, p. 15-23.
—, 1998, Road log for the geology field trip of June 13, 1997, Geology and outcrops of the trona-bearing rocks of the Green River Formation: Wyoming State Geological Survey Public Information Circular 40, p. 205-211.
Dane, C.H., 1954, Stratigraphic and facies relationships of upper part of Green River Formation and lower part of Uinta Formation in Duchesne, Uintah, and Wasatch Counties, Utah: Geological Society of America Bulletin, v. 38, p. 405-425.
—, 1955, Stratigraphic and facies relationships of the upper part of the Green River Formation and the lower part of the Uinta Formation in Duchesne, Uintah, and Wasatch Counties, Utah: U.S. Geological Survey Oil and Gas Investigations Chart OC-52, 2 sheets.
Davidson, J.R., 1987, Geology and mammalian paleontology of the Wind River Formation, Laramie Basin, southeastern Wyoming: University of Wyoming Contributions to Geology, no. 25, p. 103-132.
De Voto, R.H., 1964, Stratigraphy and structure of Tertiary rocks in southwestern South Park: The Mountain Geologist, v. 1, p. 117-126.
Deardorff, D.L., 1963, Eocene salt in the Green River Basin, Wyoming, *in* Bersticker, A.C., ed., Symposium on Salt, geology, mining, evaporated salt, solution mining, underground storag; [proceedings, 1962]: Cleveland, Northern Ohio Geological Society, p. 176-195.
DeCelles, P.G., Gray, M.B., Ridgeway, K.D., Cole, R.B., Srivastava, P., Pequera, N., and Pivnik, D.A., 1991, Kinematic history of a foreland uplift from Paleocene synorogenic conglomerate, Beartooth Range, Wyoming and Montana: Geological Society of America Bulletin, v. 103, p. 1458-1475.
Decker, R.W., 1962, Geology of the Bull Run quadrangle Elko County, Nevada: Nevada Bureau of Mines Bulletin 60, 65 p.
Denson, N.M., and Harshman, E.N., 1969, Map showing areal distribution of Tertiary rocks Bates Hole-Shirley Basin area south-central Wyoming: U.S. Geological Survey Miscellaneous Geologic Investigations Map I-570, Scale 1:125 000, 1 Sheet.
Denson, N.M., and Pipiringos, G.N., 1974, Geologic map and sections showing areal distribution of Tertiary rocks near the southeastern terminus of the Wind River Range, Fremont and Sweetwater Counties, Wyoming: U.S. Geological Survey Miscellaneous Investigations Series Map I-835, Scale 1:48 000, 2 Sheets.
Dickey, M.L., 1962, Upper Cretaceous and Cenozoic history of the Green Mountain-Whiskey Peak area Fremont County, Wyoming [M.Sc. thesis]: Laramie, University of Wyoming, 85 p.
Dickinson, W.R., Lawton, T.F., and Inman, K.F., 1986, Sandstone detrital modes, central Utah foreland region: Stratigraphic record of Cretaceous-Paleogene tectonic evolution: Journal of Sedimentary Petrology, v. 56, p. 276-293.
Doelling, H.H., 1972, Tertiary strata, Sevier-Sanpete region, *in* Baer, J.L., and Callaghan, E., eds., Plateau - Basin and Range Transition Zone, Central Utah, 1972: Salt Lake City, Utah Geological Association, Publication 2, p. 41-54.
Doi, K., 1990, Geology, and paleontology of two primate families of the Raven Ridge, northwestern Colorado and northeastern Utah [M.Sc. thesis]: Boulder, University of Colorado, 215 p.
Donnell, J.R., 1961a, Tertiary geology and oil-shale resources of the Piceance Creek Basin between the Colorado and White Rivers, northwestern Colorado: U.S. Geological Survey Bulletin 1082-L, p. 835-891.
—, 1961b, Tripartition of the Wasatch Formation near De Beque in northwestern Colorado: U.S. Geological Survey Professional Paper 424-B, p. 147-148.

—, 1969, Paleocene and lower Eocene units in the southern part of the Piceance Creek Basin Colorado: U.S. Geological Survey Bulletin 1274-M, 18 p.
—, 1982, Tongues of the Green River and Uinta Formations in the Piceance Creek Basin, *in* Gary, J.H., ed., Fifteenth Oil Shale Symposium Proceedings: Golden, Colorado, Colorado School of Mines Press, p. 29-37.
Donovan, J.H., 1950, Intertonguing of Green River and Wasatch Formations in part of Sublette and Lincoln Counties, Wyoming, *in* Harrison, J.W., ed., Southwest Wyoming: Casper, Wyoming Geological Association, 5th Annual Field Conference, Guidebook, p. 59-67.
Dorf, E., 1960, Tertiary fossil forests of Yellowstone National Park, Wyoming, *in* Campau, D.E., and Anisgard, H.W., eds., West Yellowstone-Earthquake Area: Billings, Montana, Billings Geological Society, 11th Annual Field Conference, p. 253-260.
Dorr, J.A., Jr., 1969, Mammalian and other fossils, Early Eocene Pass Peak Formation, central western Wyoming: University of Michigan Contributions from the Museum of Paleontology, v. 22, p. 207-219.
—, 1978, Revised and amended fossil vertebrate faunal lists, early Tertiary, Hoback Basin, Wyoming: University of Wyoming Contributions to Geology, v. 16, p. 79-84.
Dorr, J.A., Jr., Spearing, D.R., and Steidtmann, J.R., 1977, Deformation and deposition between a foreland uplift and an impinging thrust belt: Hoback Basin, Wyoming: Geological Society of America Special Paper 177, 82 p.
Douglass, E., 1903, New vertebrates from the Montana Tertiary: Annals of Carnegie Museum, v. 2, p. 145-199.
—, 1914, Geology of the Uinta Formation: Geological Society of America Bulletin, v. 25, p. 417-420.
Dover, J.H., 1995, Geologic map of the Logan 30' x 60' quadrangle, Cache and Rich counties, Utah, and Lincoln and Uinta Counties, Wyoming: U.S. Geological Survey Miscellaneous Investigations Series Series Map I-2210, Scale 1:100 000, 1 Sheet.
Dover, J.H., and M'Gonigle, J.W., 1993, Geologic map of the Evanston 30' x 60' quadrangle, Uinta and Sweetwater Counties, Wyoming: U.S. Geological Survey Miscellaneous Investigations Series Map I-2168, Scale 1:100 000, 1 Sheet.
Duncan, D.C., and Belser, C., 1950, Geology and oil-shale resources of the eastern part of the Piceance Creek Basin, Rio Blanco and Garfield counties, Colorado: U.S. Geological Survey Oil and Gas Investigations Map OM-119, 1 Sheet.
Duncan, D.C., Hail, W.J., Jr., O'Sullivan, R.B., and Pipiringos, G.N., 1974, Four newly named tongues of Eocene Green River Formation, northern Piceance Creek Basin, Colorado: U.S. Geological Survey Bulletin 1394-F, 13 p.
Dutcher, L.A.F., Jobling, J.L., and Dutcher, R.R., 1986, Stratigraphy, sedimentology and structural geology of Laramide synorogenic sediments marginal to the Beartooth Mountains, Montana and Wyoming, *in* Garrison, P.B., ed., Geology of the Beartooth Uplift and adjacent basins: Billings, Montana Geological Society and Yellowstone Bighorn Research Association, Field Conference and Symposium, p. 33-52.
Dyni, J.R., 1969, Structure of the Green River Formation, northern part of the Piceance Creek Basin, Colorado: The Mountain Geologist, v. 6, p. 57-66.
—, 1974, Stratigraphy and nacholite resources of the saline facies of the Green River Formation in northwest Colorado, *in* Murray, D.K., ed., Guidebook to the Energy Resources of the Piceance Creek Basin, Colorado: Denver, Colorado, Rocky Mountain Association of Geologists, 25th Annual Field Conference, p. 111-122.
—, 1976, Trioctahedral smectite in the Green River Formation, Duchesne County, Utah: U.S. Geological Survey Professional Paper 967, 14 p.
—, 1981, Geology of the nacholite deposits and associated oil shales of the Green River Formation in the Piceance Creek Basin, Colorado [PhD thesis]: Boulder, University of Colorado, 144 p.
Dyni, J.R., Hite, R.J., and Raup, O.B., 1970, Lacustrine deposits of bromine-bearing halite, Green River Formation, Northwest Colorado, *in* Rau, J.L., and Dellwig, L.F., eds., Third Symposium on Salt [papers]: Cleveland, Northern Ohio Geological Society, p. 166-180.
Dyni, J.R., Milton, C., and Cashion, W.B., 1985, The saline facies of the upper part of the Green River Formation near Duchesne, Utah, *in* Picard, M.D., ed., Geology and Energy Resources, Uinta Basin of Utah: Salt Lake City, Utah Geological Association, Publication 12, p. 51-60.

Eaton, J.G., 1980, Preliminary report on paleotological exploration of the southeastern Absaroka Range, Wyoming, *in* Gingerich, P.D., ed., Early Cenozoic paleontology and stratigraphy of the Bighorn Basin, Wyoming: Ann Arbor, University of Michigan Museum of Paleontology, Papers on Paleontology 24, p. 139-142.

—, 1982, Paleontology and correlation of Eocene volcanic rocks in the Carter Mountain area, Park County, southeastern Absaroka Range, Wyoming: University of Wyoming Contributions to Geology, v. 21, p. 153-194.

—, 1985, Paleontology and correlation of the Eocene Tepee Trail and Wiggins Formations in the north fork of Owl Creek area, southeastern Absaroka Range, Hot Springs County, Wyoming: Journal of Vertebrate Paleontology, v. 5, p. 345-370.

—, 1995, A late Eocene fauna from undescribed strata overlying the Claron Formation, Sevier Plateau, southwestern Utah: Geological Society of America Abstracts with Programs, v. 27, no. 4, p. 10.

Eaton, J.G., Hutchison, J.H., Holroyd, P.A., Korth, W.W., and Goldstrand, P.M., 1999, Vertebrates of the Turtle Basin Local Fauna, Middle Eocene, Sevier Plateau, south-central Utah, *in* Gillette, D.D., ed., Vertebrate Paleontology of Utah: Utah Geological Survey Miscellaneous Publication 99-1, p. 463-468.

Ebens, R.J., 1963, Petrography of the Eocene Tower Sandstone lenses at Green River, Sweetwater County, Wyoming [M.A. thesis]: Laramie, University of Wyoming, 46 p.

Ekren, E.B., 1985, Eocene cauldron-related volcanic events in the Challis quadrangle: U.S. Geological Survey Bulletin 1658-C, p. 43-58.

Emmons, S.F., 1877, The Green River Basin, *in* King, C., ed., Descriptive Geology: U.S. Geological Exploration of the Fortieth Parallel, p. 191-310.

Emry, R.J., 1975, Revised Tertiary stratigraphy and paleontology of the western Beaver Divide, Fremont County, Wyoming: Smithsonian Contributions to Paleobiology 25, 20 p.

—, 1990, Mammals of the Bridgerian (middle Eocene) Elderberry Canyon Local Fauna of eastern Nevada, *in* Bown, T.M., and Rose, K.D., eds., Dawn of the Age of Mammals in the Northern Part of the Rocky Mountain Interior, North America: Geological Society of America Special Paper 243, p. 187-210.

Ettinger, M., 1964, Geology of the Hartsel area South Park, Park County, Colorado: The Mountain Geologist, v. 1, p. 127-132.

Eugster, H.P., and Hardie, L.A., 1975, Sedimentation in an ancient playa-lake complex: The Wilkins Peak Member of the Green River Formation of Wyoming: Geological Society of America Bulletin, v. 86, p. 319-334.

Evanoff, E., Brand, L.R., and Murphey, P.C., 1998, Bridger Formation (Middle Eocene) of Southwest Wyoming: widespread marker units and subdivisions of Bridger B through D: Dakoterra, v. 5, p. 115-122.

Evanoff, E., Robinson, P., Murphey, P.C., Kron, D.G., Engard, D., and Monaco, P., 1994, An Early Uintan fauna from Bridger E: Journal of Vertebrate Paleontology, v. 14., no. 3, suppl, p. 24.

Fassett, J.E., 1985, Early Tertiary paleogeography and paleotectonics of the San Juan Basin area, New Mexico and Colorado, *in* Flores, R.M., and Kaplan, S.S., eds., Cenozoic Paleogeography of the West Central United States: Denver, Colorado, Rocky Mountain Section, SEPM (Society for Sedimentary Geology), Rocky Mountain Paleogeography Symposium 3, p. 317-334.

Feeley, T.C., and Cosca, M.A., 2003, Time vs. composition trends of magmatism at Sunlight volcano, Absaroka Volcanic Province, Wyoming: Geological Society of America Bulletin, v. 115, p. 714-728.

Feeley, T.C., Cosca, M.A., and Lindsay, C.R., 2002, Petrogenesis and implications of calc-alkanine cryptic hybrid magmas from Washburn Volcano, Absaroka Volcanic Province, USA: Journal of Petrology, v. 43, p. 663-703.

Fields, R.W., Rasmussen, D.L., Tabrum, A.R., and Nichols, R., 1985, Cenozoic rocks of the intermontane basins of western Montana and eastern Idaho: A summary, *in* Flores, R.M., and Kaplan, S.S., eds., Cenozoic Paleogeography of the West Central United States: Denver, Colorado, Rocky Mountain Section, SEPM (Society for Sedimentary Geology), Rocky Mountain Paleogeography Symposium 3, p. 9-36.

Fisher, F.S., McIntyre, D.H., and Johnson, K.M., compilers, 1992, Geologic map of the Challis 1° x 2° quadrangle, Idaho: U.S. Geological Survey Miscellaneous Investigations Series Map I-1819, Scale 1:250 000, 1 Sheet, 39 p. text.

Flores, R.M., and Ethridge, F.G., 1985, Evolution of intermontaine fluvial systems of Tertiary Powder River Basin, Wyoming and Montana, *in* Flores, R.M., and Kaplan, S.S., eds., Cenozoic Paleogeography of West-Central United States: Denver, Colorado,, Rocky Mountain Section, SEPM (Society for Sedimentary Geology), Rocky Mountain Paleogeography Symposium 3, p. 107-126.

Flynn, J.J., 1986, Correlation and geochronology of middle Eocene strata from the western United States: Palaeogeography, Palaeoclimatology, Palaeoecology, v. 55, p. 335-406.

Fouch, T.D., 1976, Revision of the lower part of the Tertiary system in the central and western Uinta Basin, Utah: U.S. Geological Survey Bulletin 1405-C, 7 p.

—, 1979, Character and paleogeographic distribution of upper Cretaceous (?) and Paleogene nonmarine sedimentary rocks in east-central Nevada, *in* Armentrout, J.M., Cole, M.R., and TerBest, H., Jr., eds., Cenozoic Paleogeography of the Western United States: Los Angeles, California, Pacific Section, Society of Economic Paleontologists and Mineralogists, Pacific Coast Paleogeography Symposium 3, p. 97-111.

—, 1981, Distribution of rock types, lithologic groups, and interpreted depositional environments for some lower Tertiary and upper Cretaceous rocks from outcrops at Willow Creek-Indian Canyon through the subsurface of Duchesne and Altamont oil fields, southwest to north central parts of the Uinta Basin, Utah: U.S. Geological Survey Oil and Gas Investigations Chart OC-81, 2 sheets.

Fouch, T.D., Cashion, W.B., Ryder, R.T., and Campbell, J.H., 1976, Field guide to lacustrine and related nonmarine depositional environments in Tertiary rocks, Uinta Basin, Utah, *in* Epis, R.C., and Weimar, R.J., eds., Studies in Colorado Field Geology: Golden, Colorado, Professional Contributions of Colorado School of Mines, no. 8, p. 358-383.

Fouch, T.D., Hanley, J.H., and Forester, R.M., 1979, Preliminary correlation of Cretaceous and Paleogene lacustrine and related nonmarine sedimentary and volcanic rocks in parts of the eastern Great Basin of Nevada and Utah, *in* Newman, G.W., and Goode, H.D., eds., Basin and Range Symposium and Great Basin Field Conference: Denver, Colorado, Rocky Mountain Association of Geologists, 30th Annual Field Conference, p. 305-312.

Fouch, T.D., Lawton, T.F., Nichols, D.J., Cashion, W.B., and Cobban, W.A., 1982, Chart showing preliminary correlation of major Albian to middle Eocene rock units from the Sanpete Valley in central Utah to the Book Cliffs in eastern Utah, *in* Nielson, D.L., ed., Overthrust Belt of Utah: Salt Lake City, Utah Geological Association, Publication 10, p. 267-272.

—, 1983, Patterns and timing of synorogenic sedimentation in upper Cretaceous rocks of central and northeast Utah, *in* Reynolds, M.W., and Dolly, E.D., eds., Mesozoic Paleogeography of the west-central United States: Denver, Colorado, Rocky Mountain Section, SEPM (Society for Sedimentary Geology), p. 305-336.

Franczyk, K.J., Hanley, J.H., Pitman, J.K., and Nichols, D.J., 1991, Paleocene depositional systems in the western Roan Cliffs, Utah, *in* Chidsey, T.C., Jr., ed., Geology of East-Central Utah: Salt Lake City, Utah Geological Association, Publication 19, p. 111-127.

Franczyk, K.J., Pitman, J.K., Cashion, W.B., Dyni, J.R., Fouch, T.D., Johnson, R.C., Chan, M.A., Donnell, J.R., Lawton, T.F., and Remy, R.R., 1989, Evolution of resource-rich foreland and intermontane basins in eastern Utah and western Colorado: Salt Lake City, Utah, to Grand Junction, Colorado, July 20-24, 1989: Washington, D.C., American Geophysical Union, International Geological Congress, 53 p.

Fritz, W.J., 1980, Reinterpretation of the depositional environment of the Yellowstone "fossil forests": Geology, v. 8, p. 309-313.

—, 1982, Geology of the Lamar River Formation, northeast Yellowstone National Park, *in* Reid, S.G., and Foote, D.J., eds., Geology of Yellowstone Park area: Casper, Wyoming Geological Association, 33rd Annual Field Conference, Guidebook, p. 73-101.

Froehlich, D.J., and Breithaupt, B.H., 1998, Mammals from the Eocene epoch Fossil Butte Member of the Green River Formation, Fossil Basin, Wyoming: Journal of Vertebrate Paleontology, v. 18, no. 3, suppl., p. 43-44.

Froehlich, J.F., and Froehlich, D.J., 2002, Using mammal fossil to locate the edge of the Green River Lake in the Piceance Creek Basin during the Late-Early Eocene: Geological Society of America Abstracts with Programs, v. 34, no. 6, p. 480-481.

Garner, A., and Morris, T.H., 1996, Outcrop study of the lower Green River Formation for reservoir characterization and hydrocarbon production enhancement in the Altamont-Bluebell field, Uinta Basin, Utah: Utah Geological Survey Miscellaneous Publication 96-2, 61 p.

Gazin, C.L., 1959, Paleontological exploration and dating of the early Tertiary deposits in basins adjacent to the Uinta Mountains, *in* Williams, N.C., ed., Guidebook to the Geology of the Wasatch and Uinta Mountains, Transition Area: Salt Lake City, Intermountain Association of Petroleum Geologists, 10th Annual Field Conference, p. 139-149.

—, 1962, A further study of lower Eocene mammalian faunas of southwestern Wyoming: Smithsonian Miscellaneous Collections, v. 144, no. 1, 98 p.

—, 1965, Early Eocene mammalian faunas and their environment in the vicinity of the Rock Springs Uplift, Wyoming, *in* De Voto, R.H., and Bitter, R.K., eds., Sedimentation of Late Cretaceous and Tertiary Outcrops, Rock Springs Uplift: Casper, Wyoming Geological Association, 19th Annual Field Conference, Guidebook, p. 171-180.

—, 1976, Mammalian faunal zones of the Bridger Middle Eocene: Smithsonian Contributions to Paleobiology 26, 25 p.

Gingerich, P.D., 1979, Phylogeny of Middle Eocene Adapidae (Mammalia, Primates) in North America: *Smilodectes* and *Notharctus*: Journal of Paleontology, v. 53, p. 155-163.

—, 1983, Paleocene-Eocene faunal zones and a preliminary analysis of Laramide structural deformation in the Clark's Fork Basin, Wyoming, *in* Boberg, W.W., ed., Geology of the Bighorn Basin: Casper, Wyoming Geological Association, 34th Annual Field Conference, Guidebook, p. 185-195.

Gingerich, P.D., and Clyde, W.C., 2001, Overview of mammalian biostratigraphy in the Paleocene-Eocene Fort Union and Willwood Formations of the Bighorn and Clarks Fork Basins, *in* Gingerich, P.D., ed., Paleocene-Eocene Stratigraphy and Biotic Change in the Bighorn and Clarks Fork Basins, Wyoming: Ann Arbor, University of Michigan Museum of Paleontology, Papers on Paleontology 33, p. 1-14.

Goldstrand, P.M., 1991, Tectonostratigraphy, petrology, and paleogeography of upper Cretaceous to Eocene rocks of southwest Utah [PhD thesis]: Reno, University of Nevada, 205 p.

—, 1994, Tectonic development of upper Cretaceous to Eocene strata of southwestern Utah: Geological Society of America Bulletin, v. 106, p. 145-154.

Grande, L., 1984, Paleontology of the Green River Formation, with a review of the fish fauna (second edition): The Geological Survey of Wyoming, Bulletin 63, 333 p.

Grande, L., and Buchheim, H.P., 1994, Paleontological and sedimentological variation in early Eocene Fossil Lake: University of Wyoming Contributions to Geology, v. 30, p. 33-56.

Groll, P.E., and Steidtmann, J.R., 1987, Fluvial response to Eocene tectonism, the Bridger Formation, southern Wind River Range, Wyoming, *in* Ethridge, F.G., Flores, R.M., and Harvey, M.D., eds., Recent Developments in Fluvial Sedimentology: Society of Economic Paleontologists and Mineralogists Special Publication 39, p. 263-268.

Gunnell, G.F., 1998, Mammalian fauna from the lower Bridger Formation (Bridger A, Early Middle Eocene) of the southern Green River Basin, Wyoming: University of Michigan Contributions from the Museum of Paleontology, v. 30, p. 83-130.

Gunnell, G.F., and Bartels, W.S., 1994, Early Bridgerian (middle Eocene) vertebrate paleontology and paleoecology of the southern Green River Basin, Wyoming: University of Wyoming Contributions to Geology, v. 30, p. 57-70.

—, 1999, Middle Eocene vertebrates from the Uinta Basin, Utah, and their relationship with faunas from the southern Green River Basin, Wyoming, *in* Gillette, D.D., ed., Vertebrate Paleontology of Utah: Utah Geological Survey Miscellaneous Publication 99-1, p. 429-442.

—, 2001, Basin margins, biodiversity, evolutionary innovation, and the origin of new taxa: Topics in Geobiology, v. 18, p. 403-432.

Gunnell, G.F., Bartels, W.S., Gingerich, P.D., and Torres, V., 1992, Wapiti Valley faunas: Early and middle Eocene vertebrates from the North Fork of the Shoshone River, Park County, Wyoming: University of Michigan Contributions from the Museum of Paleontology, v. 28, p. 247-287.

Gunnell, G.F., Bartels, W.S., and Zonneveld, J.-P., 2004, A late Wasatchian (late early Eocene) vertebrate assemblage preserved in meandering stream channel deposits, northern Red Desert, Wyoming: Geological Society of America Abstracts with Programs, v. 36, no. 5, p. 92.

Gunnell, G.F., and Yarborough, V.L., 2000, Brontotheriidae (Perissodactyla) from the Late Early and Middle Eocene (Bridgerian), Wasatch and Bridger Formations, southern Green River Basin, southwestern Wyoming: Journal of Vertebrate Paleontology, v. 20, p. 349-368.

Gustav, S.H., 1974, The sedimentology and paleogeography of the Bridger Formation, (Eocene) of southwestern Wyoming [M.Sc. thesis]: Boston, University of Massachusetts, 82 p.

Hail, W.J., 1965, Geology of northwestern North Park, Colorado: U.S. Geological Survey Bulletin 1188, 133 p.

—, 1968, The geology of southwestern North Park and vicinity, Colorado: U.S. Geological Survey Bulletin 1257, 119 p.

Hail, W.J., Jr., 1987, Chart showing intertongued units of the Eocene Green River and Uinta Formations, northwestern Piceance Creek Basin, northwestern Colorado: U.S. Geological Survey Miscellaneous Investigations Series Map I-1797, 1 Sheet.

Hail, W.J., Jr., and Smith, M.C., 1994, Geologic map of the northern part of the Piceance Creek Basin, northwestern Colorado: U.S. Geological Survey Miscellaneous Investigations Series Map I-2400, Scale 1:100 000, 1 Sheet.

Hail, W.J., and Leopold, E.B., 1960, Paleocene and Eocene age of the Coalmont Formation, North Park, Colorado: U.S. Geological Survey Professional Paper 400-B, p. 260-261.

Hanneman, D.L., 1989, Cenozoic basin evolution in a part of southwestern Montana [PhD thesis]: Missoula, University of Montana, 347 p.

Hansen, W.R., 1965, Geology of the Flaming Gorge area Utah-Colorado-Wyoming: U.S. Geological Survey Professional Paper 490, 196 p.

Harlan, S.S., Snee, L.W., and Geissman, J.W., 1996, $^{40}Ar/^{39}Ar$ geochronology and paleomagnetism of Independence volcano, Absaroka Volcanic Supergroup, Beartooth Mountains, Montana: Canadian Journal of Earth Sciences, v. 33, p. 1648-1654.

Harshman, E.N., 1968, Geologic map of the Shirley Basin area Albany, Carbon, Converse, and Natrona Counties, Wyoming: U.S. Geological Survey Miscellaneous Geologic Investigations Map I-539, Scale 1:48 000, 1 Sheet.

—, 1972, Geology and uranium deposits, Shirley Basin area, Wyoming: U.S. Geological Survey Professional Paper 745, 82 p.

Hay, R.L., 1956, Pitchfork Formation, detrital facies of Early Basic Breccia, Absaroka Range, Wyoming: American Association of Petroleum Geologists Bulletin, v. 40, p. 1863-1898.

Hayden, F.V., 1869, Preliminary field report of the United States Geological Survey of Colorado and New Mexico: U.S. Geological Survey of the Territories, Third Annual Report, 155 p.

Hickenlooper, J.W., and Gutmann, J.T., Jr., 1982, Geology of the Slough Creek tuff, northern Absaroka Volcanic Field, Park County, Montana, *in* Reid, S.G., and Foote, D.J., eds., Geology of Yellowstone Park Area: Casper, Wyoming Geological Association, 33rd Annual Field Conference, Guidebook, p. 55-63.

Hicks, J.F., Johnson, K.R., Obradovich, J.D., Miggins, D.P., and Tauxe, L., 2003, Magnetostratigraphy of Upper Cretaceous (Maastrichtian) to lower Eocene strata of the Denver Basin, Colorado: Rocky Mountain Geology, v. 38, p. 1-27.

Hiza, M.M., 1999, The geochemistry and geochronology of the Eocene Absaroka volcanic province, northern Wyoming and southern Montana, USA [PhD thesis]: Corvallis, Oregon State University, 243 p.

Holroyd, P.A., and Smith, K.T., 2000, Preliminary biostratigraphic evidence for age of the Wasatch and Green River Formations, Washakie Basin, Southwestern Wyoming: Geological Society of America Abstracts with Programs, v. 32, no. 7, p. 498.

Honey, J.G., 1988, A mammalian fauna from the base of the Eocene Cathedral Bluffs Tongue of the Wasatch Formation, Cottonwood Creek area, southeast Washakie Basin, Wyoming: U.S. Geological Survey Bulletin 1669-C, 14 p.

—, 1990, New Washakiin primates (Omomyidae) from the Eocene of Wyoming and Colorado, and comments on the evolution of the Washakiini: Journal of Vertebrate Paleontology, v. 10, p. 206-221.

Horsfield, B., Curry, D.J., Bohacs, K.M., Littke, R., Rullkötter, J., Schenk, H.J., Radke, M., Schaefer, R.G., Carroll, A.R., Isaksen, G., and Witte, E.G., 1994, Organic geochemistry of freshwater and alkaline lacustrine sediments in the Green River Formation of the Washakie Basin, Wyoming, U.S.A.: Organic Geochemistry, v. 22, p. 415-440.

House, M.A., Bowring, S.A., and Hodges, K.V., 2002, Implications of middle Eocene epizonal plutonism for the unroofing history of the Bitterroot metamorphic core complex, Idaho-Montana: Geological Society of America Bulletin, v. 114, p. 448-461.
Hurst, D.J., 1984, Depositional environment and tectonic significance of the Tunp Member of the Wasatch Formation, southwest Wyoming [M.Sc. thesis]: Laramie, University of Wyoming, 115 p.
Hurst, D.J., and Steidtmann, J.R., 1986, Stratigraphy and tectonic significance of the Tunp Conglomerate in the Fossil Basin, southwest, Wyoming: The Mountain Geologist, v. 23, p. 6-13.
Isbell, W.B., 1989, Converting spinner magnetometer for computer-controlled data collection and reduction & paleomagnetic study of volcanic and volcaniclastic rocks from the Absaroka Mountains, northwestern Wyoming [M.Sc. thesis]: Laramie, University of Wyoming, 105 p.
Ispolatov, V.O., 1997, $^{40}Ar/^{39}Ar$ geochronology of the Lowland Creek Volcanic Field and its temporal relations with other Eocene volcanic areas [M.Sc. thesis]: Norfolk, Virginia, Old Dominion University, 106 p.
Ispolatov, V.O., Dudas, F.O., Snee, L.W., and Harlan, S.S., 1996, Precise dating of the Lowland Creek Volcanics, west-central Montana: Geological Society of America Abstracts with Programs, v. 28, no. 7, p. 484.
Izett, G.A., Honey, J.G., and Brownfield, M.E., 1985, Geology of the Citadel Plateau quadrangle, Moffat County, Colorado: U.S. Geological Survey Miscellaneous Investigations Series Map I-1532, Scale 1:48 000, 1 Sheet.
Janecke, S., McIntosh, W., and Good, S., 1999, Testing models of rift basins: structure and stratigraphy of an Eocene-Oligocene supradetachment basin, Muddy Creek half graben, south-west Montana: Basin Research, v. 11, p. 143-165.
Janecke, S.U., Hammond, B.F., Snee, L.W., and Geissman, J.W., 1997, Rapid extension in an Eocene volcanic arc: Structure and paleogeography of an intra-arc half graben in central Idaho: Geological Society of America Bulletin, v. 109, p. 253-267.
Janecke, S.U., and Snee, L.W., 1993, Timing and episodicity of middle Eocene volcanism and onset of conglomerate deposition, Idaho: The Journal of Geology, v. 101, p. 603-621.
Janecke, S.U., VanDenburg, C.J., Blankenau, J.J., and M'Gonigle, J.W., 2000, Long-distance longitudinal transport of gravel across the Cordilleran thrust belt of Montana and Idaho: Geology, v. 28, p. 439-442.
Jepson, G.L., 1939, Dating Absaroka volcanic rocks by vertebrate fossils: Geological Society of America Bulletin, v. 50, p. 1914.
Johnson, R.B., 1959, Geology of the Huerfano Park area, Huerfano and Custer counties, Colorado: U.S. Geological Survey Bulletin 1071-D, p. 87-119.
Johnson, R.C., 1981, Stratigraphic evidence for a deep Eocene Lake Uinta, Piceance Creek Basin, Colorado: Geology, v. 9, p. 55-62.
—, 1984, New names for units in the lower part of the Green River Formation, Piceance Creek Basin, Colorado: U.S. Geological Survey Bulletin 1529-I, 20 p.
—, 1985, Early Cenozoic history of the Uinta and Piceance Creek basins, Utah and Colorado, with special reference to the development of Eocene Lake Uinta, *in* Flores, R.M., and Kaplan, S.S., eds., Cenozoic Paleogeography of the West Central United States: Denver, Colorado, Rocky Mountain Section, SEPM (Society for Sedimentary Geology), Rocky Mountain Paleogeography Symposium 3, p. 247-276.
Johnson, R.C., and Johnson, S.Y., 1991, Stratigraphic and time-stratigraphic cross sections of Phanerozoic rocks along line B-B'. Uinta and Piceance Basin area, west-central Uinta Basin, Utah to eastern Piceance Basin, Colorado: U.S. Geological Survey Miscellaneous Investigations Series Map I-2184-B, 2 Sheets.
Johnson, R.C., Nichols, D.J., and Hanley, J.H., 1988, Stratigraphic sections of lower Tertiary strata and charts showing polynomorph and mollusk assemblages, Douglas Creek Arch area, Colorado and Utah: U.S. Geological Survey Miscellaneous Field Studies Map MF-1997, 2 Sheets.
Kay, J.L., 1934, The Tertiary formations of the Uinta Basin, Utah: Annals of Carnegie Museum, v. 23, p. 357-371.
—, 1957, The Eocene vertebrates of the Uinta Basin, Utah, *in* Seal, O.G., ed., Guidebook to the Geology of the Uinta Basin: Salt Lake City, Utah, Intermountain Association of Petroleum Geologists, 8th Annual Field Conference, p. 110-114.

Keefer, W.R., 1957, Geology of the Du Noir area Fremont County Wyoming: U.S. Geological Society Professional Paper 294-E, p. 155-221.
—, 1965, Stratigraphy and geologic history of the uppermost Cretaceous, Paleocene, and Lower Eocene rocks in the Wind River Basin, Wyoming: U.S. Geological Survey Professional Paper 495-A, 77 p.
Kihm, A.J., 1984, Early Eocene mammalian faunas of the Piceance Creek basin, northwestern Colorado [PhD thesis]: Boulder, University of Colorado, 407 p.
Kistner, F.B., 1973, Stratigraphy of the Bridger Formation in the Big Island-Blue Rim area, Sweetwater County, Wyoming [M.Sc. thesis]: Laramie, University of Wyoming, 174 p.
Knight, S.H., 1937, Origin of the giant conglomerates of Green Mountain and Crook's Mountain, central Wyoming: Proceedings of the Geological Society of America for 1936, p. 84.
—, 1955, Review of the early geological explorations of the Green River Basin area 1812-1879, *in* Anderman, G.G., ed., Green River Basin: Casper, Wyoming Geological Association, 10th Annual Field Conference, Guidebook, p. 10-17.
Knowlton, F.H., 1923, Revision of the flora of the Green River Formation with descriptions of new species: U.S. Geological Survey Professional Paper 131-F, p. 133-182.
Koenig, K.J., 1960, Bridger Formation in the Bridger Basin, Wyoming, *in* McGookey, D.P., and Miller, D.N., Jr., eds., Overthrust Belt of Southwestern Wyoming and Adjacent Areas: Casper, Wyoming Geological Association, 15th Annual Field Conference, Guidebook, p. 163-168.
Korth, W.W., 1982, Revision of the Wind River faunas, early Eocene of central Wyoming. Part 2. Geologic setting: Annals of Carnegie Museum, v. 51, p. 57-78.
Krause, M.J., 1985, Early Tertiary quartzite conglomerates of the Bighorn Basin and their significance for paleogeographic reconstruction of northwest Wyoming, *in* Flores, R.M., and Kaplan, S.S., eds., Cenozoic Paleogeography of the West Central United States: Denver, Colorado, Rocky Mountain Section, SEPM (Society for Sedimentary Geology), Rocky Mountain Paleogeography Symposium 3, p. 71-91.
Krishtalka, L., and Stucky, R.K., 1986, Early Eocene artiodactyls from the San Juan Basin, New Mexico, and the Piceance Creek Basin, Colorado, *in* Flanagan, K.M., and Lillegraven, J.A., eds., Vertebrates, Phylogeny, and Philosophy: Laramie, University of Wyoming, Contributions to Geology, Special Paper 3, p. 183-196.
Lawrence, J.C., 1963, Origin of the Wasatch Formation, Cumberland Gap area, Wyoming: University of Wyoming Contributions to Geology, v. 2, p. 151-158.
—, 1965, Wasatch and Green River Formations of the southwestern part of the Green River Basin, *in* De Voto, R.H., and Bitter, R.K., eds., Sedimentation of Late Cretaceous and Tertiary Outcrops, Rock Springs Uplift: Casper, Wyoming Geological Association, 19th Annual Field Conference, Guidebook, p. 181-187.
Lee, T.-Q., and Shive, P.N., 1983, Paleomagnetic study of the volcanic and volcaniclastic rocks from the southeastern Absaroka, Wyoming: Bulletin of the Institute of Earth Sciences Academia Sinica, v. 3, p. 155-172.
Leggitt, V.L., and Cushman, R.A., Jr., 2001, Complex caddisfly-dominated bioherms from the Eocene Green River Formation: Sedimentary Geology, v. 145, p. 377-396.
Leopold, E.B., and MacGinitie, H.D., 1972, Development and affinities of Tertiary flora in the Rocky Mountains, *in* Graham, A., ed., Floristics and Paleofloristics of Asia and Eastern North America: Amsterdam, Elsevier Publishing Company, p. 147-200.
Loen, J.S., 1986, Sedimentology and gold placer deposits--Cathedral Bluffs Member of the Wasatch Formation, Dickie Springs-Pacific Butte area, Fremont County, Wyoming: U.S.Geological Survey Open-File Report 86-456, 15 p.
Love, J.D., 1939, Geology along the southern margin of the Absaroka Range, Wyoming: Geological Society of America Special Paper 20, 134 p.
—, 1947, Tertiary stratigraphy of the Jackson Hole area, northwest Wyoming: U.S. Geological Survey Oil and Gas Investigations Preliminary Chart 27, 1 Sheet.
—, 1956, Cretaceous and Tertiary stratigraphy of the Jackson Hole area, northwestern Wyoming, *in* Berg, R.R., ed., Jackson Hole: Casper, Wyoming Geological Association, 11th Annual Field Conference, Guidebook, p. 76-98.
—, 1964, Uraniferous phosphatic lake beds of Eocene age in intermontane basins of Wyoming and Utah: U.S. Geological Survey Professional Paper 474-E, 66 p.

—, 1970, Cenozoic geology of the Granite Mountains area, central Wyoming: U.S. Geological Survey Professional Paper 495-C, 154 p.
—, 1978, Cenozoic thrust and normal faulting, and tectonic history of the Badwater Area northeastern margin of Wind River Basin, Wyoming, *in* Boyd, R.G., Boberg, W.W., and Olson, G.W., eds., Resources of the Wind River Basin: Casper, Wyoming Geological Association, 30th Annual Field Conference, Guidebook, p. 235-238.
—, 1995, Uraniferous phosphatic lake beds of Eocene age in the Green River Basin, Wyoming, *in* Jones, R.W., ed., Resources of Southwestern Wyoming: Cheyenne, Wyoming Geological Association, 47th Annual Field Conference, Guidebook, p. 165-182.
Love, J.D., Keefer, W.R., Duncan, D.C., Bergquist, H.R., and Hose, R.K., 1951, Geologic map of the Spread Creek-Gros Ventre River area, Teton County, Wyoming: U.S. Geological Survey Oil and Gas Investigations Map OM-118, 2 Sheets.
Love, J.D., Leopold, E.B., and Love, D.W., 1978, Eocene rocks, fossils, and geologic history, Teton Range, northwest Wyoming: U.S. Geological Survey Professional Paper 932-B, 40 p.
Love, J.D., Reed, J.C., Jr., and Christiansen, A.C., 1992, Geologic map of Grand Teton National Park, Teton County, Wyoming: U.S. Geological Survey Miscellaneous Investigations Series Map I-2031, Scale 1:62 000, 1 Sheet, 17 p. text.
Love, J.D., Reed, J.C., Jr., Christiansen, R.L., and Stacy, J.R., 1972, Geologic block diagram and tectonic history of the Teton region, Wyoming-Idaho: U.S. Geological Survey Miscellaneous Geologic Investigations Map I-730, 1 Sheet.
Lucas, S.G., 1998, Fossil mammals and the Paleocene/Eocene series boundary in Europe, North America, and Asia, *in* Aubry, M.-P., Lucas, S.G., and Berggren, W.A., eds., Late Paleocene-Early Eocene Climatic and Biotic Events in the Marine and Terrestrial Records: New York, Columbia University Press, p. 451-500.
Lundell, L.L., 1977, Depositional environment of the Eocene Green River Formation, Piceance Creek Basin, Colorado [PhD thesis]: Laramie, University of Wyoming, 136 p.
Lundell, L.L., and Surdam, R.C., 1975, Playa-lake deposition: Green River Formation, Piceance Creek Basin, Colorado: Geology, v. 3, p. 493-497.
MacFadden, B.J., 1980, Eocene perissodactyls from the type section of the Tepee Trail Formation of northwestern Wyoming: University of Wyoming Contributions to Geology, v. 18, p. 135-143.
MacGinitie, H.D., 1969, The Eocene Green River Flora of northwestern Colorado and northeastern Utah: University of California Publications in the Geological Sciences, v. 83, 203 p.
—, 1974, An early middle Eocene flora from the Yellowstone-Absaroka Volcanic Province, northwestern Wind River Basin, Wyoming: University of California Publications in Geological Sciences, v. 108, 103 p.
Machlus, M., Hemming, S.R., Olsen, P.E., and Christie-Blick, N., 2004, Eocene calibration of geomagnetic polarity time scale reevaluated: Evidence from the Green River Formation of Wyoming: Geology, v. 32, p. 137-140.
Malone, D.H., 1995, Very large debris-avalanche deposit within the Eocene volcanic succession of the northeastern Absaroka Range, Wyoming: Geology, v. 23, p. 661-664.
—, 1996, Revised stratigraphy of Eocene volcanic rocks in the lower North and South Fork Shoshone River valleys, Wyoming, *in* Bowen, C.E., Kirkwood, S.C., and Miller, T.S., eds., Resources of the Bighorn Basin: Casper, Wyoming Geological Association, 47th Field Conference, Guidebook, p. 109-136.
Manchester, S.R., 1989, Attached reproductive and vegetative remains of the extinct American-European genus Cedrelospermum (Ulmaceae) from the Early Tertiary of Utah and Colorado: American Journal of Botany, v. 76, p. 256-276.
Mapel, W.J., 1959, Geology and coal resources of the Buffalo-Lake DeSmet area Johnson and Sheridan Counties Wyoming: U.S. Geological Survey Bulletin 1078, 148 p.
Marcantel, E.L., and Weiss, M.P., 1968, Colton Formation (Eocene: Fluviatile) and associated lacustrine beds, Gunnison Plateau, central Utah: The Ohio Journal of Science, v. 68, p. 40-49.
Mason, G.M., 1987, Mineralogic aspects of stratigraphy and geochemistry of the Green River Formation, Wyoming [PhD thesis]: Laramie, University of Wyoming, 377 p.
Masursky, H., 1962, Uranium-bearing coal in the eastern part of the Red Desert area Wyoming: U.S. Geological Survey Bulletin 1099-B, 152 p.

Matthew, W.D., 1909, The carnivora and insectivora of the Bridger Basin, middle Eocene: American Museum of Natural History Memoir, no. 9, p. 289-576.
Mauger, R.L., 1977, K-Ar ages of biotites from tuffs in Eocene rocks of the Green River, Washakie, and Uinta basins, Utah, Wyoming, and Colorado: University of Wyoming Contributions to Geology, v. 15, p. 17-41.
McCarroll, S.M., Flynn, J.J., and Turnbull, W.D., 1996a, Biostratigraphy and magnetostratigraphy of the Bridgerian-Uintan Washakie Formation, Washakie Basin, Wyoming, *in* Prothero, D.R., and Emry, R.J., eds., The Terrestrial Eocene-Oligocene Transition in North America, Cambridge University Press, p. 25-39.
—, 1996b, The mammalian faunas of the Washakie Formation, Eocene age, of southern Wyoming. Part III. The perissodactyls: Fieldiana: Geology, new series, no. 33, 38 p.
McGee, L.C., 1983, Laramide sedimentation, folding and faulting southern Wind River Range, Wyoming [M.Sc. thesis]: Laramie, University of Wyoming, 92 p.
McGookey, D.P., 1960, Early Tertiary stratigraphy of part of central Utah: American Association of Petroleum Geologists Bulletin, v. 44, p. 589-615.
McGrew, P.O., 1953, Tertiary deposits of southeastern Wyoming, *in* Blackstone, D.L., Jr., ed., Laramie Basin, Wyoming, and North Park, Colorado: Casper, Wyoming Geological Association, 8th Annual Field Conference, Guidebook, p. 61-64.
—, 1959, The geology and paleontology of the Elk Mountain and Tabernacle Butte area, Wyoming: American Museum of Natural History Bulletin, v. 117, p. 117-176.
McGrew, P.O., and Berman, J.E., 1955, Geology of the Tabernacle Butte area, Sublette County, Wyoming, *in* Anderman, G.G., ed., Green River Basin: Casper, Wyoming Geological Association, 10th Annual Field Conference, Guidebook, p. 108-111.
McGrew, P.O., and Roehler, H.W., 1960, Correlation of Tertiary units in southwestern Wyoming, *in* McGookey, D.P., and Miller, D.N., Jr., eds., Overthrust Belt of Southwestern Wyoming and Adjacent Areas: Casper, Wyoming, Wyoming Geological Association, 15th Annual Field Conference, Guidebook, p. 157-158.
McGrew, P.O., and Sullivan, R., 1970, The stratigraphy and paleontology of Bridger A: University of Wyoming Contributions to Geology, v. 9, p. 66-85.
McIntyre, D.H., Ekren, E.B., and Hardyman, R.F., 1982, Stratigraphic and structural framework of the Challis Volcanics in the eastern half of the Challis 1° x 2° quadrangle, *in* Breckenridge, R.M., and Bonnichsen, B., eds., Cenozoic Geology of Idaho: Idaho Bureau of Mines and Geology Bulletin 26, p. 3-22.
McKenna, M.C., 1955, Earliest Eocene vertebrates from the Sand Wash Basin, northwestern Colorado, *in* Ritzma, H.R., and Oriel, S.S., eds., Guidebook to the Geology of Northwest Colorado: Salt Lake City, Utah, Intermountain Association of Petroleum Geologists and Rocky Mountain Association of Geologists, 6th Annual Field Conference, p. 41-43.
—, 1972, Vertebrate paleontology of the Togwotee Pass area, northwestern Wyoming, *in* West, R.M., ed., Field Conference on Tertiary Biostratigraphy of Southern and Western Wyoming: Garden City, New York, Adelphi University, p. 80-101.
—, 1980, Late Cretaceous and early Tertiary vertebrate paleontological reconnaissance, Togwotee Pass area, northwestern Wyoming, *in* Jacobs, L.L., ed., Aspects of Vertebrate History. Essays in Honor of Edwin Harris Colbert: Flagstaff, Museum of Northern Arizona Press, p. 321-343.
M'Gonigle, J.W., and Dalrymple, G.B., 1996, $^{40}Ar/^{39}Ar$ ages of some Challis Volcanic Group rocks and the initiation of Tertiary sedimentary basins in southwestern Montana: U.S. Geological Survey Bulletin 2132, 17 p.
M'Gonigle, J.W., and Dover, J.H., 1992, Geologic map of the Kemmerer 30' x 60' quadrangle, Lincoln, Uinta and Sweetwater Counties, Wyoming: U.S. Geological Survey Miscellaneous Investigations Series Map I-2079, Scale 1:100 000, 1 Sheet.
Miller, W.E., and Hall, D.A., 1990, Earliest history of vertebrate paleontology in Utah: Last half of the 19th century: Earth Sciences History, v. 9, p. 28-33.
Moncure, G., and Surdam, R.C., 1980, Depositional environment of the Green River Formation in the vicinity of the Douglas Creek Arch, Colorado and Utah: University of Wyoming Contributions to Geology, v. 19, p. 9-24.
Moncure, G.K., 1979, Depositional environment of the Green River Formation in the vicinity of the Douglas Creek Arch, Colorado and Utah [M.Sc. thesis]: Laramie, University of Wyoming, 55 p.

Moore, S.W., and Solomon, B.J., 1982, Preliminary results of core drilling and other geologic studies of Paleogene oil shale-bearing deposits near Elko, Nevada, *in* Gary, J.H., ed., Fifteenth Oil Shale Symposium Proceedings: Golden, Colorado, Colorado School of Mines Press, p. 69-78.

Morris, T.H., Richmond, D.R., and Mariño, J.E., 1991, The Paleocene/Eocene Colton Formation: A fluvial-dominated lacustrine deltaic system, Roan Cliffs, Utah, *in* Chidsey, T.C., Jr., ed., Geology of East-Central Utah: Salt Lake City, Utah Geological Association, Publication 19, p. 129-139.

Morris, W.J., 1954, An Eocene fauna from the Cathedral Bluffs Tongue of the Washakie Basin, Wyoming: Journal of Paleontology, v. 28, p. 195-203.

Moussa, M.T., 1969, Green River Formation (Eocene) in the Soldier Summit area, Utah: Geological Society of America Bulletin, v. 80, p. 1737-1748.

Moye, F.J., Hackett, W.R., Blakley, J.D., and Snider, L.G., 1988, Regional geologic setting and volcanic stratigraphy of the Challis Volcanic Field, central Idaho, *in* Link, P.K., and Hackett, W.R., eds., Guidebook to the Geology of Central and Southern Idaho: Idaho Geological Survey Bulletin 27, p. 87-97.

Muessig, S., 1951, Eocene volcanism in central Utah: Science, v. 114, p. 234.

Murphey, P.C., 2001, Stratigraphy, fossil distribution, and depositional environments of the upper Bridger Formation (middle Eocene) of southwestern Wyoming, and the taphonomy of an unusual Bridger microfossil assemblage [PhD thesis]: Boulder, University of Colorado, 345 p.

Murphy, J.F., and Roberts, R.W., 1954, Geology of the Steamboat Butte-Pilot Butte area Fremont County, Wyoming: U.S. Geological Survey Oil and Gas Investigations Map OM 151, Scale 1:48 000, 1 Sheet.

Nace, R.L., 1939, Geology of the northwest part of the Red Desert, Sweetwater and Fremont Counties, Wyoming: Geological Survey of Wyoming Bulletin 27, 51 p.

Neasham, J.W., and Vondra, C.F., 1972, Stratigraphy and petrology of the lower Eocene Willwood Formation, Bighorn Basin, Wyoming: Geological Society of America Bulletin, v. 83, p. 2167-2180.

Nelson, M.E., 1972, Age and stratigraphic relations of the Fowkes Formation, southwestern Wyoming, *in* West, R.M., ed., Field Conference on Tertiary Biostratigraphy of Southern and Western Wyoming: Garden City, New York, Adelphi University, p. 51-62.

—, 1973, Age and stratigraphic relations of the Fowkes Formation, Eocene, of south-western Wyoming and northeastern Utah: University of Wyoming Contributions to Geology, v. 12, p. 27-31.

Nelson, M.E., Madsen, J.H., Jr., and Stokes, W.L., 1980a, A titanothere from the Green River Formation, central Utah: Teleodus uintensis (Perissodactyla: Brontotheriidae): University of Wyoming Contributions to Geology, v. 18, p. 127-134.

Nelson, W.H., and Pierce, W.G., 1968, Wapiti Formation and Trout Peak Trachyandesite northwest Wyoming: U.S. Geological Survey Bulletin 1254-H, 11 p.

Nelson, W.H., Prostka, H.J., and Williams, F.E., 1980b, Geology and mineral resources of the North Absaroka Wilderness and vicinity, Park County, Wyoming: U.S. Geological Survey Bulletin 1447, 101 p.

Nightingale, W.T., 1930, Geology of Vermillion Creek gas area in southwest Wyoming and northwest Colorado: American Association of Petroleum Geologists Bulletin, v. 14, p. 1013-1040.

Oaks, R.Q., Smith, K.A., Janecke, S.U., Perkins, M.E., and Nash, W.P., 1999, Stratigraphy and tectonics of Tertiary strata of southern Cache Valley, north-central Utah, *in* Spangler, L.E., and Allen, C.J., eds., Geology of Northern Utah and Vicinity: Salt Lake City, Utah Geological Association, Publication 27, p. 71-110.

O'Neill, J.M., Lonn, J.D., Lageson, D.R., and Kunk, M.J., 2004, Early Tertiary Anaconda metamorphic core complex, southwest Montana: Canadian Journal of Earth Sciences, v. 41, p. 63-72.

O'Neill, W.A., 1980, $^{40}Ar/^{39}Ar$ ages of selected tuff of the Green River Formation: Wyoming, Colorado, and Utah [M.Sc. thesis]: Columbus, The Ohio State University, 142 p.

Oriel, S.S., 1961, Tongues of the Wasatch and Green River Formations, Fort Hill area, Wyoming: U.S. Geological Survey Professional Paper 424-B, p. 151-152.

—, 1962, Main body of the Wasatch Formation near La Barge, Wyoming: American Association of Petroleum Geologists Bulletin, v. 46, p. 2161-2173.

Oriel, S.S., and Tracey, J.I., Jr., 1970, Uppermost Cretaceous and Tertiary stratigraphy of Fossil Basin, southwestern Wyoming: U.S. Geological Survey Professional Paper 635, 53 p.

Osborn, H.F., 1895, Fossil mammals of the Uinta Basin. Expedition of 1894: American Museum of Natural History Bulletin, v. 7, p. 71-105.
—, 1929, The titanotheres of ancient Wyoming, Dakota, and Nebraska: U.S. Geological Survey Monograph 55, v. 1, 701 p.
O'Sullivan, R.B., 1974, Chart showing correlation of selected restored stratigraphic diagram units of the Eocene Uinta and Green River Formations, east-central Piceance Creek Basin, northwestern Colorado: U.S. Geological Survey Oil and Gas Investigations Chart OC-67, 1 Sheet.
—, 1975, Coughs Creek Tongue-A new tongue of the Eocene Green River Formation, Piceance Creek Basin, Colorado: U.S. Geological Survey Bulletin 1395-G, 7 p.
—, 1987, Chart showing correlation of selected parts of the Eocene Uinta and Green River Formations, Southeastern Piceance Creek Basin, Colorado: U.S. Geological Survey Miscellaneous Field Studies Map MF-1986, 1 Sheet.
Palmer, B.A., and Shawkey, E.P., 1997, Lacustrine sedimentation processes and pattern during effusive and explosive volcanism, Challis Volcanic Field, Idaho: Journal of Sedimentary Research, v. 67, p. 154-167.
Parker, L.R., 1970, A titanothere from the Eocene Green River Formation of Utah: Geological Society of America Abstracts with Programs, v. 2, no. 6, p. 400-401.
Peale, A.C., 1876, Report of A.C. Peale: U.S. Geological and Geographic Survey of the Territories, embracing Colorado and parts of adjacent Territories, 8th Annual Report for 1874, p. 75-180.
Pekarek, A.H., Marvin, R.F., and Menhert, H.H., 1974, K-Ar ages of the volcanics in the Rattlesnake Hills, central Wyoming: Geology, v. 2, p. 283-285.
Peterson, A.R., 1976, Paleoenvironments of the Colton Formation, Colton, Utah: Brigham Young University Geology Studies, v. 23, pt.1, p. 3-35.
Picard, M.D., 1955, Subsurface stratigraphy and lithology of Green River Formation in Uinta Basin, Utah: American Association of Petroleum Geologists Bulletin, v. 39, p. 75-102.
—, 1957a, Green River and lower Uinta Formations-Subsurface stratigraphic changes in central and eastern Uinta Basin, Utah, *in* Seal, O.G., ed., Guidebook to the Geology of the Uinta Basin: Salt Lake City, Utah, Intermountain Association of Petroleum Geologists, 8th Annual Field Conference, p. 116-130.
—, 1957b, Green shale facies, lower Green River Formation, Utah: American Association of Petroleum Geologists Bulletin, v. 41, p. 2373-2376.
—, 1959, Green River and lower Uinta Formation subsurface stratigraphy in western Uinta Basin, Utah, *in* Williams, N.C., ed., Guidebook to the Geology of the Wasatch and Uinta Mountains, Transition Area: Salt Lake City, Utah, Intermountain Association of Petroleum Geologists, 10th Annual Field Conference, p. 139-149.
—, 1967, Paleocurrents and shoreline orientations in Green River Formation (Eocene), Raven Ridge and Red Wash areas, northeastern Uinta Basin, Utah: American Association of Petroleum Geologists Bulletin, v. 51, p. 383-392.
Picard, M.D., and High, L.R., Jr., 1968, Sedimentary cycles in the Green River Formation (Eocene), Uinta Basin, Utah: Journal of Sedimentary Petrology, v. 38, p. 378-383.
Pierce, W.G., 1963, Cathedral Cliffs Formation, the Early Acid Breccia unit of northwestern Wyoming: Geological Society of America Bulletin, v. 74, p. 9-22.
—, 1997, Geologic map of the Cody 1° x 2° quadrangle, northwestern Wyoming: U.S. Geological Survey Miscellaneous Investigations Series Map I-2500, Scale 1:250 000, 1 Sheet.
Pietras, J.T., Carroll, A.R., and Rhodes, M.K., 2003a, Lake basin response to tectonic drainage diversion: Eocene Green River Formation, Wyoming: Journal of Paleolimnology, v. 30, p. 115-125.
Pietras, J.T., Carroll, A.R., Singer, B.S., and Smith, M.E., 2003b, 10 k.y. depositional cyclicity in the Early Eocene: Stratigraphic and $^{40}Ar/^{39}Ar$ evidence from the lacustrine Green River Formation: Geology, v. 31, p. 593-597.
Pipiringos, G.N., 1955, Tertiary rocks in the central part of the Great Divide Basin, Sweetwater County, Wyoming, *in* Anderman, G.G., ed., Green River Basin: Casper, Wyoming Geological Association, 10th Annual Field Conference, Guidebook, p. 100-104.
—, 1961, Uranium-bearing coal in the central part of the Great Divide Basin: U.S. Geological Survey Bulletin 1099-A, 104 p.

Pipiringos, G.N., and Johnson, R.C., 1975, Preliminary geologic map of the Buckskin Point quadrangle, Rio Blanco County, Colorado: U.S. Geological Survey Miscellaneous Field Studies Map MF-651, Scale 1:24 000, 1 Sheet.

Pipringos, G.N., and Denson, N.M., 1970, The Battle Spring Formation in south-central Wyoming, *in* Enyert, R.L., ed., Symposium on Wyoming Sandstones: Casper, Wyoming Geological Association, 22nd Annual Field Conference, Guidebook, p. 161-168.

Pitman, J.K., Fouch, T.D., and Goldhaber, M.B., 1982, Depositional setting and diagenetic evolution of some Tertiary unconventional reservoir rocks, Uinta Basin, Utah: American Association of Petroleum Geologists Bulletin, v. 66, p. 1581-1596.

Pledge, N.S., 1969, Paleoenvironmental and paleoecology of part of the lower Bridger Formation, south of Opal, Wyoming [M.Sc. thesis]: Laramie, University of Wyoming, 74 p.

Powell, J.W., 1876, Report of the geology of the eastern portion of the Uinta Mountains and region of country adjacent thereto: U.S. Geological and Geographical Survey of the Territories Second Division, 218 p.

Prichinello, K.A., 1971, Earliest Eocene mammalian fossils from the Laramie Basin of southeast Wyoming: University of Wyoming Contributions to Geology, v. 10, p. 73-87.

Prostka, H.J., Blank, H.R., Jr., Christiansen, R.L., and Ruppel, E.T., 1975, Geologic map of the Tower Junction quadrangle, Yellowstone National Park, Wyoming and Montana: U.S. Geological Survey Geologic Quadrangle Map GQ-1247, Scale 1:62 500, 1 Sheet.

Prothero, D.R., 1996, Magnetic stratigraphy and biostratigraphy of the Middle Eocene Uinta Formation, Uinta Basin, Utah, *in* Prothero, D.R., and Emry, R.J., eds., The Terrestrial Eocene-Oligocene Transition in North America, Cambridge University Press, p. 25-39.

Prothero, D.R., and Emry, R.J., 1996, Summary, *in* Prothero, D.R., and Emry, R.J., eds., The Terrestrial Eocene-Oligocene Transition in North America, Cambridge University Press, p. 664-683.

Pruss, E.F., 1975, A paleomagnetic study of basalt flows from the Absaroka Mountains, Wyoming, *in* Exum, F.A., and George, G.R., eds., Geology and Mineral Resources of the Bighorn Basin: Casper, Wyoming Geological Association, 27th Annual Field Conference, Guidebook, p. 257-266.

Pusca, V.A., 2003, Wet/dry, terminal fan-dominated sequence architecture: a new, outcrop-based model for the lower Green River Formation, Utah [Ph.D. thesis]: Laramie, University of Wyoming, 175 p.

Rasmussen, D.L., 2003, Tertiary history of western Montana and east-central Idaho: A synopsis, *in* Raynolds, R.G., and Flores, R.M., eds., Cenozoic Systems of the Rocky Mountain Region: Denver, Colorado, Rocky Mountain Section, SEPM (Society for Sedimentary Geology), p. 459-477.

Rasmussen, D.T., 1999, The mammals of the Eocene Duchensne River Formation, *in* Gillette, D.D., ed., Vertebrate Paleontology of Utah: Utah Geological Survey Miscellaneous Publication 99-1, p. 421-427.

Rasmussen, D.T., Conroy, G.C., Friscia, A.R., Townsend, K.E., and Kinkel, M.D., 1999, Mammals of the Middle Eocene Uinta Formation, *in* Gillette, D.D., ed., Vertebrate Paleontology of Utah: Utah Geological Survey Miscellaneous Publication 99-1, p. 401-420.

Ratterman, N.G., and Surdam, R.C., 1981, Zeolite minerals in a tuff in the Laney Member of the Green River Formation, Wyoming: Clays and Clay Minerals, v. 29, p. 365-377.

Ray, R.G., Kent, B.H., and Dane, C.H., 1956, Stratigraphy and photogeology of the southwestern part of the Uinta Basin Duchesne and Uintah Counties, Utah: U.S. Geological Survey Oil and Gas Investigations Map OM-171, Scale 1:63 360, 2 Sheets.

Remy, R.R., 1992, Stratigraphy of the Eocene part of the Green River Formation in the south-central part of the Uinta Basin, Utah: U.S. Geological Survey Bulletin 1787-BB, 79 p.

Renne, P.R., Swisher, C.C., Deino, A.L., Karner, D.B., Owens, T.L., and DePaolo, D.J., 1998, Intercalibration of standards, absolute ages and uncertainties in $^{40}Ar/^{39}Ar$ dating: Chemical Geology, v. 145, p. 117-152.

Ripley, A.A., 1995, Tertiary carbonates in the upper Ruby and Jefferson river valleys, Montana: Northwest Geology, v. 25, p. 47-77.

Ritzma, H.R., 1955, Early Cenozoic history of the Sand Wash Basin, northwest Colorado, *in* Ritzma, H.R., and Oriel, S.S., eds., Guidebook to the Geology of Northwest Colorado: Salt Lake City, Utah, Intermountain Association of Petroleum Geologists and Rocky Mountain Association of Geologists, 6th Annual Field Conference, p. 36-40.

—, 1961, Geology and occurrence of oil and gas, Wamsutter Arch, Wyoming: American Association of Petroleum Geologists Bulletin, v. 45, p. 188-195.
—, 1965, Piceance Creek sandstone, basal Green River Sandstone Tongue, northeast Piceance Creek Basin, Colorado: The Mountain Geologist, v. 2, p. 103-107.
Robb, W.A., and Smith, J.W., 1974, Mineral profile of oil shales in Colorado core hole no. 1, Piceance Creek Basin, Colorado, *in* Murray, D.K., ed., Guidebook to the Energy Resources of the Piceance Creek Basin, Colorado: Denver, Colorado, Rocky Mountain Association of Geologists, 25th Annual Field Conference, Guidebook, p. 91-100.
Robinson, P., 1966, Fossil mammals of the Huerfano Formation, Eocene, of Colorado: Peabody Museum of Natural History Bulletin, v. 21, p. 1-95.
Roehler, H.W., 1965, Early Tertiary depositional environments in the Rock Springs Uplift area, *in* De Voto, R.H., and Bitter, R.K., eds., Sedimentation of Late Cretaceous and Tertiary Outcrops, Rock Springs Uplift: Casper, Wyoming Geological Association, 19th Annual Field Conference, Guidebook, p. 140-150.
—, 1968, Redefinition of Tipton Shale Member of Green River Formation of Wyoming: American Association of Petroleum Geologists Bulletin, v. 52, p. 2249-2256.
—, 1969, Stratigraphy and oil-shale deposits of Eocene rocks in the Washakie Basin, Wyoming, *in* Barlow, J.A., ed., Symposium on Tertiary Rocks of Wyoming: Casper, Wyoming Geological Association, 21st Annual Field Conference, Guidebook, p. 197-206.
—, 1970, Nonopaque heavy mineral from sandstone of Eocene age in the Washakie Basin, Wyoming: U.S. Geological Survey Professional Paper 700-D, p. 181-187.
—, 1973a, Stratigraphic divisions and geologic history of the Laney member of the Green River Formation in the Washakie Basin in southwestern Wyoming: U.S. Geological Survey Bulletin 1372-E, 28 p.
—, 1973b, Stratigraphy of the Washakie Formation in the Washakie Basin, Wyoming: U.S. Geological Survey Bulletin 1369, 40 p.
—, 1974, Depositional environments of rocks in the Piceance Creek Basin, Colorado, *in* Murray, D.K., ed., Guidebook to the Energy Resources of the Piceance Creek Basin, Colorado: Denver, Colorado, Rocky Mountain Association of Geologists, 25th Annual Field Conference, p. 57-64.
—, 1985, Geologic map of the Kinney Rim 30 x 60 minute quadrangle, Wyoming and Colorado: U.S. Geologic Survey Miscellaneous Investigations Series Map I-1615, Scale 1:100 000, 1 Sheet.
—, 1988, Geology of the Cottonwood Creek Delta in the Eocene Tipton Tongue of the Green River Formation, southeast Washakie Basin, Wyoming: U.S. Geological Survey Bulletin 1669-A, 14 p.
—, 1989, Correlation of surface sections of intertongued Eocene Wasatch and Green River Formations along the west flank of the Rock Springs uplift in southwest Wyoming: U.S. Geological Survey Miscellaneous Field Studies Map MF-2104, 1 Sheet.
—, 1990, Sedimentology of freshwater lacustrine shorelines in the Eocene Scheggs Bed of the Tipton Tongue of the Green River Formation, Sand Wash Basin, northwest Colorado: U.S. Geological Survey Bulletin 1911, 12 p.
—, 1991a, Correlation and oil-shale assays of measured sections of the LaClede Bed of the Laney Member of the Green River Formation in outcrops along the western margins of Washakie Basin, Wyoming, and Sand Wash Basin, Colorado: U.S. Geological Survey Miscellaneous Investigations Series Map I-2211, 2 Sheets.
—, 1991b, Godiva Rim Member-A new stratigraphic unit of the Green River Formation in southwest Wyoming and northwest Colorado: U.S. Geological Survey Professional Paper 1506-C, 17 p.
—, 1991c, Revised stratigraphic nomenclature for the Wasatch and Green River Formations of Eocene age, Wyoming, Utah, and Colorado: U.S. Geological Survey Professional Paper 1506-B, 38 p.
—, 1992a, Correlation, composition, areal distribution, and thickness of Eocene stratigraphic units, greater Green River basin, Wyoming, Utah, and Colorado: U.S. Geological Survey Professional Paper 1506-E, 49 p.
—, 1992b, Description and correlation of Eocene rocks in stratigraphic reference sections for the Green River and Washakie Basins, southwest Wyoming: U.S. Geological Survey Professional Paper 1506-D, 83 p.
—, 1993, Eocene climates, depositional environments, and geography, greater Green River basin, Wyoming, Utah, and Colorado: U.S. Geological Survey Professional Paper 1506-F, 74 p.
Roehler, H.W., Chisholm, W.A., and Schneider, G.B., 1990, Composite measured section showing nonopaque heavy minerals in sedimentary rocks of Middle Protorozoic to Late Tertiary age in the

central Rocky Mountains, southwest Wyoming and northwest Colorado: U.S. Geological Survey Miscellaneous Investigations Series Map I-2145, 1 Sheet.
Roehler, H.W., and Trudell, L.G., 1981, Surface-subsurface correlations of the Eocene Green River Formation, on the west flank of the Rock Springs Uplift, Sweetwater County, Wyoming: U.S. Geological Survey Miscellaneous Field Studies Map MF-1308, 1 Sheet.
Rohrer, W.L., 1964a, Geology of the Sheep Mountain quadrangle, Wyoming: U.S. Geological Survey Geologic Quadrangle Map GQ-310, Scale 1:24 000, 1 Sheet.
—, 1964b, Geology of the Tatman Mountain Quadrangle, Wyoming: U. S. Geological Survey Geologic Quadrangle Map GQ-311, Scale 1:24 000, 1 Sheet.
—, 1966a, Geologic map of the Kisinger Lakes Quadrangle Fremont County, Wyoming: U.S. Geological Survey Geological Quadrangle Map GQ-527, Scale 1:24 000, 1 Sheet.
—, 1966b, Geology of the Adam Weiss Peak Quadrangle, Hot Springs and Park Counties, Wyoming: U.S. Geological Survey Bulletin 1241-A, 39 p.
—, 1968, Geologic map of the Fish Lake quadrangle, Wyoming: U.S. Geological Survey Geologic Quadrangle Map GQ-724, Scale 1:24 000, 1 Sheet.
—, 1969, Preliminary geologic map of Sheridan Pass quadrangle, Fremont and Teton Counties, Wyoming: U.S. Geological Survey Open-File Report, Scale 1:24 000, 1 Sheet.
Rohrer, W.L., and Gazin, C.L., 1965, Gray Bull and Lysite faunal zone of the Willwood Formation in the Tatman Mountain area, Bighorn Basin, Wyoming: U.S. Geological Survey Professional Paper 525-D, p. 133-138.
Rohrer, W.L., and Obradovich, J.D., 1969, Age and stratigraphic relations of the Tepee Trail and Wiggins Formations, northwestern Wyoming: U.S. Geological Survey Professional Paper 650-B, p. 57-62.
Rowley, P.D., Hansen, W.R., Tweto, O., and Carrara, P.E., 1985, Geologic map of the Vernal 1º x 2º quadrangle, Colorado, Utah, and Wyoming: U.S. Geological Survey Miscellaneous Investigations Series Map I-1526, Scale 1:250 000, 1 Sheet.
Rubel, D.N., 1971, Independance Volcano: A major Eocene eruptive center, northern Absaroka Volcanic Province: Geological Society of America Bulletin, v. 82, p. 2473-2494.
Rubey, W.W., Oriel, S.S., and Tracey, J.I., Jr., 1975, Geology of the Sage and Kemmerer 15-minute quadrangles, Lincoln County, Wyoming: U.S. Geological Survey Professional Paper 855, 18 p.
—, 1980, Geologic map and structural sections of the Cokeville 30-minute quadrangle, Lincoln and Sublette Counties, Wyoming: U.S. Geological Survey Miscellaneous Investigations Series Map I-1129, Scale 1:125 000, 2 Sheets.
Ryder, R.T., Fouch, T.D., and Elison, J.H., 1976, Early Tertiary sedimentation in the western Uinta Basin, Utah: Geological Society of America Bulletin, v. 87, p. 496-592.
Sanborn, A.F., and Goodwin, J.C., 1965, Green River Formation at Raven Ridge, Uintah County, Utah: The Mountain Geologist, v. 2, p. 109-114.
Savage, D.E., Waters, B.T., and Hutchison, J.H., 1972, Northwestern border of the Washakie Basin, *in* West, R.M., ed., Field Conference on Tertiary Biostratigraphy of Southern and Western Wyoming: Garden City, New York, Adelphi University, p. 32-50.
Schmidtt, L.J., Jr., 1979, Geologic map of the Crooks Peak quadrangle, Fremont and Sweetwater Counties, Wyoming: U.S. Geological Survey Geologic Quadrangle Map GQ-1517, Scale 1:24 000, 1 Sheet.
Schoff, S.L., 1951, Geology of the Cedar Hills: Geological Society of America Bulletin, v. 62, p. 619-646.
Schultz, A.R., 1920, Oil possibilities in and around Baxter Basin, in the Rock Springs Uplift, Sweetwater County, Wyoming: U.S. Geological Survey Bulletin 702, 107 p.
Sears, J.D., and Bradley, W.H., 1924, Relations of the Wasatch and Green River Formations in northwestern Colorado and southern Wyoming: U.S. Geological Survey Professional Paper 132-F, p. 93-107.
Sears, J.W., and Ryan, P.C., 2003, Cenozoic evolution of the Montana Cordillera: Evidence from paleovalleys, *in* Raynolds, R.G., and Flores, R.M., eds., Cenozoic Systems of the Rocky Mountain Region: Denver, Colorado, Rocky Mountain Section, SEPM (Society for Sedimentary Geology), p. 289-301.
Seeland, D., 1992, Depositional systems of a synorogenic continental deposit-The upper Paleocene and lower Eocene Wasatch Formation of the Powder River Basin: U.S. Geological Survey Bulletin 1917-H, 20 p.
Seeland, D.A., 1978a, Eocene fluvial drainage patterns and their implications for uranium and hydrocarbon exploration in the Wind River Basin, Wyoming: U.S. Geological Survey Bulletin 1446, 21 p.

—, 1978b, Sedimentology and stratigraphy of the lower Eocene Wind River Formation, central Wyoming, *in* Boyd, R.G., Boberg, W.W., and Olson, G.W., eds., Resources of the Wind River Basin: Casper, Wyoming Geological Association, 30th Annual Field Conference, Guidebook, p. 181-198.
—, 1998, Late Cretaceous, Paleocene, and early Eocene paleogeography of the Bighorn Basin and northwestern Wyoming, *in* Keefer, W.R., and Goolsby, J.E., eds., Cretaceous and Lower Tertiary Rocks of the Bighorn Basin, Wyoming and Montana: Aurora, Colorado, Wyoming Geological Association, 49th Annual Field Conference, Guidebook, p. 137-165.
Sheliga, C.M., 1980, Sedimentation of the Eocene Green River Formation in Sevier and Sanpete Counties, Central Utah [M.Sc. thesis]: Columbus, The Ohio State University, 166 p.
Sheridan, D.M., Maxwell, C.H., and Collier, J.T., 1961, Geology of the Lost Creek schroeckingerite deposits Sweetwater County, Wyoming: U.S. Geological Survey Bulletin 1087-J, p. 391-478.
Shive, P.N., Pekarek, A.K., and Zawislak, R.L., 1977, Volcanism in the Rattlesnake Hills of central Wyoming: A paleomagnetic study: Geology, v. 5, p. 563-566.
Shive, P.N., and Pruss, E.F., 1977, A paleomagnetic study of basalt flows from the Absaroka Mountains, Wyoming: Journal of Geophysical Research, v. 82, p. 3039-3048.
Siems, P.L., 1964, Correlation of Tertiary strata in mountain basins, southern Colorado and northern New Mexico: The Mountain Geologist, v. 1, p. 161-180.
Simnacher, F., 1970, Stratigraphy, depositional environments, and paleontology of the Cathedral Bluffs tongue of the Wasatch Formation, Parnelle Creek area Sweetwater County, Wyoming [M.Sc. thesis]: Laramie, University of Wyoming, 101 p.
Sinclair, W.J., and Granger, W., 1911, Eocene and Oligocene of the Wind River and Bighorn Basins: American Museum of Natural History Bulletin, v. 30, p. 83-117.
Sklenar, S.E., and Anderson, D.W., 1985, Orgin and early evolution of an Eocene lake system within the Washakie Basin of southwestern Wyoming, *in* Flores, R.M., and Kaplan, S.S., eds., Cenozoic Paleogeography of the West Central United States: Denver, Colorado, Rocky Mountain Section, SEPM (Society for Sedimentary Geology), Rocky Mountain Paleogeography Symposium 3, p. 231-245.
Smedes, H.W., 1962, Lowland Creek Volcanics, and upper Oligocene Formation near Butte, Montana: The Journal of Geology, v. 70, p. 255-266.
Smedes, H.W., and Hanna, W.F., 1977, Paleomagnetism of the lower Eocene Lowland Creek Volcanics, Montana: Geological Society of America Abstracts with Programs, v. 7, no. 6, p. 763.
Smedes, H.W., and Prostka, H.J., 1972, Stratigraphic framework of the Absaroka Volcanic Supergroup in the Yellowstone National Park region: U.S. Geological Survey Professional Paper 729-C, 33 p.
Smith, J.D., 1984, Depositional environments of the Tertiary Colton and basal Green River Formations in Emma Park, Utah: Brigham Young University Geology Studies, v. 33, pt. 1, p. 135-174.
Smith, K.T., and Holroyd, P.A., 2003, Rare taxa, biostatigraphy, and the Wasatchian-Bridgerian boundary in North America, *in* Wing, S.R., Gingerich, P.D., Schmitz, B., and Thomas, E., eds., Causes and Consequences of Globally Warm Climates in the Early Paleogene: Geological Society of America Special Paper 369, p. 501-511.
Smith, L.N., Lucas, S.G., and Elston, W.E., 1985, Paleogene stratigraphy, sedimentation and volcanism of New Mexico, *in* Flores, R.M., and Kaplan, S.S., eds., Cenozoic Paleogeography of the West Central United States: Denver, Colorado, Rocky Mountain Section, SEPM (Society for Sedimentary Geology), Rocky Mountain Paleogeography Symposium 3, p. 293-315.
Smith, M.E., Singer, B., and Carroll, A.R., 2003, $^{40}Ar/^{39}Ar$ geochronology of the Eocene Green River Formation, Wyoming: Geological Society of America Bulletin, v. 115, p. 549-565.
—, 2004, $^{40}Ar/^{39}Ar$ geochronology of the Eocene Green River Formation, Wyoming; Reply: Geological Society of America Bulletin, v. 116, p. 253-256.
Smith, M.E., Singer, B.S., Carroll, A.R., and Fournelle, J.H., 2006a, High-resolution calibration of Eocene strata: $^{40}Ar/^{39}Ar$ geochronology of biotite in the Green River Formation: Geology, v. 34, p. 393-396.
—, 2006b, Precise dating of biotite in distal ash: Isolating subtle alteration using $^{40}Ar/^{39}Ar$ laser incremental heating and electron microprobe techniques: Geochimica et Cosmochimica Acta, p. (in review).
Smoot, J.P., 1983, Depositional subenvironments in an arid closed basin; the Wilkins Peak Member of the Green River Formation (Eocene), Wyoming, U.S.A.: Sedimentology, v. 30, p. 801-827.

Snider, L.G., 1995, Stratigraphic framework, geochemistry, geochronology, and eruptive styles of Eocene volcanic rocks in the White Knob Mountains area, southeastern Challis Volcanic Field, central Idaho [M.Sc. thesis]: Pocatello, Idaho State University, 212 p.

Snider, L.G., and Moye, F.J., 1989, Regional stratigraphy, physical volcanology, and geochemistry of the southeastern Challis Volcanic Field: U.S. Geological Survey Open-File Report 89-639, p. 122-127.

Snow, C.B., 1970, Stratigraphy of basal sandstones in the Green River Formation northeast Piceance Basin, Rio Blanco County, Colorado: The Mountain Geologist, v. 7, p. 3-32.

Soister, P.E., 1968, Stratigraphy of the Wind River Formation in south-central Wind River Basin, Wyoming: U.S. Geological Survey Professional Paper 594-A, 50 p.

Solomon, B.J., 1981, Geology and oil shale resources near Elko, Nevada: U.S. Geological Survey Open-File Report 81-709, 146 p.

Solomon, B.J., McKee, E.H., and Anderson, D.W., 1979, Stratigraphy and depositional environments of Paleogene rocks near Elko, Nevada, *in* Armentrout, J.M., Cole, M.R., and TerBest, H., Jr., eds., Cenozoic paleogeography of the western United States: Los Angeles, California, Pacific Section, Society of Economic Paleontologists and Mineralogists, Pacific Coast Paleogeography Symposium. 3, p. 75-88.

Spieker, E.M., 1946, Late Mesozoic and early Cenozoic history of central Utah: U.S. Geological Survey Professional Paper 205-D, p. 117-161.

—, 1949, The transition between the Colorado Plateaus and the Great Basin in central Utah: Salt Lake City, Utah Geological Society, 106 p.

Stagner, W.L., 1941, The paleogeography of the eastern part of the Uinta Basin during Uinta B (Eocene) time: Annals of Carnegie Museum, v. 28, p. 273-308.

Stands, R.E., 1992, Relative ages of major coal beds in the Coalmont Formation (Paleocene-Eocene), North Park Basin, Jackson County, Colorado [M.Sc. thesis]: Golden, Colorado School of Mines, 91 p.

Stanley, K.O., and Collinson, J.W., 1979, Depositional history of Paleocene-lower Eocene Flagstaff Limestone and coeval rocks, central Utah: American Association of Petroleum Geologists Bulletin, v. 63, p. 311-323.

Stanley, K.O., and Surdam, R.C., 1978, Sedimentation on the front of Eocene Gilbert-type deltas, Washakie Basin, Wyoming: Journal of Sedimentary Petrology, v. 48, p. 557-573.

Steidtmann, J.R., 1969, Stratigraphy of the early Eocene Pass Peak Formation, central-western Wyoming, *in* Barlow, J.A., ed., Symposium on Tertiary Rocks of Wyoming: Casper, Wyoming Geological Association, 21st Annual Field Conference, Guidebook, p. 55-63.

Steidtmann, J.R., and Middleton, L.T., 1991, Fault chronology and uplift history of the southern Wind River Range, Wyoming: Implications for Laramide and post-Laramide deformation in the Rocky Mountain foreland: Geological Society of America Bulletin, v. 103, p. 472-485.

Steidtmann, J.R., Middleton, L.T., Bottjer, R.J., Jackson, K.E., McGee, L.C., Southwell, E.H., and Lieblang, S., 1986, Geometry, distribution, and provenance of tectogenic conglomerates along the southern margin of the Wind River Range, Wyoming, *in* Peterson, J.A., ed., Paleotectonics and Sedimentation in the Rocky Mountain Region, United States: American Association of Petroleum Geologists Memoir 41, p. 321-332.

Stephens, J.G., and Healey, D.L., 1964, Geology and uranium deposits at Crooks Gap, Fremont County Wyoming: U.S. Geological Survey Bulletin 1147-F, 82 p.

Stuart, W.J., Jr., 1963, Stratigraphy of the Green River Formation west of the Rock Springs Uplift, Sweetwater County, Wyoming [M.Sc. thesis]: Laramie, University of Wyoming, 51 p.

—, 1965, Stratigraphy of the Green River Formation, west of the Rock Springs Uplift, *in* De Voto, R.H., and Bitter, R.K., eds., Sedimentation of Late Cretaceous and Tertiary Outcrops, Rock Springs Uplift: Casper, Wyoming Geological Association, 19th Annual Field Conference, Guidebook, p. 159-166.

Stucky, R.K., 1982, Mammalian fauna and biostratigraphy of the upper part of the Wind River Formation (early to middle Eocene), Natrona County, Wyoming, and the Wasatchian-Bridgerian Boundary [PhD thesis]: Boulder, University of Colorado, 285 p.

—, 1984a, Revision of the Wind River faunas, early Eocene of central Wyoming. Part 5. Geology and biostratigraphy of the upper part of the Wind River Formation, northeastern Wind River Basin: Annals of Carnegie Museum, v. 53, p. 231-294.

—, 1984b, The Wasatchian-Bridgerian land mammal age boundary (early to middle Eocene) in Western North America: Annals of Carnegie Museum, v. 53, p. 347-382.
Stucky, R.K., Krishtalka, L., and Dawson, M.R., 1989, Paleontology, geology and remote sensing of Paleogene rocks in the northeastern Wind River Basin, USA, *in* Flynn, J.J., ed., Mesozoic/Cenozoic Vertebrate Paleontology: Classic Localities, Contemporary Approaches: Washington, D.C., American Geophysical Union, International Geological Congress, 28th, Field Trip Guidebook T322, p. 34-44.
Stucky, R.K., Prothero, D.R., Lohr, W.G., and Snyder, J.R., 1996, Magnetic stratigraphy, sedimentology, and mammalian faunas of the early Uintan Washakie Formation, Sand Wash Basin, northwestern Colorado, *in* Prothero, D.R., and Emry, R.J., eds., The Terrestrial Eocene-Oligocene Transition in North America, Cambridge University Press, p. 40-51.
Sullivan, R., 1980, A stratigraphic evaluation of the Eocene rocks of southwestern Wyoming: Wyoming Geological Survey Report of Investigations 20, 50 p.
—, 1985, Origin of lacustrine rocks of the Wilkins Peak Member, Wyoming: American Association of Petroleum Geologists Bulletin, v. 69, p. 913-922.
Sundell, K.A., 1982, Geology of the headwater area of the North Fork of the Owl Creek, Hot Springs County, Wyoming: Geological Survey of Wyoming Report of Investigations 15, 51 p.
Sundell, K.A., Shive, P.N., and Eaton, J.G., 1984, Measured sections, magnetic polarity and biostratigraphy of the Eocene Wiggins, Tepee Trail and Aycross Formations within the southeastern Absaroka Range, Wyoming: Wyoming Geological Association Earth Science Bulletin, v. 17, p. 1-48.
Surdam, R.C., and Stanley, K.O., 1979, Lacustrine sedimentation during the culminating phase of Eocene Lake Gosiute, Wyoming (Green River Formation): Geological Society of America Bulletin, v. 90, p. 93-110.
—, 1980a, Effects of changes in drainage-basin boundaries on sedimentation in Eocene Lakes Gosiute and Uinta of Wyoming, Utah, and Colorado: Geology, v. 8, p. 135-139.
—, 1980b, The stratigraphic and sedimentologic framework of the Green River, Formation, Wyoming, *in* Hollis, S., ed., Stratigraphy of Wyoming: Casper, Wyoming Geological Association, 31st Annual Field Conference, Guidebook, p. 205-221.
Tabrum, A.R., Prothero, D.R., and Garcia, D., 1996, Magnetostratigraphy and biostratigraphy of the Eocene-Oligocene transition, southwestern Montana, *in* Prothero, D.R., and Emry, R.J., eds., The Terrestrial Eocene-Oligocene Transition in North America, Cambridge University Press, p. 40-51.
Tauxe, L., Gee, J., Gallet, Y., Pick, T., and Bown, T., 1994, Magnetostratigraphy of the Willwood Formation, Bighorn Basin, Wyoming: New constraints on the location of Paleocene/ Eocene boundary: Earth and Planetary Science Letters, v. 125, p. 159-172.
Thaden, R.E., 1980a, Geologic map of the Guffy Peak quadrangle, showing chromatolithofacies in the Wind River Formation, Fremont and Hot Springs Counties, Wyoming: U.S. Geological Survey Geologic Quadrangle Map GQ-1527, Scale 1:24 000, 1 Sheet.
—, 1980b, Geologic map of the Picard Ranch quadrangle, showing chromatolithofacies and coal beds in the Wind River Formation, Fremont County, Wyoming: U.S. Geological Survey Geologic Quadrangle Map GQ-1539, Scale 1:24 000, 1 Sheet.
Thomas, R.C., Sears, J.W., Ripley, A.A., and Berg, R.B., 1995, Tertiary extensional history of southwestern Montana: Field trip guide for the Sweetwater and upper Ruby valleys, Montana: Northwest Geology, v. 25, p. 5-25.
Torres, V., 1985, Stratigraphy of the Eocene Willwood, Aycross, and Wapiti Formations along the North Fork of the Shoshone River, north-central Wyoming: University of Wyoming Contributions to Geology, v. 23, p. 83-97.
Torres, V., and Gingerich, P.D., 1983, Summary of Eocene stratigraphy at the base of the Jim Mountain, North Fork of the Shoshone River, northwestern Wyoming, *in* Boberg, W.W., ed., Geology of the Bighorn Basin: Casper, Wyoming Geological Association, 34th Annual Field Conference, Guidebook, p. 205-208.
Tracey, J.I., Jr., Oriel, S.S., and Rubey, W.W., 1961, Diamictite facies of the Wasatch Formation in the Fossil Basin, southwestern Wyoming: U.S. Geological Survey Professional Paper 424-B, p. 149-150.
Trudell, L.G., Beard, T.N., and Smith, J.W., 1970, Green River Formation lithology and oil-shale correlations in the Piceance Creek Basin, Colorado: U.S. Bureau of Mines Report of Investigations 7357, 226 p.

—, 1974, Stratigraphic framework of Green River Formation oil shales in the Piceance Creek Basin, Colorado, *in* Murray, D.K., ed., Guidebook to the Energy Resources of the Piceance Creek Basin, Colorado: Denver, Colorado, Rocky Mountain Association of Geologists, 25th Annual Field Conference, p. 65-69.
Trudell, L.G., Mason, G.M., Smith, J.W., and Beard, T.N., 1982, Utah's principle oil shale resources in the Uinta Basin, *in* Gary, J.H., ed., Fifteenth Oil Shale Symposium Proceedings: Golden, Colorado, Colorado School of Mines Press, p. 38-49.
Trudell, L.G., Roehler, H.W., and Smith, J.W., 1973, Geology of Eocene rocks and oil yields of Green River oil shales on part of Kinney Rim, Washakie Basin, Wyoming: U.S. Bureau of Mines Report of Investigations 7775, 151 p.
Turnbull, W.D., 1972, The Washakie Formation of Bridgerian-Uintan ages, and the related faunas, *in* West, R.M., ed., Field Conference on Tertiary Biostratigraphy of Southern and Western Wyoming: Garden City, New York, Adelphi University, p. 20-31.
—, 1978, The mammalian faunas of the Washakie Formation, Eocene age, of southern Wyoming: Fieldiana: Geology, v. 33, p. 569-601.
Tweto, O., 1980, Summary of Laramide Orogeny in Colorado, *in* Kent, H.C., and Porter, K.W., eds., Colorado Geology: Denver, Colorado, Rocky Mountain Association of Geologists, Symposium on Colorado Geology, p. 129-134.
Van Houten, F.B., 1955, Volcanic-rich middle and upper Eocene rocks northwest of Rattlesnake Hills central Wyoming: U.S. Geological Survey Professional Paper 274-A, 14 p.
—, 1964, Tertiary geology of the Beaver Rim area Fremont and Natrona counties, Wyoming: U.S. Geological Survey Bulletin 1164, 99 p.
Vandenburg, C.J., Janecke, S.U., and McIntosh, W.C., 1998, Three-dimensional strain produced by >50My of episodic extension, Horse Prairie Basin area, SW Montana, U.S.A.: Journal of Structural Geology, v. 20, p. 1747-1767.
Veatch, A.C., 1907, Geography and geology of a portion of southwestern Wyoming: U.S. Geological Survey Professional Paper 56, 178 p.
Ver Ploeg, A.J., 1992, Geologic map of the Nowater Creek 30' x 60' quadrangle, northcentral Wyoming: Geologic Survey of Wyoming Map Series 39, Scale 1:100 000, 1 Sheet.
Walsh, S.L., Prothero, D.R., and Lundquist, D.J., 1996, Stratigraphy and paleomagnetism of the middle Eocene Friars Formation and Poway Group, southwestern San Diego County, California, *in* Prothero, D.R., and Emry, R.J., eds., The Terrestrial Eocene-Oligocene Transition in North America, Cambridge University Press, p. 120-154.
Walton, A.H., 1992, Magnetostratigraphy of the lower and middle members of the Devil's Graveyard Formation (Middle Eocene), Trans-Pecos Texas, *in* Prothero, D.R., and Berggren, W.A., eds., Eocene-Oligocene Climatic and Biotic Evolution: Princeton, Princeton University Press, p. 74-87.
Wedow, H., Jr., Gatskill, D.L., Banister, D.P., and Pattee, E.C., 1975, Mineral resources of the Absaroka Primitive Area and vicinity, Park and Sweet Grass Counties, Montana: U.S. Geological Survey Bulletin 1391-B, 115 p.
Weiss, M.P., 1982, Relation of the Crazy Hollow Formation to the Green River Formation, central Utah, *in* Nielson, D.L., ed., Overthrust Belt of Utah: Salt Lake City, Utah Geological Association, Publication 10, p. 285-289.
Weiss, M.P., and Warner, K.N., 2001, The Crazy Hollow Formation (Eocene) of Central Utah: Brigham Young University Geology Studies, v. 46, p. 143-161.
Weiss, M.P., Witkind, I.J., and Cashion, W.B., 1990, Geologic map of the Price 30' x 60' quadrangle, Carbon, Duchesne, Uintah, Utah, and Wasatch Counties, Utah: U.S. Geological Survey Miscellaneous Investigations Series Map I-1981, Scale 1:100 000, 1 Sheet.
West, R.M., 1970, Sequence of mammalian faunas of Eocene age in the northern Green River Basin, Wyoming: Journal of Paleontology, v. 44, p. 142-147.
—, 1973, Geology and mammalian paleontology of the New Fork-Big Sandy area, Sublette County, Wyoming: Fieldiana: Geology, v. 29, 193 p.
—, 1976, Paleontology and geology of the Bridger Formation, southern Green River Basin, southwestern Wyoming: Milwaukee Public Museum Contributions in Biology and Geology, no. 7, 10 p.
—, 1990, Vertebrate paleontology of the Green River Basin, Wyoming, 1840-1910: Earth Sciences History, v. 9, p. 45-56.

West, R.M., and Atkins, E.G., 1970, Additional Middle Eocene (Bridgerian) mammals from Tabernacle Butte, Sublette County, Wyoming: American Museum Novitates, no. 2404, 26 p.
West, R.M., and Dawson, M.R., 1973, Fossil mammals from the upper part of the Cathedral Bluffs Tongue of the Wasatch Formation (Early Bridgerian), northern Green River Basin, Wyoming: University of Wyoming Contributions to Geology, v. 12, p. 33-41.
—, 1975, Eocene fossil mammalia from the Sand Wash Basin, northwest Moffat County, Colorado: Annals of Carnegie Museum, v. 45, p. 231-253.
West, R.M., and Huchison, J.H., 1981, Geology and Paleontology of the Bridger Formation, southern Green River Basin, southwestern Wyoming. Part 6. The fauna and correlation of Bridger E: Milwaukee Public Museum Contributions in Biology and Geology, no. 46, 8 p.
Wiegman, R.W., 1964, Late Cretaceous and early Tertiary stratigraphy of the Little Mountain area, Sweetwater County, Wyoming [M.Sc. thesis]: Laramie, University of Wyoming, 53 p.
Wilf, P., 2000, Late Paleocene-early Eocene climate changes in southwestern Wyoming: Paleobotanical analysis: Geological Society of America Bulletin, v. 112, p. 292-307.
Wilson, A.B., and Elliott, J.E., 1997, Geologic maps of western and northern parts of Gallatin National Forest, south-central Montana: U.S. Geological Survey Geological Investigations Series Map I-2584, Scale 1:126 720, 2 Sheets.
Winfrey, M.W., Jr., 1958, Stratigraphy, correlation, and oil potential of the Sheep Pass Formation, east-central Nevada: Geological Record, Rocky Mountain Section, American Association of Petroleum Geologists, p. 77-82.
—, 1960, Stratigraphy, correlation, and oil potential of the Sheep Pass Formation, east-central Nevada, *in* Boettcher, J.W., and Sloan, W.W., Jr., eds., Guidebook to the Geology of East Central Nevada: Salt Lake City, Utah, Intermountain Association of Petroleum Geologists, 11th Annual Field Conference, p. 126-133.
Wing, S.L., Alroy, J., and Hickey, L.J., 1995, Plant and mammal diversity in the Paleocene to early Eocene of the Bighorn Basin: Palaeogeography, Palaeoclimatology, Palaeoecology, v. 115, p. 117-155.
Wing, S.L., Bao, H., and Koch, P.L., 2000, An early Eocene cool period? Evidence for continental cooling during the warmest part of the Cenozoic, *in* Huber, B.T., Macleod, K.G., and Wing, S.L., eds., Warm Climates in Earth History: Cambridge, Cambridge University Press, p. 197-237.
Wing, S.L., Bown, T.M., and Obradovich, J.D., 1991, Early Eocene biotic and climatic change in interior western North America: Geology, v. 19, p. 1189-1192.
Winterfield, G.F., 1990, Summary of Laramide depositional and tectonic events East Fork area, northwestern Wind River Basin and adjacent Washakie Range, Wyoming, *in* Specht, R.W., ed., Sedimentation and Tectonics: Casper, Wyoming Geological Association, 41st Annual Field Conference, Guidebook, p. 167-177.
Winterfield, G.F., and Conard, J.B., 1983, Laramide tectonics and deposition, Washakie Range and northwestern Wind River Basin, Wyoming, *in* Lowell, J.D., and Gries, R., eds., Rocky Mountain Foreland Basins and Uplifts: Denver, Colorado, Rocky Mountain Association of Geologists, 34th Annual Field Conference, Guidebook, p. 137-148.
Wolfbauer, C.A., and Surdam, R.C., 1974, Origin of nonmarine dolomite in Eocene Lake Gosiute, Green River Basin, Wyoming: Geological Society of America Bulletin, v. 85, p. 1733-1740.
Wolfe, J.A., Forest, C.E., and Molnar, P., 1998, Paleobotanical evidence of Eocene and Oligocene paleoaltitudes in midlatitude western North American: Geological Society of America Bulletin, v. 110, p. 664-678.
Wood, C.B., 1966, Stratigraphy and paleontology of the Bridger Formation northeast of Opal, Lincoln County, Wyoming [M.Sc. thesis]: Laramie, University of Wyoming, 112 p.
Wood, H.E., II, 1934, Revision of the Hyrachyidae: American Museum of Natural History Bulletin, v. 67, p. 181-285.
Wood, H.E., II, Seton, H., and Hares, C.J., 1936, New data on the Eocene of the Wind River Basin: Geological Society of America Proceedings for 1935, p. 394-395.
Yuretich, R.F., 1984, Yellowstone fossil forests: New evidence for burial in place: Geology, v. 12, p. 159-162.
Zawiskie, J., Chapman, D., and Alley, R., 1982, Depositional history of the Paleocene-Eocene Colton Formation, north-central Utah, *in* Nielson, D.L., ed., Overthrust Belt of Utah: Salt Lake City, Utah Geological Association, Publication 10, p. 273-284.

Zonneveld, J.-P., Bartels, W.S., and Clyde, W.C., 2003, Stratal architecture of an Early Eocene fluvial-lacustrine depositional system, Little Muddy Creek area, southwestern Green River Basin, Wyoming, *in* Raynolds, R.G., and Flores, R.M., eds., Cenozoic Systems of the Rocky Mountain Region: Denver, Colorado, Rocky Mountain Section, SEPM (Society for Sedimentary Geology), p. 253-287.

Zonneveld, J.-P., Gunnell, G.F., and Bartels, W.S., 2000, Early Eocene fossil vertebrates from the southwestern Green River Basin, Lincoln and Uinta Counties, Wyoming: Journal of Vertebrate Paleontology, v. 20, p. 369-386.